
[All ETDs from UAB](#)

[UAB Theses & Dissertations](#)

2021

A Role for INF- γ -Inducible Transcription Factors in Antibody Secreting Cell Differentiation

Jessica N. Peel
University Of Alabama At Birmingham

Follow this and additional works at: <https://digitalcommons.library.uab.edu/etd-collection>

 Part of the [Medical Sciences Commons](#)

Recommended Citation

Peel, Jessica N., "A Role for INF- γ -Inducible Transcription Factors in Antibody Secreting Cell Differentiation" (2021). *All ETDs from UAB*. 627.
<https://digitalcommons.library.uab.edu/etd-collection/627>

This content has been accepted for inclusion by an authorized administrator of the UAB Digital Commons, and is provided as a free open access item. All inquiries regarding this item or the UAB Digital Commons should be directed to the [UAB Libraries Office of Scholarly Communication](#).

A ROLE FOR IFN- γ -INDUCIBLE TRANSCRIPTION FACTORS IN ANTIBODY
SECRETING CELL DIFFERENTIATION

by

JESSICA N. PEEL

AMY S. WEINMANN, COMMITTEE CHAIR
ANDRE BALLESTEROS-TATO
LAURIE E. HARRINGTON
JOHN F. KEARNEY
FRANCES E. LUND

A DISSERTATION

Submitted to the graduate faculty of The University of Alabama at Birmingham,
in partial fulfillment of the requirements for the degree of
Doctor of Philosophy.

BIRMINGHAM, ALABAMA

2021

ABSTRACT

Viral infections remain a major cause of morbidity and mortality. Within a viral, interferon (IFN)- γ -driven inflammatory microenvironment, B cells may produce antibody which is critical for rapid viral clearance and continued protection from reinfection. However, the roles of IFN- γ and IFN- γ -induced transcription factors (TFs) in driving antibody secreting cell (ASC) development from their B cell precursors are poorly understood. Herein, we identify two IFN- γ -inducible transcription factors (TFs), T-bet and interferon regulatory factor 1 (IRF1), that are essential for the differentiation of ASCs from IFN- γ -activated B cell precursors. T-bet repressed an IFN- γ -inducible inflammatory gene program that was incompatible with ASC formation *in vitro*. In contrast, IRF1 is required for dampening BCR signaling thus supporting development of a marginal zone innate-like ASC precursor. Both, T-bet and IRF1, contribute to protective antigen-specific antibody responses upon influenza infection. While B cell-intrinsic T-bet was required for the generation of long-lived ASCs upon viral infection, B cell-intrinsic IRF1 was indispensable for the development of early antigen-specific IgM in response to both viral infection and bacterial immunization. Lastly, we find that immunization with an intranasal Ad5COVID vaccine induces local IFN- γ producing T cell responses and the production of durable receptor binding (RBD) specific antibody. Thus, IFN- γ and IFN- γ -inducible TFs are essential for generating protective humoral immunity.

TABLE OF CONTENTS

	<i>Page</i>
ABSTRACT	<i>ii</i>
LIST OF FIGURES.....	<i>v</i>
INTRODUCTION	1
Overview.....	1
B cell development.....	3
B cell development-bone marrow.....	3
Transitional B cells- peripheral B cell development.....	5
The mature B cells	6
B-1 B cells.....	7
B-2 B cells.....	8
Follicular B cells.....	8
MZ B cells.....	9
B cell differentiation: B memory cells (Bmem) and ASCs.....	11
B cell activation/ CSR/SHM.....	11
T-independent (T-I)	13
T-I Bmem	13
T-I ASCs	13
T-dependent (T-D).....	14
The Germinal center.....	15
T-D Bmem	17
T-D ASCs	17
Transcriptional regulation of Bmem and ASCs.....	18
Signals 1,2, and 3: For B cell development and differentiation.....	19
Signal 1: BCR.....	20
Selection-B cell development.....	20
Clonal positive selection	20
Clonal negative selection	21
BCR signaling threshold-mediated selection	22
Altered selection driving autoimmunity	22
Signaling: The good.....	24
Signaling: The bad	24
Signal 2: Co-stimulation and TLR ligands	26

Signal 3: Cytokine	27
The bare essentials.....	28
IFN- γ and IFN- γ -inducible transcriptional regulation	29
T-bet.....	30
IRF1	32
Summary	33
T-BET TRANSCRIPTION FACTOR PROMOTES ANTIBODY SECRETING CELL DIFFERENTIATION BY LIMITING THE INFLAMMATORY EFFECTS OF IFN- γ ON B CELLS	35
A ROLE FOR DUAL BCR AND TLR- INDUCED IRF1 IN B CELL FATE SPECIFICATION	93
SINGLE-DOSE INTRANASAL ADMINISTRATION OF ADCOVID ELICITS SYSTEMIC AND MUCOSAL IMMUNITY AGAINST SARS-COV-2 IN MICE	151
DISCUSSION	191
T-bet and IFN- γ represses alternate B cell fates.....	192
T-bet paradox: Stable B effector state	194
IRF1 as a regulator of protective, innate-like B cells.....	195
The influence of TLR signaling in the development of mature B cells.....	196
IRF1 and the development of autoimmunity	197
COVID-19 vaccination strategies.....	199
Future directions and concluding remarks.....	200
GENERAL LIST OF REFERENCES	202
APPENDIX IACUC APPROVAL	224

LIST OF FIGURES

Main

<i>Figure</i>		<i>Page</i>
1	Resolution and characterization of B cell development.	4
2	Transitional B cell subsets-continued B cell development in periphery.....	6
3	Heterogeneity amongst mature b cell subsets	7
4	The splenic marginal zone.....	11
5	The germinal center	16
6	A model of intraclonal competition.....	23
7	A model of ifng-inducible irf1 contributing to the generation of asc precursors	34
8	A model of bcr/tlr-inducible irf1 in transitional b cells.....	191
9	T-bet opposes iga-producing cells in response to influenza infection in the lung.....	193
10	T-bet represses gc b cell formation after influenza infection.....	195

T-BET TRANSCRIPTION FACTOR PROMOTES ANTIBODY SECRETING CELL DIFFERENTIATION BY LIMITING THE INFLAMMATORY EFFECTS OF IFN- γ ON B CELLS

<i>Figure</i>		<i>Page</i>
1	ASC Development Is Preferentially Initiated in Th1 Cell-Primed B Cells.	69
2	IFN- γ R Signals Control Be1 Differentiation into ASCs.....	71
3	T-bet Controls Be1 Differentiation but Does Not Regulate Early ASC Programming.....	72
4	T-bet Represses Inflammatory Gene Expression in Be1	

	Cells	73
5	T-bet Supports Be1 ASC Formation by Repressing the IFN- γ R-Regulated Inflammatory Gene Program	75
6	T-bet-Expressing B Cells Regulate Humoral Immunity to Influenza	78
7	ASC Development after Flu Challenge Infection Requires T-bet ⁺ Memory B Cells	80
S1	Be1 cells upregulate Blimp-1 by day 2 and commit to the ASC lineage between days 2- 3 (related to Fig. 1).	82
S2	PageRank analysis predicts TF activity in day 2 Be1 and Be2 cells (related to Fig.2)	83
S3	T-bet regulates ASC development in Be1 cells (related to Fig. 3)	84
S4	T-bet represses the IRF and STAT induced inflammatory signature in Be1 cells (related to Fig. 4)	86
S5	Sustained TLR and NF- κ B signaling prevents ASC development in Be1 cells (related to Fig. 5)	88
S6	Identification of T-bet expressing B cells in flu-infected T-bet reporter mice and B cell bone marrow chimeras (related to Fig. 6)	89
S7	Identification of B cell subsets following induced deletion of <i>Tbx21</i> in memory B cells (related to Fig. 7)	91

A ROLE FOR DUAL BCR AND TLR- INDUCED IRF1 IN B CELL FATE SPECIFICATION

<i>Figure</i>	<i>Page</i>	
1	IRF1-expressing B cells are required for IFN γ -dependent IgM antibody responses and early IgM responses to influenza infection.	132
2	IRF1 regulates IgM Ab responses to TLR ligands and T-independent antigens	134
3	The marginal zone B cell and macrophage compartments rely on IRF1	135
4	MZ B cells and T cell independent responses require IRF1 expression by B cells	137
5	TLR and BCR signals cooperate to induce IRF1 expression in	

	transitional B cells	139
6	IRF1 regulates Notch signaling in transitional B cells	141
7	IRF1 regulates selection of B cells into the polyreactive and autoreactive repertoire	142
S1	Generation of bone marrow chimeric mice and identification of influenza, nucleoprotein (NP)-specific GC B cells and ASCs.....	144
S2	Characterization of splenic MZ B cells in naïve WT and <i>Irf1</i> ^{-/-} mice.....	145
S3	<i>Irf1</i> is dispensable for BM and splenic B cell development and integrin and chemokine receptor expression is intact in absence of <i>Irf1</i>	146
S4	IRF1 expression in transitional and MZ B cells does not require IFN signals.	147
S5	Activated <i>Irf1</i> ^{-/-} transitional B cells do not adopt a mature MZ B cell phenotype <i>in vitro</i>	148
S6	IRF1 regulates selection of B cells into the polyreactive and autoreactive repertoire.	149

SINGLE-DOSE INTRANASAL ADMINISTRATION OF ADCOVID ELICITS SYSTEMIC AND MUCOSAL IMMUNITY AGAINST SARS-COV-2 IN MICE

<i>Figure</i>		<i>Page</i>
1	Spike-specific IgG responses in sera following a single intranasal administration of AdCOVID	172
2	A single intranasal administration of AdCOVID elicits anti-SARS-CoV-2 neutralizing antibodies	173
3	Spike-specific IgA responses in BAL following single intranasal administration of AdCOVID.	174
4	Flow cytometry analysis of immune cells in lungs from C57BL/6J mice following a single intranasal dose of AdCOVID.	175
5	Intranasal AdCOVID vaccination elicits mucosal and systemic IFN- γ ⁺ T cells.....	176
6	Intracellular cytokine production by pulmonary and splenic T cells 14 days after intranasal AdCOVID vaccination.	177

7	Intranasal AdCOVID vaccination elicits polyfunctional memory T cell populations in the lung 14 days after vaccination	178
8	Intranasal AdCOVID vaccination does not elicit a Th2 or Th17-biased immune response	179
S1	A single intranasal dose of AdCOVID generates long-lived anti-RBD IgG-secreting B cell populations in the periphery	180
S2	A single intranasal dose of AdCOVID generates long-lived anti-RBD IgA-secreting B cell populations.....	181
S3	Flow cytometry analysis of immune cells in BAL from C57BL/6J mice following intranasal vaccination with single dose of AdCOVID	182
S4	Flow cytometry analysis of immune cells in medLN from C57BL/6J mice following intranasal vaccination with single dose of AdCOVID	183
S5	Flow cytometry analysis of immune cells in spleens from C57BL/6J mice following intranasal vaccination with single dose AdCOVID	184
S6	Representative flow cytometry plots for gating of T cells isolated from mice	186
S7	Representative flow cytometry plots for gating B cells isolated from mice.....	187
S8	Representative flow cytometry plots for gating of myeloid cells isolated from mice.....	188
S9	Representative flow cytometry plots for gating of Trm cells isolated from mice.....	189

TABLE OF ABBREVIATIONS

Abbreviation	Definition
Ab	antibody
Ag	antigen
ASC	antibody secreting cell(s)
BCR	B cell receptor
Be	B effector
BM	bone marrow
Bmem	B memory cell(s)
DC	dendritic cell
FDC	follicular dendritic cell
FoB	follicular B cell(s)
GC B	germinal center B cell
IFN	interferon
IFNg-R	interferon gamma receptor
Ig	immunoglobulin
IL	interleukin
IRF	interferon regulatory factor
LL-PC	long-lived plasma cell(s)
MZ B	marginal zone B cell(s)
PB	plasmablast(s)
PC	phosphorylcholine
T-D	T-dependent
T-I	T-independent
TCR	T cell receptor
TF	transcription factor
Tfh	T follicular helper
Th	T helper cells
TLR	toll-like receptor

INTRODUCTION

Overview

Antibodies are an essential component of innate-like and adaptive immunity, immunologic memory, and immunopathology¹. Capable of binding to components of fungi, bacteria, viruses, and self-antigens, antibody is produced by antibody-secreting cells (ASCs) that develop from their B cell precursors. Arising from the fetal liver, populations of innate-like B cells, or “natural memory” cells, predominate in neonatal life and are poised to secrete broadly reactive antibody rapidly in response to pathogens in a T-independent (T-I) manner². In contrast, the continually replenished bone marrow-derived conventional B-2 B cells depend on interactions with cognate T cells and specialized stromal cells to undergo affinity maturation in transient structures known as germinal centers (GCs) upon antigen encounter³⁻⁵. It is thought that these highly proliferative, activated GC B cells give rise to long-lived pools of ASCs and B memory cells (Bmem)^{6,7}. While there is a well-appreciated role for antibodies in conferring protection in health and mediating pathogenicity in disease, we do not yet fully understand the mechanisms by which ASCs differentiate, nor have we fully identified the pathways that grant longevity to some populations of ASCs⁸.

It is currently understood that the differentiation of activated B cells into ASCs is a lineage switch, coordinating the loss of B cell identity genes with the acquisition of ASC specific regulators¹⁰. While informative, many of these studies have only described this transition following model antigen immunization and largely focusing on contributions of antigen receptor engagement and co-stimulation¹¹⁻¹⁴. Only relatively recently have cytokine and cytokine-inducible transcription factors been appreciated in governing not only isotype switching, but also B cell terminal differentiation.

B cells expressing the IFN- γ -inducible transcription factor, T-bet, have been identified *in vivo* following immunization, viral infection or in chronic disease states, such as systemic lupus erythematosus (SLE) and rheumatoid arthritis (RA)¹⁵⁻²¹. These studies posited that populations of T-bet⁺ B cells, with distinct phenotypical characteristics, are a correlate of protection or disease¹⁵⁻²¹. These studies, however, only focused early post

infection/immunization or are assessed in chronic infection or disease states¹⁵⁻²¹. Additionally, the role of T-bet is largely ascribed to B cell class switching to IgG2a/c rather than B cell fate decisions^{15,21}. Therefore, the role of T-bet in the generation of long-lived ASCs, and, further, the molecular mechanism by which T-bet promotes the differentiation of ASCs has not been adequately addressed.

We recently showed that T helper 1 (Th1)-activated B cells require expression of T-bet and the interferon gamma receptor (IFN- γ R) to differentiate into ASCs²². We found that IFN- γ and not T-bet was required for expression of an ASC specifying transcription factor, Blimp-1^{10,22}. Instead, T-bet repressed an inflammatory gene program which was incompatible with ASC formation²². At the intersect of four different bioinformatic analysis, IRF1 was the only other predicted upstream regulator, besides T-bet, of IFN- γ -induced ASC development²². Therefore, we predicted that IRF1 would be required for the initiation of *Prdm1* (the gene encoding for Blimp-1) and, thus, IFN- γ -induced ASC differentiation.

Very little is known about IRF1 in B cell fate decisions. The development of mature B cells appears to be intact in *Irf1* deficient mice²⁵. Relatively recently, it has been shown that B cell-specific loss of *Irf1* results in fewer GC B cells following murine gammaherpesvirus 68, MHV-68, infection²⁴. Despite this marked reduction in GC B cells, the generation of long lived, antigen specific antibody is intact in the absence of *Irf1*^{23,24}. This study, while informative, only thoroughly evaluated *Irf1* expressing B cells relatively early following chronic viral infection^{23,24}. It is well appreciated that long-lived ASCs begin to accumulate 20-30 days after acute viral infection and that persistent antigenic stimulation and inflammation results in fewer ASCs^{26,27}. Therefore, it is not possible to determine whether IRF1 is required for the development of long-lived antibody responses from those studies.

We, therefore, hypothesized that IRF1 would promote ASC differentiation. Our studies evaluate the role of IRF1 expressing B cells, not only in IFN- γ -induced ASC differentiation *in vitro*, but also humoral responses following influenza infection and immunization with bacterial particulate antigen *in vivo*. Furthermore, we propose a mechanism by which IRF1 may promote the generation of a developmentally distinct ASC precursor, thus establishing protection against infection and prevention of autoimmune disease. Lastly, we identify a local IFN- γ -producing T cell response as a correlate of durable RBD-specific antibody upon intranasal Ad5COVID vaccination. Thus, we establish that IFN- γ and IFN- γ -

inducible transcription factors may promote long-lived antibody responses upon viral infection and vaccination. To introduce these topics, mechanisms of B cell development, activation, and differentiation, will be discussed. While relatively limited, we will focus on B cell activation and differentiation in the context viral infection and autoimmune disease. Additionally, we will discuss the established mechanisms driving those processes of B cell biology.

B cell development

B cell precursors progress through an ordered series of developmental and selection steps before reaching maturity. The well appreciated heterogeneity in peripheral, mature B cell subsets is largely due to clonal selection defined by BCR specificities as well as BCR signaling strength. While innate-like B cell subsets, B-1 and marginal zone (MZ) B cells, enrich for self-reactive specificities, conventional follicular (FoB) cells are highly diversified and monospecific. Herein, we describe B cell development and the selection events that give rise to mature B cells.

B cell development- bone marrow

B cells develop from hematopoietic stem cells (HSCs) in the liver before birth and in the bone marrow (BM) thereafter²⁸. The earliest BM B cell precursors include cells that do not express surface immunoglobulin (sIg) but do express the B cell lineage marker B220²⁹. This BM derived B220⁺sIg^{neg} fraction is heterogeneous with respect to cell surface expression of BP-1 and CD24 and three populations can be identified as BP-1^{neg}CD24^{neg}, BP-1^{neg}CD24⁺, and BP-1⁺CD24⁺ subsets²⁹. After culture of these populations with a fetal liver derived stromal cell line, the sequential order of early B cell development can be resolved. Briefly, the BP-1^{neg}CD24^{neg} fraction is the most immature and is referred to as Pre-pro B cells, or Fraction A²⁹. Fraction A cells upon expression of CD24 (BP-1^{neg}CD24⁺), matured into early Pro- B cells, or Fraction B cells. The Fraction B cells upregulated BP-1 and matured into late Pro- B cells, or Fraction C cells (BP-1⁺CD24⁺) and the Fraction C cells upregulated expression of the B cell receptor, sIg²⁹.

These early BM fractions were functionally distinct in that they were the only BM derived B cell lineages to proliferate and survive in the *in vitro* cultures. This was thought to be due to the presence of a pro-survival factor, IL-7, which was required primarily by Fractions

B and C for proliferation, whereas Fraction A was also dependent on stromal cell contact *in vitro*²⁹. Additional analysis described the status of Ig gene rearrangement in each of these early BM B cell fractions, thus reinforcing the progressive early B cell developmental stage assigned by the cell surface phenotype^{29,30}.

After productive IgH gene rearrangement and pairing with surrogate light chain, B cells are permitted to enter a rapidly proliferating phase, Fraction C', followed by a resting stage known as Pre- B cells, or Fraction D²⁹. At this stage, rearrangement with a variety of light chains results in a functional antigen receptor, the hallmark of an adaptive immune cell²⁹. This process generates a B cell repertoire capable of theoretically recognizing more than 10¹⁶ antigenic determinants⁹. Considering this vast diversity, a balance of immunity and tolerance must be achieved. Therefore, a B cell expressing a receptor that engages self-antigens “too strongly” may undergo clonal deletion or gene editing^{29,31-33}, thus establishing central tolerance³⁴. However, once a tolerable B cell receptor (BCR) signal occurs, immature B cells are competent to exit from the bone marrow for further selection in the periphery^{28,29,36}.

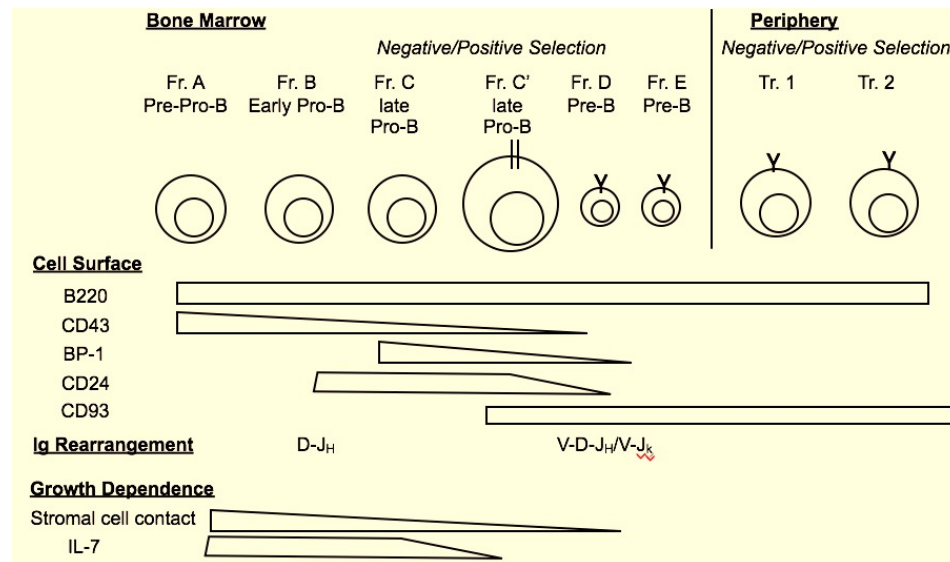


Figure 1 Resolution and characterization of B cell development. Summary of the changes in cell surface molecule expression during B cell developmental stages in the bone marrow and in the spleen correlated with Ig gene rearrangement status and growth dependence.

Hardy *Immunol Rev.* (2000) DOI: <https://doi.org/10.1111/j.1600-065X.2000.imr017517.x>

Transitional B cells- peripheral B cell development

Originally described as CD24^{hi} splenic B cells, the immature transitional B cells reconstitute the spleen before CD24^{low} mature B cells after sublethal dose of irradiation³⁵. Additionally, CD24^{hi} splenic B cells are rapidly cycling which parallel that of the BM derived immature B cell fraction^{35,36}. Furthermore, unlike the mature B cell compartment, CD24^{hi} splenic B cells undergo apoptosis in response to B cell receptor (BCR) ligation³⁵. However, this is likely a function due to dosage of antigen receptor stimulation rather than a ubiquitous response to BCR ligation as it has been demonstrated that low dose BCR crosslinking results in improved splenic immature B cell survival rather than apoptosis³⁷. Alternatively, amongst these studies are differing cell surface definitions of splenic immature B cells. Whereas some define splenic immature as CD24^{hi}, others have also included cell surface expression of CD93 and varying levels of CD21^{35,36,38}. This suggests an underappreciated heterogeneity in this population. Indeed, earlier studies defining transitional B cells on the basis of CD24 expression concluded that the earliest newly formed splenic B cells, transitional 1 (T1) B cells, were more vulnerable to apoptosis when compared to the more mature transitional (T2) B cells³²². Additionally, this study, while informative, cultured T1 and T2 B cells in the presence of high dose BCR stimulation which later studies demonstrated results in low cell viability of these splenic newly formed cells^{37,322}. Furthermore, in response to high dose BCR stimulation T2 B cells upregulate CD69 and enter cell cycle³²². This could suggest that based on this cell surface definition, along with high dose BCR stimulation that there were contaminating mature B cells within this population. However, it has also been shown that T2 cells have augmented responses to BAFF, a prosurvival factor, suggesting that T2 cells may be more able to overcome relatively strong BCR signals³²³.

Given the inherent heterogeneity of the splenic immature transitional B cells, it has been proposed that T1 and T2 cells have differing propensities to seed the mature marginal zone (MZ) B cell or follicular (Fo) B cell compartment (discussed at length later). Indeed, in mice lacking a serine/threonine kinase, TAOK3, T1 cells do not efficiently express ADAM10, a metalloproteinase responsible for the initiation of a hallmark MZ B cell developmental pathway⁹⁵. However, this study, while informative, monitored ADAM10 expression on all transitional B cells rather than B cells fated to be selected into the MZ B cell pool. Additionally, this study also indicated that ADAM10^{neg} T1 and T2 B cells may also yield to MZ B cell precursors, which is consistent with previous studies^{3,38,95,323}. While it is observed

that T2 B cells can predominantly give rise to FoB cells, there is also an appreciated plasticity amongst mature B cell subsets. FoB cells may migrate through bridging channels into the red pulp where FoB cells can subsequently experience signals to then acquire qualities of a MZ B cell^{62,324}. Therefore, it is clear that there is no one precursor to either FoB or MZ B cells. In sum, peripheral transitional B cells are considered distinct developmental intermediates in the generation of mature B cells and are thought to experience selection pressures that shape the mature B cell repertoire (Figure 2)³⁹.

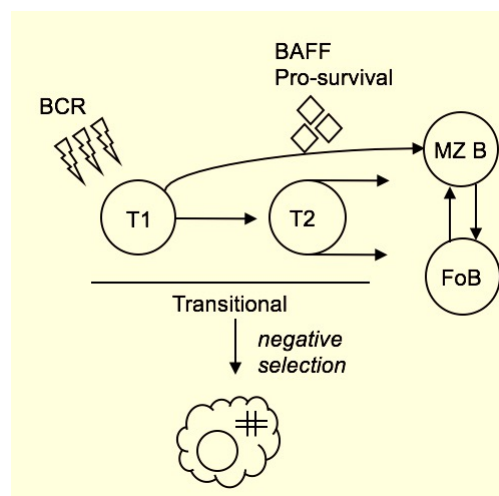


Figure 2 Transitional B cell subsets- continued B cell maturation in the periphery. Summary of the signals and selective pressures transitional 1 (T1) and transitional 2 (T2) B cells experience to give rise to mature B cell subsets.

Allman *Curr. Opin. Immunol* (2008) DOI: 10.1016/j.coi.2008.03.014

The mature B cells

Upon completion of development, mature peripheral B cells are typically classified as B-1 or B-2 B cells on the basis of developmental ontogeny. Whereas the B-1 B cells arise from the fetal liver with the capacity to self-renew, the predominant B-2 are continually replenished from the adult bone marrow and are further categorized into follicular (Fo) and MZ B cells. Given this heterogeneity within the mature B cell compartment, the characteristics of these phenotypically, topographically, and functionally distinct B cell lineages will be discussed (Figure 3).

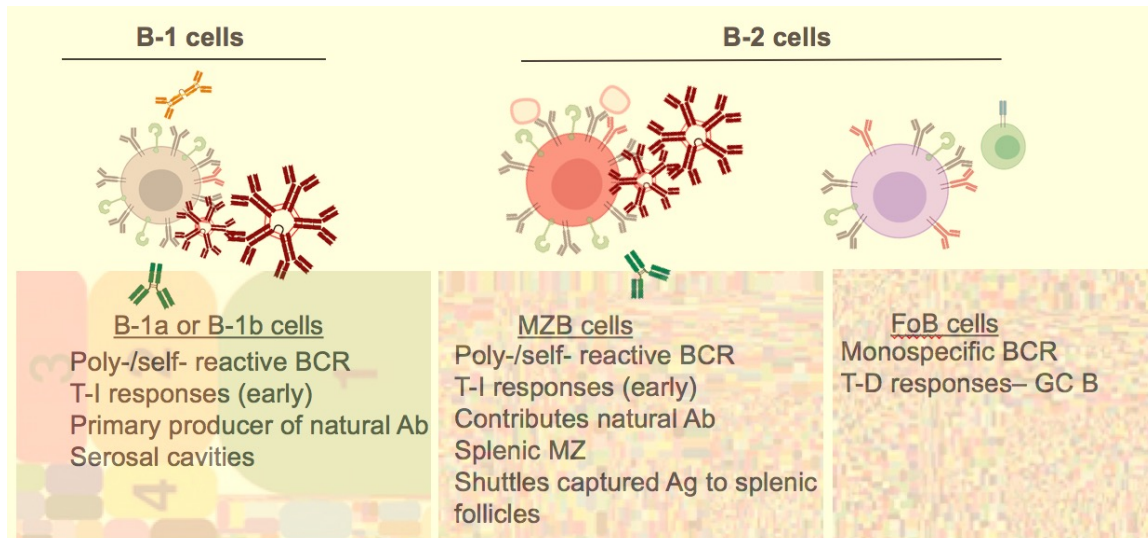


Figure 3 Heterogeneity amongst mature B cell subsets. Summary of the developmental and functional distinctions between mature B cell compartments.

Attanavanich *J Immunol.* (2004) DOI: [10.4049/jimmunol.172.2.803](https://doi.org/10.4049/jimmunol.172.2.803)

New *Viral Immunol.* (2020) DOI: [10.1089/vim.2019.0136](https://doi.org/10.1089/vim.2019.0136)

Yang *Elife.* (2015) DOI: [10.7554/eLife.09083](https://doi.org/10.7554/eLife.09083)

B-1 B cells

According to the lineage hypothesis, it is thought that the innate-like, self-renewing B-1 B cells represent a separate lineage derived largely from the fetal liver that cannot give rise to conventional or B-2 cells^{69,70}. Arising from distinct progenitors, B-1 B cells have a restricted and biased BCR repertoire through unique developmental constraints⁶⁹⁻⁷². These limitations are essential to the establishment of conserved specificities capable of recognizing diverse antigens, including those originating from self⁶⁹⁻⁷³. Thus, B-1 B cells are the primary producers of natural, cross-reactive antibody that is continuously produced in the absence of immunization, infection, or microbial antigen⁷³⁻⁷⁷. However, it has been recently shown that populations of B-1 B cells may be directly influenced by microbial components³²¹. Given this distinct function, it is thought that the B-1 B cell lineage is regulated differently than B-2 B cells and in part contributes to their unique phenotype.

B-1 B cells were originally identified as expressing “Ly-1” or CD5⁺, a known negative regulator of antigen receptor signaling⁷⁰. B-1 B cells are known to highly co-express CD9, CD36, CD72, CD73, CD11b and CD22. Expression of these proteins is indicative of the ability of B-1 B cells to effectively capture and present antigen (CD36), migrate to sites of inflammation (CD11b), and to manage continuous BCR activation (CD72 and CD22)⁷⁸⁻⁸². CD73 expressing-B-1 B cells may be indicative of their previous antigenic experience⁸³. Owing to this distinctive phenotype, B-1 B cells are sometimes referred to as “natural memory cells,” and as such are positioned in serosal cavities to readily re-encounter antigen^{69,70}.

B-1 B cells are further distinguished on the basis of CD5 expression, where the earliest B-1a B cells express CD5 and arise before birth the B-1b B cells do not express CD5 and can be replenished through adult bone marrow³²⁵. Due to this difference in developmental ontogeny, B-1a B cells are continually replenished through self-renewal, whereas B-1b B cells can be derived from an adult bone marrow precursor³²⁵.

B-2 B cells

The continually replenished, adult bone marrow derived B-2 B cell lineage are further categorized into follicular B (FoB) and marginal zone B cells (MZ B) on the basis of phenotype, position, and function.

Follicular B cells

Most mature B cells are recirculating cells that home to B cell follicles in secondary lymphoid tissues and therefore are referred to as follicular B (FoB) cells⁴⁵. B cell follicles are in close proximity to the periarteriolar lymphoid sheath (PALS) in the spleen and the paracortex in the lymph nodes, which are areas mainly populated by T cells⁴⁵. Therefore, it is more likely that FoB cells may communicate with T cells. Composed of a highly-diversified BCR repertoire, it is unlikely that FoB cells experience any strong peripheral selection event and, presumably, is an additional basis for T-dependent activation, expansion, and affinity maturation (discussed later) in response to protein antigens⁷⁴. However, the even more diversified BM-derived immature B cell fraction would suggest FoB cells undergo some clonal selective pressure⁸⁴. Altogether, FoB cells represent an expansive pool of mature B cells capable of responding to a vast number of antigenic determinants.

Marginal zone B cells

Located at the interface of the lymphoid white pulp and non-lymphoid red pulp of the spleen, the marginal zone (MZ) is a unique microenvironment where senescent cells, cellular debris, and blood-borne pathogens are efficiently removed from the blood by the resident immune cells (Figure 4)^{46,85}. One such MZ resident immune cell are the phenotypically distinct CD21^{hi}CD23^{low} MZ B cells⁴⁶. Similar to B-1 B cells, MZ B cells co-express CD1d, CD36 and CD9, presumably to aid in antigen capture and presentation^{78,79,86}. Due to their positioning and continual exposure to the circulation MZ B cells embody some functional properties of innate immunity⁸⁷. Indeed, it has been shown MZ B cells, rather than FoB cells, have an enhanced capacity to prime T cells⁸⁸. However, their most prominent role is providing a first line of defense through rapidly producing cross-reactive antibody to bridge the temporal gap required by later arising T-dependent responses⁸⁷. Therefore, the innate-like MZ B cells are spatially, phenotypically, and functionally distinct B cell subset⁴⁶.

The production of cross-reactive, natural antibody (NAb) primarily relies on B-1 B cells and, to a lesser extent, MZ B cells⁸⁷. Thus, MZ B cells express BCRs that react with microbial and self antigens^{46,47,51,52}. Indeed, autoreactive 81X or M167-V_H-bearing B cells are selected into the MZ B cell pool from their splenic transitional precursors^{46,47,51,52}. By virtue of a repertoire enriched with self-reactive specificities, MZ B cells participate in “housekeeping” functions. Certainly, a primary role of NAb is to promote the clearance of potentially proinflammatory apoptotic cells, and thus, the prevention of autoimmune disease^{54,89,90}. Although, unlike B-1 B cells, mechanisms for Ig diversification are intact in MZ B cell progenitors thereby enhancing the breadth of the MZ B cell repertoire^{87,71,72}. Although, the FoB cell repertoire is certainly more vast⁷⁴. Therefore, the MZ B cell pool may possess a relatively restricted, self-reactive repertoire that assists in the clearance of senescent cells and cellular debris in the circulation.

In addition to strong, peripheral clonal selection events, MZ B cells depend on signaling through a membrane bound receptor, Notch2 by engaging its ligand, delta-like 1 (DLL-1) expressed on stromal cells of the MZ^{91,92}. Indeed, mice lacking Notch2 or components of this hallmark pathway have fewer MZ B cells⁹¹⁻⁹³. Similarly, there are more MZ B cells in transgenic mice where Notch2 pathway is constitutively activated⁹². The primary function of the Notch2 pathway is to direct MZ B cell development from their splenic transitional B cell precursors^{3,45,91-95}. While it is well appreciated that the activation of the

Notch2 pathway is required for MZ B cell development, the underlying molecular mechanism supporting that development is unknown. It has been suggested that a predicted downstream target of Notch2 signaling, c-Fos, drives MZ B cell development by sensitizing transitional B cells to toll-like-receptor (TLR)-induced proliferation^{96,97}. However, it is currently understood that TLR signaling is mostly dispensable for mature B cell development^{98,99}. Therefore, how Notch2 governs MZ B cell development remains largely unexplored. Thus, through the communication with neighboring DLL-1 expressing MZ resident stromal cells, MZ B cells require Notch2 signaling for their development.

In addition to the developmental cues imparted to the MZ B cells by the other resident cells of the MZ, MZ B cells communicate with populations of MZ macrophages to efficiently capture antigen^{87,100-102}. Strategically interposed between the lymphoid white pulp and the circulation, the blood flow slows within the MZ allowing for the efficient capture of particulate antigens by populations of scavenger receptor expressing MZ macrophages^{87,100-102}. Studies have shown that the scavenger receptor, SIGN-R1, is required for antigen trapping in the MZ^{87,101,102} and that its expression requires the presence of MZ B cells³²¹. Indeed, *Cd19* or *Notch2* deficient mice, which have markedly fewer MZ B cells, have diminished SIGN-R1 expression on populations of MZ macrophages (MZMs)^{100,103}. Consequently, antigen is inefficiently trapped in the MZ and, in turn, MZ B cells are unable to capture antigen¹⁰⁰. Therefore, the cooperation between MZMs and MZ B cells is required to effectively filter antigen from the circulation, one of the principle functions of the spleen.

Additional interactions with stromal cells expressing adhesion molecules, ICAM1 and VCAM1, are required for the retention of MZ B cells within the MZ¹⁰⁴. Indeed, MZ B cells selectively express the integrins, $\alpha\text{L}\beta\text{2}$ and $\alpha\text{4}\beta\text{1}$, which interact with ICAM1 and VCAM1, respectively¹⁰⁴. S1PR1 and S1PR3 expressing MZ B cells are also diverted from entry into B cell follicles by overcoming response to the chemoattractant CXCL13 produced by follicular dendritic cells (FDCs)¹⁰⁵⁻¹⁰⁶. Therefore, owing to their selective expression of receptors and integrins, MZ B cells are positioned within the splenic MZ. Altogether, the development and function of MZ B cells are largely influenced by niche specific signals resulting in a distinctive B cell population essential for the protection from blood borne pathogens and the filtration of potentially inflammatory cellular debris.

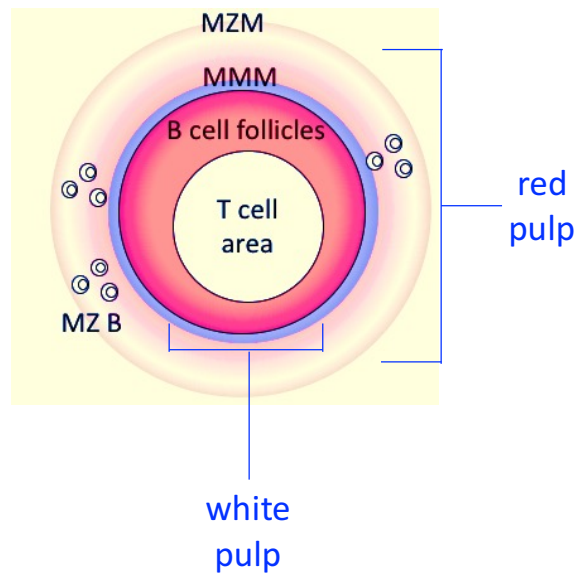


Figure 4 The splenic marginal zone. Immunofluorescent staining of a naïve mouse splenic section. Located at the interface of the lymphoid white pulp and the circulation the splenic marginal zone (MZ) is strategically positioned to filter cellular debris and pathogens from the blood.

Won et al. *J. Immunology* (2006)

DOI:<https://doi.org/10.4049/jimmunol.177.5.2749>

B cell differentiation: Bmem and ASCs

For B cells, there exists two different B cell effector fates upon activation: memory B cells (Bmem) and antibody-secreting cells (ASCs). ASCs are terminally differentiated B effectors that produce antibody. Whereas, Bmem are defined as antigen experienced, B cells that have returned to a quiescent state and may differentiate into ASCs upon reencounter with antigen. There is a well appreciated diversity in the cellular mechanisms driving B cell differentiation into ASCs or Bmem, thus, an overview of these processes will be provided.

B cell activation and CSR/SHM

Antigens can be transported passively through blood or lymph and, if of a small molecular size, diffuse through a reticular network within lymphoid tissues for delivery to dendritic cells (DCs) and B cells¹⁰⁷⁻¹⁰⁹. As for large molecules, DCs may shuttle antigen to B cell follicles to initiate early antibody responses¹¹⁰⁻¹¹¹. Furthermore, B cells may participate in

antigen capture and transport to load follicular DCs (FDCs) and prime CD4⁺ T cells^{88,112}. Therefore, it is very likely that B cells encounter antigen through many mechanisms *in vivo* and as such experience various cytokine and co-stimulatory signals to support BCR-induced activation.

Naïve B cells primarily express IgM/IgD¹¹³⁻¹¹⁷. Upon activation with antigen or toll-like receptor (TLR) ligands, B cells may undergo class switch recombination (CSR), which is a DNA recombination process that switches the immunoglobulin (Ig) constant region for a mostly cytokine directed-secondary Ig isotype or class¹¹³⁻¹¹⁷. Therefore, after CSR, the activated B cell will express either an IgG (subclasses are IgG1, IgG2b, IgG2a/c, or IgG3, in mice), IgA, or IgE Ig constant region on their surface rather than IgM/IgD¹¹³⁻¹¹⁷. Additionally, processes of somatic hypermutation (SHM) involves the introduction of point mutations within the variable region of Ig genes, thus augmenting the affinity for antigen¹¹⁶. Historically, it was thought that CSR and SHM predominately occurred in germinal centers (GCs) as both processes required activation-induced cytidine deaminase (AID), which is most highly expressed in the GC B cells¹¹⁷. However, very recently, it was shown that at least CSR occurs infrequently in GCs¹¹³. By enforcing synchronicity and tracking hen egg lysozyme (HEL)-specific B cells, it was shown that *Ighg1*-germline transcripts (GLTs) were most highly expressed just 2.5 days post immunization¹¹³. In this model, the peak of the GC response occurs at 5.5 days after immunization, suggesting that *Ighg1* GLTs could not have originated from the GC B cells¹¹³. Additionally, this observation is consistent with early extrafollicular responses producing class switched antibody. Thus, at least CSR is a process initiated very early after B cell activation, resulting in an altered Ig response most suitable to provide protection upon vaccination or infection.

While the molecular and cellular mechanisms of CSR and SHM have been thoroughly characterized, relatively few reports have addressed how affinity of the BCR influences B cell fate decisions. Nor have the contributions of inherit signaling differences between different Ig isotypes been adequately explored¹¹⁸. However, it has been shown that high affinity antigenic engagement preferentially biases B cells towards ASC differentiation whereas B cells expressing BCRs with weaker affinities for the antigen were primarily directed to germinal centers^{11,119}. Furthermore, it has been observed that over the course of immunization the affinity of serum antibody increases over time, suggesting that B cells bearing a BCR of high affinity are selected into the long-lived ASC pool¹²⁰⁻¹²². Therefore, BCR affinity may drive ASC

differentiation directly, independent of T cell help, or bias B cells towards participation in GCs.

T-independent (T-I) generation of Bmem and ASCs

T-I antigens are classified as type I or type II. Whereas type I T-I antigens are classified as mitogens and engage polyclonal receptors like TLRs, type II T-I antigens are typically highly repetitive structures like polysaccharides. Upon immunization with T-I antigen, rapid generation of Bmem and ASCs ensues.

T-I Bmem

Historically, it was thought that the Bmem compartment is generated from B cells activated by proteinaceous antigens and have received cognate CD4⁺ T cell help. These notions were based on the observations that many Bmem had undergone CSR and SHM¹²³. However, it has been shown that populations of Bmem can emerge independently from T cell help. Upon immunization with a type II T-I antigen, a quiescent, antigen specific B cell population persisted 120 days post immunization¹²⁴. Generated in the absence of T cells, this population resembled characteristic Bmem by secondary Ig expression and cell surface phenotype¹²⁴. Therefore, Bmem can be generated in the absence of T cell help, however the longevity of these cells is not entirely clear, though some suggest a lifespan of at least 60 days¹²⁵.

T-I ASCs

Mature B cells can give rise to two categorically distinct antibody-secreting cell (ASC) populations defined on the basis of lifespan: rapidly dividing, short-lived plasmablasts or long-lived plasma cells (LL-PCs)^{6,10,126,127}. It is often assumed that innate-like B cells may differentiate into extrafollicular, short-lived plasmablasts upon encounter with T-I antigens, whereas conventional FoB B cells give rise to LL-PCs in a T-D manner^{6,10,126,127}. However, lifespan of ASCs cannot be determined solely based on the putative precursor nor the quality of the immunizing antigen. Indeed, upon immunization with haptenated polysaccharide, a type I T-I antigen, antigen specific B cells differentiate into ASCs that migrated to the bone marrow, a long-lived niche, where the ASCs persisted for 150 days or longer after immunization¹²⁶. This observation was unchanged even in the absence of T cells¹²⁶. Furthermore, a polysaccharide vaccine, Pneumovax, confers long-lived humoral immunity to 23 pneumococcal bacterial subtypes for up to 10 years in humans, which persisted even after

splenectomy¹²⁷⁻¹²⁹. Therefore, it is prudent to also consider how lifelong humoral immunity is maintained. It has been proposed long-lived antibody is supported through the continual replenishment of short-lived plasma cells generated by persistent antigen activating Bmem¹²⁷⁻¹²⁹. Consequently, through the adoptive transfer of LL-PCs into syngeneic, naive recipients, it has been shown that antigen-specific antibody can be maintained in the absence of immunizing antigen¹³⁰. Therefore, T-I antibody responses have the capacity to be long-lived and can be maintained independently from immunizing antigen.

It is also often assumed that antibody arising from ASCs formed independently of T cell help are of low-affinity. Indeed, the very process, SHM, that can generate high affinity BCRs, takes place largely within in T cell-dependent GCs. Although, it has been shown that some germline encoded specificities are inherently of high affinity for particular antigens, thereby dispelling the notion that SHM is required to generate such a response¹³¹. More recently, it has been suggested that severe acute respiratory syndrome coronavirus 2 (SARS-CoV-2) can induce production of germline encoded receptor-binding domain (RBD)-specific antibodies capable of potent virus neutralization in at least some individuals¹³². Therefore, while SHM can certainly augment affinity for antigen, it is not required.

Regardless of whether an antibody is of high affinity or not, T-I antibody has proven beneficial in providing protection against infection. It has been shown in the absence of T cell help, influenza-specific antibody promotes the resolution of primary influenza infection¹³³. Additionally, B-1 B cells contribute to protection from influenza infection even before encounter with the virus through the generation of natural IgM^{134,135}. Furthermore, an expanded population of B-1 B cells have been shown to provide local IgM upon influenza infection¹³⁶. Therefore, ASCs arising independent of T cell help are protective through the production of naturally derived and antibody.

T-dependent (T-D) generation of Bmem and ASCs

Upon immunization with proteinaceous T-dependent antigen (T-D), highly transient and dynamic structures arise in the form of GCs. This well-orchestrated response requires the participation of CD4+ T cells and follicular dendritic cells (FDCs) to generate populations of Bmem and ASCs.

The Germinal Center

GCs were first described as distinct microanatomical regions of secondary lymphoid organs that contained dividing cells^{137,138}. As such, GCs were thought to be the site of developing lymphocytes, however it was later shown that GCs are induced upon immunization resulting in B cell expansion¹³⁸. As mentioned previously, GCs are the site of SHM, and therefore drive Darwinian-like selection of B cells that express high affinity BCRs¹³⁸. Affinity based selection and iterative rounds of SHM occur in disparate “zones,” which are clearly visible by conventional histology (Figure 5)^{139,140}. Whereas antigen loaded follicular dendritic cells (FDC) and CD4⁺ T follicular helper (Tfh) cells, are found in the light zone (LZ), highly proliferating B cells are located in the dark zone (DZ)¹³⁸. Thus, affinity-based selection occurs through B cells competing for antigen displayed on the surface of FDCs and interactions with Tfh cells.

The notion that affinity based selection occurs over the course of vaccination has been shown by very early experiments monitoring the dissociation rate of antibody/antigen conjugates over time¹³⁷. It is also recognized that limiting amounts of antigen promoted affinity whereas abundant antigen resulted in delayed affinity maturation^{138,141-143}. From this observation, it has been proposed that GC B cells of high affinity would “block” access to antigen depots, thus putting those of low affinity at a competitive disadvantage^{138,141-143}. Indeed, GC B cells of higher affinity acquire more antigen and expand^{144,145}. However, this model is not supported by more recent data as it appears that GC B cells do not form lasting interactions with FDCs^{146,147}. Furthermore, GCs are formed without functional FDCs altogether¹⁴¹⁻¹⁴³. Although, the lifespan of the antibody response was impaired, suggesting that interactions with FDCs may grant longevity to ASCs¹⁴¹⁻¹⁴³. Altogether, these observations underscore the importance of interactions with other cell subsets. While not required for the formation of the GC, engagement of GC B cells with FDCs can alter the quality of the humoral immune response.

An alternate limiting source for driving affinity maturation is help derived from the Tfh cells^{13,138}. It is thought that Tfh cells select high affinity B cells on the basis of peptide MHC (pMHC) displayed on their surface, where B cells of the highest affinity would proportionally present antigen¹⁴⁸. Therefore, only GC B cells with the highest affinity would be competitive for Tfh cell interactions^{138,148}. Indeed, Tfh cell derived signals determines the magnitude of GC B cell expansion, therefore influencing affinity based selection^{138,148,149}.

Clearly, Tfh cells provide help selectively to GC B cells of the highest affinity, but how do the Tfh cells support GC B cells? Crosslinking of CD40 on the surface of GC B cells promotes cell proliferation and slows the rate of apoptosis *in vitro*¹⁵⁰. Furthermore, blocking CD40 ligand (CD40L), expressed on Tfh cells, potently abrogates established GCs *in vivo*¹⁵¹. Additional support is provided by the Tfh cells through the secretion of the cytokine, IL-21, which promotes GC B cell proliferation and maintenance^{152,153,166}. Therefore, Tfh are indispensable in supporting affinity based selection, survival and proliferation.

Germinal centers may persist for one year, primarily due to the availability of antigen and T cell help^{154,155}. Given the prolonged lifespan of the GC, generation of Bmem and ASCs are separated by time, thus imparting different qualities to each respective population¹²⁵. GC-derived Bmem are thought to be of moderate affinity (higher than naïve B cells), whereas GC-derived ASCs are uniformly of high affinity¹⁵⁶. Since antigen specific antibody of varying affinities are generated throughout the course of immunization, an antibody-driven affinity based selection mechanism has been proposed¹⁵⁷. This notion of “antibody masking” would drive affinity based selection by blocking antigen on the surface of FDCs and may promote GC resolution¹⁵⁷. Therefore, the GC generates layered populations of Bmem and ASCs with varying affinities, the latter producing antibody which may then terminate the GC through blocking antigen displayed on the surface of FDCs.

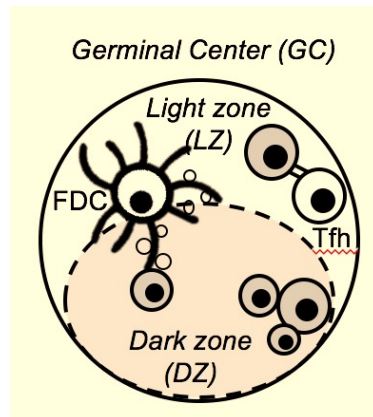


Figure 5 The germinal center. illustration depicted the organization of the germinal center (GC).

Light Zone (LZ)- the site of affinity-based selection and where follicular dendritic cells and T follicular helper cells reside. Dark Zone (DZ)- the site of clonal expansion and somatic hypermutation (SHM).

Victora et al. *Blood* (2012) DOI:10.1182/blood-2012-03-415380

T-D Bmem

While Bmem are thought to be generated before the onset of a robust GC response, some subsets emerge with delayed kinetics suggesting the dependency on T cell help¹²⁵. Certainly, class switched, IgG1⁺ Bmem arise after IgM⁺ Bmem exhibiting qualities of GC experience in the form SHM^{125,158,159}. Furthermore, Bmem are functionally classified on the basis of Ig isotype¹⁶⁰. Upon rechallenge, the IgM⁺ Bmem generate GCs, while the IgG⁺ Bmem differentiate into ASCs¹⁶⁰. This observation could suggest that class switched BCRs provide unique signals that promote ASC differentiation¹¹⁸. Alternatively, as IgG⁺ Bmem arise later through the course of immunization, they may experience signals deriving from T cell help^{125,161}. These additional T cell derived cues may poise IgG⁺ Bmem to rapidly differentiate into ASCs upon antigen reencounter¹⁶¹. Indeed, *Bcl6* deficient B cells generate Bmem that had significantly fewer SHMs, indicating that at least the affinity of the Bmem is dependent on T cell help¹⁶². Others have shown a subset of LZ GC B cells identifiable by the surface expression of CCR6, a chemokine receptor important for Bmem positioning, transcriptionally resembles the mature Bmem compartment^{163,164}. Therefore, Bmem are incredibly diverse in regards to origin and functionality and arguably represents the least understood B cell subset.

T-D ASCs

As mentioned previously, LL-PCs are uniformly of high affinity and it is thought that this very quality drives their differentiation^{11,122}. Indeed, it was shown that antigen specific B cells experiencing a range of affinities through antigen variants were biased towards ASC differentiation in the presence of high affinity interactions^{11,122}. Although, this observation did not determine whether this mechanism applied to GC B cells, only that high affinity interactions could direct ASC differentiation. Additionally, Bcl-2 overexpression in transgenic mouse models had an expansion of antigen specific cells suggesting that the stringency of selection had lessened¹⁶⁵. However, affinity-based selection appeared intact, as antibody arising later after immunization remained of high affinity. Therefore, it is thought that high affinity BCRs are a prerequisite for ASC differentiation.

Additionally, it is thought that ASCs arising from GCs are long-lived^{6,10,11,125,126,130}. Indeed, abrogation of GCs through loss of T cell help, FDCs, or key transcriptional regulators

of the GC B cell program coincides with waning antigen specific antibody titers^{142,166-168}. Most notably, in the absence of CD40 or MHCII, influenza specific IgG antibody returns to baseline, naïve titers 100 days post infection, whereas no remarkable difference in early influenza specific antibody is observed¹⁶⁸. This suggests that CD4⁺ T cell help is required to generate durable antibody responses after influenza infection¹⁶⁸. Furthermore, it has been shown that antibody generated in the absence of T cell derived signals are remarkably reduced in affinity^{138,169}. It could be argued that durable antibody requires the sum of all ASCs over time, regardless of the quality of affinity or dependency of T cell help. However, adoptive transfer of ASCs into naïve, syngeneic recipients would suggest otherwise^{27,130}. Additionally, it has been well appreciated that maintenance of LL-PCs requires contributions of the cytokines BAFF, APRIL, and IL-6¹⁷⁰⁻¹⁷³. Are there other factors selectively required for LL-ASCs? It remains to be seen how polarizing, infection induced cytokine may influence the differentiation or lifespan of ASCs. Therefore, while much is known about the initial selection of ASCs very little is known about selective requirements that grant ASCs longevity.

Transcriptional Regulation of Bmem and ASCs

The generation of ASCs from activated B cell precursors requires the repression of B cell identity genes with coordinated activation of a unique ASC-specific program¹⁰. The primary function of this program is to achieve high rate antibody production while maintaining the integrity of the cell. This balance is principally driven by key transcriptional regulators IRF4, Blimp-1, and XBP-1¹⁰. As a titratable transcription factor, the expression of IRF4 dictates function¹⁷⁴. Activated B cells require low expression of IRF4 for CSR and GC formation, whereas high expression of IRF4 can activate *Prdm1*, the gene encoding for Blimp-1¹⁷⁴⁻¹⁷⁶. Once Blimp-1 is expressed, Blimp-1 may act as a transcriptional repressor of key B cell identity genes like *Pax5* and *Spib*^{177,178}. Although Blimp-1 is thought to be required for the generation of ASCs, some populations of ASCs appear to form independently of this key transcriptional regulator^{179,180}. Indeed, Blimp-1 is dispensable for IgG3-secreting B-1 B cells¹⁸⁰. Thus, while a Blimp-1-dependent program is characteristic of most ASCs, there exists some unique B cell lineages that utilize unconventional mechanisms for antibody production.

Along with the transcriptional rewiring required by ASCs, it is equally important for ASCs to manage the immense endoplasmic reticulum (ER) stress due to high rate antibody production. One critical transcription factor, XBP-1, has been shown to be required for late

stage ASC development¹⁸¹. Indeed, B cells deficient in *Xbp1* are capable of expressing CD138, a defining cell surface phenotype of most ASCs¹⁸¹. Additionally, *Irf4* and *Prdm1* transcript level expression is unchanged, suggesting that *Xbp1* is dispensable for the initiation of ASC differentiation¹⁸¹. Furthermore, characteristic morphological changes associated with ER remodeling are not observed in B cells lacking *Xbp1*¹⁸¹. This result correlates with a remarkable reduction of antibody production in the absence of *Xbp1*¹⁸¹. Therefore, in addition to the regulation of distinguishing transcription factors and phenotypes, ASCs require significant ER remodeling to support their most significant function.

Very little is known about the transcriptional regulation of the quiescent, relatively low affinity population of Bmem. It is thought that low affinity GC B cells undergo apoptosis because they are rendered competitively unfit, which further supports the notion that many Bmem are generated independent of T cell help^{138,159,160}. Although, more recently, low affinity populations of LZ GC B cells have been shown to represent a “PreBmem” pool¹⁸². PreBmem expressed higher amounts of the transcriptional repressor, *Bach2*, which is required for CSR and SHM, and reduction of *Bach2* expression resulted in fewer Bmem¹⁸². Although, it could be argued that GC B cells were not effectively generated, therefore it only be concluded that *Bach2* is required for T-I Bmem. Furthermore, the anti-apoptotic transcription factor, Bcl-2, has been shown to promote generation of Bmem. Indeed, constitutive expression of *Bcl2* resulted in a larger Bmem pool¹⁶⁵. Until very recently only factors promoting the generation of Bmem through antagonizing the effects of apoptosis had been described. Hhex is shown to be a critical driver of Bmem through the repression of a key GC B cell identity transcription factor, Bcl-6¹⁸³. Thus, the transcriptional regulation of Bmem, while still very unclear, requires the coordinated activation of anti-apoptotic factors with the repression of other activated B cell programs.

Signals 1, 2, and 3: For B cell development and differentiation

The above review focused on the stages of B cell development, activation, and differentiation. The following will discuss the signals responsible for those processes. Thus, BCR signaling, co-stimulation, and cytokine, often referred to as signals 1,2, and 3, respectively, will be reviewed.

Signal 1: BCR

Selection- B cell development

During formative, transitional developmental stages, BCR signaling in response to self-antigens underlies negative and positive selection events that determine which B cells expressing a unique Ig rearrangement, or clone, form the mature B cell repertoire. It is often thought that these secondary selection mechanisms establish peripheral tolerance, eliminating or inactivating potentially pathogenic, autoreactive B cells while sparing non-autoreactive B cells, thereby generating an innocuous mature B cell repertoire⁴⁰.

However, in the production of the mature B cell repertoire a balance between activation and tolerance must be achieved or else immunity could not be established. Therefore, an alternative view is that all mature peripheral B cell subsets, follicular (FoB), marginal zone (MZ), and B-1 B cells, have some autoreactivity⁴⁰. Indeed, continued BCR signaling is required for mature B cell survival⁴¹. Therefore, it is likely that these selection mechanisms function on the basis of a signaling threshold, only eliminating cells bearing a BCR that respond “too strongly” to self-antigens^{40,42}. Thus, in addition to antigenic based selection, response to BCR ligation must be appropriately tuned for developmental progression^{40,42,43-45}. Indeed, MZ B cells have been shown to require weak BCR signals⁴³, whereas FoB and B-1 B cells favor stronger BCR signals for their development⁴³⁻⁴⁵. Accordingly, there are different positive and negative selection signals involved in the generation of various mature B cell compartments⁴⁶. Thus, a brief overview of positive and negative peripheral selection as well as BCR signaling mechanisms will be provided.

Clonal Positive Selection

In contrast to the strong evidence supporting positive selection of T cells in the thymus, it is currently not known whether a defined ligand is required for BCR dependent positive selection⁴⁷. It is well appreciated that persistent BCR signaling provides some positive signal that allows mature B cells to survive⁴¹. Indeed, mature B cells are lost upon conditional deletion of surface IgM (sIgM)⁴¹. Furthermore, mouse models that have compromised BCR signaling have fewer mature B cells^{43,44,48-50}. Therefore, the existence of natural, *in vivo* self or commensal ligands that continue to provide BCR stimulation have been proposed for all mature B cells⁴⁸⁻⁵⁰.

Although, innate-like B cell subsets are thought to experience stronger peripheral antigenic selective pressures. An example of this is a functional germline encoded IgH gene, V_H81X, that is reactive towards intracytoplasmic antigens^{51,52}. V_H81X-bearing B cells are preferentially selected into the MZ B cell pool^{51,52}. Other examples are the V_HS107.1-expressing B cells, or T15⁺ B cell clonotypes, which confer protection against *Streptococcus pneumoniae* through the recognition of phosphorylcholine (PC)^{53,54}. While PC is ubiquitously expressed amongst altered self and microbial antigens, T15⁺ B cell clonotypes are expanded in mice raised in specific pathogen free conditions⁵³⁻⁵⁵. Therefore, it is proposed that T15⁺ B cell clonotypes are selected by autoantigens⁵³. These autoreactive specificities dominate in neonatal life and are preferentially selected into B-1 B cell pools^{51,52,56,57}. Thus, there are some well-characterized specificities enriching in the innate-like B cell subsets that constitute a significant portion of the natural, preimmune repertoire.

Clonal Negative Selection

The mechanism of central tolerance is often incomplete and potentially pathogenic, self-reactive B cells may emerge into peripheral lymphoid tissues. Therefore, secondary, peripheral tolerance mechanisms eliminate or functionally silence autoreactive B cells^{31,40,42,58-60}.

Studies of “double-transgenic” mice expressing neo-self antigen, hen egg lysozyme (HEL), and B cells bearing an Ig-transgene encoding for high affinity anti-lysozyme antibody demonstrates the mechanisms of peripheral tolerance^{31,40,59}. In the presence of soluble HEL, Ig-transgenic B cells do not undergo clonal deletion in the bone marrow and are in normal numbers in the periphery, although are competitively excluded from B cell follicles by non-transgenic B cells^{31,40,42,59,60}. While B cell development seemed intact, Ig-transgenic B cells display reduced sIgM expression and are unable to produce anti-lysozyme antibody, thus are considered functionally unresponsive or anergic^{31,40,59}. Reduced sIgM could be a mechanism of tolerance induction through counteracting persistent antigenic stimulation^{59,60}. Alternatively, IgM^{hi} B cells could be deleted, allowing for expansion of an IgM^{low} B cell population⁵⁹. The precise role for the change in sIgM expression, whether cause or effect, in functionally inactivating autoreactive B cells remains to be seen. Thus, the autoreactive B cells that escape clonal deletion in the bone marrow are rendered functionally inactive in the periphery^{31,59,60}.

BCR signaling threshold-mediated selection

In addition to clonal selection, perhaps equally important is the different BCR signaling thresholds required by distinct populations of B cells for their development⁴⁴. Studies of transgenic mouse models that overexpress positive regulators of BCR signaling, such as *Cd19* and *Btk*, showed an enrichment of B-1 B cells⁶¹. Similarly, mice deficient in negative regulators of BCR signaling, such as SHP-1 (encoded by the gene *Ptprn6*), also have an expanded B-1 B cell compartment and fewer MZ B cells^{43,61}. However these mice also exhibit an overall severe B cell immunodeficiency suggesting that BCR signaling was “too strong” for most mature B cells⁶¹. Through these studies an optimal BCR signaling threshold has been suggested, although an exact threshold is difficult to ascertain as there are contributions of BCR specificity and avidity to also consider.

Additional studies have suggested a BCR signaling threshold independently of BCR specificity⁴⁴. This was shown through the generation of BCR-deficient mice expressing different amounts of the Epstein-Barr virus (EBV) protein LMP2A (BCR^{neg}LMP2A⁺ mice). LMP2A is able to mimic some aspects of BCR signaling and, therefore, support B cell survival⁴⁴. In this study, weak constitutive signaling through LMP2A in BCR deficient mice favored FoB cell and MZ B cell development while an increased expression of LMP2A generated mostly B-1 B cells⁴⁴. However, other studies show that FoB cells require relatively strong BCR signaling through activation of BTK, though BTK is also required for clonal MZ B cell survival and accumulation^{47,62,63}. Thus, a BCR signaling continuum, or “Goldilocks hypothesis” is proposed^{40,43,58}. B-1 and FoB B cells favor relatively strong BCR signals, whereas MZ B cells require relatively weak BCR signals^{44,62,63}.

Altered selection driving development of autoimmunity

Despite the rigorous tolerance mechanisms that aim to give rise to a diverse yet innocuous repertoire, pathogenic, self-reactive B cells may breach those selection mechanisms leading to the development of autoimmunity^{40,42,43,48,49,58}. As mentioned above, the combinatorial rearrangement process that generates the nascent Ig receptor produces a vast B cell repertoire potentially capable of recognizing 10¹⁶ antigenic determinants⁹. However, as the mature B cell repertoire is limited by the absolute number of B cells occupying the periphery, only a fraction of the potential repertoire can be present at any given time⁴⁰. Thus,

a model of intraclonal competition (Figure 6) has been proposed for the generation of the ‘fittest’ and ‘safest’ mature B cell repertoire.

This model may be illustrated by phenotypes observed in mice with altered components of BCR signaling. For example, mice deficient in *Ptprc*, the gene encoding for CD45 and positive regulator of BCR signaling, have fewer mature B cells when bearing a restricted Ig receptor^{40,41,64,65}. However, in the presence of selecting autoantigen mature B cells accumulated in periphery suggesting that loss of activating BCR signals may result in the retention of autoreactive specificities instead of elimination^{40,41,64,65}. Thus, autoreactive B cells may be allowed to expand and survive in the absence of other B cells.

In contrast, loss in negative BCR signaling molecules may lead to B cell immunodeficiency by promoting excessive B cell elimination. As described above, absence of *Ptgn6*, or SHP-1, results in BCR signals that are “too strong” and a severe B cell immunodeficiency ensues^{40,43,60}. This, in turn, may drive autoimmunity by permitting a greater frequency of autoreactive B cells to persist in the periphery due to absence of other competing B cells^{40,43,60}. Additionally, strongly autoreactive B cells may become competitively fit in response to “accessory” pro-survival factors, such as BAFF, or toll-like receptor (TLR) signaling^{59,66-68}. Indeed, B cells rendered anergic may be redeemed through activation with TLR ligation and sufficient BAFF^{59,66-68}. Therefore, a strict BCR signaling threshold promotes the retention of the most competitively fit B cells.

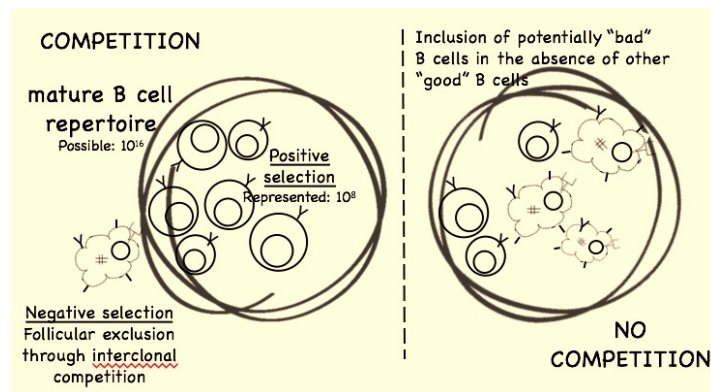


Figure 6 Model of interclonal competition. Ig rearrangement generates a repertoire capable of recognizing up to 10^{16} antigenic determinants, however only 10^8 B cell clones can be represented in the periphery. Self-reactive B cells that signal “too strongly” are excluded from B cell follicles to prevent the formation of autoantibody.

Signaling: The good

Upon antigen engagement and cross-linking of the membrane-bound BCR, Src family kinases, like Lyn, and the spleen tyrosine kinase (Syk) regulate a cascade of phosphorylation events that initiate BCR signaling¹⁸⁴⁻¹⁸⁶. These early phosphorylation events result in the assembly of intracellular proteins, phospholipase C- γ 2 (PLC- γ 2), Vav, Bruton tyrosine kinase (Btk), Phosphoinositide 3-kinase (PI3K), and the adaptor protein B-cell linker (BLNK) to form a multicomponent complex known as the signalosome¹⁸⁴⁻¹⁸⁶. Coordinated activity of the signalosome results in the production of secondary messengers, diacylglycerol (DAG) and inositol-1,4,5-triphosphate (IP3), which initiates calcium influx¹⁸⁴⁻¹⁸⁶. Subsequently, calcium signals differentially activate transcriptional regulators of the NF- κ B, MAPK and NFAT pathways¹⁸⁴⁻¹⁸⁶, thereby promoting proliferation, survival, and differentiation.

Strict negative regulation of BCR signaling is also required to prevent inappropriate B cell activation. Some transmembrane receptors are potent negative regulators of BCR activation, such as Fc γ RIIb, CD5, CD72, and CD22¹⁸⁷⁻¹⁸⁹. Signaling through those receptors recruits inhibitory proteins, SHIP, SHP-1, and Lyn, which inactivate BCR signaling through dephosphorylation of BCR activating kinases¹⁹¹⁻¹⁹². Thus, the engagement of BCR, and subsequent signal transduction, is an elegantly balanced signaling cascade that equilibrates activation with inhibition appropriately tuning B cell development and differentiation.

In addition to the immediate signaling cascade, it is well appreciated that IRF family members are influenced by antigen receptor signaling¹⁷⁴⁻¹⁷⁶. Through the immunization of HEL variants with differing affinity for BCR, it is shown that high affinity interactions are a correlate of high IRF4 induction and, thus, ASC differentiation *in vivo*¹⁷⁵. While less is known about the expression of other IRF family members in response to antigen receptor signaling, it was shown that IRF1 is required for the positive selection of developing CD8⁺ T cells, and in the absence of IRF1, TCR-mediated signal transduction is impaired¹⁹³. Thus, it is conceivable that IRF1, like IRF4, could direct B cell maturation and differentiation in response to antigenic stimulation.

Signaling: The bad

As discussed previously, the interplay of positive and negative selection generates a B cell repertoire that is capable of providing immunity while maintaining tolerance^{40,58,68}.

Continued “weak” BCR signaling, presumably through engagement of self-antigen, provides some positive signal that allows mature B cells to survive⁴¹. However, should the engagement of self-antigen surpass a BCR signaling threshold, the potentially autoreactive B cell is eliminated through clonal deletion or the induction of anergy^{31-34,40,42}. Therefore, BCR signaling of an “intermediate” signaling strength promotes the positive selection of innocuous, yet protective B cells^{31-34,40,42,68}.

Alterations to components of BCR signaling are associated with the development of autoimmune manifestations. B cells deficient in the Src family kinase, *Lyn*, have enhanced BCR signaling determined by augmented calcium influx and increased activation of the MAPK pathway^{184,194-196}. Consequently, mice with a B cell-specific deletion in *Lyn* have fewer B cells. However, despite this B cell immunodeficiency, these mice develop high amounts of pathogenic, class-switched autoantibodies with age¹⁹⁷. Similarly, mice that overexpress an activator of BCR signaling, *Btk*, display symptoms of systemic lupus erythematosus (SLE)-like disease, characterized by chronic inflammation, spontaneous GC formation, and production of autoantibody^{198,199}. Conversely, X-linked agammaglobulinemia (XLA) is a disease caused by deleterious mutations in the *BTK* gene and these patients present with a near loss of all mature B cells^{200,201}. While XLA patients typically do not develop autoimmune disease, it has been reported the few remaining B cells bear autoreactive specificities²⁰¹. Therefore, alterations in BCR signaling often results in the development of autoimmune manifestations that is characterized by the expansion of activated B cells and the generation of autoantibodies.

Although not yet well understood, protein tyrosine phosphatase nonreceptor 22 (PTPN22) is thought to be a negative regulator of BCR signaling⁶⁸. Single nucleotide polymorphisms in the gene, *PTPN22* (C1858T; R620W), are associated with SLE, rheumatoid arthritis (RA), and type 1 diabetes (T1D)^{68,202-205}. In accordance with alterations in BCR signaling, individuals carrying the autoimmune-associated variants of *PTPN22* have expanded populations of circulating transitional and anergic B cells^{68,206,207}. Furthermore, studies of mice carrying a mutation in *Ptpn22* (analogous to the human *PTPN22*^{C1858T} variant) have enhanced BCR signaling, expanded populations of immature B cells, and an increased proportion of FoB cells to MZ B cells²⁰⁸. These results support a model where the risk variant enhances BCR signaling, thereby promoting the selection of autoreactive specificities into the FoB cell compartment. However, in opposition to that model, it has also been proposed that *Ptpn22* is completely dispensable for BCR signaling²⁰⁹. Indeed, PTPN22 is predominantly expressed

in T cells^{209,210}. Furthermore, no significant difference in BCR signaling is observed in the absence of *Ptpn22*²¹⁰. Although, while informative, these reports only evaluate BCR signaling in all mature B cells. Therefore, given the inherent heterogeneity within a pool of all mature B cells, it cannot be determined whether *Ptpn22* is dispensable for every categorically distinct population of B cells. Thus, the role of PTPN22 in BCR signaling remains very much unclear.

Signal 2: Co-stimulation: Cellular interaction and TLR ligands

Co-stimulation is typically thought of as interactions formed between 2 cells through cell surface receptor/ligand pairs²¹¹. However, this definition could include any signal that supports antigen-induced activation. While antigen receptor signaling is critical for the activation of B and T cells, it is insufficient to maintain proliferation and drive differentiation²¹¹. Therefore, a brief description of co-stimulation will be provided.

Co-stimulatory signals to CD40-expressing B cells are provided by CD40 ligand (CD40L)-expressing CD4⁺ T cells²¹¹. Early studies showed that by stimulating B cells with agonistic anti-CD40 antibodies plus BCR stimulation induces robust B cell proliferation and CSR²¹². This result suggests that B cells benefit from direct T cell contact²¹². Furthermore, additional CD40 signaling promoted survival in *ex vivo* human GC B cells²¹³. Other molecules abundantly expressed by T cells are equally as important for the generation of class switched antibody²¹¹. In the absence of CD28 on T cells, or its respective receptors CD80/CD86 on B cells and antigen presenting cells (APCs), vesicular stomatitis virus (VSV)-infected mice failed to efficiently mount a class switched antigen specific IgG1 or IgG2a²¹⁴. Additional studies have shown impaired GC formation and altered CSR in the absence of *Icos*, a co-stimulatory molecule abundantly expressed on T cells, and *Icoslg*, the respective ICOS ligand predominantly expressed on B cells and APCs^{215,216}. Therefore, through the interaction of ligand/receptor pairs, T cells can support B cell activation and antibody production.

Other co-stimulatory signals that inform and alter B cell development and differentiation are wholly independent of cellular interactions. B cells express toll like receptors (TLRs) that can recognize components of bacteria and viruses, such lipopolysaccharide (LPS, TLR4), single-stranded RNA (ssRNA, TLR9), and CpG-containing DNA (TLR9)²¹⁷. TLRs signal through adaptor proteins MyD88 and TRIF²¹⁷. While it is typically thought that TLR signaling is largely dispensable for B cell development, there is some evidence to support otherwise. B cells stimulated with CpGs (TLR9 ligands) become

more responsive to the pro-survival factor, BAFF, which is essential for the development of mature B cells^{98,218-220}. Furthermore, it has been proposed that engagement of BCR and TLR promotes the positive selection of developing B cells by overcoming pro-apoptosis factors induced by BCR signaling^{68,221,222}. Therefore, while not required, TLR signaling can certainly support B cell development.

It has been shown *Myd88* and *Ticam1* (the gene encoding for TRIF), are mostly dispensable for mounting antigen-specific antibody in response to T-I and T-D immunizing antigen⁹⁸. Although, upon challenge of *Streptococcus pneumoniae* or influenza, B cell intrinsic *Myd88* is indispensable for eliciting a robust antigen specific IgG2a response^{223,224}. Additionally, in the absence of *Myd88* and *Ticam1* there is a significant reduction in total IgG3 antibody in the preimmune sera of these mice⁹⁸. Since innate-like B cell subsets are the primary producers of natural IgG3 antibodies, this result suggests B-1 and MZ B cells may be impaired by the inability to sense microbial or self-components⁵⁴. Thus, the contributions of TLR in B cell biology remains unclear and requires further study in the context of homeostasis and infectious disease.

The signaling through co-stimulatory molecules principally activates NF- κ B, MAPK, STAT and IRF families of transcription factors^{225,226}. Notably, TLR signaling appears to require IRF family members for the expression of type I interferon (IFN)^{225,226}. Indeed, it has been shown that pDCs depend on *Myd88* to activate IRF7 which is required for the production of IFN α/β ²²⁷. Interestingly, type I IFN production is independent of TLR-driven IRF7 and IRF3 activity in myeloid DCs (mDCs) and instead requires IRF1²²⁸. This result is unexpected, as IRF1 is thought to be induced by IFN- γ . Thus, this study suggested an IRF1-dependent link between TLR and IFN- γ , where IFN- γ enhances TLR signaling. Indeed, dual TLR and IFN- γ R signaling augments the production of IFN β , IL12-p35, and iNOS in an IRF1-dependent fashion²²⁹. While well described in myeloid derived lineages, the role of TLR-induced IRF family members in B cell development or differentiation remains relatively unexplored.

Signal 3: Cytokine

Cytokines are secreted pleiotropic effector molecules that mediate the communication between cells²³⁰. Acting through cell surface receptors, cytokines are known to influence the development, activation, and differentiation of a broad range of cells²³⁰. Therefore, the effects

of cytokines on B cells with a focus on IFN- γ will be discussed. However, since relatively little is known about the mechanisms of IFN- γ -inducible transcription factors (TFs) in B cells, IFN- γ -inducible TFs in CD4⁺ T cells will also be reviewed.

The bare essentials

It is well appreciated that IL-7 is indispensable for B and T cell lymphopoiesis^{230,231,232}. Although IL-7 is not required for the earliest stages of B cell development, Fraction A in the bone marrow, it is essential for the expansion of late pro- and pre- B cells, Fractions B and C, respectively^{28-30,231,232}. As IL-7 is required for B cell development progression, mature B cells are markedly lost in its absence^{28-30,231,232}. Peripheral, transitional B cells are vulnerable to apoptosis and are dependent on the pro-survival cytokine, BAFF^{67,219,221}. It has been proposed that BAFF signaling overcomes the pro-apoptotic effects of BCR engagement at this developmental stage^{67,68,219,221}. Furthermore, in response to elevated BAFF mice develop autoantibodies⁶⁸. Thus, BAFF may be strictly regulated to maintain B cell survival without triggering autoimmunity⁶⁸. Therefore, IL-7 and BAFF are essential for B cell development and survival.

As discussed previously, T follicular helper (T_{fh}) cells support B cell differentiation by providing co-stimulation and IL-21^{13,138,166}. Indeed, mice deficient in *Il21r* are unable to produce antigen specific IgG1, IgG2b, and IgG3 in response to T-D immunization¹⁶⁶. Although, it appears that *Il21r* is dispensable for the generation for antigen-specific Bmem¹⁶⁶. Additionally, it has been well appreciated that maintenance of LL-ASCs requires the contributions of the cytokines BAFF, APRIL, and IL-6^{170,172}. Therefore, while BAFF, APRIL, IL-6, and IL-21 are required for ASC responses, relatively little is known about the contribution of cytokine to Bmem^{166,170,172}.

Largely ascribed to roles in CSR, other cytokines are known to influence the activation and recruitment of B cells. However, these will not be discussed at length here. Instead the following table will offer a brief overview of some functions of these other cytokines:

TABLE 1: Description of cytokines in B cell biology.

Cytokine	Function	Reference
IL-1 α/β	enhancement of T-D antibody production; Antigen presentation.	233,234
IL-2	B cell survival; ASC differentiation.	234,235
IL-4	IgG1 and IgE CSR/production; supports IgA production; IL-4 production; repression of alternate B cell fates; GC B cell support; B cell proliferation	235-242
IL-10	ASC differentiation; regulatory functions	243,244
IL-12/IL-18	supports B effector 1 function	238,245
IL-17	supports IgA CSR; migration by CCR6; B cell mucosal immunity	246-248
IFN α/β	Transitional B cell survival/autoimmunity; enhancement of BCR signaling.	68,249
TGF- β	IgA and IgG2b CSR	250,251

IFN- γ and IFN- γ -induced transcriptional regulation

Respiratory epithelial cells are the primary targets for influenza virus³⁵². After influenza infection, inflammatory cytokines, IL-1 and type I and II interferon (IFN) drives the recruitment of innate and adaptive immune cells to the lung²⁵². Type II IFN, IFN- γ , is produced by NK cells and T cells and is required to promote viral clearance and reduce viral burden^{253,254}. IFN- γ , binds to a receptor that is composed of two subunits, IFNGR1 and IFNGR2²⁵⁵. Each subunit, IFNGR1 and IFNGR2 interacts with an intracellular Janus activated kinase, JAK1 and JAK2, respectively^{256,257}. Activation of JAK1 and JAK2 results in phosphorylation of signal transducer and activator of transcription 1, STAT1^{256,257}. STAT1

homodimers translocate to the nucleus to drive the transcription of *Irf1*, *Tbx21* (gene encoding for T-bet), and other interferon stimulated genes (ISGs)²⁵⁵. Therefore, IFN- γ is induced upon viral infection and promotes transcription of *Irf1*, *Tbx21*, and ISGs.

T-bet *CD4⁺ T cells*

CD4⁺ helper T cells differentiate into distinct lineages upon pathogen-specific priming, and as a result, produce polarizing cytokines to effectively respond to a variety of infections²⁵⁸. In response to IL-12 and/or IFN- γ , CD4⁺ T cells will activate Th1 cell specific genes while opposing genes of alternative CD4⁺T helper cell fates²⁵⁸⁻²⁶⁰. Upon activation with IL-12 and/or IFN- γ , CD4⁺ T cells will express T-bet, a principle TF for Th1 cell fate commitment²⁵⁹. Indeed, T-bet is required to activate *Ifng*, which in turn establishes a feed-forward reinforcement of the Th1 cell program²⁵⁸⁻²⁶³. Additionally, given optimal T cell receptor (TCR) activation, full Th1 cell generation is achieved through an IFN- γ -autocrine mechanism, and blocking IFN- γ results in fewer IFN- γ -producing Th1 effectors²⁶³. However, upon suboptimal TCR stimulation, both IL-12 and IFN- γ are required for the generation of Th1 cells, where IL-12 enhances production of IFN- γ ²⁶³. Therefore, it is thought that the extent of dependency of either IL-12 or IFN- γ may rely on TCR signaling strength²⁶³. Altogether, T-bet will activate lineage specific genes to establish an IFN- γ -driven Th1 cell program.

Along with activation of Th1 cell specific programs, T-bet has been shown to be a potent repressor of alternative CD4⁺ T helper cell fates^{259,260}. Certainly, T-bet cooperates with Runx3 to silence IL-4, the signature cytokine of the Th2 cell²⁶⁰. Furthermore, T-bet has been shown to physically interact with and redirect Bcl-6, thus obstructing Tfh cell commitment²⁶⁴. More recently, T-bet has been shown to repress an inflammatory type I IFN gene program in response to IFN- γ ²⁶⁵. Thus, it appears that T-bet functions to activate Th1 lineage genes, while simultaneously blocking alternative CD4⁺T helper cell fates and functions.

B cells

Relatively little is known about IFN- γ and T-bet directing B cell fate decisions. Early studies identified that T-bet is required to direct class switch to IgG2a in response to IFN- γ ^{21,269}. This would remain the primary role of T-bet in B cells, although others find that a

population of T-bet⁺B cells are generated after mice are infected with an intracellular bacterial pathogen, *Ehrlichia muris*²⁶⁶. Interestingly, these T-bet⁺ B cells are described as a subset of T cell-dependent (T-D) IgM⁺Bmem responsible for the production of antigen-specific IgG upon rechallenge²⁶⁶⁻²⁶⁸. T-bet⁺ B cells are also required for the development of antigen-specific antibody following chronic viral infections, lymphocytic choriomeningitis virus (LCMV) and murine gamma-herpesvirus 68 (MHV-68)^{15,16,266,267}. Additionally, T-bet expressing B cells are consistently observed in the enlarged spleens of aged mice and in murine models of autoimmune diseases³²⁷. These “age-associated” B cells exhibit a profound proliferative response to TLR7 and TLR9 agonists and are refractory to BCR ligation³²⁷. Those distinctive functional features distinguish this subset from other mature B cell subsets³²⁷. These findings from murine mouse models have been extended to human studies. Indeed, T-bet expressing B cells with enhanced responsiveness to TLR7 agonists have been associated with the development of autoreactive, naïve PC precursors in systemic lupus erythematosus (SLE) patients³²⁶. However, these studies only evaluated antibody responses during persistent antigen stimulation and inflammation. Furthermore, the conclusions of those studies largely focused on the production of IgG2a rather than how T-bet may direct the differentiation of Bmem or ASCs.

Similar to T cells, B cells can produce IFN- γ in response to IL-12/IL-18 *in vitro*²⁴⁵. B cells also secrete IFN- γ when activated with antigen and cognate, IFN- γ -producing Th1 cells (B effector 1, Be1 cells)^{238,245}. Interestingly, IFN- γ production by Be1 cells is dependent on *Ifngr1* and *Tbx21*, but can occur in the absence of *Stat1*²⁴⁵. Furthermore, production of IFN- γ by Be1 cells is required to maintain the transcription of *Ifng*²⁴⁵. This suggests, like T cells, B cells may depend on the feed-forward reinforcement of the B effector program. While relatively little is known about how T-bet regulates B effectors, even less is known about how T-bet may promote ASC differentiation. It has been shown that Be1 cells produced more antibody when compared to B cells activated in the presence of antigen and IL-4-producing Th2 cells (B effector 2, Be2, cells)²³⁸. Therefore, the exact mechanism of how T-bet directs ASC fate commitment remains an open question.

IRF1
CD4⁺ T cells

It is observed IRF1 deficient mice are susceptible to intracellular bacterial pathogens, *Listeria monocytogenes* and *Leishmania major* infection^{270,271}. These early experiments suggest that susceptibility to at least *Listeria monocytogenes* is due to a defect in the generation of Th1-mediated immunity²⁷¹. Indeed, CD4⁺ T cells exhibit a refractory response to IL-12 in that a small, but significant amount of IL-4 is produced instead of IFN- γ ^{271,272}. Thus, it appears that Th1 cell differentiation is compromised in the absence of *Irf1*. Subsequently, it has been shown that IRF1 directly activates transcription of *Ii12b1* through binding to an interferon-stimulated response element (ISRE) consensus sequence within the promoter region of *Ii12b1*²⁷². This observation suggests that IRF1 is required for the IL-12/IFN- γ feedback mechanism that is essential for the establishment of the Th1 cell program. Therefore, similar to T-bet, IRF1 promotes Th1 cell commitment through the activation of lineage specifying genes. Additionally, IRF1 appears to repress some aspects of Th2-directed immunity^{270,271}. In the absence of *Irf1*, mice exhibit elevated production of Th2-signature cytokines, IL-4 and IL-5, and are resistant to the nematode infection, *Nippostrongylus brasiliensis*^{270,271}. Furthermore, IRF1 binds to 3 distinct regulatory elements in the *Ii4* gene which correlates with reduced *Ii4* expression in CD4⁺ T cells²⁷³. Thus, IRF1 activates Th1 lineage specifying genes while directly opposing alternative T cell fates.

B cells

It is relatively unknown whether IRF1 participates in B cell fate decisions. The development of mature B cells appears to be intact in *Irf1* deficient mice²⁵. Although, it is also proposed that IRF1 may contribute to the termination of proliferation in developing B cells²⁷⁴. Relatively recently, it has been shown that GC B cells require *Irf1* following MHV-68 infection²⁴. However, it appears *Irf1* is dispensable for the generation of long lived, antigen specific antibody²⁴. Interestingly, it is proposed that IRF1 may activate a negative regulator of BCR signaling, SHP1²⁴. Although, how IRF1 regulates SHP1 activity remains an open question²⁴. This study, while informative, only thoroughly evaluated *Irf1* expressing B cells during the first 42 days following chronic viral infection²⁴. Therefore, it cannot be determined whether IRF1 is required for the development of long-lived antibody responses from this study. Thus, the role of IRF1 in B cell biology has not been adequately addressed.

Summary

Fungi, bacteria, viruses, and self-antigens all have the potential to incite an immune response. In health, we are granted immunity from infection while maintaining tolerance, otherwise we succumb to disease. How is protection from disease achieved? Certainly, antibody is one essential component underlying protection and pathology. Some decades ago two concepts revolutionized our understanding of the generation of antibody: 1) antigen must interact with respective membrane bound antigen receptor and 2) the consequences of that interaction involve clonal expansion and differentiation²⁷⁵. While these concepts emerged many years ago, we have yet to fully understand the mechanistic basis for the development of the cells that secrete antibody. As described above, what we do know has been limited to simplistic immunization models with particular focus on BCR signaling and co-stimulation with relatively little understanding of the contribution of cytokines to the process. Therefore, in order to develop efficacious vaccines, it will be absolutely essential to recognize how infection induced cytokine would promote protective antibody responses upon encounter with pathogen.

Herein, we describe the role of two IFN- γ -inducible transcription factors, T-bet and IRF1, in driving ASC differentiation. We find that T-bet, unlike other ASC specifying transcription factors, promotes ASC differentiation through extinguishing an IFN γ -induced pro-inflammatory program which is incompatible with completion of terminal ASC differentiation *in vitro*. In contrast, IRF1 is required for dampening BCR signaling thus supporting development of an innate-like ASC precursor. Both, T-bet and IRF1, contribute to protective antigen-specific antibody responses upon influenza infection. While T-bet is required to generate long-lived humoral responses, IRF1 is essential for early antigen-specific IgM. Although, IRF1 is also induced upon BCR and TLR engagement, the contribution of IFN- γ cannot be understated, as we clearly show how an IFN- γ -driven inflammatory program initiates ASC differentiation (Figure 7). Accordingly, we show a significant local IFN- γ -producing T cell response which correlates with the production of durable RBD-specific antibody upon intranasal Ad5COVID vaccination. Thus, we show for the first time, how IFN- γ and IFN- γ -inducible transcription factors promote ASC differentiation, thus informing efficacious vaccine strategies.

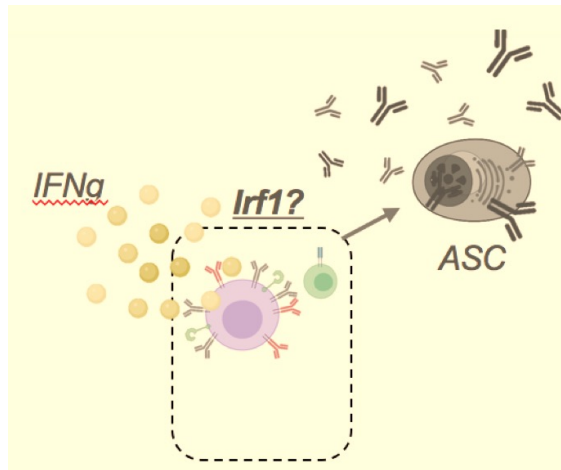


Figure 7 Model of IFN γ -inducible IRF1 contributing to the generation of ASC precursors. IRF1-expressing B cells are required for optimal antibody responses early post following influenza infection and T-I immunization models. While IRF1 can be induced upon IFN γ stimulation TLR/BCR-inducible IRF1 is critical for the generation of a protective, innate-like PC precursor, marginal zone (MZ) B cells.

T-BET TRANSCRIPTION FACTOR PROMOTES ANTIBODY-SECRETING CELL
DIFFERENTIATION BY LIMITING THE INFLAMMATORY EFFECTS OF IFN-
 γ ON B CELLS

by

SARA L. STONE, JESSICA N. PEEL, CHRISTOPHER D. SCHARER, CHRISTOPHER
A. RISLEY, DANIELLE A. CHISOLM, MICHAEL D. SCHULTZ, BINGFEI YU,
ANDRE BALLESTEROS-TATO, WOJCIECH WOJCIECHOWSKI, BETTY
MOUSSEAU, RAVI S. MISRA, ADEDAYO HANIDU, HUIPING JIANG, ZHENHAO
QI, JEREMY M. BOSS, TROY D. RANDALL, SCOTT R. BRODEUR, ANANDA W.
GOLDRATH, AMY S. WEINMANN, ALEXANDER F. ROSENBERG, FRANCES E.
LUND

Immunity

Stone SL, Peel JN, Scharer CD, et al. T-bet Transcription Factor Promotes Antibody-
Secreting Cell Differentiation by Limiting the Inflammatory Effects of IFN- γ on B Cells.
Immunity. 2019;50(5):1172-1187.e7. doi:10.1016/j.immuni.2019.04.004

Copyright

2019

by

Frances E. Lund

Used by permission

Format adapted for dissertation

SUMMARY

Although viral infections elicit robust interferon- γ (IFN- γ) and long-lived antibody-secreting cell (ASC) responses, the roles for IFN- γ and IFN- γ -induced transcription factors (TFs) in ASC development are unclear. We showed that B cell intrinsic expression of IFN- γ R and the IFN- γ -induced TF T-bet were required for T-helper 1 cell-induced differentiation of B cells into ASCs. IFN- γ R signaling induced Blimp-1 expression in B cells but also initiated an inflammatory gene program that, if not restrained, prevented ASC formation. T-bet did not affect Blimp-1 upregulation in IFN- γ -activated B cells but instead regulated chromatin accessibility within the *Ifng* and *Ifngr2* loci and repressed the IFN- γ -induced inflammatory gene program. Consistent with this, B cell intrinsic T-bet was required for formation of long-lived ASCs and secondary ASCs following viral, but not nematode, infection. Therefore, T-bet facilitates differentiation of IFN- γ -activated inflammatory effector B cells into ASCs in the setting of IFN- γ -, but not IL-4-, induced inflammatory responses.

KEYWORDS

T-bet, B cell differentiation, IFN γ , antibody secreting cells, inflammation

INTRODUCTION

The interferon- γ (IFN- γ) inducible T-box transcription factor (TF), T-bet, regulates the activation, proliferation, differentiation, lifespan, and effector functions of T cells (Lazarevic et al., 2013) by modulating gene expression through its interactions with histone-modifying enzymes and other master regulator TFs, like Bcl6 and Blimp-1 (Oestreich and Weinmann, 2012, Xin et al., 2016). T-bet promotes T helper-1 (Th1) development by activating effector cell gene programs (Zhu et al., 2012) and by repressing alternate cell fates (Lazarevic et al., 2013) and type I interferon (IFN)-induced inflammatory gene programs (Iwata et al., 2017). Although T-bet is required for IFN- γ -driven switching to the immunoglobulin G2c (IgG2c) (B6) or IgG2a (BALB/c) isotype in mice (Peng et al., 2002), remarkably little is known about whether T-bet can also influence B cell-fate decisions. However, recent studies showing that T-bet-expressing B cells are expanded in aging, chronically infected, and autoimmune mice and humans (Jenks et al., 2018, Karnell et al., 2017, Knox et al., 2017, Lau et al., 2017, Naradikian et al., 2016, Rubtsov et al., 2011, Rubtsova et al., 2017, Wang et al., 2018) suggest that T-bet may influence B cell transcriptional programming and cell-fate decisions. In support of this idea, autoantibody responses in some systemic lupus erythematosus (SLE)-prone mice are dependent on B cell intrinsic T-bet expression (Rubtsova et al., 2017), and expansion of an unusual population of T-bet-expressing CD11c+CXCR5neg IgDnegCD27neg (DN2) human B cells correlates with disease severity in a subset of SLE patients (Jenks et al., 2018, Wang et al., 2018). Moreover, T-bet+ DN2 cells (Jenks et al., 2018, Wang et al., 2018) as well as T-bet+ CD27+CD21lo-activated human memory B cells (Knox et al., 2017, Lau et al., 2017) exhibit phenotypic, molecular, and functional similarities to antibody (Ab)-secreting cell (ASC) precursors.

Given the association between T-bet expression and pre-ASC formation, we tested whether T-bet was required for commitment to the ASC lineage. We showed that ASC development by B cells activated *in vitro* in the presence of IFN- γ -producing T cells required B cell intrinsic expression of T-bet and the IFN- γ R. T-bet, despite facilitating IFN- γ -dependent ASC development, was not required for IFN- γ -induced upregulation of ASC programming TFs, like Blimp-1, interferon-regulatory factor (IRF)4, and XBP1 (Nutt et al., 2015). Instead, T-bet

repressed an IFN- γ -induced inflammatory gene program that was incompatible with ASC differentiation. Moreover, we found that B cell intrinsic T-bet expression was required for long-lived ASC (LL-ASC) formation following primary infection with influenza virus and memory B cell differentiation into ASCs following influenza challenge infection. By contrast, T-bet-expressing B cells were not required for ASC differentiation following a Th2-inducing nematode infection. Therefore, unlike the core TFs that are required for ASC commitment in all settings (Nutt et al., 2015), T-bet promotes ASC development by preventing B cells from assuming an alternate inflammatory effector cell fate in response to IFN- γ , which is produced in response to some but not all pathogens and autoantigens.

RESULTS

The Blimp-1-Dependent ASC Gene Program Is Enhanced in Th1-Activated B Cells

We reported that cultures of Th1 cell-stimulated B cells (Be1 cells) contained more secreted Ab than cultures of Th2 cell-stimulated B cells (Be2 cells) (Harris et al., 2005b). To test whether ASC development was enhanced in the Be1 cultures, we subdivided the day 4 Be1 cells into 4 discrete populations using the ASC markers CD138 and CD93 (Figure 1A) and measured Ab production by the sort-purified cells. We found that the CD138+CD93+ subset produced the most Ab, as measured by Ab secretory rates, following re-culture of an equivalent number of cells for 5 h (Figure 1B) or by ELISPOT (Figure 1C). Next, we quantitated CD138+CD93+ ASCs and Ab secretory rates in day 4 Be1 and Be2 cultures. CD138+CD93+ cells were more prevalent in day 4 Be1 cultures (Figures 1D and 1E), and day 4 Be1 cells produced more Ab than day 4 Be2 cells (Figure 1F), indicating enhanced ASC formation in Be1 cultures.

To determine when ASC lineage commitment occurs in Be1 cells, we used gene set enrichment analysis (GSEA; Subramanian et al., 2005) and evaluated when TFs that are differentially expressed between bone marrow (BM) ASCs and follicular B cells (FOBs) (Shi et al., 2015) were enriched in the Be1 transcriptome (Table S1; Figure S1A). Since many ASC-specific TFs were significantly enriched in the Be1 transcriptome by day 3 (Figure 1G; Figure S1B), we examined day 2 cells and found that only two ASC-promoting TFs, Prdm1 (Blimp-1) and Jun, were upregulated at this time point in Be1 cells relative to Be2 cells (Figure 1H; Figure S1C).

Consistent with this, day 2 Be1 cells generated from Blimp-1-reporter mice (Rutishauser et al., 2009) expressed detectable amounts of Blimp-1 (Figure 1I). Next, we performed assay for transposase-accessible chromatin sequencing (ATAC-seq) (Buenrostro et al., 2015) on day 2 Be1 and Be2 cells (Table S2). We identified 611 differentially accessible regions (DARs) (Figure 1J) and observed significant enrichment ($p = 3.77 \times 10^{-90}$) of accessible Blimp-1-binding motifs in the day 2 Be1 cells compared to the Be2 cells (Figure 1K). Finally, we observed few CD138+CD93+ ASCs (Figures 1L and 1M) and significantly decreased Ab secretory rates in Be1 cultures containing Prdm1^{-/-} Be1 cells (Figure 1N). Thus, antigen and Th1 cell-activated B cells rapidly upregulate Blimp-1, undergo chromatin remodeling at Blimp-1-binding sites, and differentiate in a Blimp-1-dependent fashion into CD138+CD93+ ASCs.

IFN- γ Controls Early Blimp-1 Expression and ASC Development in Be1 Cells

To identify the upstream TFs that might promote early Blimp-1 expression in Be1 cells, we examined day 2 Be1 and Be2 ATAC-seq and transcriptome datasets using the PageRank (PR) algorithm (Yu et al., 2017; Table S3; Figure S2), ingenuity pathway analysis (IPA; Krämer et al., 2014), and HOMER motif analysis. We also identified the differentially expressed genes (DEGs) in the day 2 datasets. Fourteen of the 357 PR-predicted TFs were also identified in at least 2 of the other 3 analyses and 2 of these TFs, T-bet (Tbx21) and Irf1, were identified in each analysis (Figure 2A; Table S3). Expression of Tbx21 and Irf1 was induced in Be1 cells within 1 day (Figures 2B and 2C) and by day 2 chromatin-accessible regions containing binding motifs for T-bet (Figure 2D) and IRF1, including the interferon-sensitive response element (ISRE), ETS-IRF composite element (EICE) and AP1-IRF composite element (AICE) binding sites (Figures 2E–2G), were significantly enriched in Be1 cells. Expression of Tbx21 and Irf1 was ablated in IFN- γ R1-deficient (Ifngr1^{-/-}) Be1 cells (Figure 2H), demonstrating that expression of these TFs was controlled by IFN- γ . To test whether Be1 differentiation was dependent on IFN- γ signals, we examined Prdm1 expression in Ifngr1^{-/-} Be1 cells. Expression of Prdm1 was significantly lower in day 2 Ifngr1^{-/-} Be1 cells compared to day 2 B6 Be1 and Be2 cells (Figure 2I). Moreover, expression of Prdm1 and other ASC promoting TFs, like Irf4, Pou2af1, and Xbp1, remained low even out to day 4 in Ifngr1^{-/-} Be1 cells (Figure 2J), and these B cells did not form CD138+CD93+ ASCs or secrete Ab (Figures 2K–

2M). Thus, IFN- γ controls rapid upregulation of Tbx21, Irf1, and Prdm1 in Be1 cells and is necessary for the development of Be1 ASCs.

T-bet Controls IFN- γ -Dependent ASC Development but Does Not Regulate Early Expression of Blimp-1

Since T-bet is known to regulate Blimp-1 expression in T cells (Oestreich et al., 2012, Xin et al., 2016), and Blimp-1 was required for Be1 ASC formation, we tested whether Be1 differentiation was T-bet dependent. We found that ASC formation and Ab secretion (Figures 3A–3C) were significantly impaired in Tbx21 $^{-/-}$ Be1 cultures. Consistent with this, GSEA using RNA sequencing (RNA-seq) data (Table S4) from day 4 B6 and Tbx21 $^{-/-}$ Be1 cells revealed that the transcriptome of Tbx21 $^{-/-}$ Be1 cells was not enriched for ASC-specific TFs (Shi et al., 2015) and was instead enriched in FOB TFs (Figures 3D and 3E; Figure S3A). To examine whether T-bet facilitates ASC development by promoting Blimp-1 expression or activity, we analyzed quantitative PCR and ATAC-seq (Table S2) data from day 2 B6 and Tbx21 $^{-/-}$ Be1 and Be2 effectors. We identified 561 DARs between day 2 B6 Be1 and Tbx21 $^{-/-}$ Be1 cells but only 30 DARs between day 2 B6 Be2 and Tbx21 $^{-/-}$ Be2 cells (Figure 3F). In addition, we observed significantly increased chromatin accessibility in the 100 bp immediately surrounding T-bet consensus binding motifs in B6 Be1 cells relative to Tbx21 $^{-/-}$ Be1 cells and B6 Be2 cells (Figure 3G; Figure S3B). However, chromatin accessibility near Blimp-1-binding motifs was unchanged (Figure 3G; Figure S3B), and Prdm1 mRNA expression was equivalent (Figure 3H) between the day 2 B6 and Tbx21 $^{-/-}$ Be1 cells. Similarly, expression of other ASC-inducing TFs (Nutt et al., 2015; Figure 3H) and chromatin accessibility near binding sites for any of these TFs (Figure 3G; Figure S3B) were only modestly affected in the day 2 Tbx21 $^{-/-}$ Be1 cells. Thus, T-bet appeared to promote IFN- γ -dependent ASC formation via a distinct mechanism.

Tbx21 $^{-/-}$ Be1 Cells Maintain an Activated Inflammatory Gene Signature

Although T-bet was not required to induce early Prdm1 expression in Be1 cells, we identified >2,000 DEGs between day 4 Tbx21 $^{-/-}$ and B6 Be1 cells (Table S4). To understand which T-bet-regulated genes were responsible for ASC development, we first examined the IPA-predicted upstream regulator TFs in B6 Be1 and Be2 cells and Tbx21 $^{-/-}$ Be1 cells (Table S5). As expected, IFN- γ -induced TFs, like STAT1, T-bet, and IRF family members, were predicted to be activated (positive Z-score) by day 1 in Be1 cells compared to Be2 cells

(Figure 4A; Table S5). Moreover, by day 2, downstream inflammatory and anti-viral gene targets of STAT1, IRF3, and IRF7 were more highly expressed in Be1 cells compared to day 2 Be2 cells (Figure 4B). However, expression of these genes declined by day 4 in Be1 cells, and the predicted Z-scores for STAT1, IRF3, and IRF7 shifted from activated to inhibited (negative Z-score) (Figure 4B). By contrast, the majority of the downstream gene targets of IRF3, IRF7, and STAT1 were more highly expressed in day 4 Tbx21^{-/-} Be1 cells compared to day 4 Be1 cells (Figure 4B), and IRF3, STAT1, and IRF7, which were the top IPA-identified upstream regulators of the day 4 Tbx21^{-/-} Be1 transcriptome (Figure 4C; Table S5), were predicted to be activated in these cells (Figure 4C). The time-dependent downmodulation of the inflammatory gene signature in the B6 Be1 cells was not limited to downstream targets of IRF3, IRF7, and STAT1 as mRNA expression of multiple TFs from the IRF (Figure 4D), STAT (Figure 4E), and nuclear factor κ B (NF- κ B) (Figure 4F) families also declined by day 4 in the B6 Be1 cells. Similarly, mRNA expression of receptors that activate NF- κ B and IRF, including members of the Toll-like receptor (TLR) (Figure 4G) and TNFR (Figure 4H) families, decreased by day 4 in B6 Be1 cells. By contrast, expression of many STAT, IRF, and NF- κ B TFs (Figures 4D–4F), as well as receptors and ligands that activate NF- κ B and IRF signaling, including TLRs (Figure 4G) and TNF and TNFR family members (Figure 4H), was increased in day 4 Tbx21^{-/-} Be1 cells relative to B6 Be1 cells. The enhanced inflammatory gene signature observed in the Tbx21^{-/-} Be1 cells was not due to the lack of ASCs in the Tbx21^{-/-} Be1 cultures as we observed similar results comparing the transcriptomes of day 4 Tbx21^{-/-} Be1 cells and the non-ASCs present in the day 4 Be1 cultures (Figures S4A–S4G; Table S5). Thus, an inflammatory “effector-like” transcriptional signature, which is transiently observed in B6 Be1 cells, is maintained in Tbx21^{-/-} Be1 cells.

T-bet Is a Transcriptional Repressor in Be1 Cells

Although T-bet is well characterized as a transcriptional activator of T cell effector development (Zhu et al., 2012) its role as a repressor is less appreciated. However, a recent report (Iwata et al., 2017), showing that commitment to the Th1 cell lineage requires T-bet-directed repression of IFN- α -driven inflammatory gene expression, suggested that T-bet might promote ASC development by repressing the inflammatory transcriptional program in Be1 cells. We therefore compared our RNA-seq dataset with published B6 and Tbx21^{-/-}

Th1 cell RNA-seq and chromatin immunoprecipitation sequencing (ChIP-seq) data (Iwata et al., 2017) and found that many of the T-bet-repressed target genes in Th1 cells were also repressed in a T-bet-dependent fashion in Be1 cells (Figure 4I). Indeed, GSEA revealed that the day 4 *Tbx21*^{-/-} Be1 transcriptome was significantly enriched relative to day 4 B6 Be1 transcriptome in targets that are normally repressed by T-bet in Th1 cells (Figure 4J). Moreover, this T-bet-dependent repression of inflammatory genes in Be1 cells was time dependent as expression of known targets of T-bet repression declined in Be1 cells between days 1 and 3 (Figures 4K and 4L; Figure S4H). Thus, deletion of T-bet in Be1 cells resulted in the sustained expression of inflammatory and anti-viral genes, including many already described (Iwata et al., 2017) targets of T-bet repression in T cells.

Sustained TLR and NF- κ B Signaling in Be1 Cultures Prevents ASC Development

Tbx21^{-/-} Be1 cells sustained expression of many inflammatory genes and TFs, including NF- κ B and NF- κ B activators, that are normally suppressed during Be1 differentiation. Since NF- κ B can regulate B cell development, activation, and ASC formation (Gerondakis and Siebenlist, 2010, Klein and Heise, 2015), we assessed whether sustained NF- κ B activation blocked differentiation of IFN- γ -activated Be1 cells. We found that maintaining NF- κ B activity in Be1 cultures, by adding the NF- κ B activator betulinic acid (Kasperczyk et al., 2005) beginning on day 2, significantly suppressed the formation of ASCs and Ig-secreting cells (Figures 5A and 5B; Figure S5A) in the Be1 cultures. Next, we exposed Be1 cells, beginning on day 2, to NF- κ B-activating TLR ligands. We found that ASC development declined significantly (Figures 5C and 5D; Figure S5B). This was not due to reduced cell recovery as the Be1 cells proliferated equally well in the TLR7 and TLR9 ligand exposed cultures (data not shown). Thus, sustained TLR and NF- κ B signaling is sufficient to suppress Be1 ASC development, suggesting that ASC differentiation is likely to be impaired in B cells that cannot downmodulate the inflammatory gene network that activates NF- κ B.

*T-bet Regulates IFN- γ R Signaling in Be1 Cells by Repressing *Ifng* and *Ifngr2* Expression*

T-bet facilitates Th1 cell commitment by repressing *Ifna* expression and preventing initiation of an IFN- α -driven autocrine inflammatory loop (Iwata et al., 2017). Since *Ifna* and the *Ifnar* were not overexpressed in *Tbx21*^{-/-} Be1 cells (data not shown), we hypothesized that T-bet

might facilitate ASC commitment in IFN- γ -activated B cells by inhibiting expression of inflammatory genes that are normally induced by IRF and NF- κ B TFs following activation with IFN- γ or intracellular TLR ligands. We therefore performed IPA upstream regulator analysis on the T-bet-repressed genes that were either unique to Be1 cells or shared between Be1 and Th1 cells (Iwata et al., 2017; Figure 5E; Tables S6 and S7). In agreement with our hypothesis, IFN- γ and TLRs were predicted by IPA to be the top upstream regulators of the 1,220 T-bet-repressed genes that were unique to Be1 cells (Figure 5F; Table S7). Furthermore, many of the genes that were repressed by T-bet in both Th1 and Be1 cells (Figure 5G; Table S7) were also predicted by IPA to be downstream targets of IFN- γ and/or TLR signaling (Figure 5H; Table S7). Thus, both unique targets of T-bet repression in B cells and shared targets of T-bet repression in Be1 and Th1 cells can be induced by IFN- γ R and/or TLR signaling.

Next, we determined the overlap between T-bet-repressed genes in day 4 Be1 cells (Table S6) with genes containing T-bet-dependent DARs in day 2 Be1 cells (Table S2). We identified 40 genes that were repressed in a T-bet-dependent fashion in Be1 cells and mapped to T-bet-dependent DARs that also contained one or more consensus T-bet binding motifs (Figure 5I). The DARs from 17 of these genes contained AICE binding motifs for AP1-IRF complexes or EICE binding sites for Ets-IRF complexes (Figure 5I), suggesting that many of the T-bet-repressed genes in Be1 cells may be co-regulated by IFN- γ -induced IRF TFs. Two of the genes identified in this analysis included *Ifngr2* and *Ifng* (Figures 5I–5K). Both loci contained DARs with T-bet binding motifs (Figures 5L and 5M) that also co-localized with binding motifs for IRF family members. To address whether these T-bet-regulated chromatin-accessible regions in the *Ifngr2* (Figure 5L) or the *Ifng* (Figure 5M) loci were conserved between Be1 and Th1 cells, we compared the day 2 Be1 cell ATAC-seq data with day 4 Th1 cell ATAC-seq data and published Th1 cell T-bet ChIP-seq data (Zhu et al., 2012). We found DARs that were shared between Be1 and Th1 cells and DARs that were specific to either Be1 or Th1 cells. The Be1 unique DAR in the *Ifngr2* locus contained T-bet, EICE, and AICE binding motifs, while the Be1 unique DAR in the *Ifng* locus contained IRF4 and T-bet binding motifs (Figure 5M). Chromatin accessibility in the B cell unique *Ifng* and *Ifngr2* DARs increased in a T-bet-dependent fashion (Figures 5L and 5M), despite the fact that the genes were downregulated in a T-bet-dependent fashion in Be1 cells (Figures 5J and 5K). These results suggest that T-

bet orchestrates chromatin opening in loci undergoing repression and may repress gene expression either through direct binding or by indirectly facilitating recruitment of other repressors to these loci.

T-bet Tunes Expression of IFN- γ R-Regulated Inflammatory Genes

Since T-bet dampened inflammatory gene expression in Be1 cells, we predicted that Tbx21 $^{-/-}$ Be1 cells would make enhanced inflammatory responses following activation with ligands of TLR or TNFR family receptors. Consistent with this, significantly more IFN- γ (Figure 5N) and IFN- γ -induced cytokines, like interleukin-6 (IL-6) (Figure 5O), were produced by day 4 Tbx21 $^{-/-}$ Be1 cells stimulated with TLR7 + TLR9 ligands or TLR ligands plus anti-CD40 and anti-Ig. Given this result, we examined whether T-bet prevented establishment of an IFN- γ R-induced inflammatory feedback loop. We found that inflammatory genes like *Ifng*, *Irf1*, *Stat1*, *Tlr7*, *Tnfsf10*, and *Hif1a* (Figure 5P) were expressed at significantly higher amounts in day 2 Tbx21 $^{-/-}$ Be1 cells and at significantly reduced amounts in day 2 *Ifngr1* $^{-/-}$ Be1 cells when compared to control day 2 B6 Be1 cells. Therefore, expression of these IFN- γ -inducible genes appeared to be restrained by T-bet. However, other genes, like *Ifngr2*, *Irf5*, *Relb*, *Il6*, *Batf*, and *Rorc*, were more highly expressed in both *Ifngr1* $^{-/-}$ and Tbx21 $^{-/-}$ Be1 cells relative to B6 Be1 cells (Figure 5Q), suggesting that IFN- γ R signaling could also repress, in a T-bet-dependent fashion, expression of inflammatory genes and alternate fate-specifying TFs in Be1 cells. Collectively, these data show that T-bet does not directly initiate IFN- γ -dependent ASC programming. Instead, T-bet blocks inappropriate activation of the IFN- γ -induced inflammatory gene program and prevents establishment of alternate effector cell fates in IFN- γ -activated B cells.

T-bet $^{+}$ B Cells Regulate Primary ASC Responses to Viral Infection

To test whether B cell intrinsic expression of T-bet was required for ASC development in vivo, we first infected ZsGreen (ZsG) T-bet reporter mice (Zhu et al., 2012) with influenza A/Puerto Rico/8/1934 H1N1 (PR8) virus or the parasite *Heligmosomoides polygyrus* (Hp) and characterized the T-bet-expressing B cells. Consistent with our in vitro Be1 and Be2 data (Figure S6A), ZsG (T-bet) was expressed by lymph node (LN) FOBs, ASCs, and germinal center B (GCB) cells from the flu but not Hp-infected mice (Figures 6A and 6B). ZsG was also expressed by flu nucleoprotein (NP) (Allie et al., 2019)-specific GCB, ASC, and memory

B cells (Figures 6C–6H). Although ZsG could be detected in early NP-specific plasmablasts (Figure 6C), by day 60 post-infection only a fraction of splenic ASCs (Figure 6D; Figure S6B) and few of the BM LL-ASCs continued to express ZsG (Figure 6E; Figure S6C). By contrast, most flu NP+ memory LN B cells continued to express ZsG (Figures 6F and 6G; Figure S6D) as well as intracellular T-bet protein (Figure 6H).

To address whether T-bet expression by B cells was required for ASC development *in vivo*, we generated BM chimeras that selectively lacked T-bet in all B cells (B-*Tbx21*^{-/-} mice) or were T-bet sufficient in all lineages (B-WT mice) (Figure S6E) and measured day 60 *Hp*- and flu-specific responses. Although *Hp*-specific IgG and IgG1 (Figures 6I and 6J) responses were similar in both groups, flu-specific IgG Ab (Figure 6K) and BM ASC (Figures 6L and 6M) responses were significantly decreased in the B-*Tbx21*^{-/-} chimeras. Thus, T-bet-expressing B cells facilitate LL-ASC and Ab responses to an IFN- γ -inducing viral infection but not to an IL-4-dominated nematode infection.

Although flu-specific Ab and ASC responses were significantly decreased in B-*Tbx21*^{-/-} mice, humoral immunity was not completely ablated in these mice. Since B cell intrinsic T-bet is required for isotype-switch to IgG2a (Peng et al., 2002), we assessed the isotype distribution of the NP-specific Ab and memory B cell responses to flu to determine whether the loss of IgG2c B cells was sufficient to account for the decline in flu-specific Abs in B-*Tbx21*^{-/-} mice. As expected, (Baumgarth et al., 1999), the flu-specific IgM Ab response was short lived in both groups of mice (Figure 6N). Consistent with a requirement for T-bet in switching to IgG2c (Barnett et al., 2016, Peng et al., 2002, Wang et al., 2012), NP-specific IgG2c Abs (Figure 6O) and day 60 IgG2c+ NP+ memory B cells (Figure S6F; Figures 6P–6R) were missing from B-*Tbx21*^{-/-} mice. By contrast, both the NP-specific IgG2b Ab (Figure 6O) and the NP+ IgG2b+ memory B cell (Figures 6P–6R) responses were intact in the B-*Tbx21*^{-/-} mice. However, despite normal frequencies and numbers of IgG1+ flu NP+ memory B cells in B-*Tbx21*^{-/-} mice (Figures 6P–6R), the NP-specific IgG1 Ab response was significantly decreased in B-*Tbx21*^{-/-} mice (Figure 6O). These data therefore indicate that T-bet not only regulates switching to IgG2c following flu infection but also directs the formation of IgG1 long-lived flu-specific Ab responses.

ASC Recall Responses to Flu Require T-bet+ Memory B Cells

Although the total number of flu NP+ memory B cells was not altered in B-Tbx21^{-/-} mice (Figure 6R), T-bet was expressed by many memory B cells (Figures 6G and 6H). To address whether T-bet+ memory B cells contributed to secondary ASC formation, we infected Tbx21fl/fl.hCD20-TAM-cre mice (Figure 7A; Figure S7A) and control B6 mice with PR8 virus. On day 90 post-infection, we exposed the Tbx21fl/fl.hCD20-TAM-cre mice and B6 controls to tamoxifen (TAM) to selectively and inducibly (Khalil et al., 2012) delete Tbx21 from B cells in the flu memory Tbx21fl/fl.hCD20-TAM-cre mice (Figure 7A; Figure S7A). Eight days after the last TAM treatment, we examined expression of CXCR3 (Figure 7B), a known T-bet target gene (Zhu et al., 2012), in B and T lineage cells. TAM treatment of memory Tbx21fl/fl.hCD20-TAM-cre mice did not affect CXCR3 expression by T cells (Figure 7C) but did cause significant reductions in the frequencies of CXCR3+ B cells and CXCR3+NP+ memory B cells (Figures 7D and 7E; Figure S7B). However, inducible deletion of T-bet in the CD20+ compartment did not affect the number of total LN cells, B cells, or T cells (data not shown) or the number of LN NP+ memory B cells (Figure 7F; Figure S7B). Therefore, continued expression of T-bet by memory B cells is not required for short-term maintenance of the flu NP+ memory B cell pool.

Next, we infected naive B6 mice (“X31 primary” mice) and the TAM-treated B6 and Tbx21fl/fl.hCD20-TAM-cre PR8 flu memory mice with X31 (H3N2) influenza (Figure 7A; Figure S7A). Since the H1-specific Abs generated during the primary PR8 infection do not neutralize the H3 X31 virus, we were able to productively infect the PR8 memory mice and follow the response to NP, which is conserved between both viruses (Kees and Krammer, 1984). Similar to our prior experiment, T-bet was efficiently and specifically deleted in B cells from the TAM-treated Tbx21fl/fl.hCD20-TAM-cre mice as measured by decreased CXCR3 expression by total B cells (Figures S7C and S7D) and NP+ GCB cells and ASCs (Figure 7G; Figures S7F and S7G) on day 5 post-X31 challenge. However, CXCR3 continued to be expressed by T lineage cells (Figure S7E). NP+ GCB cells, while not yet detectable in the X31 primary infected mice (Figure 7H), were present in equal numbers in LNs from X31-challenged TAM-treated B6 and Tbx21fl/fl.hCD20-TAM-cre mice (Figure 7H; Figure S7F). However, the number of NP+ ASCs in the challenged memory Tbx21fl/fl.hCD20-TAM-cre

mice was decreased 10-fold compared to the X31-challenged PR8 memory B6 animals (Figure 7I; Figure S7G). Thus, T-bet expression by memory B cells regulates the differentiation of reactivated flu-specific memory B cells.

Secondary Flu-Specific IgG2c ASC Responses Require T-bet+ Memory B Cells

Since our data showed that T-bet was not required for the maintenance of the memory B cell pool (Figure 7F), we used the Tbx21^{-/-}.hCD20-TAM-cre mice to address whether T-bet regulates the differentiation of flu NP⁺ memory B cells into IgG2c-producing ASCs. Consistent with our earlier results, TAM treatment of day 90 PR8 memory hCD20-TAM-cre controls and Tbx21^{fl/fl}.hCD20-TAM-cre mice had no impact on the number of flu NP⁺ memory B cells (Figure 7J; Figure S7H). This was true whether we looked at the NP⁺ IgM-expressing IgD^{neg}CD38⁺ memory B cells or the IgG1 and IgG2c NP⁺ memory B cells (Figures 7K and 7L; Figure S7H). Next, we challenged the mice with heterologous X31 virus and measured the ASC response 5 days post-challenge. Again, we observed a significant reduction in the number of NP⁺ ASCs in the Tbx21^{fl/fl}.hCD20-TAM-cre mice compared to control animals (Figure 7M; Figure S7I). Moreover, IgG2c NP⁺ ASCs, which were easily detected in the challenged control group, were significantly decreased in the TAM-treated Tbx21^{fl/fl}.hCD20-TAM-cre mice (Figure 7M; Figure S7I). Therefore, T-bet controls the differentiation of flu-specific memory B cells into IgG2c⁺ ASCs. Taken together, these data support the conclusion that T-bet expression by B cells does facilitate the development of ASC and Ab responses following primary and secondary flu infections. However, T-bet, unlike Blimp-1 or IRF4 (Nutt et al., 2015), is not a master regulator of ASC development since some types of ASC responses remain intact in the absence of T-bet-expressing B cells. The importance of the T-bet controlled ASC developmental pathways in health and disease is discussed.

DISCUSSION

In IFN- γ -activated T cells, T-bet regulates cell-fate decisions by activating lineage-specific programs and repressing alternate fates and inflammatory feedback loops (Iwata et al., 2017, Lazarevic et al., 2013). Although T-bet is expressed by human DN2 and memory pre-ASCs

(Jenks et al., 2018, Lau et al., 2017, Wang et al., 2018), and T-bet-expressing B cells are required for autoAb responses in some autoimmune mice (Peng et al., 2002, Rubtsova et al., 2017), the role for T-bet in ASC lineage commitment had not been well studied. We previously reported that cognate encounters between antigen-presenting B cells and IFN- γ -producing Th1 cells results in rapid upregulation of T-bet (Harris et al., 2005a) and robust Ab production (Harris et al., 2005b). This result was initially quite puzzling as at that time Th2 cytokines were thought to promote B cell differentiation (Randolph et al., 1999), and IFN- γ was thought to induce B cell apoptosis (Bernabei et al., 2001). However, more recent publications revealing that IFN- γ R, STAT1 and T-bet-expressing B cells are required for autoAb responses in some mouse models of autoimmunity (Domeier et al., 2016, Jackson et al., 2016, Rubtsova et al., 2017, Thibault et al., 2008), suggested that IFN- γ signaling might also be important for ASC development. Our data showing that IFN- γ -producing T cells not only induced IFN- γ - and T-bet-dependent B cell differentiation but were even more effective in promoting ASC development than IL-4-producing T cells demonstrated that potent B cell-fate cues can be provided by an inflammatory cytokine that is often associated with viral infection and autoimmunity.

Although we fully expected to find that T-bet induced B cell differentiation by promoting TFs that initiate ASC commitment, we realized that T-bet did not regulate the early expression or activity of any of the well-described ASC-associated TFs (Nutt et al., 2015) including Blimp-1, which can be modulated in a T-bet-dependent fashion in T cells (Oestreich et al., 2012, Xin et al., 2016). Likewise, T-bet did not function to repress TFs like Pax5 that maintain B cell identity and prevent ASC differentiation (Nutt et al., 2015). Instead, we found that IFN- γ , rather than T-bet, was responsible for early induction of Prdm1 and that T-bet functioned to repress anti-viral and inflammatory genes that are known downstream targets of type I and type II IFN signaling (Pollard et al., 2013). These results were similar to data (Iwata et al., 2017) showing that T-bet prevents *Ifna* expression and represses initiation of an autocrine type I IFN inflammatory circuit in developing Th1 cells. Although expression of *Ifna*, *Ifnb*, and *Ifnar* was not impacted in *Tbx21*^{-/-} Be1 cells, we observed that expression of *Ifng* and *Ifngr2* was higher in *Tbx21*^{-/-} Be1 cells relative to B6 Be1 cells and that *Tbx21*^{-/-} Be1 cells produced more IFN- γ following TLR stimulation. These data suggested that T-bet might repress an IFN- γ -induced autocrine or paracrine inflammatory circuit in differentiating B cells.

In fact, IPA revealed that many of the >1,000 T-bet-repressed genes in Be1 cells were predicted to be activation targets of IFN- γ R and/or TLR signaling. Since engagement of IFN- γ R, TLR, and TNF family receptors can activate IRF and NF- κ B TFs (Hiscott, 2007, Rickert et al., 2011, Schroder et al., 2004), we postulate that a key function of T-bet in B cells is to restrain IRF and NF- κ B-directed transcriptional programs and prevent the establishment of feedforward inflammatory circuits. Furthermore, we predict that once NF- κ B and IRF inflammatory loops are initiated in Tbx21 $^{-/-}$ Be1 cells, additional IFN- γ R signaling may not be required to sustain the inflammatory phenotype, as several TNF family ligand and receptor pairs capable of driving NF- κ B inflammatory loops (Rickert et al., 2011) were upregulated in Tbx21 $^{-/-}$ Be1 cells.

Our data showed that T-bet prevented sustained activation of TFs from the STAT and IRF and NF- κ B families. While expression of many Nfkb family members declined rapidly in Be1 cells compared to Be2 cells, Tbx21 $^{-/-}$ Be1 cells maintained high expression of Nfkb family members relative to B6 Be1 cells. Enforced NF- κ B activation in the B6 Be1 cells, either through addition of a NF- κ B activator or exogenous TLR ligands to the Be1 cultures, significantly suppressed ASC formation. Thus, sustained NF- κ B activation was sufficient to prevent IFN- γ -induced B cell differentiation. This was somewhat unexpected since many of the cues that drive B cell activation and proliferation promote NF- κ B activity (Hoffmann and Baltimore, 2006). Moreover, deletion or mutation of some NF- κ B family members, specifically within mature B cell compartment, is reported to impair ASC commitment in some settings (Grossmann et al., 2000, Heise et al., 2014, Kaisho et al., 2001). However, a recent publication shows that c-REL (Rel), which is overexpressed and predicted by IPA to be in an activated state in Tbx21 $^{-/-}$ Be1 cells, blocks ASC differentiation in response to TLR ligands (Roy et al., 2019). Furthermore, we found that two IPA-predicted activation targets of c-REL, Bach2 and Cd40, were downregulated in a T-bet-dependent fashion in differentiating Be1 cells. Given that downmodulation of both Bach2 and CD40 is required for ASC development (Igarashi et al., 2014, Lee et al., 2005, Randall et al., 1998), it is tempting to speculate that one way T-bet facilitates ASC formation is by preventing sustained NF- κ B and c-REL signaling that promotes continued expression of pro-proliferation and anti-differentiation genes like Cd40 and Bach2.

In addition to repressing expression of Nfkb family members, T-bet also downmodulated genes, like Irf1 and Stat1, that are induced in an Ifngr1-dependent fashion in Be1 cells. These data suggested that IFN- γ R signals induce an inflammatory IFN-stimulated gene (ISG) transcriptional program and simultaneously engage a T-bet-mediated negative feedback loop to tune the magnitude and duration of ISG expression. However, genes such as Baft, Rorc, Ifih1, and Il6 were highly expressed in both Tbx21 $^{-/-}$ and Ifngr $^{-/-}$ Be1 cells, suggesting IFN- γ and T-bet cooperate to repress some genes. Since we identified overlap between T-bet-repressed genes and DARs with EICE or AICE binding motifs, one possible mechanism is through recruitment of repressive IRF complexes by T-bet. Given that IRF TFs were identified by PR, IPA, and HOMER as putative upstream regulators of the Be1 transcriptome network, we speculate that T-bet, perhaps through its capacity to recruit chromatin modifying enzymes to DNA (Miller and Weinmann, 2010), may increase chromatin accessibility and allow for binding of IFN- γ -induced IRF-containing repressive TF complexes. Regardless, the data support a model in which IFN- γ and T-bet cooperate to prevent expression of alternate cell-fate-specifying transcriptional programs in the activated Be1 cells—similar to the role that T-bet plays in cementing commitment to the Th1 cell lineage (Oestreich and Weinmann, 2012).

Our *in vivo* experiments using B-Tbx21 $^{-/-}$ chimeras demonstrated that B cell intrinsic T-bet was required for the development of a primary IgG1 long-lived Ab response and the secondary IgG2c ASC response to influenza virus but was not required for the development or maintenance of flu-specific memory B cells. This result initially appeared inconsistent with a previous study reporting that T-bet was required for maintenance of IgG2c memory B cells (Wang et al., 2012). However, this study, which actually evaluated the memory B cell recall response following *in vivo* reactivation with B cell receptor (BCR) ligands, showed reduced formation of secondary ASCs following reactivation of memory IgG2c cells. Thus, this result is very consistent with our data showing that inducible deletion of T-bet in memory cells greatly impairs the IgG2c ASC recall response to flu. However, our experiments, which also examined memory cell maintenance under steady state following T-bet deletion, demonstrated that T-bet was not required for memory cell maintenance, at least over a 10-day period. This result is similar to CD8 T cells where T-bet is not required for memory formation (Joshi et al., 2007) but does regulate memory cell differentiation to secondary effectors (Joshi et al., 2011).

While our *in vivo* data clearly showed a role for B cell intrinsic T-bet in regulating some primary and secondary ASC responses to influenza, our data also indicated that B cell intrinsic expression of T-bet is dispensable for the IgG1 Ab response to *Hp* and the IgG2b Ab response to influenza. These data indicated that, unlike Blimp-1 or IRF4, T-bet is not a universal ASC lineage commitment factor; instead, T-bet regulates IFN- γ -induced ASC differentiation. We believe that these results are very consistent with our *in vitro* data that suggested that T-bet primarily functions to prevent IFN- γ -activated B cells from being “locked into” an effector inflammatory cell fate that is not compatible with commitment to the ASC lineage. If this is correct, then T-bet should be completely dispensable when B cells are activated in an environment with few IFN- γ -producing cells or have received previous programming signals that render the B cells non-responsive to IFN- γ signals. We think this is likely to be the case for the B cells responding to *Hp* infection as the response to this pathogen is dominated by IL-4-producing Th2 and Tfh2 cells (León et al., 2012). While we cannot yet explain why flu-specific IgG2b⁺ ASC formation is intact in the B-*Tbx21*^{-/-} mice, transforming growth factor β (TGF- β) is the cytokine most often associated with IgG2b class-switch recombination (Deenick et al., 2005, McIntyre et al., 1993, Sellars et al., 2009), and it is known, at least in T cells, that TGF- β potently suppresses IFN- γ signaling (Lin et al., 2005). Thus, it is possible that IgG2b⁺ B cells are unable to respond to IFN- γ signaling and differentiate in an IFN- γ and T-bet-independent manner. In summary, *in vivo* activated B cells must integrate a complex array of microenvironmental cues during the processes of class switch recombination, proliferation, and differentiation. We propose that T-bet, while not a universal regulator of B cell differentiation, acts in a cytokine-dependent manner in the settings of virus infection and autoimmunity to finely tune the IFN-induced inflammatory gene network and allow B cells to transition from an activated inflammatory “effector” cell to a terminally differentiated ASC.

EXPERIMENTAL MODEL AND SUBJECT DETAILS

Mice and generation of bone marrow chimeras.

All experimental animals were bred and maintained in the UAB animal facilities. All procedures involving animals were approved by the UAB Institutional Animal Care and Use Committee and were conducted in accordance with the principles outlined by the National Research Council. Mouse strains used in these experiments include the following: CD45.1+OT-II (intercrossed C57BL/6-Tg(TcraTcrb)425Cbn/J and B6.SJL-Ptprca Pepcb/BoyJ (CD45.1+ B6 mice), B6.129S7-Ifngr1tm1Agt/J (Ifngr1^{-/-}), B6.129P2(C)-Cd19tm1(Cre)Cgn/J (Cd19Cre/+), Cd19Cre/+Prdm1fl/fl (intercrossed B6.129-Prdm1tm1Clme/J and Cd19Cre/+ mice), hCD20-TAM-cre, Tbx21fl/fl.hCD20-TAM-cre (intercrossed hCD20-TAM-cre and B6.129-Tbx21tm2Srnrl/J mice), B6.Blimp-1-YFP reporters and B6.T-bet-ZsGreen reporters. Blimp-1 (Rutishauser et al., 2009) and T-bet (Zhu et al., 2012) reporter mice were obtained from Dr. Meffre (Yale University) and Dr. Zhu (NIH), respectively. hCD20-TAM-cre mice (Khalil et al., 2012) were obtained from Mark Shlomchik (University of Pittsburgh) and all other strains were obtained from Jackson Laboratory. Bone marrow (BM) chimeric mice were generated by irradiating B cell deficient μ MT (B6.129S2-Ighmtm1Cgn/J) recipient animals with 950 Rads from a high-energy X-ray source, delivered in a split dose 4 hrs apart, and then reconstituting the recipients with 10⁷ BM cells by retro-orbital injection. BM cell mixtures were as follows: 80% μ MT BM + 20% Tbx21^{-/-} BM (B-Tbx21^{-/-} chimeras) or with 80% μ MT BM + 20% B6 (C57BL/6J) BM (B-WT). BM chimeras were used in experiments 8-12 weeks post-reconstitution. Both male and female mice were used in this study. Within each experiment, animals were matched for age, 8-12 weeks at time zero, and sex. No differences were observed between cohorts of male versus female mice.

Infections and tamoxifen exposure.

BM chimeric mice were infected (i.n.) with a sublethal dose (1.5×10^4 VFU) of the H1N1 influenza virus, A/PR/8/34 (PR8) or by gavage with 200 *H. polygyrus* (*Hp*) L3 larvae. To

terminate *Hp* infection, 10 mg pyrantel pamoate (Pin-X, Quartz) was administered by gavage 28 days post infection. In some experiments, mice were given a primary infection with PR8, allowed to recover for ≥ 90 days, injected i.p. 5 times over 8 days with tamoxifen (Sigma, 200 μ l of 10 mg/ml drug dissolved in 10% ethanol and 90% corn oil) and then analyzed or challenged i.n. (1.25×10^6 VFU) with the heterosubtypic H3N2 influenza virus, A/Aichi/68 (X31) before analysis.

T and B cell effector generation and stimulation.

Th1 and Th2 cells were generated *in vitro* as previously described (Harris et al., 2005a). Briefly, splenic CD4⁺ CD45.1⁺ OT-II TCR Tg T cells were purified by positive selection (Miltenyi Biotec) and cultured in complete medium in the presence of platebound anti-CD3 (2 μ g/ml) and anti-CD28 (5 μ g/ml) and either IL-12 (2 ng/ml) and anti-IL-4 (11B11, 20 μ g/ml) (Th1 cell conditions) or IL-4 (50 units/ml) and anti-IFN γ (XMG1.2, 10 μ g/ml) (Th2 cell promoting conditions). T cells were transferred into new plates after 48-72 hrs and cultured for an additional 48 hours in media supplemented with IL-2 (20 units/ml). Polarized Th1 and Th2 cells were treated with mitomycin C, washed and then co-cultured at a 1:1 ratio with positively selected (Miltenyi Biotec) CD19⁺ splenic B cells in complete B cell media supplemented with OT-II peptide (5 μ M), anti-IgM F(ab')₂ (10 μ g/ml), and IL-2 (20 Unit/ml). “Be1” refers to B cells from cultures containing Th1 cells, “Be2” refers to B cells from cultures containing Th2 cells, and “BeA” refers to cells cultured under the same conditions but without T cells. In some experiments IKK α & IKB α activator, betulinic acid at 10 μ g/ml; TLR7 agonist, R848 at 12.5 μ g/ml, (InvivoGen); TLR9 agonist, CpG ODN1826 at 12.5 μ g/ml, (InvivoGen); or vehicle, DMSO (Sigma) were added to cultures at day 2, prior to analysis on day 4. For analysis of the cytokines made by effector B cell subsets, B cells were collected, purified by positive selection using B220 microbeads and MACS, assessed for purity by FACS and then restimulated at 1×10^6 cells/ml with TLR ligands (CpG + LPS) or with a restimulation cocktail (LPS + CpG + anti-IgM + anti-CD40 (10 μ g/ml) for 24h. Supernatants were collected and tested for IFN γ and IL-6 using Luminex array beads.

METHOD DETAILS

ELISPOT and Ab secretory rate assay.

Day 4 B effector cells were harvested, washed and recultured in fresh media for 5-6 hr at 1×10^6 live cells/ml. Secreted Ab was quantified using an anti-Kappa ELISA (Southern Biotechnology) and a Kappa standard (Sigma). Secretory rates were reported as ng Kappa chain secreted/hour/106 cells. For ELISPOT, Day 4 B effector cells were harvested, washed and in some experiments sort-purified before being recultured in duplicate in fresh media for 5 hrs on multiscreen cellulose filter ELISPOT plates (Millipore) coated with goat anti-mouse kappa light chain (Southern Biotech). Bound Ab was detected with AP-conjugated goat anti-mouse Ig(H+L) Ab (Southern Biotech) and the AP substrate 5-bromo-4-chloro-3'-indolyphosphate p-toluidine salt and nitro-blue tetrazolium chloride (BCIP/NBT, Moss Substrates). ELISPOTS were counted using a dissecting microscope and imaged using S6 Ultra-V Analyzer (Cellular Technology Limited).

Hp and flu Ab titers.

Immune serum samples were serially diluted in ELISA plates coated with purified PR8 virus proteins (Lee et al., 2005) or Hp extract (Harris et al., 2000). Bound Ab was detected using HRP-conjugated goat anti-mouse heavy chain IgG, IgG 1, IgG2c or IgG2b-specific Abs (Southern Biotechnology) and ABTS substrate followed by oxalic acid stop. Absorbance values at 405nm (OD) were read and endpoint titers were determined using the average OD from naive samples as baseline.

Ex vivo ELISPOT.

BM cells were isolated from flu-infected mice (2 tibia + 2 femur/mouse), run over lymphocyte separation media gradient (Corning, 1.077-1.080g/ml) to remove dead cells, serially diluted in duplicate in complete media and incubated for 5 hr at 37°C on multiscreen cellulose filter ELISPOT plates (Millipore) coated with purified PR8 virus protein. Bound Ab was detected with AP-conjugated goat anti-mouse heavy chain-specific pan-IgG Ab (Jackson ImmunoResearch) and the AP substrate BCIP/NBT (Moss Substrates). ELISPOTS were counted using a dissecting microscope and imaged using S6 Ultra-V Analyzer (Cellular Technology Limited).

Cell isolation, flow cytometry analysis and cell sorting.

Spleen and BM single cell suspensions were prepared by gently disrupting tissue on fine wire mesh then red blood cells were lysed. LN single cell suspensions prepared by gently disrupting tissue between glass slides. Cell suspensions were filtered through 70 μ m nylon mesh then incubated in FcR blocking mAb 2.4G2 (10 μ g/ml). Cells were stained with fluorochrome-conjugated Abs, PNA or recombinant flu nucleoprotein (NP) B cell tetramers, prepared as previously described (Allie et al., 2019), and 7-aminoactinomycin D (7AAD, Sigma). For IgG isotype staining, immunoglobulin antibodies were stained in a separate step prior to other cell surface markers and all incubations were performed in staining media supplemented with 5% goat serum (Invitrogen) and 5% rat serum (Invitrogen). For IgG isotype staining cells were stained with the LIVE/DEAD fixable stain (ThermoFisher) before fixation with 10% neutral buffered formalin (Sigma). For intracellular T-bet staining, stained cells were incubated with LIVE/DEAD fixable stain, then fixed and permeabilized with the TF staining buffer set (eBioscience) before intracellular staining. Stained cells were analyzed using a FACSCanto II (BD Bioscience) and Attune NxT (Invitrogen, ThermoFisher) or were sort-purified with a FACSARIA (BD Biosciences) located in the UAB Comprehensive Flow Cytometry Core.

Antibodies used in this study include: anti-mouse CD19 (6D5), B220 (RA3-6B2), CD93 (AA4.1), CD138 (281-2), CD38 (90), CXCR3 (CXCR3-173), IgM (II-41), IgD (AMS 9.1 and 11-26c.2a), IgG1 (RMG1-1), IgG2b (RMG2b-1 and polyclonal goat anti-mouse), IgG2c (polyclonal goat antimouse), CD45.1 (A20), CD45.2 (104), CD8 (53-6.7), CD3 (17A2), CD4 (GK1.5 and RM4-5) and T-bet (4B10). Monoclonal Abs were obtained from BioLegend, E-Bioscience and Southern Biotech.

Quantitative RT-PCR.

TRIzol (ThermoFisher) or RNeasy (Qiagen) was used to isolate total RNA from sort-purified B effector cells (CD19+CD4negCD45.2+CD45.1neg). RNA quantity and quality were assessed using the Nanodrop 6000 and the Agilent 2100 Bioanalyzer. cDNA was generated from total RNA using SuperScript II double stranded cDNA synthesis kit (Invitrogen) with random hexamers according to manufacturer's protocols. Real-time PCR was performed using TaqMan Gene Expression Master Mix, with the following parameters on a Roche LightCycler 480: 50°C for 2 min, 95 °C for 10 min, followed by 45 two-step cycles at 95°C for 15 sec and at 60° C for 1 min. Applied Biosystems pre-designed TaqMan Gene Expression Assays were used for real-time PCR (Batf Mm00479410_m1, Bcl6 Mm00477633_m1, Cxcl10 Mm00445235_m1, Ets1 Mm01175819_m1, Gapdh Mm99999915_g1, Hif1a Mm00468869_m1, Ifih1 Mm00459183_m1, Ifng Mm01168134_m1, Ifngr2 Mm01210592_m1, Il6 Mm00446190_m1, Irf4 Mm00516431_m1, Irf5 Mm00496447_m1, Irf7 Mm00516788_m1, Jun Mm00495062_s1, Pax5 Mm00435501_m1, Pou2af1 Mm004488326_m1, Prdm1 Mm00476128_m1, Relb Mm00485664_m1, Rorc Mm01261022_m1, Runx3 Mm00490666_m1, Spib Mm03048233_m1, Stat2 Mm00490880_m1, Stat4 Mm00448881_m1, Tbkbp1 Mm00446590_m1, Tbx21 Mm00450960_m1, Tlr7 Mm00446590_m1, Tnfsf4 Mm00437214_m1, Tnfsf10 Mm01283606_m1, Xbp1 Mm00457359_m1). B effector gene expression analyses included three experimental replicates/group. At least three independent experiments were performed for each analysis. For quantification of gene expression, each sample was normalized to expression of an endogenous control gene, Gapdh for Be1. The fold change in expression of each gene compared to a control sample, set at 1.0 was calculated as $2^{-\Delta\Delta CT}$. Samples with CT values above 32 were considered negative.

Affymetrix array sample preparation.

Total RNA was purified (TRIzol) from day 1-4 Be1 and Be2 cells (n= 7 independent experimental samples/timepoint/group) and converted to biotin-labeled cRNA using the Affymetrix one-cycle cDNA synthesis and IVT kit. Labeled cRNA was fragmented to an average size of 35 to 200 bases by incubation at 94°C for 35 min. Hybridization (16 hr), washing, and staining of the Affymetrix GeneChip® Mouse Genome U430 Plus 2.0 Array was conducted according to manufacturer specifications.

RNA-seq sample preparation

500 ng of total RNA (TRIzol) from three biological replicates of day B6 and Tbx21^{-/-} Be1 cells, and one replicate of CXCR3⁺CCR6⁺ B6 Be1 and CXCR3⁺CCR6^{neg} B6 Be1 cells, was used as input for the Illumina TruSeq RNA-seq library kit. Following quality assessment on a bioanalyzer, RNA-seq libraries were pooled and sequenced on one lane of a HiSeq2500 using 50 bp paired-end chemistry as previously described (Barwick et al., 2016).

ATAC-seq sample preparation.

ATAC-seq was performed on Be1 and Be2 cells as previously described (Buenrostro et al., 2015) and Th1 and Th2 cells as previously described (Chisolm et al., 2017). Nuclei from 50,000 cells were extracted and incubated with Tn5 transposase (Illumina) for 30 minutes at 37°C. DNA samples were purified with the MinElut Kit (Qiagen). Library amplification was performed using Nextara primers with Next High-Fidelity 2× PCR Master Mix (New England BioLabs), followed by purification with the PCR Purification Kit (Qiagen). The libraries were sequenced using a 1×50bp paired end run at the UAB Heflin Genomics Center.

QUANTIFICATION AND STATISTICAL ANALYSIS

Statistical details of all experiments including tests used, n, and number of experimental repeats are provided in figure legends. FlowJo (Tree Star) used for flow cytometric analyses. Prism graphpad used for statistical analyses and graphing except where indicated. Details of transcriptomics library generation and statistical analysis are provided below.

Affymetrix array analysis.

The signal value of each probe set (gene) was calculated using the Microarray Suite 5 (MAS5) algorithm and normalized using global scaling which set the average signal intensity of an array to 750. MAS5 values were log₂-transformed and a p value for each probe set was calculated using an unpaired t-test. Positive FDR and q values were computed using Matlab (The Mathworks Inc., Natick MA) based on the method of Storey (Storey, 2002). FC data reported as log₂ expression ratio of indicated groups.

RNA-seq analysis.

Sequencing reads were quality checked using the FASTX-Toolkit and mapped to the mm9 genome using TopHat2 (Kim et al., 2013) with the default settings and the mm9 UCSC Known Gene table as a reference transcriptome. HOMER software (Heinz et al., 2010) was used to summarize reads in transcripts using the analyzeRepeats.pl script with the following options ‘-strand both –count exons –condenseGenes –noadj’. Genes that contained 2 or more reads in at least 3 samples were deemed expressed (13,924 of 24,016) and used as input for edgeR (Robinson et al., 2010) to identify differentially expressed genes using the HOMER script ‘getDiffExpression.pl –repeats’. Following edgeR analysis, p-values for genes with 2-fold change or greater were false-discovery rate (FDR) corrected using the Benjamini-Hochberg method.

Genes with a FDR of <0.05 and fold change ≥ 2 were considered significant between B6 and Tbx21^{-/-} Be1 cells. Expression data was normalized to reads per kilobase per million mapped reads (FPKM) using the analyzeRepeats.pl script with the following options “-strand both – count exons – condenseGenes – rpkm”. Data visualization was performed using custom scripts and the R/Bioconductor package, which are available upon request. FC data reported as log₂ expression ratio of indicated groups.

GSEA.

Gene set enrichment analysis (GSEA) was performed using the GSEA program (<http://software.broadinstitute.org/gsea/index.jsp>). For analysis of Be1 and Be2 Affymetrix microarray data, non-log transformed expression data from Be1 (n=7) and Be2 (n=7) samples were submitted to GSEA. Analysis metrics (Subramanian et al., 2005) are summarized briefly as follows: Probe sets were collapsed to genes, which were then ranked by the signal-to-noise metric based on the Be1 vs. Be2 phenotype comparison. Nominal p-values were calculated empirically using 1000 random phenotype label permutations to produce a null distribution of enrichment score. When comparing against a database of large numbers of gene sets, enrichment scores were normalized to account for differences in set sizes, and false discovery rates were computed to control for multiple comparisons.

For GSEA analysis of RNA-seq data, all detected genes were ordered by their score ($-\log_{10}$ of the p-value from edgeR multiplied by the sign of the fold change) from most upregulated in Tbx21^{-/-} Be1 cells to most downregulated in Tbx21^{-/-} Be1 cells and used as input for the GSEA Preranked analysis, where nominal p-values are based on gene set permutations.

Bioinformatic identification of predicted upstream regulatory TFs.

To define the TFs that participate in the Be1 transcriptional network we integrated four datasets including HOMER motif analysis, Ingenuity Pathway Analysis (IPA) upstream regulator analysis (Kramer et al., 2014), PageRank analysis (Yu et al., 2017), and differential expression of each factor. Putative Be1 network TFs were selected based on being predicted as a Be1 TF in all four or three of the four different analyses. For the HOMER motif analysis, TF motifs specifically enriched in either Be1 or Be2 cells were first defined. Next, where specific motifs matched multiple factors, the motif was assigned to a TF family (i.e., IRF3 = IRF/ISRE or cJun = AP-1). TFs overlapping the Be1 list were annotated. For PageRank analysis the log₂ fold change (logFC) of the Be1 versus the Be2 PageRank statistic was computed. TFs with positive logFC values were assigned to the Be1 network and negative logFC values the Be2 network.

Significant expression changes at day 2 by MA analysis was determined based on $FDR < 0.05$ and absolute value \log_2 ratio of > 1 . For IPA upstream regulator analysis TFs were grouped into Be1 or Be2 and annotated accordingly. Activation Z-scores were used to characterize regulators as activated or inhibited based on the observed pattern of up-/down-regulation of the target molecules compared with expected directions of changes documented in Ingenuity's curated database.

The Z-score captures the degree to which the directions of changes of the individual DEGs in the regulator's target set is consistent with its activated or inhibited state based on the IPA curated, expected influences of the regulator on each target. Statistical analysis of the IPA upstream regulator analysis was measured using overlap p-value as previously described (Kramer et al., 2014). Briefly, the overlap p-value (bar height after $-\log_{10}$ transform) characterizes the enrichment of a regulator's target set within a DEG set based on Fisher's exact test, which can suggest involvement of a regulator even if that regulator is not a DEG. Genes with an overlap p value < 0.05 by IPA were predicted to be upstream regulators. Unless otherwise indicated, all IPA upstream regulator analyses were performed using only direct interactions.

ATAC-seq analysis

Data processing was performed as previously described (Scharer et al., 2016). Specifically, raw sequencing data was mapped to the mm9 version of the mouse genome using Bowtie (Langmead et al., 2009) with the default settings. Duplicate reads were marked using the Picard Tools MarkDuplicates function (<http://broadinstitute.github.io/picard/>) and eliminated from downstream analyses. Enriched accessible peaks were identified using the HOMER findPeaks.pl script with setting “-style dnase”. Genomic annotations were computed for ATAC-seq peaks using the HOMER annotatePeaks.pl script and gene expression data annotated using the Entrez ID as a reference. Significantly differential accessible loci (DAR) were identified by the following steps. First, a composite list of all peaks occurring in any sample were obtained using the HOMER mergePeaks.pl script resulting in 62,925 unique regions. Next, the unnormalized read counts for all peaks were annotated for each sample from the bam file using the Genomic Ranges (Lawrence et al., 2013) R/Bioconductor package. This matrix was used as input for edgeR (Robinson et al., 2010) and a pairwise differential analysis was performed between all groups. p-values were FDR corrected for multiple testing using the Benjamini-Hochberg method. Peaks with an FDR < 0.05 were called significant. De novo motif enrichment was determined for peaks that mapped to DAR for the indicated comparison using the HOMER findMotifsGenome.pl script with the default settings. Locations of individual specific motifs (Blimp-1, T-bet, ISRE, AICE, EICE, PAX5, SpiB, Bcl6, XBP1, IRF4, OCT2) were identified in peaks using the findMotifs.pl script with the “-m <factor> -mbed” and ATAC-seq reads in the 100 bp surrounding each motif were annotated for each sample. All other analyses and data display was performed using R/Bioconductor with custom scripts that are available upon request.

DATA AND SOFTWARE AVAILABILITY

The Microarray data have been deposited in the Gene Expression Omnibus (GEO) database under ID code GSE84948. The RNA-seq data have been deposited in the GEO database under ID code GSE83697. The ATAC-seq data have been deposited in the GEO database under ID code GSE118984. Software used in transcriptomics analysis is detailed in METHODS DETAILS and KEY RESOURCES TABLE. Custom scripts for RNA-seq and ATAC-seq data display in R/Bioconductor are available by request.

ACKNOWLEDGEMENTS

We thank Thomas Scott Simpler, Uma Mudunuru, Rebecca Burnham and Holly Bachus for technical support and Drs. Eric Meffre (Yale University), Shane Crotty (LIAI), Mark Shlomchik (Univ. Pittsburgh) for providing mouse strains that were used in the experiments. Boehringer Ingelheim Pharmaceutical Inc. (to FEL, SRB, and HJ) provided support for Affymetrix transcriptome analysis. Funding for all other experiments was provided by the US National Institutes of Health (NIH): P01 AI078907, R01 AI110508, (to FEL), P01 AI125180 (to FEL and ASW), U19 AI109962 (to FEL and TDR), R01 HL069409 and R01 AI097357 (to TDR), AI061061 (to ASW) and AI23733-01 (to JMB and CDS). SLS received grant support from the UAB Medical Scientist Training Program NIGMS T32GM008361. NIH P30 AR048311 and P30 AI027767 provided support for the UAB consolidated flow cytometry core and G20RR022807-01 provided support for the UAB Animal Resources Program X-irradiator.

REFERENCES

- Allie SR, Bradley JE, Mudunuru U, Schultz MD, Graf BA, Lund FE, and Randall TD (2019). The establishment of resident memory B cells in the lung requires local antigen encounter. *Nature immunology* 20, 97–108.
- Barnett BE, Staupe RP, Odorizzi PM, Palko O, Tomov VT, Mahan AE, Gunn B, Chen D, Paley MA, Alter G, et al. (2016). Cutting Edge: B Cell-Intrinsic T-bet Expression Is Required To Control Chronic Viral Infection. *Journal of immunology* 197, 1017–1022.
- Barwick BG, Scharer CD, Bally AP, and Boss JM (2016). Plasma cell differentiation is coupled to division-dependent DNA hypomethylation and gene regulation. *Nature immunology* 17, 1216–1225.
- Baumgarth N, Herman OC, Jager GC, Brown L, Herzenberg LA, and Herzenberg LA (1999). Innate and acquired humoral immunities to influenza virus are mediated by distinct arms of the immune system. *Proceedings of the National Academy of Sciences of the United States of America* 96, 2250–2255.
- Bernabei P, Coccia EM, Rigamonti L, Bosticardo M, Forni G, Pestka S, Krause CD, Battistini A, and Novelli F (2001). Interferon-gamma receptor 2 expression as the deciding factor in human T, B, and myeloid cell proliferation or death. *J Leukoc Biol* 70, 950–960.
- Buenrostro JD, Wu B, Chang HY, and Greenleaf WJ (2015). ATAC-seq: A Method for Assaying Chromatin Accessibility Genome-Wide. *Curr Protoc Mol Biol* 109, 21.29.21–29.
- Chisolm DA, Savic D, Moore AJ, Ballesteros-Tato A, Leon B, Crossman DK, Murre C, Myers RM, and Weinmann AS (2017). CCCTC-Binding Factor Translates Interleukin 2- and alpha-Ketoglutarate-Sensitive Metabolic Changes in T Cells into Context-Dependent Gene Programs. *Immunity* 47, 251–267 e257.
- Deenick EK, Hasbold J, and Hodgkin PD (2005). Decision criteria for resolving isotype switching conflicts by B cells. *European journal of immunology* 35, 2949–2955.
- Domeier PP, Chodisetti SB, Soni C, Schell SL, Elias MJ, Wong EB, Cooper TK, Kitamura D, and Rahman ZS (2016). IFN-gamma receptor and STAT1 signaling in B cells are central to spontaneous germinal center formation and autoimmunity. *The Journal of experimental medicine* 213, 715–732.
- Gerondakis S, and Siebenlist U (2010). Roles of the NF-kappaB pathway in lymphocyte development and function. *Cold Spring Harb Perspect Biol* 2, a000182.

- Grossmann M, O'Reilly LA, Gugasyan R, Strasser A, Adams JM, and Gerondakis S (2000). The anti-apoptotic activities of Rel and RelA required during B-cell maturation involve the regulation of Bcl-2 expression. *EMBO J* 19, 6351–6360.
- Harris DP, Goodrich S, Gerth AJ, Peng SL, and Lund FE (2005a). Regulation of IFN-gamma production by B effector 1 cells: essential roles for T-bet and the IFN-gamma receptor. *Journal of immunology* 174, 6781–6790.
- Harris DP, Goodrich S, Mohrs K, Mohrs M, and Lund FE (2005b). Cutting edge: the development of IL-4-producing B cells (B effector 2 cells) is controlled by IL-4, IL-4 receptor alpha, and Th2 cells. *Journal of immunology* 175, 7103–7107.
- Harris DP, Haynes L, Sayles PC, Duso DK, Eaton SM, Lepak NM, Johnson LL, Swain SL, and Lund FE (2000). Reciprocal regulation of polarized cytokine production by effector B and T cells. *Nature immunology* 1, 475–482.
- Heinz S, Benner C, Spann N, Bertolino E, Lin YC, Laslo P, Cheng JX, Murre C, Singh H, and Glass CK (2010). Simple combinations of lineage-determining transcription factors prime cis-regulatory elements required for macrophage and B cell identities. *Molecular cell* 38, 576–589.
- Heise N, De Silva NS, Silva K, Carette A, Simonetti G, Pasparakis M, and Klein U (2014). Germinal center B cell maintenance and differentiation are controlled by distinct NF-kappaB transcription factor subunits. *The Journal of experimental medicine* 211, 2103–2118.
- Hiscott J (2007). Convergence of the NF-kappaB and IRF pathways in the regulation of the innate antiviral response. *Cytokine Growth Factor Rev* 18, 483–490.
- Hoffmann A, and Baltimore D (2006). Circuitry of nuclear factor kappaB signaling. *Immunological reviews* 210, 171–186.
- Igarashi K, Ochiai K, Itoh-Nakadai A, and Muto A (2014). Orchestration of plasma cell differentiation by Bach2 and its gene regulatory network. *Immunological reviews* 261, 116–125.
- Iwata S, Mikami Y, Sun HW, Brooks SR, Jankovic D, Hirahara K, Onodera A, Shih HY, Kawabe T, Jiang K, et al. (2017). The Transcription Factor T-bet Limits Amplification of Type I IFN Transcriptome and Circuitry in T Helper 1 Cells. *Immunity* 46, 983–991 e984.
- Jackson SW, Jacobs HM, Arkatkar T, Dam EM, Scharping NE, Kolhatkar NS, Hou B, Buckner JH, and Rawlings DJ (2016). B cell IFN-gamma receptor signaling promotes autoimmune germinal centers via cell-intrinsic induction of BCL-6. *The Journal of experimental medicine* 213, 733–750.
- Jenks SA, Cashman KS, Zumaquero E, Marigorta UM, Patel AV, Wang X, Tomar D, Simon Z, Burgovsky R, Blalock EL, et al. (2018). A new B cell effector pathway with defective regulation of TLR7 signaling in human SLE. *Immunity* in press.

- Joshi NS, Cui W, Chandele A, Lee HK, Urso DR, Hagman J, Gapin L, and Kaech SM (2007). Inflammation directs memory precursor and short-lived effector CD8(+) T cell fates via the graded expression of T-bet transcription factor. *Immunity* 27, 281–295.
- Joshi NS, Cui W, Dominguez CX, Chen JH, Hand TW, and Kaech SM (2011). Increased numbers of preexisting memory CD8 T cells and decreased T-bet expression can restrain terminal differentiation of secondary effector and memory CD8 T cells. *Journal of immunology* 187, 4068–4076.
- Kaisho T, Takeda K, Tsujimura T, Kawai T, Nomura F, Terada N, and Akira S (2001). IkappaB kinase alpha is essential for mature B cell development and function. *The Journal of experimental medicine* 193, 417–426.
- Karnell JL, Kumar V, Wang J, Wang S, Voynova E, and Ettinger R (2017). Role of CD11c(+) T-bet(+) B cells in human health and disease. *Cellular immunology* 321, 40–45.
- Kasperczyk H, La Ferla-Bruhl K, Westhoff MA, Behrend L, Zwacka RM, Debatin KM, and Fulda S (2005). Betulinic acid as new activator of NF-kappaB: molecular mechanisms and implications for cancer therapy. *Oncogene* 24, 6945–6956.
- Kees U, and Krammer PH (1984). Most influenza A virus-specific memory cytotoxic T lymphocytes react with antigenic epitopes associated with internal virus determinants. *The Journal of experimental medicine* 159, 365–377.
- Khalil AM, Cambier JC, and Shlomchik MJ (2012). B cell receptor signal transduction in the GC is short-circuited by high phosphatase activity. *Science* 336, 1178–1181.
- Kim D, Pertea G, Trapnell C, Pimentel H, Kelley R, and Salzberg SL (2013). TopHat2: accurate alignment of transcriptomes in the presence of insertions, deletions and gene fusions. *Genome biology* 14, R36.
- Klein U, and Heise N (2015). Unexpected functions of nuclear factor-kappaB during germinal center B-cell development: implications for lymphomagenesis. *Curr Opin Hematol* 22, 379–387.
- Knox JJ, Buggert M, Kardava L, Seaton KE, Eller MA, Canaday DH, Robb ML, Ostrowski MA, Deeks SG, Slifka MK, et al. (2017). T-bet+ B cells are induced by human viral infections and dominate the HIV gp140 response. *JCI Insight* 2.
- Kramer A, Green J, Pollard J Jr., and Tugendreich S (2014). Causal analysis approaches in Ingenuity Pathway Analysis. *Bioinformatics* 30, 523–530.
- Langmead B, Trapnell C, Pop M, and Salzberg SL (2009). Ultrafast and memory-efficient alignment of short DNA sequences to the human genome. *Genome biology* 10, R25.

Lau D, Lan L, Andrews SF, Henry C, Thatcher Rojas K, Neu KE, Huang M, Huang Y-P, DeKosky B, Palm A-KE, et al. (2017). Low CD21 expression defines a population of recent germinal center graduates primed for plasma cell differentiation. *Science Immunol* 1.

Lawrence M, Huber W, Pages H, Aboyoun P, Carlson M, Gentleman R, Morgan MT, and Carey VJ (2013). Software for computing and annotating genomic ranges. *PLoS Comput Biol* 9, e1003118.

Lazarevic V, Glimcher LH, and Lord GM (2013). T-bet: a bridge between innate and adaptive immunity. *Nature reviews. Immunology* 13, 777–789.

Lee BO, Rangel-Moreno J, Moyron-Quiroz JE, Hartson L, Makris M, Sprague F, Lund FE, and Randall TD (2005). CD4 T cell-independent antibody response promotes resolution of primary influenza infection and helps to prevent reinfection. *Journal of immunology* 175, 5827–5838.

Leon B, Ballesteros-Tato A, Browning JL, Dunn R, Randall TD, and Lund FE (2012). Regulation of T(H)2 development by CXCR5+ dendritic cells and lymphotoxin-expressing B cells. *Nature immunology* 13, 681–690.

Lin JT, Martin SL, Xia L, and Gorham JD (2005). TGF-beta 1 uses distinct mechanisms to inhibit IFN-gamma expression in CD4+ T cells at priming and at recall: differential involvement of Stat4 and T-bet. *Journal of immunology* 174, 5950–5958.

McIntyre TM, Klinman DR, Rothman P, Lugo M, Dasch JR, Mond JJ, and Snapper CM (1993). Transforming growth factor beta 1 selectivity stimulates immunoglobulin G2b secretion by lipopolysaccharide-activated murine B cells. *The Journal of experimental medicine* 177, 1031–1037.

Miller SA, and Weinmann AS (2010). Molecular mechanisms by which T-bet regulates T-helper cell commitment. *Immunological reviews* 238, 233–246.

Naradikian MS, Hao Y, and Cancro MP (2016). Age-associated B cells: key mediators of both protective and autoreactive humoral responses. *Immunological reviews* 269, 118–129.

Nutt SL, Hodgkin PD, Tarlinton DM, and Corcoran LM (2015). The generation of antibody-secreting plasma cells. *Nature reviews. Immunology* 15, 160–171.

Oestreich KJ, Mohn SE, and Weinmann AS (2012). Molecular mechanisms that control the expression and activity of Bcl-6 in TH1 cells to regulate flexibility with a TFH-like gene profile. *Nature immunology* 13, 405–411.

Oestreich KJ, and Weinmann AS (2012). T-bet employs diverse regulatory mechanisms to repress transcription. *Trends in immunology* 33, 78–83.

- Peng SL, Szabo SJ, and Glimcher LH (2002). T-bet regulates IgG class switching and pathogenic autoantibody production. *Proceedings of the National Academy of Sciences of the United States of America* 99, 5545–5550.
- Pollard KM, Cauvi DM, Toomey CB, Morris KV, and Kono DH (2013). Interferon-gamma and systemic autoimmunity. *Discov Med* 16, 123–131.
- Randall TD, Heath AW, Santos-Argumedo L, Howard MC, Weissman IL, and Lund FE (1998). Arrest of B lymphocyte terminal differentiation by CD40 signaling: mechanism for lack of antibody-secreting cells in germinal centers. *Immunity* 8, 733–742.
- Randolph DA, Huang G, Carruthers CJ, Bromley LE, and Chaplin DD (1999). The role of CCR7 in TH1 and TH2 cell localization and delivery of B cell help in vivo. *Science* 286, 2159–2162.
- Rickert RC, Jellusova J, and Miletic AV (2011). Signaling by the tumor necrosis factor receptor superfamily in B-cell biology and disease. *Immunological reviews* 244, 115–133.
- Robinson MD, McCarthy DJ, and Smyth GK (2010). edgeR: a Bioconductor package for differential expression analysis of digital gene expression data. *Bioinformatics* 26, 139–140.
- Roy K, Mitchell S, Liu Y, Ohta S, Lin Y. s., Metzger MO, Nutt SL, and Hoffmann A (2019). A Regulatory Circuit Controlling the Dynamics of NFκB cRel Transitions B Cells from Proliferation to Plasma Cell Differentiation. *Immunity* 50, 616–628. e616.
- Rubtsov AV, Rubtsova K, Fischer A, Meehan RT, Gillis JZ, Kappler JW, and Marrack P (2011). Toll-like receptor 7 (TLR7)-driven accumulation of a novel CD11c(+) B-cell population is important for the development of autoimmunity. *Blood* 118, 1305–1315.
- Rubtsova K, Rubtsov AV, Thurman JM, Mennona JM, Kappler JW, and Marrack P (2017). B cells expressing the transcription factor T-bet drive lupus-like autoimmunity. *The Journal of clinical investigation* in press.
- Rutishauser RL, Martins GA, Kalachikov S, Chandele A, Parish IA, Meffre E, Jacob J, Calame K, and Kaech SM (2009). Transcriptional repressor Blimp-1 promotes CD8(+) T cell terminal differentiation and represses the acquisition of central memory T cell properties. *Immunity* 31, 296–308.
- Scharer CD, Blalock EL, Barwick BG, Haines RR, Wei C, Sanz I, and Boss JM (2016). ATAC-seq on biobanked specimens defines a unique chromatin accessibility structure in naive SLE B cells. *Sci Rep* 6, 27030.
- Schroder K, Hertzog PJ, Ravasi T, and Hume DA (2004). Interferon-gamma: an overview of signals, mechanisms and functions. *J Leukoc Biol* 75, 163–189.

Sellars M, Reina-San-Martin B, Kastner P, and Chan S (2009). Ikaros controls isotype selection during immunoglobulin class switch recombination. *The Journal of experimental medicine* 206, 1073–1087.

Shi W, Liao Y, Willis SN, Taubenheim N, Inouye M, Tarlinton DM, Smyth GK, Hodgkin PD, Nutt SL, and Corcoran LM (2015). Transcriptional profiling of mouse B cell terminal differentiation defines a signature for antibody-secreting plasma cells. *Nature immunology* 16, 663–673.

Storey JD (2002). A direct approach to false discovery rate. *J. R. Stat. Soc. Ser. B* 64, 479–498.

Subramanian A, Tamayo P, Mootha VK, Mukherjee S, Ebert BL, Gillette MA, Paulovich A, Pomeroy SL, Golub TR, Lander ES, and Mesirov JP (2005). Gene set enrichment analysis: a knowledge-based approach for interpreting genome-wide expression profiles. *Proceedings of the National Academy of Sciences of the United States of America* 102, 15545–15550.

Thibault DL, Chu AD, Graham KL, Balboni I, Lee LY, Kohlmoos C, Landrigan A, Higgins JP, Tibshirani R, and Utz PJ (2008). IRF9 and STAT1 are required for IgG autoantibody production and B cell expression of TLR7 in mice. *The Journal of clinical investigation* 118, 1417–1426.

Wang NS, McHeyzer-Williams LJ, Okitsu SL, Burris TP, Reiner SL, and McHeyzer-Williams MG (2012). Divergent transcriptional programming of class-specific B cell memory by T-bet and RORalpha. *Nature immunology* 13, 604–611.

Wang S, Wang J, Kumar V, Karnell JL, Naiman B, Gross PS, Rahman S, Zerrouki K, Hanna R, Morehouse C, et al. (2018). IL-21 drives expansion and plasma cell differentiation of autoreactive CD11c(hi)T-bet(+) B cells in SLE. *Nat Commun* 9, 1758.

Xin A, Masson F, Liao Y, Preston S, Guan T, Gloury R, Olshansky M, Lin JX, Li P, Speed TP, et al. (2016). A molecular threshold for effector CD8(+) T cell differentiation controlled by transcription factors Blimp-1 and T-bet. *Nature immunology* 17, 422–432.

Yu B, Zhang K, Milner JJ, Toma C, Chen R, Scott-Browne JP, Pereira RM, Crotty S, Chang JT, Pipkin ME, et al. (2017). Epigenetic landscapes reveal transcription factors that regulate CD8(+) T cell differentiation. *Nature immunology* 18, 573–582.

Zhu J, Jankovic D, Oler AJ, Wei G, Sharma S, Hu G, Guo L, Yagi R, Yamane H, Punkosdy G, et al. (2012). The transcription factor T-bet is induced by multiple pathways and prevents an endogenous Th2 cell program during Th1 cell responses. *Immunity* 37, 660–673.

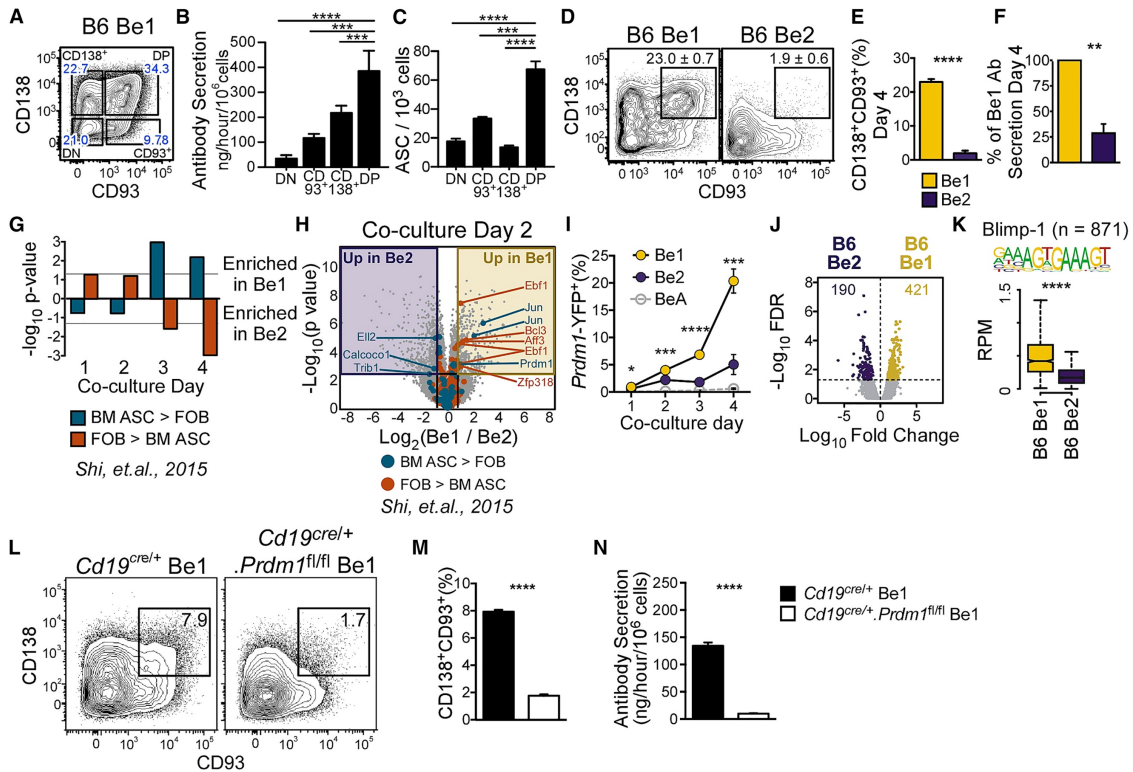


Figure 1 ASC Development Is Preferentially Initiated in Th1 Cell-Primed B Cells

(A–C) Identification of ASCs in sort-purified day 4 Be1 cell subsets (A) divided using CD138 and CD93. Ab secretory rates (B) and ELISPOT (C) analyses of each subset are shown.

(D–F) Identification (D) and enumeration (E) of CD138⁺CD93⁺ ASCs in day 4 Be1 and Be2 cultures. Ab secretory rates (F) of Be1 and Be2 cells are shown as percentage of Be1 Ab secretion.

(G and H) Gene set expression analysis (GSEA) for differentially expressed TF genes in BM ASCs versus FOB cells (Shi et al., 2015) in day 1–4 Be1 and Be2 microarray (MA) data (G). Day 2 Be1 and Be2 volcano plot (H) highlighting TF genes significantly (false discover rate [FDR] < 0.05, ≥1.75 fold change [FC]) upregulated in BM ASCs or FOBs (Shi et al., 2015).

(I–N) Analysis of Blimp-1 in Be1 and Be2 cells.

(I) Enumeration of Blimp-1 reporter (YFP⁺) expressing Be1, Be2, and control BeA cells generated from Blimp-1 reporter mice by flow. Be1 versus Be2 p values are shown.

(J) Volcano plot of day 2 B6 Be1 and Be2 cell ATAC-seq data showing 611 DARs (FDR < 0.05).

(K) Chromatin accessibility within 100 bp surrounding Blimp-1 binding motifs in day 2 Be1 and Be2 cells by ATAC-seq. n = number of motif-containing DARs analyzed. $p = 3.8 \times 10^{-90}$.

(L–N) Identification (L) and quantification (M) of CD138⁺CD93⁺ ASCs in day 4 Be1 cultures containing control (*Cd19^{cre/+}*) or Blimp-1-deficient (*Cd19^{cre/+}.Prdm1^{fl/fl}*) B cells. Day 4 Ab secretory rates (N) are shown.

Data are representative of ≥ 2 independent experiments (A–E, I, and L–N), representative pooled data from 4 independent experiments (F), 7 independent experimental samples/time point/group (MA), or 3 independent experimental samples per group (ATAC-seq). Data are presented as mean \pm SD of ≥ 3 experimental replicates (B, C, E, I, M, and N); mean \pm SEM of 4 independent experiments (F); bar plot of nominal p values (G) or box and whisker plots (showing interquartile range and upper and lower limit) are shown (K). p values were determined using one-way ANOVA (B and C) or Student's t test (E, F, I, K, M, and N). See [STAR Methods](#) for description of Be1 and Be2 cultures, DAR identification, and statistical analyses of GSEA and MA datasets. * $p < 0.05$, ** $p \leq 0.01$ *** $p \leq 0.001$, **** $p \leq 0.0001$, ns, not significant.

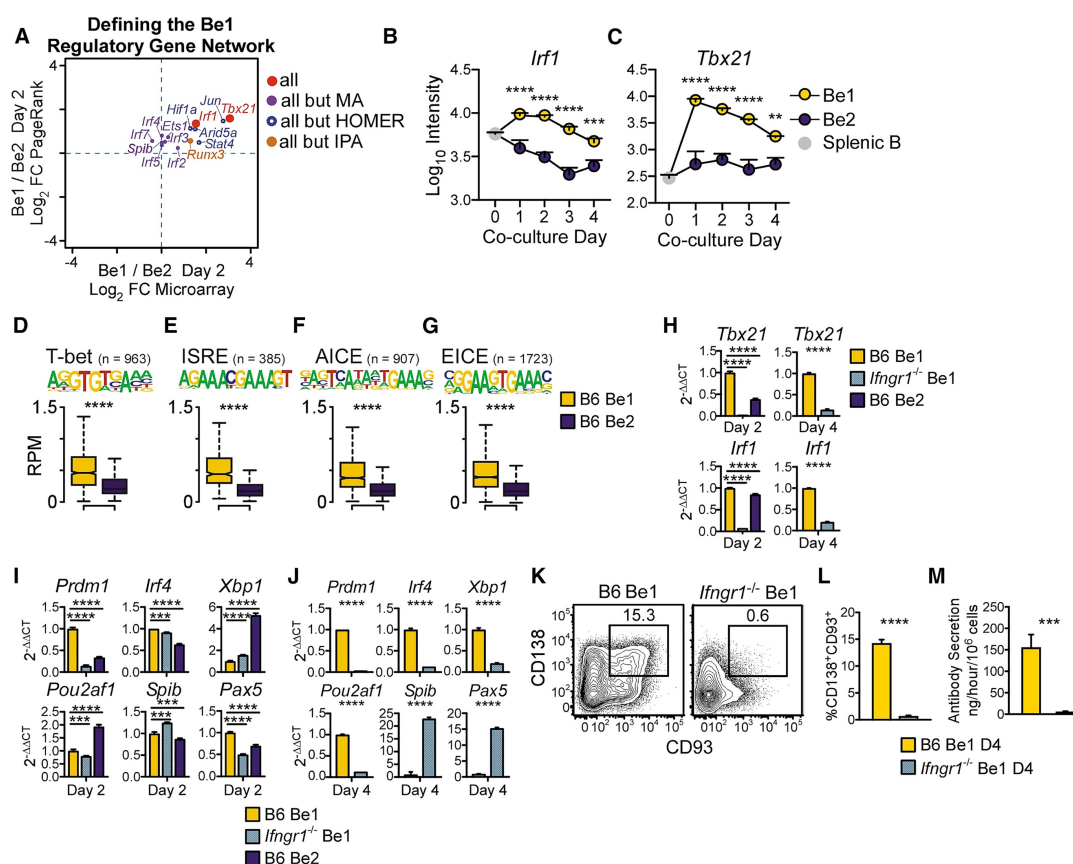


Figure 2 IFN- γ R Signals Control Be1 Differentiation into ASCs

(A) TF regulators of the day 2 Be1 gene network as predicted by HOMER motif, ingenuity pathway (IPA) upstream regulator, PageRank (PR), and DEG analyses using day 2 Be1 and Be2 MA and ATAC-seq data. TFs predicted by all 4 analyses or 3 of 4 analyses are shown as MA Log₂ FC versus PR Log₂ FC.

(B and C) MA expression of *Irf1* (B) and *Tbx21* (C) by day 0 (splenic B) and day 1–4 Be1 and Be2 cells. Be1 versus Be2 p values shown.

(D–G) Chromatin accessibility within 100 bp surrounding T-bet (D) and IRF (E–G) binding motifs in day 2 Be1 and Be2 cells by ATAC-seq. n = number of motif-containing DARs analyzed. p = 1.6×10^{-68} (D), p = 3.1×10^{-49} (E), p = 5.9×10^{-74} (F), and p = 5×10^{-137} (G).

(H–J) qPCR analysis (see [STAR Methods](#)) of day 2 (H and I) or day 4 (H and J) B6 Be1, *Ifngr1*^{-/-} Be1, or B6 Be2 cells.

(K–M) Identification (K) and quantification (L) of CD138⁺CD93⁺ ASCs in day 4 B6 and *Ifngr1*^{-/-} Be1 cultures. Day 4 Ab secretory rates (M) are shown.

Data in (H)–(M) are representative of 2 (H and I) or ≥ 3 (J–M) independent experiments. Shown as the mean \pm SD of ≥ 3 PCR (H–J) or experimental (L and M) replicates. MA data are shown as mean \pm SEM of 7 experiments (B and C). ATAC-seq data are shown as box and whisker plots of 3 independent experimental samples per group (D–G). p values were determined by Student's t test (D–G, J, L, and M), one-way ANOVA (H and I), or two-way ANOVA (B and C). **p \leq 0.01
p \leq 0.001, *p \leq 0.0001, ns, not significant.

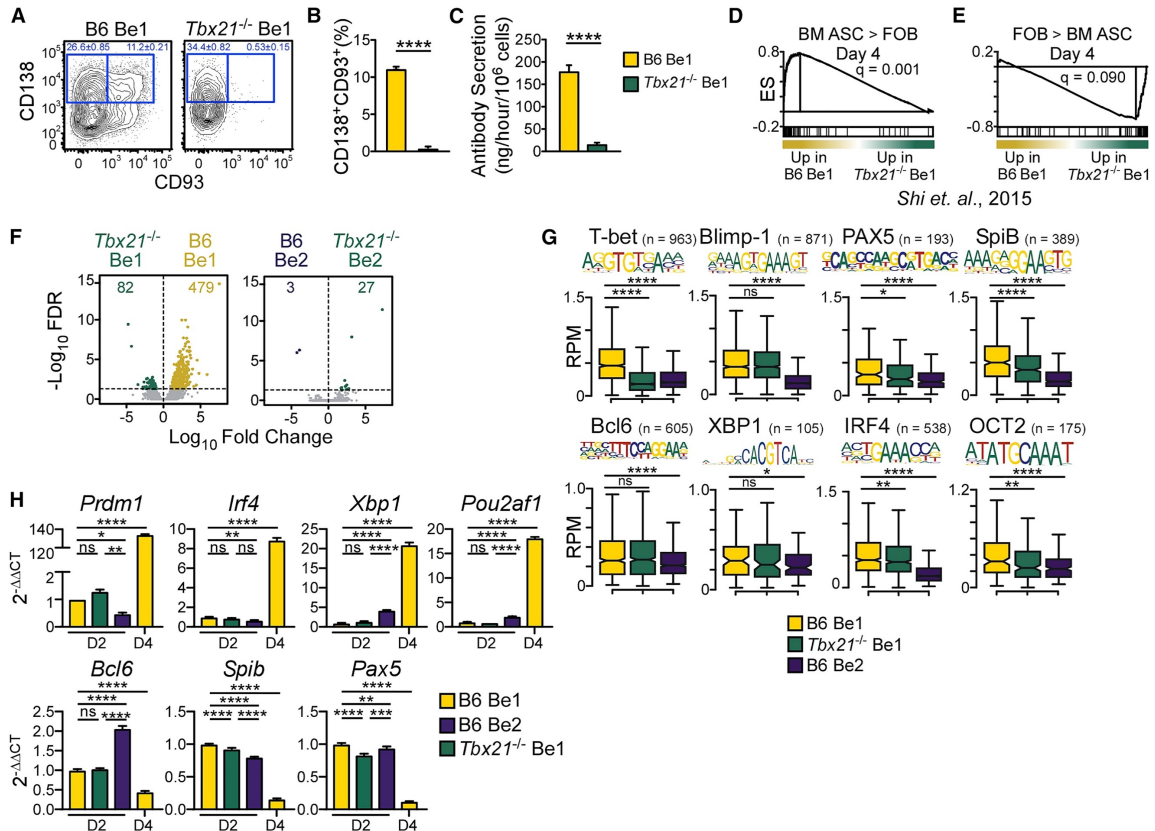


Figure 3 T-bet Controls Be1 Differentiation but Does Not Regulate Early ASC Programming

(A–C) Identification (A) and enumeration (B) of CD138⁺CD93⁺ ASCs in day 4 B6 and *Tbx21*^{-/-} Be1 cultures. Day 4 Ab secretory rates (C) are shown.

(D and E) GSEA enrichment plots for differentially expressed TF genes in BM ASC (D) versus FOB (E) cells (Shi et al., 2015) in day 4 B6 and *Tbx21*^{-/-} Be1 RNA-seq data. Enrichment score (ES) are shown.

(F) Day 2 ATAC-seq volcano plots showing DARs (FDR < 0.05) between B6 Be1 and *Tbx21*^{-/-} Be1 (561 DARs, left) and B6 Be2 and *Tbx21*^{-/-} Be2 (30 DARs, right).

(G) Chromatin accessibility within 100 bp surrounding the indicated TF binding motifs in 2 B6 Be1, B6 Be2, and *Tbx21*^{-/-} Be1 cells by ATAC-seq. n = number of motif-containing DARs analyzed. p values are provided in [Figure S3B](#).

(H) qPCR analysis (see [STAR Methods](#)) of days 2 or 4 *Tbx21*^{-/-} Be1, B6 Be1, and B6 Be2 cells.

RNA-seq and ATAC-seq data are from 3 independent experiments. Data are representative of 2 (H) or ≥ 3 (A–C) independent experiments. Shown as the mean \pm SD of ≥ 3 experimental replicates. Statistical significance determined by Student's t test (B, C, and G), one way-ANOVA (H), or FDR q analysis (D–F). * $p < 0.05$, ** $p \leq 0.01$, *** $p \leq 0.001$, or **** $p \leq 0.0001$, ns, not significant.

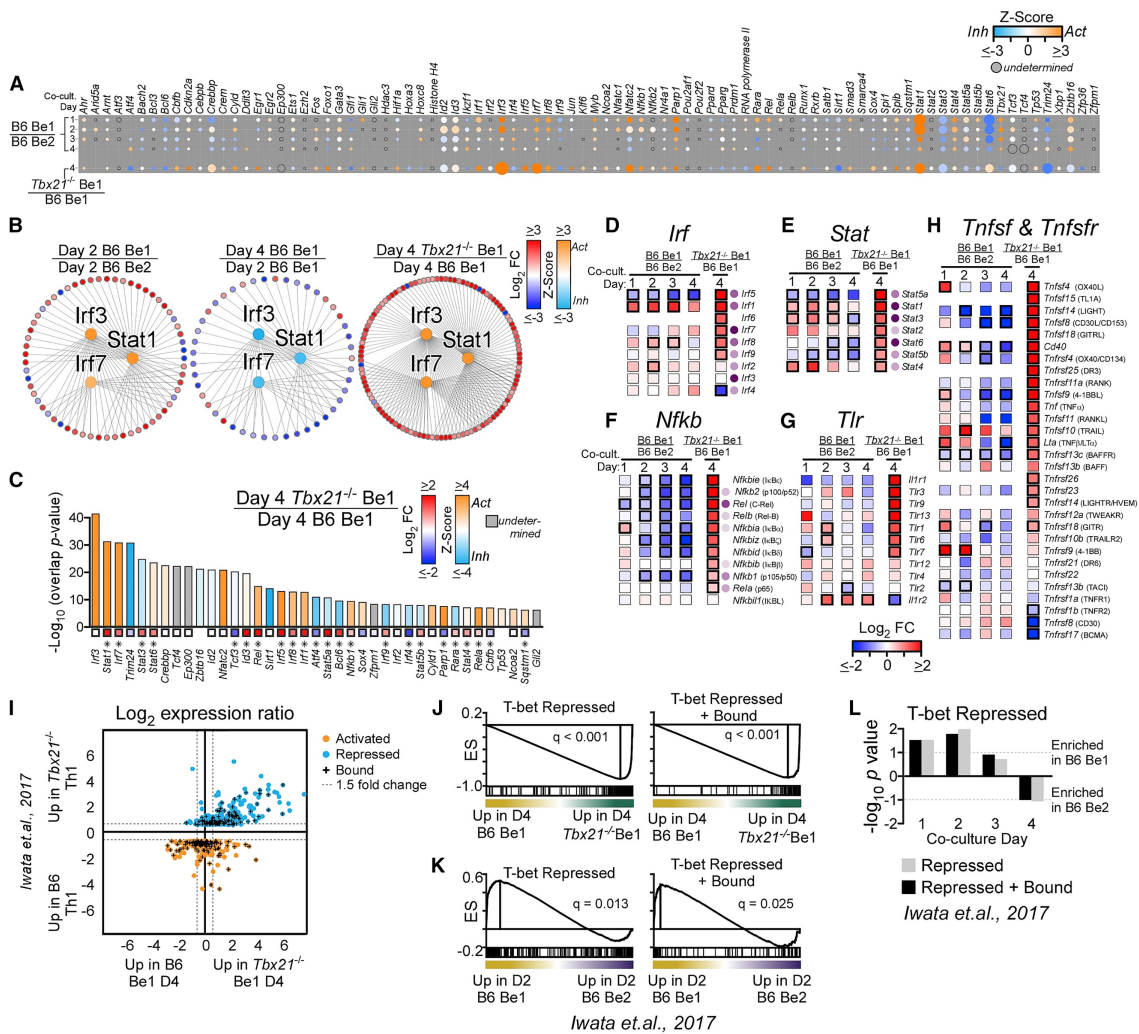


Figure 4 T-bet Represses Inflammatory Gene Expression in Be1 Cells

(A) Activation Z-score heatmap for IPA-predicted upstream regulator TFs in B6 Be1 over B6 Be2 (MA) or *Tbx21*^{-/-} Be1 over B6 Be1 (RNA-seq). Circle size is proportional to $-\log_{10}$ overlap p value.

(B) Predicted upstream regulators (center; *Irf3*, *Irf7*, *Stat1*, colored by Z-score) and target genes (outer circle, colored by FC) in day 2 B6 Be1 over day 2 B6 Be2 (left), day 4 B6 Be1 over day 2 B6 Be1 (middle), and day 4 *Tbx21*^{-/-} Be1 over day 4 B6 Be1 (right).

(C) IPA-predicted upstream regulators from day 4 *Tbx21*^{-/-} Be1 over day 4 B6 Be1, showing activation Z-score (bars) and FC (asterisk indicates FDR < 0.05).

(D–H) mRNA expression heatmaps (squares with black borders = FDR < 0.05) of *Irf* (D), *Stat* (E), *Nfkb* (F), *Tlr* (G), *Tnfsf* and *Tnfsfr* (H) family members in B6 Be1 over B6 Be2 (MA), or *Tbx21*^{-/-} Be1 over B6 Be1 (RNA-seq). Purple circles show $-\log_{10}$ overlap p values from IPA upstream regulator analysis described in (A) with darker shades increasing in significance. Protein names are provided in parentheses.

(I) Intersection of T-bet-regulated genes in day 3 Th1 cells ([Iwata et al., 2017](#)) with genes expressed by day 4 *Tbx21*^{-/-} Be1 or B6 Be1 cells (RNA-seq data, n = 497) shown as FC expression in day 3 *Tbx21*^{-/-} Th1 over B6 Th1 cells (y axis) versus FC in day 4 *Tbx21*^{-/-} Be1 over B6 Be1 cells (x axis). Activated (orange), repressed (blue), and direct targets of T-bet (“+”) in Th1 cells ([Iwata et al., 2017](#)) are indicated.

(J–L) GSEA enrichment plots for T-bet-repressed or T-bet-repressed+bound gene targets in day 4 Th1 cells ([Iwata et al., 2017](#)) in day 4 B6 and *Tbx21*^{-/-} Be1 cells by RNA-seq (J) or in B6 Be1 and B6 Be2 cells by MA (K). Enrichment score (ES). Bar plot (L) shows GSEA nominal p values.

Analysis includes 3 (RNA-seq) or 7 (MA) samples/group/time point. Statistical significance was assessed using overlap p value (A–H) or GSEA FDR value analysis (J–L). Genes with an overlap p < 0.05 by IPA (see [STAR Methods](#) for description) were predicted to be upstream regulators.

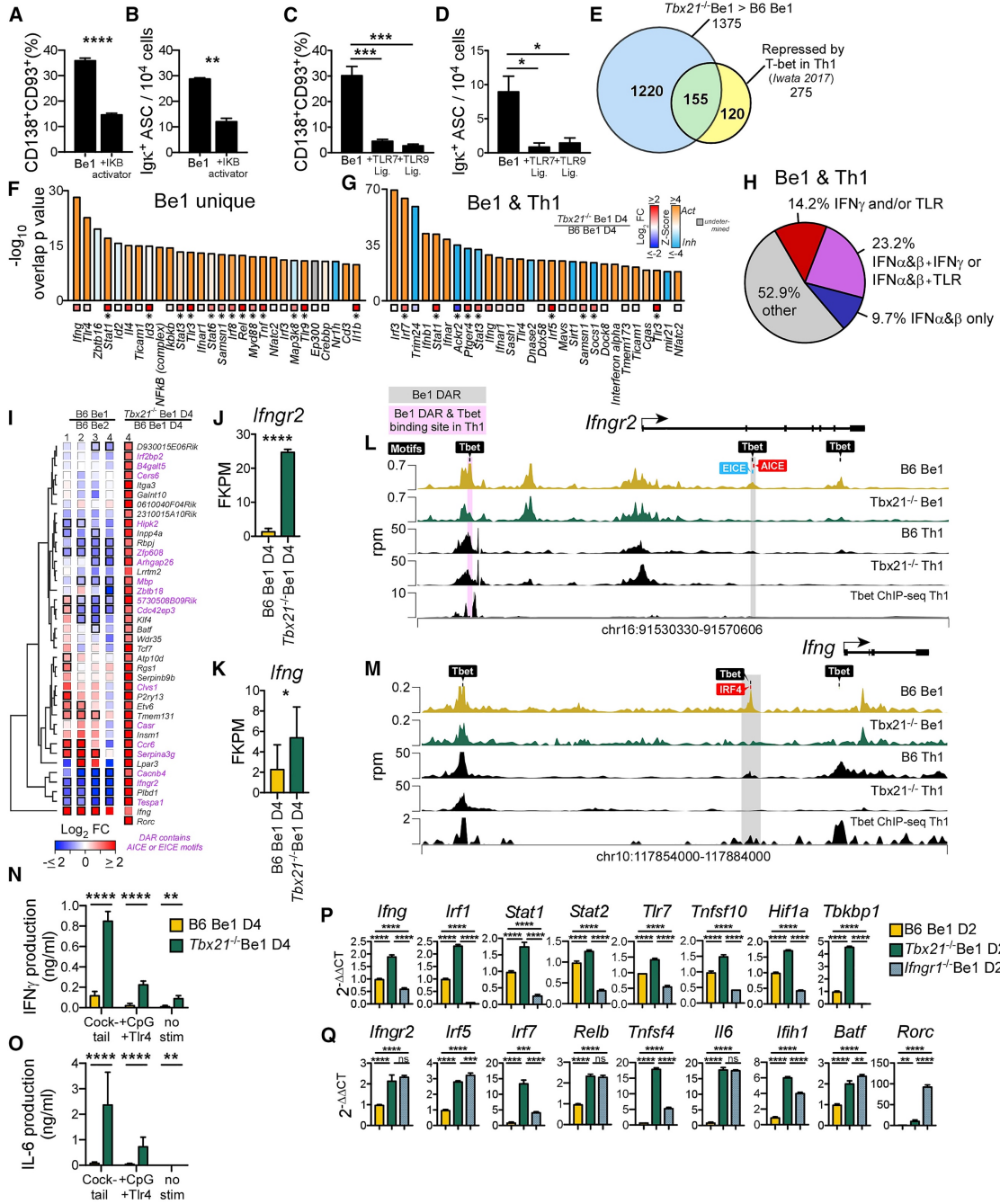


Figure 5 T-bet Supports Be1 ASC Formation by Repressing the IFN- γ -Regulated Inflammatory Gene Program

(A–D) NF- κ B activator (Betulinic acid, A and B), R848 (C and D), CpG (C and D), or vehicle (A–D) was added to day 2 B6 Be1 cultures. ASCs enumerated by flow (A and C) or ELISPOT (B and D) on day 4.

(E) Venn diagram showing T-bet-repressed genes in Th1 cells ([Iwata et al., 2017](#), n = 275) and in Be1 cells (n = 1,375). Indicated are genes unique to Be1 cells (1,220, blue), unique to Th1 cells (120, yellow), or shared (155, green).

(F and G) IPA predicted regulators of T-bet-repressed genes identified in (E) that are unique to Be1 cells (F) or shared between Be1 and Th1 cells (G), showing overlap p value (see [STAR Methods](#)) and activation Z-score (bars) and FC expression in day 4 *Tbx21*^{-/-} Be1 over B6 Be1 (asterisk indicates FDR < 0.05).

(H) IPA analysis of the 155 T-bet-repressed genes shared between Be1 and Th1 cells to identify genes that are induced (activated) by IFN- α (or IFN- β) \pm IFN- γ \pm TLR signals. Data are shown as percentage of targets that are activated by individual or multiple upstream regulators.

(I) mRNA expression heatmap of 40 T-bet-repressed genes, based on FC >2, p < 0.05 in day 4 *Tbx21*^{-/-} Be1 over B6 Be1 cells by RNA-seq that also map to T-bet binding motif containing DARs (FDR < 0.05 by ATAC-seq in in day 2 B6 and *Tbx21*^{-/-} Be1 cells). FC B6 Be1 over B6 Be2 (MA) or *Tbx21*^{-/-} Be1 over B6 Be1 (RNA-seq) is shown. Bold borders indicate FDR < 0.05. Genes with DARs containing AICE or EICE binding motifs are noted in pink. Genes (rows) are clustered based on Euclidean distance of FC and complete linkage. *Rorc* not detected in Be1 or Be2 MA samples.

(J and K) RNA-seq expression (FPKM) for *Ifngr2* (J) and *Ifng* (K) in day 4 *Tbx21*^{-/-} Be1 and B6 Be1 cells.

(L and M) Chromatin accessibility (rpm, reads per million) by ATAC-seq, within *Ifngr2* (L) and *Ifng* (M) loci in day 2 B6 Be1 (gold) and *Tbx21*^{-/-} Be1 (green) cells and day 4 B6 and *Tbx21*^{-/-} Th1 cells (black). Shaded boxes indicate DARs (FDR < 0.05) in Be1 only (gray) or Be1 and Th1 cells (pink; [Zhu et al., 2012](#)). Binding motifs for T-bet, AICE, EICE, and IRF4 are indicated.

(N and O) IFN- γ (N) and IL-6 (O) production by day 4 *Tbx21*^{-/-} Be1 and B6 Be1 cells before or after stimulation with anti-Ig F(ab')₂+anti-CD40+LPS+CpG (cocktail) or LPS+CpG.

(P and Q) qPCR analysis (described in [STAR Methods](#)) of day 2 *Tbx21*^{-/-}, *Ifngr1*^{-/-}, and B6 Be1 cells.

Data shown are representative of 2 (B, N, O, P, and Q) or 3 (A, C, and D) independent experiments and reported as mean \pm SD of 3–4 experimental replicates (A and C), duplicate dilutions (B, D, N, and O), or PCR triplicates (P and Q). Analysis includes 3 (RNA-seq) or 7 (MA) samples per group per time point. Statistical analysis was performed using Student's t test (A, B, J, and K), one-way ANOVA (C, D, P, and Q), or two-way ANOVA (N and O). Genes with an overlap $p < 0.05$ by IPA (see [STAR Methods](#) for description) were predicted to be upstream regulators. * $p < 0.05$, ** $p \leq 0.01$, *** $p \leq 0.001$, **** $p \leq 0.0001$, ns, not significant.

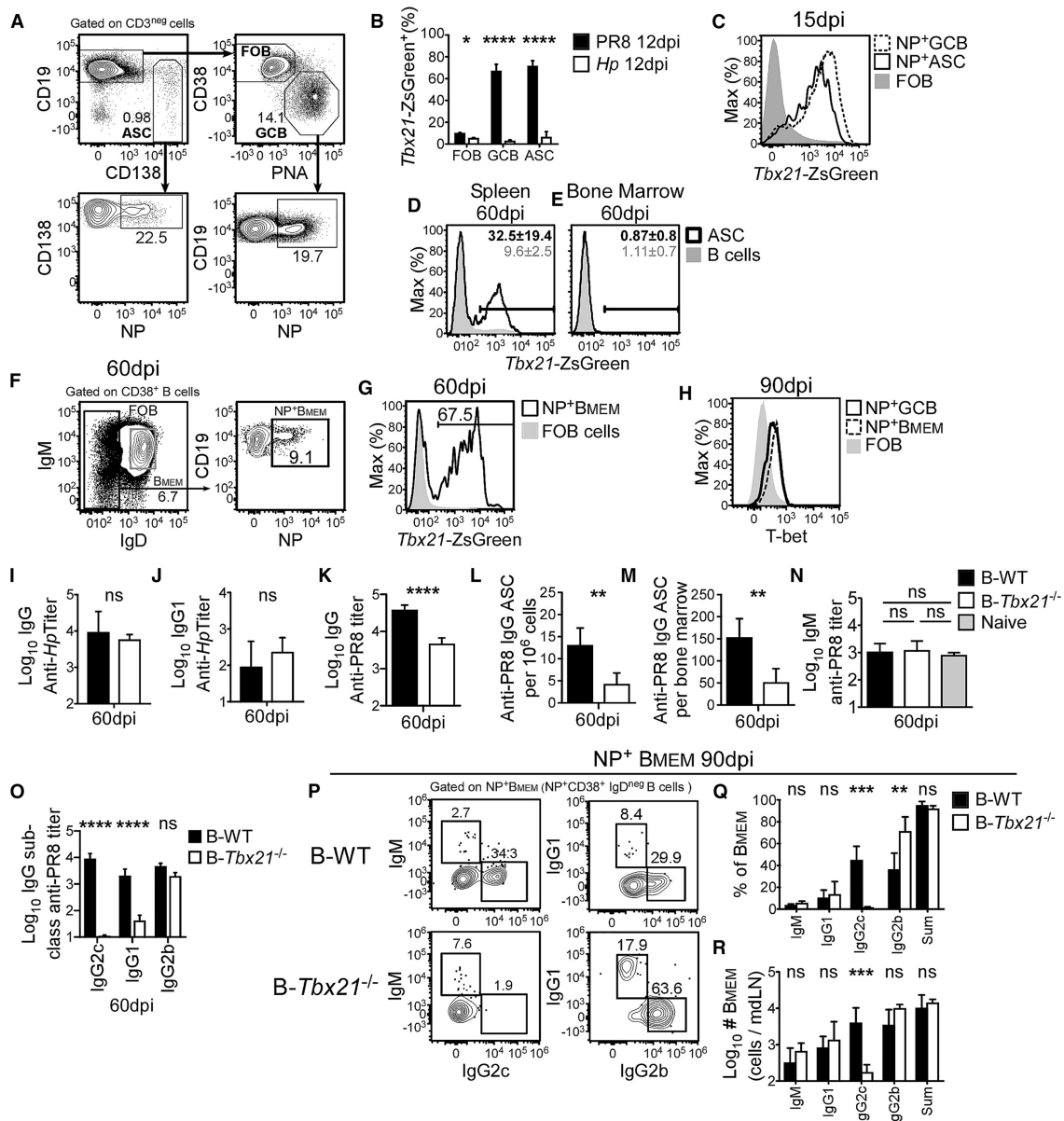


Figure 6 T-bet-Expressing B Cells Regulate Humoral Immunity to Influenza *Tbx21* reporter (A–G), B6 (H), and BM chimeric mice, generated with 80% μ MT BM + 20% B6 BM (B-WT) or 80% μ MT BM + 20% *Tbx21*^{-/-} BM (B-*Tbx21*^{-/-}) (I–R), were infected with PR8 influenza virus (A–H and K–R) or *Hp* (B, I, and J).

(A–H) Gating strategy (A) for ASC, FOB, and GCB cells (top) and for flu nucleoprotein (NP)-specific ASC and GCB cells (bottom) in mdLN 15 days post-PR8 infection. Frequencies (B) of T-bet reporter (ZsG⁺) ASC, GCB, and FOB B cells from draining LN (gated as in A) day 12 post-PR8 or *Hp* infection. T-bet reporter expression (C) by mdLN NP⁺ ASC and NP⁺ GCB cells (gated as in A) day 15 day post-PR8 infection. T-bet reporter expression day 60 post-PR8 infection in splenic (D) and BM (E) ASCs and mdLN NP-specific switched memory B cells (F

and G). Intracellular staining day 90 post-PR8 infection for T-bet (H) in mdLN NP⁺ GCB, NP⁺ switched memory B cells and FOB cells.

(I–O). Titers of *Hp*-specific IgG (I) *Hp*-specific IgG1 (J) and PR8-specific IgG (K, all subclasses) in B-WT and B-*Tbx21*^{-/-} mice 60 days post-*Hp* (I and J) or PR8 (K) infection. Frequency (L) and number (M) of PR8-specific BM IgG⁺ ASCs (ELISPOT) and titers of PR8-specific IgM (N), IgG2c, IgG1, and IgG2b (O) Abs in B-WT and B-*Tbx21*^{-/-} mice 60 days after infection.

(P–R) Gating strategy (P) to identify Ig isotype of NP⁺ memory B cells, gated on NP⁺ CD38⁺IgD^{neg} B cells. Frequency (Q) and number (R) of NP⁺ mdLN memory B cells from B-WT and B-*Tbx21*^{-/-} chimeras day 90 post-infection.

Data are representative of 2 (C–G, I–J, and P–R) or ≥3 (A, B, H, and L–N) independent experiments with 3–5 (A–J, L, M, and P–R) or 7–10 (N) mice per group and reported as mean ± SD. Data were pooled from 5 independent experiments and shown as mean ± SEM of 26–29 mice/group (K and O). p values were determined using Student's t test, *p ≤ 0.05, **p ≤ 0.01, ***p ≤ 0.001, ****p ≤ 0.0001, ns, not significant.

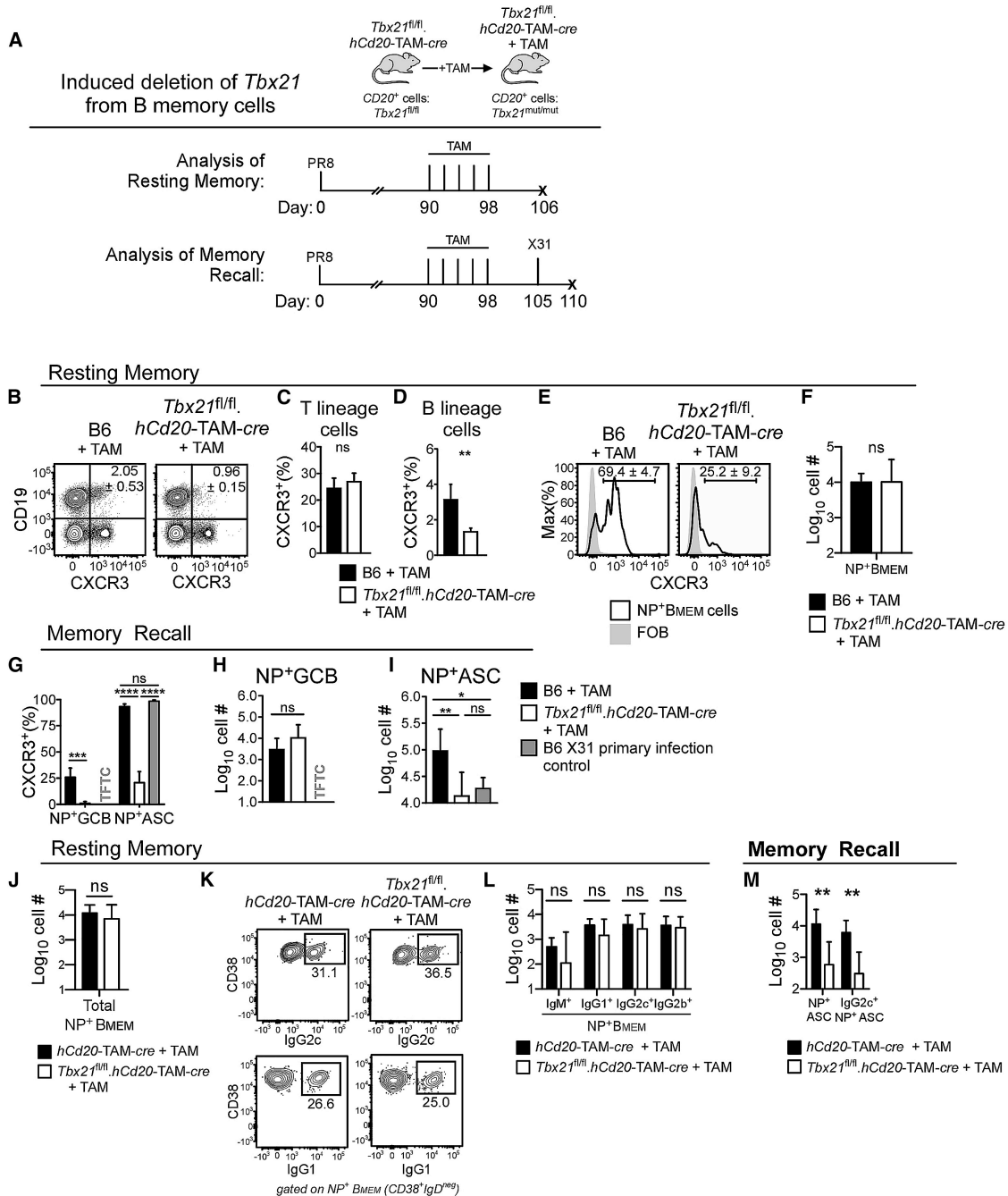


Figure 7 ASC Development after Flu Challenge Infection Requires T-bet⁺ Memory B Cells

(A–M) Experimental design (A) showing tamoxifen (TAM) treatment of day 90 PR8 flu memory *Tbx21^{fl/fl}.hCD20-TAM-cre* (B–M), *hCD20-TAM-cre* (J–M), and B6 (B–I) mice in order to inducibly delete T-bet from B cells in *Tbx21^{fl/fl}.hCD20-TAM-cre* mice. Mice analyzed (resting memory, B–F and J–L) 8 days following last TAM

treatment or challenged with X31 influenza and analyzed 5 days later (memory recall, G–I and M).

(B–E) Enumeration of CXCR3⁺ mdLN cells following TAM treatment, showing flow plots (B and E) and frequency of CXCR3⁺ T cells (C), B cells (D), and NP⁺CD38⁺IgD^{neg} memory B cells (Bmem; E).

(F) Enumeration of NP-specific Bmem cells following TAM treatment.

(G–I) Enumeration of mdLN CXCR3⁺ NP⁺ GCB cells and ASCs (G) and NP⁺ GCB cells (H) and ASCs (I) in day 5 primary X31-infected B6 mice and X31-challenged, TAM-treated B6 and *Tbx21^{fl/fl}.hCD20-TAM-cre* flu memory mice.

(J–L) Enumeration of mdLN NP⁺ memory (NP⁺CD38⁺IgD^{neg}) B cells (J) 8 days post-TAM treatment of *Tbx21^{fl/fl}.hCD20-TAM-cre* and *hCD20-TAM-cre* mice. Identification (K) and enumeration (L) of IgM, IgG1, IgG2c, and IgG2b-expressing NP⁺ Bmem cells.

(M) Enumeration of total and IgG2c⁺ NP⁺ mdLN ASCs in TAM-treated memory *Tbx21^{fl/fl}.hCD20-TAM-cre* and *hCD20-TAM-cre* mice 5 days after X31 challenge.

Representative data from one of 2 (K–M) or 3 (B–J) independent experiments are shown as the mean ± SD of 3–6 mice/group. p values were determined using one-way ANOVA (G [for NP⁺ ASCs] and I) or Student's t test (all others). *p < 0.05, **p ≤ 0.01, ***p ≤ 0.001, ****p ≤ 0.0001, ns, not significant. TFTC, too few to count (<10 cells per sample).

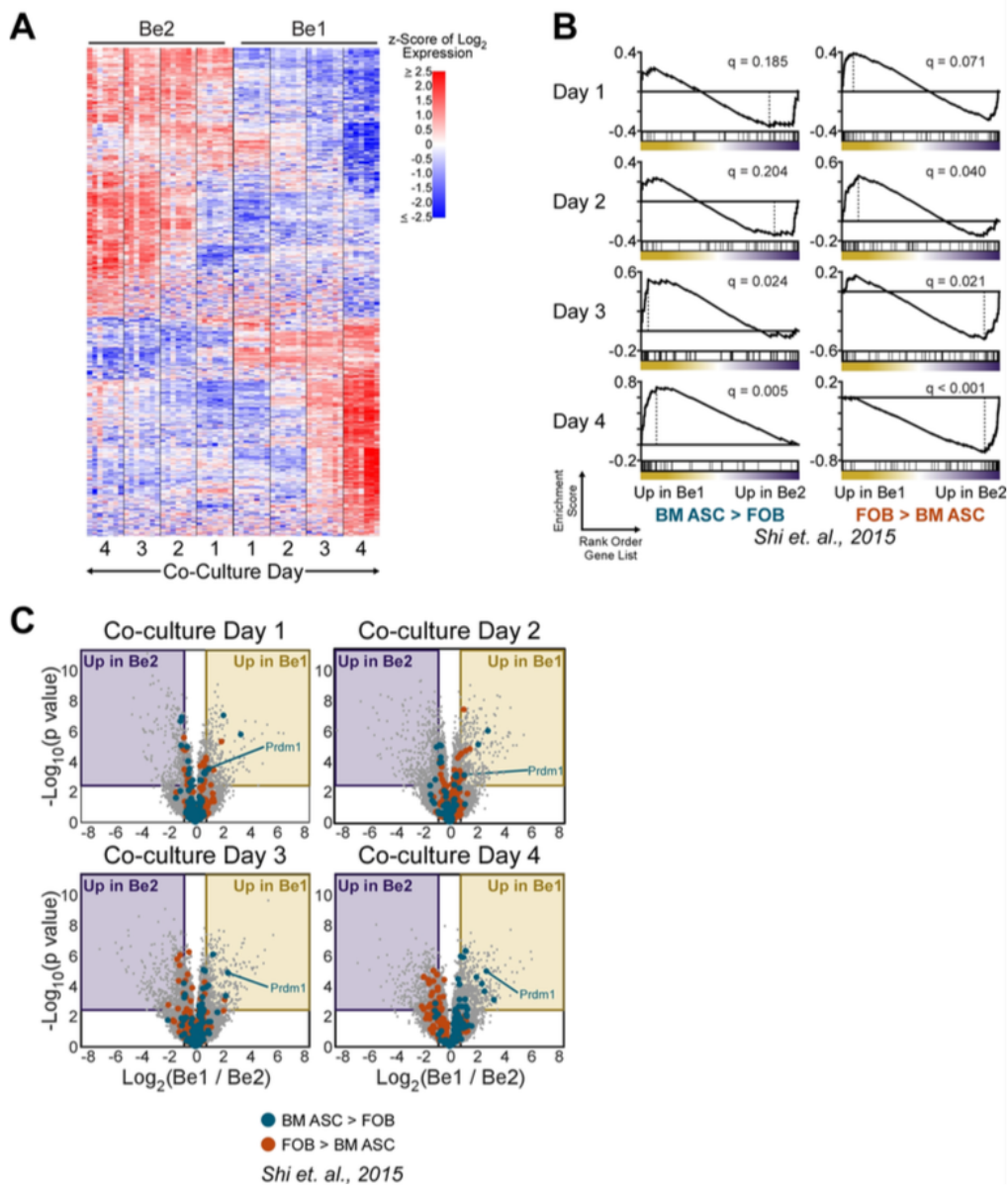


Figure S1. Be1 cells upregulate Blimp-1 by day 2 and commit to the ASC lineage between days 2- 3 (related to Fig. 1).

(A) Expression on days 1-4 of 760 genes (1022 probe sets) that exhibited a ≥ 2 -fold change and $\text{FDR} < 0.05$ between day 4 Be1 and Be2 from Affymetrix microarray (MA) data sets. Heat map showing clustered gene expression patterns over time (see also Table S1). Color corresponds to Z-score (per gene) of log_2 expression. Euclidean distance and average linkage were used for clustering.

B) GSEA plots of days 1-4 Be1 and Be2 cell MA data sets compared to TF genes reported (Shi et al., 2015) to be significantly upregulated in BM ASC or FOB. Enrichment score (ES) is plotted against the ranked gene list (n = 17186) for TF genes upregulated in BM ASC (left) or FOB (right). Dashed vertical lines indicates the cutoff for leading edge genes. See also Fig. 1G.

C) Volcano plots of Be1 and Be2 MA data showing DEGs on days 1-4 based on $q < 0.05$ and ≥ 1.75 -fold change cutoff. TFs differentially expressed in BM ASCs (blue) and FOB (red) (Shi et al., 2015) are indicated. See also Fig. 1H. MA analysis was performed with seven independent experimental samples/group/timepoint. FDR q values (B) computed based on 1000 random phenotype permutations.

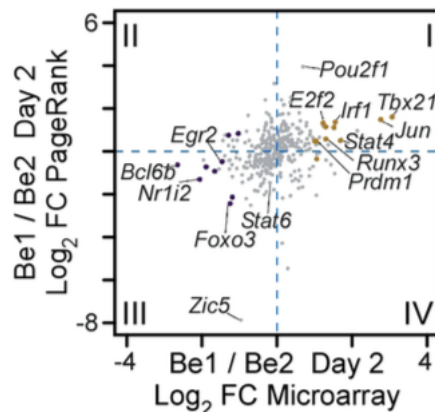


Figure S2. PageRank analysis predicts TF activity in day 2 Be1 and Be2 cells (related to Fig. 2).

Assignment of TFs to Be1 (gold) or Be2 (purple) network by PageRank analysis (Yu et al., 2017). Log₂ fold change in expression of genes by MA (X axis) is plotted against the log₂ fold change in the Be1 versus the Be2 PageRank statistic (Y axis). In quadrant I, genes shown in gold were assigned to the Be1 PageRank network, based on having both a positive log₂FC by PageRank statistic and log₂FC of > 1 and FDR < 0.05 by MA. In quadrant III, genes shown in purple were assigned to the Be2 PageRank network based on both a negative log₂FC by PageRank statistic and log₂FC of < -1 and FDR < 0.05 by MA (See also Fig. 2A and Table S3).

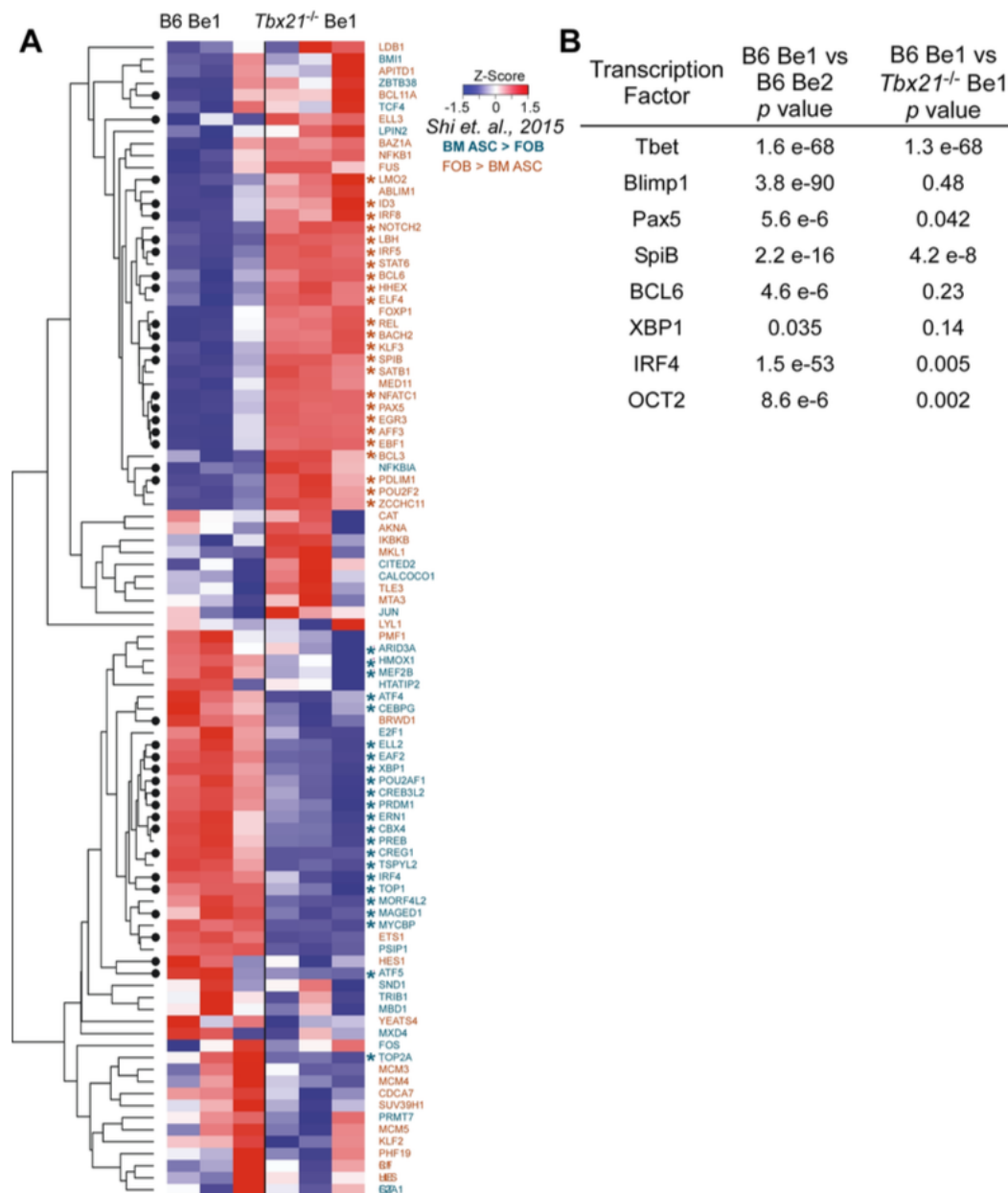


Figure S3. T-bet regulates ASC development in Be1 cells (related to Fig. 3).
 A) Heat map showing expression levels of 96 TF genes that were previously defined as differentially expressed in BM ASC and FOB (Shi et al., 2015) and were also present in the Day 4 B6 and *Tbx21*^{-/-} Be1 cell RNA-seq data sets. Heat map color corresponds to Z-score of log₂ expression of day 4 B6 and *Tbx21*^{-/-} Be1 samples from the RNA-seq data set (n= 3 independent biological samples/group).

Solid circles on dendrogram indicate genes that exhibited a ≥ 2 FC in expression and $q < 0.05$ between day 4 B6 and Tbx21^{-/-} Be1 cells. (n=3/group). Genes labeled in blue font (41 genes) are those reported to be more highly expressed in BM ASC relative to FOB and genes labeled in red font (55 genes) are those reported to be more highly expressed in FOB relative to BM ASCs (Shi et al., 2015). Asterisks indicate leading edge genes based on GSEA. See also Fig. 3D-E and Table S4. (B) p values for Fig. 3G, chromatin accessibility at transcription factor consensus DNA binding motifs in ATAC-seq data (See also Table S4). RNA-seq and ATAC-seq analysis was performed with 3 independent samples/group.

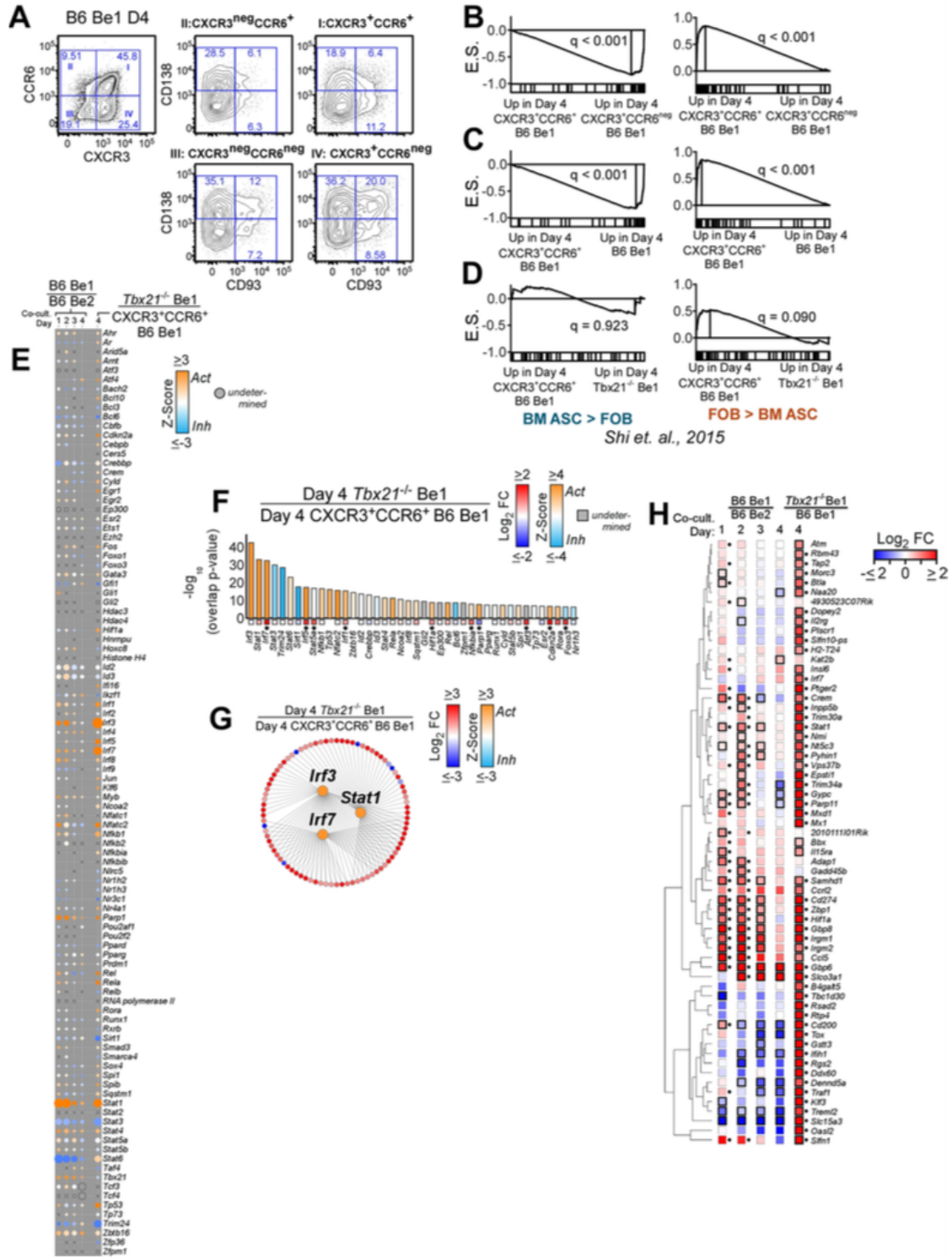


Figure S4. T-bet represses the IRF and STAT induced inflammatory signature in Be1 cells (related to Fig. 4).

(A-D) Identification of a non-ASC enriched effector cell population (CXCR3+CCR6+) in day 4 Be1 cultures. Expression of CXCR3 and CCR6 (A, left side) in B6 Be1 cells on day 4 of co-culture and expression of ASC markers CD93 and CD138 within the CXCR3 and CCR6 subsets (A, right side). Frequency of cells within gated regions are noted. GSEA plots (B-D) comparing day 4 total Be1, CXCR3+CCR6+ effector Be1, CXCR3+CCR6neg Be1 and Tbx21-/- Be1 to TF genes that are reported (Shi et al., 2015) to be significantly upregulated in BM ASC or FOB. Enrichment score (ES) is plotted against the ranked gene list for TF genes upregulated in BM ASC (left) or FOB (right). Dashed vertical lines indicates the cutoff for leading edge genes. GSEA reveals that day 4 CXCR3+CCR6neg cells are enriched in BM ASC TFs relative to the CXCR3+CCR6+ effector cells, suggesting that the CXCR3+CCR6+ population contains fewer ASCs than the CXCR3+CCR6neg population. Consistent with this conclusion, Day 4 CXCR3+CCR6+ effector Be1 cells are enriched in FOB TF genes when compared to the CXCR3+CCR6neg subset or the total Be1 cells. Moreover, CXCR3+CCR6+ effector Be1 cells and the Tbx21-/- Be1 cells show similar low expression of BM ASC TFs and GSEA reveals no significant enrichment in expression of the ASC (or FOB) defined TFs between the CXCR3+CCR6+ effector Be1 cells and Tbx21-/- Be1 cells. See Table S4 for detailed transcriptional profiling showing that the CXCR3+CCR6+ “effector” subset of Be1 cells is predominantly composed of non-ASC effector populations.

(E-G) IPA upstream regulator analysis of RNA-seq data from day 4 Tbx21-/- and B6 CXCR3+CCR6+ effector Be1 cells and MA data from days 1-4 Be1 and Be2 cells. Heatmap (E) of activation Z-scores (activated (Act), orange; inhibited (Inh), blue; or undetermined, grey) for TFs predicted by IPA to be upstream regulators of B6 Be1 over B6 Be2 (days 1-4) or day 4 Tbx21-/- Be1 over day 4 B6 CXCR3+CCR6+ effector Be1 cells. Circle size is proportional to $-\log_{10}$ overlap p value. Top IPA predicted upstream regulators (F) from the day 4 Tbx21-/- over day 4 B6 CXCR3+CCR6+ effector Be1 cells comparison ranked by overlap p value, colored by activation Z-score. Squares below bars indicate \log_2 FC in expression for each predicted regulator with * indicating FDR < 0.05. Regulator-target circular graphs (G) based on IPA upstream regulator analysis of Day 4 Tbx21-/- Be1 over Day 4 B6 CXCR3+CCR6+ effector Be1 cells. Shown are 3 selected predicted upstream regulators (center; Irf3, Irf7, Stat1) and their target genes (outer circle) with lines connecting regulators to target genes. Predicted regulators are colored by Z-score and target genes by \log_2 FC in expression determined from RNA-seq datasets. (see also Table S5 and Fig. 4A-C).

(H) Expression of genes, which are reported to be direct targets of T-bet repression in Th1 cells, in Be1 cells. Heat map display of leading edge genes identified in the GSEA comparison (see Fig. 4J-L) of day 1 Be1 vs Be2, day 2 Be1 vs Be2 and day 4 Tbx21^{-/-} Be1 vs B6 Be1 to genes that were reported to be repressed and bound by T-bet in day 4 Th1 cells (Iwata et al., 2017). Data shown as FC (log₂ expression ratio of MA data Be1 over Be2 days 1-4 and RNA-seq data Tbx21^{-/-} Be1 over B6 Be1 day 4) with black borders indicating $q < .05$ for the corresponding differential expression comparison, and black dots indicating membership in the leading-edge subset for the corresponding GSEA analysis. Genes were clustered based on Euclidean distance of the fold-change data and complete linkage.

Data shown are representative of 3 independent experiments (A). RNA-seq analysis was performed with 3 Tbx21^{-/-} Be1, 1 CXCR3⁺CCR6⁺ B6 Be1, 1 CXCR3⁺CCR6^{neg} B6 Be1, and 3 day 4 B6 Be1 samples. MA analysis was performed with 7 samples/group/timepoint. Statistical significance between samples was determined using FDR p analyses (E-G) or FDR q analyses (B-D). Genes which had on overlap p value < 0.05 by IPA were predicted to be upstream regulators (E-G).

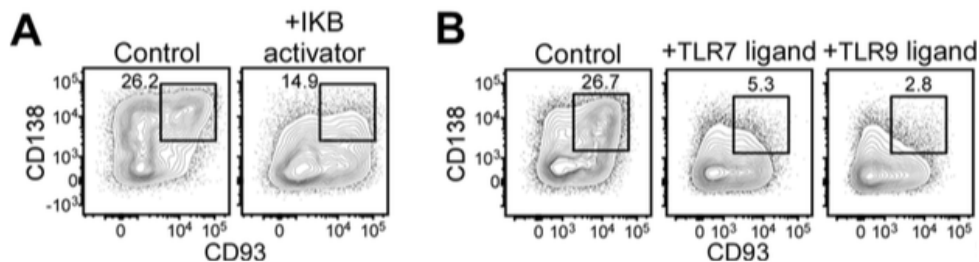


Figure S5. Sustained TLR and NF- κ B signaling prevents ASC development in Be1 cultures (related to Fig. 5).

(A) Vehicle or IKK/NF- κ B, Betulinic acid, was added to day 2 B6 Be1 cultures generated as in Fig. 1. On day 4 ASCs were quantified as CD138⁺CD93⁺ cells by flow cytometry. (See also Fig. 5A).

(B) Vehicle, TLR7 ligand R848, or TLR9 ligand CpG, was added to day 2 B6 Be1 cultures. On day 4 ASCs were identified as CD138⁺CD93⁺ cells by flow cytometry. (See also Fig. 5C). Data shown are representative of 3 independent experiments.

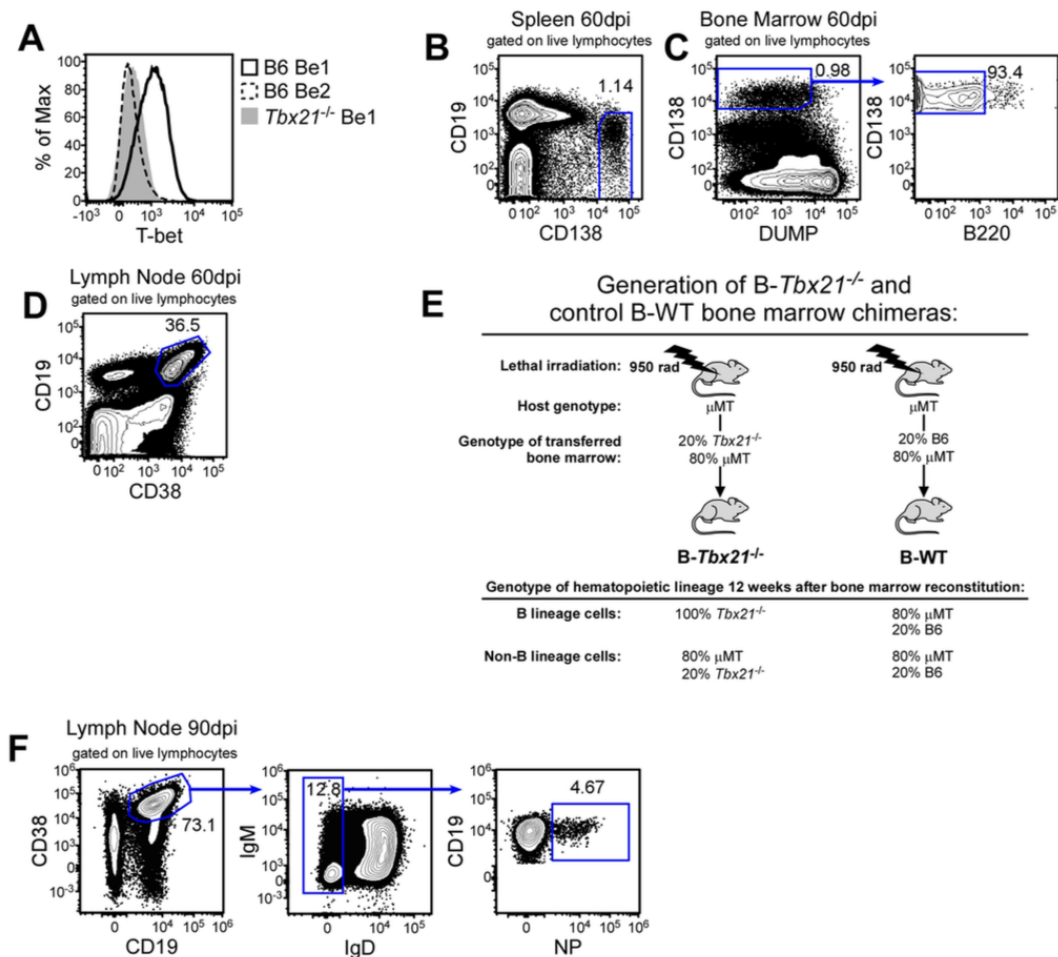


Figure S6. Identification of T-bet expressing B cells in flu-infected T-bet reporter mice and B cell bone marrow chimeras (related to Fig. 6).

(A) T-bet intracellular staining in B6 Be1, B6 Be2, and *Tbx21*^{-/-} Be1 cells on day 4 of co-culture.

(B-D) Gating strategies to identify B cell subsets in T-bet-ZsGreen reporter mice 60 days post-PR8 infection. Gating to identify splenic plasma cells ((B), see also Fig. 6D), bone marrow plasma cells ((C) see also Fig. 6E) and LN CD38+CD19+ cells ((D), see also Fig. 6F-G). Dump channel includes CD3, CD4, CD43, NK1.1, Ly6G, and Ter119.

(E) Cartoon showing generation of bone marrow chimeric mice harboring *Tbx21*^{-/-} B cells (B-*Tbx21*^{-/-} mice), and control chimeras with WT B cells (B-WT mice). Top, recipient (host) μ MT mice were lethally irradiated (950 rad) prior to adoptive transfer of a mixture of bone marrow cells, as depicted. Bottom, genotype of

hematopoietic cells after allowing 12 weeks for engraftment of transferred bone marrow.

(F) Gating strategy to identify NP+CD38+IgDneg memory B cells (BMEM) in LN of B-WT mice 90 days post-infection (See also Fig. 6P). Shown in the far-right panel are 9700 cells.

Representative data from one of 3 independent experiments with 3-4 experimental replicates (A) or 3-5 mice (B-D, F) per group.

A

Treatment Groups	Treatments Administered			Effect of Tamoxifen Treatment on B memory cells	Purpose of control
	1° infection PR8	Tamoxifen Treatment 90dp PR8	2° infection X31 (if assessing memory recall)		
Experimental Group <i>Tbx21^{fl/fl}.hCd20-TAM-cre</i> + TAM	X	X	X	T-bet deficient B memory cells	N/A
Control Groups <i>hCd20-TAM-cre</i> + TAM	X	X	X	WT B memory cells	Effect of tamoxifen-induced Cre activity in CD20+ cells
	B6 + TAM	X	X		Effect of Tamoxifen on non-transgenic cells
B6 X31 1° infection control			X	N/A (lacks B memory cells)	Lacks pre-formed PR8-specific memory cells & antibodies

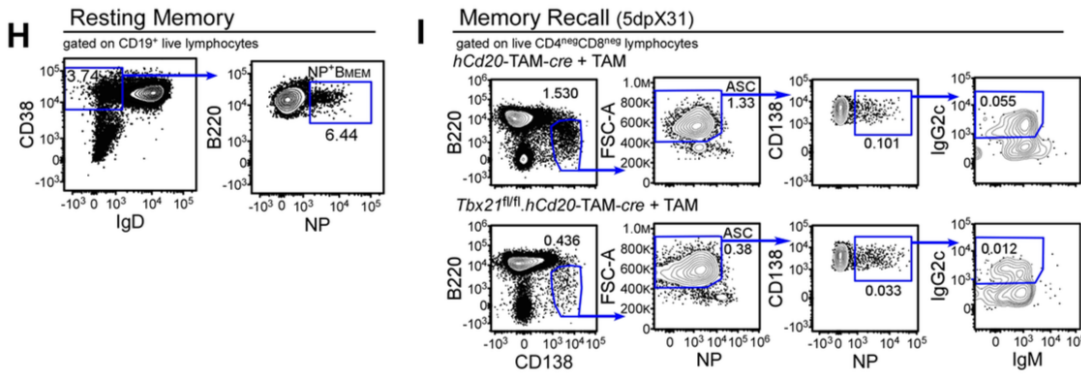
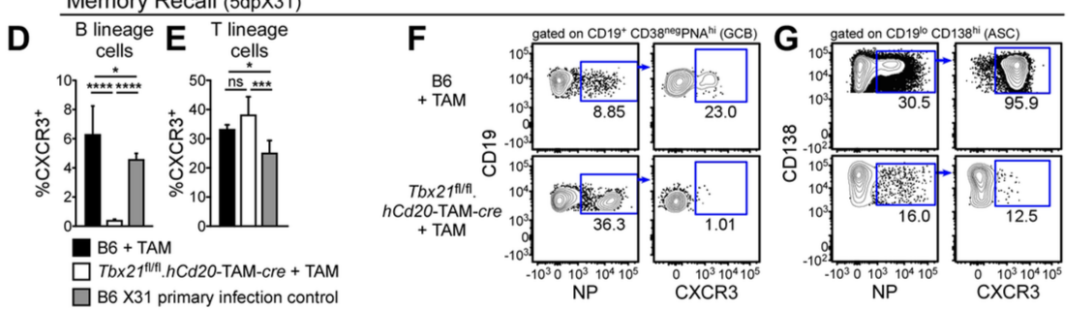
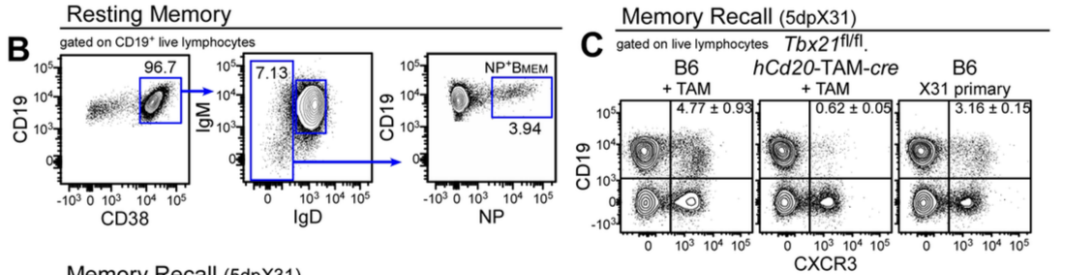


Figure S7. Identification of B cell subsets following induced deletion of Tbx21 in memory B cells (related to Fig. 7)

(A) Table depicting experimental design and rationale for controls in experiments designed to assess the effect of induced Tbx21 deletion in memory B cells (BMEM) after establishment of the memory B cell compartment (see also Fig. 7A). Following Tbx21 deletion in BMEM cells of flu memory mice, analyses were performed on the resting flu-specific BMEM compartment (see Fig. 7B-F and J-L). Alternatively, following Tbx21 deletion in BMEM cells of flu memory mice, mice were challenged with a heterosubtypic influenza virus and the BMEM-derived flu-specific GCB and ASC responses were measured (see Fig. 7G-I and M).

(B) Gating strategy to identify NP+CD38+IgDneg memory B cells (BMEM) following inducible deletion of Tbx21 in LN BMEM cells (See also Fig. 7E).

(C-E) CXCR3 expression by T and B lineage LN cells on day 5 post-challenge flu infection in tamoxifen-treated memory recall B6 and Tbx21fl/fl.hCd20-TAM-cre mice and primary infected B6 mice. Example flow plots(C) and the frequency of CXCR3+ B lineage cells (sum of CD19+ CD138neg B cells and CD19loCD138hi ASCs) (D) and CXCR3+ CD3+ T lineage cells (E).

(F-G) Gating strategy to identify NP+CXCR3+ GCB (F) and ASC (G) 5 days after X31 challenge infection, pregated on total ASC and GCB (see Fig. 6A for pre-gates). See also Fig. 7G-I for quantitation. (H) Gating strategy to identify NP+CD38+IgDneg BMEM cells. See also Fig. 7J-L for quantitation of flu-specific BMEM subsets.

(I) Gating strategy to identify NP+IgG2c+ ASC 5 days after X31 challenge infection. The frequency of each gated population within the total live lymphocyte population is indicated. See also Fig. 7M for quantitation. Representative data from one of 2 (I) 3 (B-H) independent experiments, shown as the mean + SD of 3- 6 mice/group. p values were determined using one-way ANOVA *p<0.05, ***p≤0.001, ****p≤0.0001 or “ns” not significant.

A ROLE FOR DUAL BCR AND TLR-INDUCED IRF1 EXPRESSION IN B CELL
FATE SPECIFICATION

by

JESSICA N. PEEL, AARON SILVA-SANCHEZ, JOHN F. KEARNEY, FRANCES E.
LUND

In preparation for *Nature Immunology*
Format adapted for Dissertation

SUMMARY

IRF1, an interferon (IFN)-inducible transcription factor, regulates T cell and macrophage fate specification and function, however a role for IRF1 in controlling B lineage fate decisions has not been established. We show that IRF1 expression specifically in B cells is necessary for optimal T cell independent antibody responses and is required for marginal zone (MZ) B cell development. While IFNs can induce IRF1 expression in MZB precursors, IFN signaling is not required for MZB cell development. Instead, BCR and TLR signals, which influence MZB commitment, cooperate to promote IRF1 expression and nuclear translocation in MZB precursors. In turn, IRF1 facilitates the development of the MZB cell compartment but also prevents selection of autoreactive B cells into the follicular B cell repertoire. Thus, IRF1 integrates BCR and TLR signals to ensure appropriate selection of B cells into the mature, non-autoreactive follicular and MZB cell compartments.

KEYWORDS

IRF1, Marginal Zone B cells, BCR, TLR, interferon, transitional B cells

INTRODUCTION

The mature B cell compartment is composed of B1 cells, follicular B cells (FoB) and marginal zone (MZB) B cells (Kantor et al., 1992; Martin et al., 2002). These mature B cell subsets, which develop from different progenitor populations (Hayakawa et al., 1983; Hayakawa et al. 1985), exhibit distinct B cell receptor (BCR) repertoires and specificities (Yang et al., 2015) that influence the functional attributes of each subset. For example, the BCR repertoire of the fetal liver-derived, innate-like B1 B cells is skewed toward polyreactive specificities (Martin et al., 2002; Baumgarth et al., 2005). These cells, which reside in the serosal cavities (Kantor et al., 1992), can be activated in a T cell independent (T-I) manner to produce “natural” antibodies that mediate rapid protection from infection across a broad range of pathogens (Baumgarth et al., 2005; Bos et al., 1989; Haury et al., 1997; Hayakawa et al., 1983; Hayakawa et al., 1985; Hooijkaas et al., 1984). The BCR repertoire of the MZB cells, which are derived from bone marrow progenitor cells, is also restricted (Yang et al., 2015) and enriched for reactivity to pathogen-associated carbohydrate and lipid antigens (Durbin et al., 2018; Huflejt et al., 2009). The MZB cells, like the B1 cells, can be activated to produce antibodies in the absence of T cell help (Martin et al., 2000; Martin et al., 2002). Thus, the MZB cell subset, which is predominately sessile (shuttling?) and found within the marginal zone of the spleen (Martin et al., 2000; Martin et al., 2002), is geographically poised to rapidly respond to antigens derived from systemic pathogens (Martin et al., 2001; Martin et al., 2002; Oliver et al., 1997). By contrast, the BCR repertoire of the adult bone marrow-derived conventional FoB cells is very diverse (Yang et al., 2015) and encompasses specificities across a wide range of protein epitopes (MacLennan et al., 1997). FoB cells, which recirculate through secondary lymphoid tissues (Bajénoff et al., 2006; Cyster et al., 2010), typically participate in T cell-dependent (TD) immune responses (MacLennan et al., 1997) that are initiated in interfollicular regions of secondary lymphoid tissues (De Silva et al., 2015) and within days highly specialized germinal center (GC) structures are formed (De Silva et al., 2015).

Despite differences in ontogeny, localization, BCR specificity and functional properties, the development of all three mature B cell subsets from their hematopoietic progenitors is a highly-regulated process (Hardy et al., 1991) that integrates signals provided by (self)-antigens, the cellular microenvironment and endogenous or pathogen associated ligands of Toll-Like Receptors (TLRs) (Martin et al., 2002). These signals also play key roles

in the commitment of all three mature B cell subsets to the antibody secreting cell (ASC) lineage. For example, although the B cell receptor (BCR) signaling thresholds required to support development and differentiation differ between the B cell subsets (Cyster et al., 1995; Cyster et al., 1996; Cyster et al., 1997), BCR signaling regulates positive and negative selection of all B progenitors and the activation and proliferation of all mature B cells (Pillai et al., 1999, Martin et al., 2002; Nutt et al., 2015). Similarly, while TLR expression levels differ between the different developing and mature B cell subsets (Hua et al., 2013), TLR ligands broadly influence B cell selection, activation, proliferation and differentiation (Gavin et al., 2007; Rawlings et al., 2012; New et al., 2020). Finally, while the different mature B cell subsets reside in distinct locations, each subset receives microenvironment-derived cellular cues that support subset specification and differentiation. These niche-specific cells, which can include stromal cells, T cells, dendritic cells and macrophages (You et al., 2011; Pirgova et al., 2020; Fasnacht et al., 2014), provide direct contact-dependent co-stimulatory signals to B cells (Chen et al., 2013), capture antigen for sampling by B cells (Hannum et al., 2000) and produce cytokines that regulate B cell survival, proliferation, class switch recombination (CSR) and differentiation (Jandl et al., 2016).

Key microenvironment-derived developmental programs mediated by resident neighboring cells must coordinate with a continuum of BCR signaling thresholds to ensure the selection of newly formed B cells into the appropriate mature B cell compartment (Pillai et al., 2009; Hammad et al., 2017; Wen et al., 2005). For example, deleterious mutations in activating factors of BCR signaling, thereby attenuating BCR signaling strength, results in the relative preservation of the MZB cell compartment and a loss of the FoB cells (Hardy et al., 1983; Hikida et al., 2003; Wen et al., 2003; Pillai et al., 2009). Similarly, in the absence of inhibitory regulators of BCR signaling, thereby enhancing BCR signaling strength, MZB cells are markedly decreased (Samardzic et al., 2002; Pillai et al., 2009). Therefore, MZB cells appear to require relatively “weak” BCR signals whereas FoB cells depend on “strong” BCR signals for their development.

How the cues provided by antigen, the cellular microenvironment and TLR ligands are integrated to specify different B cell fate decisions remains unclear, however transcription factors that are expressed or activated in response to these signals are clearly important. Indeed, we know that signaling through cytokine receptors, TLRs and the BCR induces expression and/or activation of multiple transcription factors including members of the

STAT, T-box, NF-KB and IRF families (Luu et al., 2014; Xu et al., 2015; Stone et al., 2019). Many of these transcription factors are intimately involved in B cell fate decisions. For example, IRF8 supports maintenance of the B cell identity program (Xu et al., 2015) while the T-box family member T-bet prevents B cells from adopting an alternate inflammatory effector cell fate (Stone et al., 2019). By contrast, IRF4 promotes commitment of the mature B cells to the ASC transcriptional program (Xu et al., 2015). Thus, it is the balance of transcription factors that control cell fate specification and initiate the new transcriptional and epigenetic programs that endow the B cells and ASCs with unique functional attributes.

We previously showed that mature B cells activated in the presence of the inflammatory cytokine IFN γ upregulate expression of the transcription factors, T-bet and IRF1 (Stone et al., 2019). We further demonstrated that T-bet is required for IFN γ -dependent ASC development (Stone et al., 2019). Notably, our transcriptome and epigenome analyses of the mature B cells induced to differentiate to ASCs in an IFN γ -dependent fashion, also identified IRF1 as a key transcriptional regulator of this process (Stone et al., 2019). This was intriguing as IRF1 was previously shown to regulate Th1 cell differentiation by initiating expression of lineage specifying genes and repressing alternative effector cell fates (Taki et al., 1997; Kano et al., 2008). Although less is known about the role for IRF1 in B cells, early studies revealed that IRF1 can block cell cycle in B cells (Yadama et al., 1991). Consistent with this finding, global deletion of *Irf1* resulted in increased numbers of GC B cells and ASCs in the MHV-68 viral infection model (Mboko et al., 2016). By contrast, B cell-selective deletion of *Irf1* resulted in fewer GC B cells and ASCs in the setting of chronic MHV-68 infection (Jondle et al., 2020).

The published results, while suggesting an intrinsic role for *Irf1* in B cell responses, were complicated to interpret as MHV-68 is a chronic pathogen that infects and establishes latency in B cells (Flaño et al., 2002) and it is known that EBV-family viruses can alter the transcriptional programming of B cells (Hatton et al., 2014). Therefore, we set out to test the hypothesis that IFN γ -induced IRF1, like other IRF family members, can influence B cell lineage specification and/or lineage commitment. We show that *Irf1* expression by mature B cells is required for ASC differentiation in response to IFN γ and TLR signals. We demonstrate that B cell intrinsic expression of *Irf1* is required for T-I antibody responses and for the development of the innate-like MZB cell compartment. Surprisingly, *Irf1*-dependent MZB cell development does not require IFN γ signaling. Instead, BCR and TLR signals cooperate

to induce IRF1 expression and IRF1 nuclear translocation in immature transitional B cell precursors. In turn, *Irf1* supports the selection of self-reactive developing B cells into the MZB cell pool. Importantly, *Irf1*^{-/-} self-reactive B cells undergo altered selection into the FoB cell compartment thereby predisposing autoreactive B cells to T cell help. Consistent with this, we observe that *Irf1* deletion in B cells results in the spontaneous emergence of GCB cells and the production of autoantibodies. Collectively, these data indicate that IRF1, induced in response to BCR and TLR signals, regulates B cell fate decisions and the development of a normal non-autoreactive mature B cell compartment.

RESULTS

IRF1-expressing B cells regulate early IgM responses to influenza infection.

We previously identified the IFN γ -inducible transcription factor, IRF1 as a potential upstream regulator of ASC commitment in B cells activated with antigen in the presence of IFN γ -producing Th1 cells (Stone et al 2019). To test whether IRF1 was required for the formation of ASCs we co-cultured Th1 cells with C57BL/6J (wildtype, WT) B cells or *Irf1*^{-/-} B cells in the presence of anti-IgM Fab'2 + IL-2 for 4 days and enumerated ASCs and secreted antibody (Ab). We observed a significant reduction in the frequency of CD93⁺CD138⁺ ASCs in the *Irf1*^{-/-} Be1 co-cultures compared to WT Be1 co-cultures (Fig. 1A-B). Consistent with this, Ab secretory rates were also significantly decreased in the *Irf1*^{-/-} Be1 cultures (Fig. 1C). Therefore, B cell intrinsic expression of IRF1 is important for Th1-induced ASC development *in vitro*.

While our data demonstrated a B cell intrinsic role for IRF1 during Be1 cell differentiation, the requirement for IRF1-expressing B cells *in vivo* is less clear with a prior report revealing that antibody responses in mice selectively deficient in *Irf1* expression in B cells were unaffected following LCMV infection but significantly decreased after MHV68 infection (Jondle et al., 2020). Since our prior data indicated that influenza infection induces expansion of Be1-like cells (Stone et al., 2019), we hypothesized that IRF1-expressing B cells would be required for development of flu-specific ASCs and serum Ab. To test this, we generated bone marrow (BM) chimeric mice (Fig. S1A), which were either *Irf1* sufficient in all lineages (B-WT mice) or lacked *Irf1* in B cell lineage cells (B-*Irf1*^{-/-} mice), and infected the reconstituted chimeras with influenza A/Puerto Rico/8/1934 H1N1 (PR8) virus. On day 15 (D15) post-infection, we enumerated the T cell-dependent influenza nucleoprotein (NP)-specific (Allie et

al., 2019) GC B cells and ASCs (Fig. S1B) in the draining mediastinal LN (medLN). In opposition to the MHV-68 infection studies that showed a decrease in the number of total GC B cells in B-*Irf1*^{-/-} mice (Jondle et al., 2020), we observed a significant expansion in the frequency and number of flu NP-specific GC B cells in B-*Irf1*^{-/-} chimeric mice (Fig. 1D-F). However, unlike what was observed after MHV-68 infection where ASC numbers were reduced in the B-*Irf1*^{-/-} mice (Jondle et al., 2020), the frequency and number of NP-specific ASCs in the B-*Irf1*^{-/-} mice were unchanged on D15 post-influenza infection (Fig. 1G-I). Furthermore, and consistent with this result, flu-specific Ab titers were equivalent between B-WT and B-*Irf1*^{-/-} mice on D60 post-infection (Fig. 1J). This outcome, which was similar to what was reported for LCMV infected B-*Irf1*^{-/-} mice (Jondle et al., 2020), suggested that IRF1 expression by B cells is not required for T cell-dependent (T-D) long-lived Ab responses to influenza.

Although we did not identify a role for *Irf1* expression by B cells in the T-D Ab response to influenza, flu infection also induces a T cell-independent (T-I) IgM Ab response (Lee et al., 2011). To assess a potential role for IRF1 in B cells during the T-I response to flu infection, we evaluated the D10 flu-specific IgM antibody response in B-WT and B-*Irf1*^{-/-} chimeras. Interestingly, PR8-specific IgM on D10 post-flu infection was significantly decreased in serum from B-*Irf1*^{-/-} chimeric mice compared to B-WT animals (Fig. 1K). Thus, while *Irf1* expression by B cells is not required for the development of the T-D and GC-dependent flu-specific ASC and IgG Ab responses, IRF1 does appear to play a role in the development of the early flu-specific IgM Ab response.

Irf1-expressing B cells are required for T cell independent antibody responses

Since *Irf1*-expressing B cells regulated the early IgM response but not the GC-dependent IgG response to PR8 infection, we hypothesized that *Irf1* expression by B cells might be important for ASC differentiation in response to signals delivered in the absence of cognate interactions between B cells and T cells. To test this hypothesis, we evaluated the ASC differentiation potential of splenic WT or *Irf1*^{-/-} CD19⁺ B cells activated with anti-IgM, cytokines (IFN γ , IL-21, and IL-2) and either LPS (Toll-Like Receptor 4 (TLR4) ligand) or R848 (TLR7 ligand). We found that the D3 TLR-stimulated *Irf1*^{-/-} B cell cultures contained significantly fewer CD93⁺CD138⁺ ASCs relative to the WT B cell cultures (Fig. 2A-B). We also observed that Ab

secretion by the stimulated *Irf1*^{-/-} B lineage cells was impaired relative to WT B cells (Fig. 2C). These data therefore show that IRF1 can promote ASC differentiation in response to signals delivered by cytokines, TLR ligands and antigen, at least *in vitro*.

Given that IRF1 appears to regulate ASC development independently of T:B cognate signals, we next asked whether IRF1-expressing B cells are required for T-I Ab responses *in vivo*. We immunized WT and *Irf1*^{-/-} mice with a model T-I antigen, Ficoll haptenated with trinitrophenyl (TNP-Ficoll), and measured the anti-hapten IgM response on D7 post-vaccination. In agreement with the *in vitro* data, we observed a significant decrease in anti-nitrophenyl specific IgM titers in the *Irf1*^{-/-} mice (Fig. 2D). To confirm these results, we intravenously vaccinated WT and *Irf1*^{-/-} mice with heat-killed *Streptococcus pneumoniae*, a well-characterized, physiologic activator of T-I Ab responses directed against the outer membrane constituent phosphorylcholine (PC). We observed a significant reduction in PC-specific IgM responses in *Irf1*^{-/-} mice (Fig. 2E). Thus, *Irf1* is required for the development of multiple T-I antigen driven Ab responses.

Splenic marginal zone B cells and macrophages are decreased in Irf1^{-/-} mice

T-D and T-I responses are directed by distinct mature B cell populations with follicular B cells (FoB) playing a key role in T-D humoral immunity and splenic marginal zone B cells (MZ B) and serous cavity B1 cells contributing to T-I responses (Martin et al., 2002). To assess whether the MZ B and B1 compartments were intact in the *Irf1*^{-/-} mice, we enumerated the B1 cells in the peritoneal cavity (PerC) and MZ B cells in the spleen of WT and *Irf1*^{-/-} mice. The B1 compartment, which contains the CD5⁺ B1a and CD5^{neg} B1b cells (Fig. 3A), was not appreciably different between the *Irf1*^{-/-} and WT mice (Fig. 3B-C). Likewise, no differences were seen (data not shown) in the number of PerC CD11b^{+/+} B1 B cell subsets (Ghosn et al., 2011). Similarly, when we examined the spleen of WT and *Irf1*^{-/-} mice (Fig. 3D) we observed no differences in the number of CD23⁺CD21^{lo} FoB cells (Fig. 3E). However, the number of splenic CD23^{neg}CD21^{hi} MZ B cells was significantly reduced in the *Irf1*^{-/-} mice (Fig. 3F). This finding remained true even when we used alternate markers such as CD1d, CD9 and CD36 (Won et al., 2002; Won et al., 2008; Amano et al., 1998), to identify MZ B cells (Fig. S2A-F). Thus, *Irf1* appears to regulate the size of the splenic MZ B cell compartment.

The splenic MZ is unique microenvironment at the interface of the white and red pulp, which is occupied by specialized subsets of MZ B cells and SIGNR1⁺ marginal zone macrophages (MZM) that are poised to sample and respond to blood-borne antigens (Pillai et al. 2005) and to clear cell debris and apoptotic bodies (New et al., 2016). Prior studies revealed that close association of the MZM and MZ B cells is required for the development and maintenance of both populations and is necessary for optimal T-I Ab responses (You et al., 2011). Given the reduction in the phenotypically defined MZ B subset in the *Irf1*^{-/-} mice, we hypothesized that *Irf1* would be critical for the establishment of the anatomically-defined MZ. To test this, we used fluorescence microscopy to visualize the MZ in the spleens of WT and *Irf1*^{-/-} mice. Consistent with our flow cytometric analyses, the characteristic ring of CD1d⁺B220⁺ MZ B cells outlining the white pulp areas appeared to be missing in the spleens of *Irf1*^{-/-} mice (Fig. 3G). To quantify this observation, we identified the MZ B cells in the section by examining the fluorescence intensities of CD1d and B220 in all nucleated cells (Fig. 3H). Consistent with our flow cytometric analysis, the frequency of CD1d⁺B220⁺ cells was significantly reduced in the spleens of the *Irf1*^{-/-} mice (Fig. 3I). Next, we used an x and y grid to assign the location of the CD1d⁺B220⁺ cells within the spleen section (Fig. 3J) and then calculated the area occupied by these cells (Fig. 3K). In agreement with the reduced numbers of MZ B cells in the *Irf1*^{-/-} mice, the splenic area occupied by the CD1d⁺B220⁺ *Irf1*^{-/-} B cells was reduced relative to the area occupied by the WT CD1d⁺B220⁺ B cells (Fig. 3K). However, the localization of the CD1d⁺B220⁺ B cells within the spleen was similar between the *Irf1*^{-/-} and WT mice. Indeed, the few remaining CD1d⁺B220⁺ B cells in the spleens of *Irf1*^{-/-} mice were found adjacent to B cell follicles in close proximity to the MZ and were not present in the white or red pulp (Fig. 3J). Thus, *Irf1* is required for the establishment or maintenance of the anatomically defined MZ B cell subset.

Given that the differentiation, maintenance and functional properties of MZ B cells and MZM are intertwined (You et al., 2011), we next asked whether the loss of *Irf1* impacted the architecture and cellular composition of the MZ. In accordance with previous publications demonstrating the loss of the SIGNR1⁺ MZM population in mice lacking MZ B cells (You et al., 2011), quantitative image analysis (Fig. 3L) revealed a significant reduction in the area occupied by the SIGNR1⁺ MZM (Fig. 3G) within the spleens of *Irf1*^{-/-} mice. To confirm this result, we used flow cytometry to assess whether the CD11b⁺Tim4⁺ MZM population, which

is reported to be dependent on MZ B cells (Fujiyama et al., 2019), was affected by the loss of *Irf1* (Fig. 3M). In support of the histologic analysis, significantly fewer Tim4⁺ MZM were identified in the *Irf1*^{-/-} mice (Fig. 3N-O). Taken together, these data suggest that IRF1 regulates T-I responses by controlling the development or maintenance of the splenic MZ B cells and macrophages that respond to blood-borne particulate antigens.

B cell intrinsic expression of Irf1 is required for MZ B cell responses.

Our data showed that the splenic MZ B cell and MZM compartments were significantly decreased in *Irf1*^{-/-} mice. Given that the survival or maintenance of these two subsets is linked (You et al., 2011; Fujiyama et al., 2019) and that IRF1 can be expressed by myeloid (Langlais et al., 2016) and lymphoid lineage (Penninger et al., 1997) cells, it was important to assess whether IRF1 directly influences the development or maintenance of MZ B cells. To address this question, we first examined whether MZ B cell development was intact in the *Irf1*^{-/-} mice. We therefore used the well-characterized (Van Epps et al., 2006) Hardy B cell development scheme (Fig. S3A) to enumerate early pre-pro B (Fr. A), pro-B (Fr. B-C), pre-B (Fr. D) and immature (Fr. E) cells in the bone marrow (BM) of WT and *Irf1*^{-/-} mice. Interestingly, the *Irf1*^{-/-} mice exhibited a small but significant reduction in the frequency and number (Fig. 4-B) of Fraction C cells, which include late pro-B cells that are undergoing selection for expression of the IgH pro-B cell receptor (Hardy et al., 2001). However, no differences were seen in any of the other BM subsets, including Fraction D that is undergoing pre-B cell receptor selection (Fig. 4A-B). These data suggest that IRF1 expression is not obligate for B cell development in the BM.

Although we didn't identify any major role for IRF1 in B cell development in the BM, B cell maturation continues in the spleen where the BM-derived mature B cells undergo additional negative and positive selection steps as transitional (T1 and T2) cells that then commit to the mature MZ B or FoB lineages (Metzler et al 2015). To assess the role of IRF1 in the final stages of B cell development we analyzed the splenic T1 and T2 subsets (Fig. S3B) in WT and *Irf1*^{-/-} mice. Again, we found that the frequency and numbers of these cells were unchanged between WT and *Irf1*^{-/-} mice (Fig. 4C-D).

The data showed that IRF1 is not required for the development of the direct splenic precursors of the FoB and MZ B cell subsets. Therefore, we hypothesized that IRF1 may play a B cell intrinsic role during the commitment of transitional cells to the MZ B lineage. To assess this possibility we examined the transitional, MZ B and FoB compartments in B-WT and B-*Irf1*^{-/-} mice (Fig. S1A). Similar to what we observed in animals with a global deletion of *Irf1*, deletion of *Irf1* in the B lineage alone did not affect the number of T1 and T2 cells present in the spleen of these mice (Fig. 4E-G). However, we observed a significant reduction in the number of splenic MZ B cells in the B-*Irf1*^{-/-} mice compared to B-WT mice (Fig. 4H-I). Moreover, we found that the number of FoB cells was significantly increased in the B-*Irf1*^{-/-} animals (Fig. 4H, J). Since the splenic transitional compartment is intact in these animals, the data suggested that *Irf1* may play a role at the bifurcation step where transitional cells are selected into either the FoB or MZ B cell lineage.

Although the phenotypically defined MZ B subset was clearly reliant on *Irf1* expression by B cells, we could not exclude the possibility that other IRF1-expressing cells, like the MZM, might influence the development, placement or maintenance of these cells within the anatomically defined MZ. To address whether B cell intrinsic *Irf1* was critical for appropriate placement of B cells within the MZ, we generated 50:50 BM chimeric mice that were reconstituted with equivalent numbers of BM cells from CD45.1⁺ WT mice and CD45.2⁺ *Irf1*^{-/-} mice. Following reconstitution, we examined the proportion of FoB and MZ B cells derived from each genotype (Fig. 4K). As expected, the percentages of CD45.1⁺ WT and CD45.2⁺ *Irf1*^{-/-} cells present the spleens of the 50:50 chimeras were largely equivalent (Fig. 4L). Likewise, the fractions of CD45.1⁺ WT FoB and CD45.2⁺ *Irf1*^{-/-} FoB were similar (Fig. 4M). By contrast, the percentage of WT MZ B cells was approximately 3.5-fold increased relative to the *Irf1*^{-/-} MZ B cells in the same animals (Fig. 4N). These data again support the conclusion that B cell intrinsic expression of IRF1 is necessary for the establishment or maintenance of the MZ B cell subset.

Next, we examined the architecture of the spleen in the WT and *Irf1*^{-/-} 50:50 BM chimeras (Fig. 4O). We first identified the CD45.1⁺ and CD45.2⁺B220⁺ B cells (Fig. 4P) and mapped the location of these cells relative to the CD169⁺ metallophilic marginal zone macrophages (MMMs) that line the border between the white pulp and MZ (Fig. 4Q). We then enumerated

the CD45.1⁺ WT and CD45.2⁺ *Irf1*^{-/-} B cells that were located outside of the B cell follicle and within the MZ (Fig. 4R-S). Similar to the flow cytometric analysis of MZ B cells in the mixed BM chimeras, significantly fewer *Irf1*^{-/-} B cells were localized within the MZ of the spleen (Fig. 4S). However, the relative proportions of WT and *Irf1*^{-/-} B cells localized in the MZ of the spleen (Fig. 4S) were very similar to the proportions of MZ B cells identified by flow cytometry in the mixed BM chimeras (Fig. 4N). Moreover, expression of integrins and chemokine receptors, like CD11a, CD18, CD49d, CD29 and CXCR7, which are known to regulate localization of B cells within the MZ (Lu et al., 2002; Wang et al., 2012), was very similar between the WT and *Irf1*^{-/-} B cells (Fig. S4). These data therefore argue that B cell intrinsic expression of *Irf1* is not required for placement of B cells within the MZ region and may play a more important role during the development of these cells.

Finally, given the B cell intrinsic role for IRF1 in the establishment of the MZ B cell compartment, we predicted that B cell intrinsic expression of *Irf1* is necessary for optimal T-I immune responses. To test this prediction, we generated B-WT and B-*Irf1*^{-/-} chimeras (Fig. S1A), immunized the mice with either TNP-Ficoll or heat-killed *S. pneumoniae* and measured nitrophenyl-specific (Fig. 4T) or PC-specific (Fig. 4U) IgM responses. Consistent with our prediction, we observed a significant decrease in the Ag-specific IgM response to both T-I antigens (Fig. 4T-U). Taken together, we conclude that IRF1 expression in B lineage cells is necessary for the development and/or survival of MZ B cells that can rapidly respond to T-I antigens.

BCR and TLR signals cooperate to induce IRF1 expression in transitional B cells

Since our data showed B cell-intrinsic expression of *Irf1* was not required for seeding of transitional/MZ B cell precursors in the spleen, but appeared to be required for MZ B cell development from these precursors, we predicted that IRF1 would be expressed by the transitional and MZ B cells. Consistent with this prediction, we observed low but detectable levels of IRF1 in the T1 and T2 precursors (Fig. 5A-B, Fig. S5A) and significantly higher expression of IRF1 in the mature MZ B cells (Fig. 5A-B). Interestingly, IRF1 levels were the lowest in mature splenic FoB cells (Fig. 5B), suggesting that IRF1 is downregulated when B cells commit to the FoB lineage.

Next, we set out to identify the signals that promote IRF1 expression in the transitional and MZ B cell compartments. We first used Ingenuity Pathway Analysis (IPA) to identify predicted regulators of the published transcriptome profiles (Table S1) of murine FoB and MZ B cells. As expected, known negative regulators of MZ B cell development, like TRAF2, which activates the canonical NF-KB pathway (Grech et al., 2004), and FOXO1, which is activated by BCR and CD19 signaling (Chen et al., 2010), were predicted as upstream activators of the FoB transcriptional program (Fig. 5C, Table S2). Conversely, transcriptional regulators that promote MZ B cell commitment and function like Notch (Zhang et al., 2012) and TLR (Oliver et al., 1997) family members were predicted by IPA to be upstream activators of the MZ B cell transcriptome (Fig. 5C, Table S2). Interestingly, IFN receptors and members of the Type I (IFN α /b) and Type II (IFN γ) IFN cytokine family were predicted by IPA (Fig. 5C, Table S2) to activate the MZ B transcriptional program. Since IFNs induce expression of IRF1 in many cell types (Elser et al., 2002; Negishi et al. 2006; Stone et al. 2019), we predicted that these inflammatory cytokines might induce IRF1 expression in the MZ B precursors and support commitment of these cells to the MZ B lineage. To test this, we cultured WT transitional B cells for 24 hrs in the presence of the survival factor BAFF or with BAFF in combination with IFN α or IFN γ and then measured expression of IRF1. As expected, IRF1 expression increased >4-fold in the IFN γ -exposed transitional B cells (Fig. 5D-E). Moreover, we observed a very modest (25%), but significant increase in IRF1 expression in the transitional B cells exposed to IFN α (Fig. 5D-E).

Since IFN γ exposure dramatically increased IRF1 expression by the transitional B cells, we hypothesized that IFN γ R signaling might be necessary for establishment or maintenance of the MZ B cell compartment. To test this possibility, we reconstituted lethally irradiated recipient animals with a 50:50 mixture of CD45.1⁺ WT BM plus CD45.2⁺ WT BM or with a 50:50 mixture of CD45.1⁺ WT BM plus CD45.2⁺ *Ifngr1*^{-/-} BM. 8 weeks following reconstitution we determined the ratio of CD45.1⁺ B cells to CD45.2⁺ B cells in each recipient. Despite the fact that IFN γ was a potent inducer of IRF1 expression in transitional B cells, IFN γ R expression by B cells was not required for the establishment of mature splenic B cells (Fig. 5F) nor for the development of the FoB and MZB compartments (Fig. 5G-H). Moreover, we observed similar results when we enumerated the splenic B cell subsets in WT:*Ifnar1*^{-/-} BM chimeras (Fig. S5B-D). Thus, while IRF1 is necessary for the development or maintenance of

a normal MZ B cell compartment, signaling through Type I and Type II IFN receptors appears to be dispensable for MZ development.

Although IRF family members are prototypic IFN inducible transcription factors (Tamura et al., 2008), it is appreciated that some IRF members, including IRF8 and IRF4, can be upregulated in response to other types of stimuli, including BCR and TLR ligands (Xu et al., 2015; Negishi et al., 2005). Furthermore, previous reports indicate that IRF1 is induced upon TLR signaling in dendritic cells (DCs) (Negishi et al., 2006; Schmitz et al., 2007) and following T cell receptor engagement in T cells (Penninger et al., 1997). Given that both BCR and TLR signaling pathways are implicated in MZ B cell development and function (Wen et al., 2005; Oliver et al., 1997), we considered the possibility that IRF1 expression levels might be regulated by these stimuli in B cells. We therefore cultured transitional B cells for 24 hrs in the presence of BAFF alone or BAFF in combination with LPS and/or anti-IgM and then measured the expression of IRF1. We observed a significant increase in IRF1 expression within the transitional B cells following either TLR or BCR stimulation (Fig. 5I-J). Moreover, the combination of BCR and TLR signaling induced the highest levels of IRF1 by the transitional B cells (Fig. 5I-J). Since both BCR and TLR ligands can induce IFN γ production by B cells (Bao et al., 2014), we assessed whether upregulation of IRF1 in the BCR and TLR stimulated transitional B cells was due to autocrine IFN γ signaling. We therefore measured IRF1 levels in WT and *Ifng*^{-/-} transitional B cells following stimulation with BAFF or BAFF in combination with LPS and/or anti-IgM. We observed no differences in IRF1 induction levels between the stimulated WT and *Ifng*^{-/-} transitional B cells (Fig. S5E-F), indicating that IRF1 upregulation of BCR and TLR stimulated transitional cells is controlled by an IFN γ -independent mechanism.

Prior reports showed that IRF1-dependent transcription requires cooperation between IFN signals, which induce expression of IRF1 mRNA and protein, and TLR-derived signals, which direct IRF1 to the nucleus (Negishi et al., 2006). To assess whether cooperative BCR and TLR signals are required to initiate expression and nuclear translocation of IRF1 in transitional B cells we stimulated transitional B cells with BAFF alone or BAFF in combination with anti-IgM and/or LPS and used ImageStream to analyze IRF1 expression and localization within the cells. Similar to the flow cytometry data, IRF1 expression was significantly increased in the

cells cultured in the presence of anti-IgM or TLR4 ligand relative to B cells cultured in BAFF alone (Fig. 5K-L). IRF1 expression was even higher when transitional B cells were cultured in the presence of both anti-IgM and LPS (Fig. 5K-L). Next, we quantified nuclear translocation of IRF1 under the different stimulation conditions by determining the overlap (measured as the similarity index) between IRF1 staining and the nuclear stain Hoescht in individual cells. We observed a positive similarity index value for the vast majority of single cells analyzed from the LPS, anti-IgM and LPS+anti-IgM stimulated cultures (Fig. 5M). Moreover, there was no difference in the mean similarity index score between the groups (Fig. 5M). These data indicate that although the combination of BCR and TLR4 stimulation induces the highest expression of IRF1, ligands for either the BCR or TLR4 are sufficient to induce expression and nuclear translocation of IRF1 in transitional B cells.

IRF1 regulates Notch signaling in transitional B cells.

Our data showed that IRF1 is required for the development or survival of the splenic MZ B cell compartment and that IRF1 expression can be induced in response to TLR and BCR ligand signals, which are known to regulate MZ B cells (Oliver et al., 1997; Wen et al., 2005). In particular, BCR and TLR signals have both been implicated in regulating the expression or activity of members of the Notch transcription factor family (Wen et al., 2005; Gamrekelashvili et al., 2020) and Notch2 expression by B cells is critical for commitment to the MZ B cell lineage (Saito et al., 2003; Tanigaki et al., 2002). To assess whether IRF1, induced in response to TLR and/or BCR signals, is required for Notch2 controlled commitment of transitional cells to the MZ B lineage, we co-cultured WT or *Irf1*^{-/-} transitional B cells with parental OP9 stromal cells or OP9 stromal cells expressing Notch2 ligand, Delta-like 1 (DLL1), in the presence of BAFF or BAFF plus anti-IgM and/or LPS. After 3 days, we assessed the ability of these activated transitional B cells to adopt a mature MZ B cell phenotype by determining the frequencies of CD23^{neg}CD21⁺IgM⁺ MZ-like B cells present in the cultures (Fig. S6). Not surprisingly, co-culturing either WT (Fig. 6A) or *Irf1*^{-/-} (Fig. 6B) transitional B cells with the control DLL1^{neg} stromal cells induced few if any MZ-like B cells, even in the presence of BAFF. Moreover, addition of LPS and/or anti-IgM to these cultures did not initiate MZ B cell development (Fig. 6A-B). By contrast, culturing WT transitional B cells in the presence of DLL1-expressing stromal cells and BAFF significantly increased the frequency of CD23^{neg}CD21⁺IgM⁺ MZ-like B cells in the cultures (Fig. 6C). Although the addition of anti-

IgM alone did not increase the frequency of CD23^{neg}CD21⁺IgM⁺ B cells in these cultures, we observed a significant boost in the frequency of the MZ-like B cells in the cultures that contained LPS and these cells were further amplified when LPS plus anti-IgM were included in the co-cultures (Fig. 6C). Strikingly, *Irf1*^{-/-} transitional B cells did not adopt a mature MZ B cell phenotype following co-culture with BAFF and DLL1-expressing stromal cells, regardless of whether anti-IgM and/or LPS were included in the cultures (Fig. 6D-E). Thus, the combination of TLR and anti-IgM signals potently cooperate with Notch2 and BAFF to promote the development or survival of MZ B cells from IRF1-expressing MZ B precursors.

Our data showed that *Irf1* expression by transitional B cells is required for Notch2-dependent development of B cells with the phenotypic properties of mature MZ-like B cells. To assess whether Notch2 was activated in an *Irf1*-controlled fashion in the transitional B cells, we isolated RNA from WT and *Irf1*^{-/-} transitional B cells that were co-cultured for 5 hrs with parental OP9 stromal cells or with DLL1-expressing OP9 stromal cells. We then analyzed mRNA expression levels of several Notch target genes, including *Dtx*, *Hes1*, *Hes5* and *Hey1*, in the transitional B cells. As expected, expression of all 4 Notch target genes increased in the WT transitional B cells that were co-cultured with DLL1-expressing stromal cells compared to WT transitional B cells co-cultures with parental OP9 cells (Fig. 6F-I). By contrast, and consistent with our prediction, Notch2-dependent induction of these target genes was significantly impaired in the *Irf1*^{-/-} transitional B cells (Fig. 6F-I). Taken together, these data show that Notch2-dependent gene expression and commitment of transitional B cells to the MZ B cell lineage is dependent on IRF1 expression by the transitional B cells and can be further enhanced by TLR signals delivered alone or in combination with BCR ligation.

IRF1 regulates the polyreactive and autoreactive B cell repertoire.

Our data showed that *Irf1*^{-/-} transitional B cells are unable to respond to Notch2 signaling even when stimulated with LPS or LPS + anti-IgM. Given that these signals both upregulate IRF1 expression in the transitional B cells and promote maturation to the MZ B lineage, the data suggested that IRF1 acts downstream of TLR and BCR signals to regulate the final maturation and selection steps of B cell development. Since BCR signals are one of the key regulators of selection into the MZ B or FoB lineage (Cyster et al., 1995; Cyster et al., 1996; Cyster et al., 1997), we hypothesized that IRF1 regulates this BCR-dependent step. To test this hypothesis,

we took advantage of the VH81X IgH transgenic mouse model (Chen et al., 1997; Martin et al., 1997). These animals express a functional, fetal-liver-derived VH81X IgH transgene (Chen et al., 1997; Martin et al., 1997). This IgH chain, which pairs with a variety endogenous Ig light chains (IgL), the most predominant Vk1C IgL, gives rise to mature B cells that express a BCR that is reactive to intracellular antigens (Chen et al., 1997; Martin et al., 1997). B cells expressing the IgMa VH81X transgene and Vk1C light chain are preferentially and positively selected into the MZ B cell compartment (Chen et al., 1997; Martin et al., 1997) and can be detected by flow cytometry using allotype and IgL chain idiotype specific antibodies.

To assess whether IRF1 contributes to selection of B cells expressing the VH81X transgene into the MZ B cell compartment, we generated control WT.VH81X and *Irf1*^{-/-}.VH81X animals. We analyzed the splenic B cells by flow cytometry to identify CD21⁺CD23^{neg} MZ B and CD21^{lo}CD23⁺ FoB cells. As expected (Chen et al., 1997; Martin et al., 1997), the frequency (Fig. 7A-C) and number (Fig. 7D) of total MZ B cells present in the VH81X transgenics was higher than that normally seen in non-transgenic B6 mice (~25% vs ~3-5%, respectively). However, and consistent with our prior results, the frequency (Fig. 7A-C) and number (Fig. 7D) of total MZ B cells was significantly less in the *Irf1*^{-/-}.VH81X animals relative to the WT transgenics. Next, we analyzed the splenic B cells expressing the VH81X transgene (IgMa) and the IgL VK1C (Fo27⁺) in both groups of mice (Fig. 7E-F). Importantly, there was no difference (Fig. 7G) between the frequencies of splenic B cells expressing the stereotypic transgenic BCR in WT.VH81X and *Irf1*^{-/-}.VH81X mice (14-16% of CD19⁺ splenic B cells in both groups). As expected, the vast majority (>70%) of the transgenic WT B cells were selected into the MZ B cell compartment (Fig. 7H) with <20% being selected into the FoB compartment (Fig. 7I). In striking contrast, only ~50% of the transgene-expressing *Irf1*^{-/-} B cells were selected into the MZ B cell compartment (Fig. 7H) with significantly more of the transgenic B cells directed to the FoB cell compartment (Fig. 7I). Together, these data show that *Irf1* plays a key role in supporting selection of B cells expressing polyreactive BCRs into the MZ B cell compartment. Importantly, *Irf1*^{-/-} polyreactive B cells do not appear to be lost to negative selection and apoptosis but rather are selected into the FoB compartment.

Our data argue that *Irf1* plays an important role in ensuring that polyreactive BCR expressing B cells, which can rapidly respond to conserved pathogen-derived molecules and TLR ligands,

are restricted to the MZ B cell compartment where T-D interactions are geographically limited. However, if these polyreactive B cells are selected into the FoB compartment, the polyreactive B cells will have the opportunity to interact with Th cells in the B cell follicles and GCs. Prior publications indicated that MZ B cells that are unable to recycle back to the MZ and remain within the B cell follicle can be diverted with T cell help into the autoreactive B cell repertoire (Zhou et al., 2011). Our data examining the T-D influenza response showed that the number of GC B cells was significantly increased in the *Irf1*^{-/-} mice (Fig. 1E), suggesting that loss of *Irf1* may lead to dysregulated T-D GC responses. Based on these data, we hypothesized that the *Irf1*^{-/-} FoB repertoire is enriched in polyreactive B cells that have the potential to respond to endogenous antigens in a T-D manner. To test this, we generated 50:50 BM chimeric mice that were reconstituted with CD45.1⁺ WT and CD45.2⁺ *Irf1*^{-/-} BM. We aged the mice for 6 months and enumerated activated GC B cells, memory B cells and ASCs in the spleens (Fig. 7J). The WT and *Irf1*^{-/-} total live cells were equivalently represented in the 50:50 chimeras (Fig. 7K). Within the CD19⁺ B cell compartment, >25% of the cells exhibited a GC phenotype (Fig. 7K), suggesting that these aged but non-experimentally manipulated animals were actively responding to endogenous or environmental antigens. Interestingly, the “spontaneous” GC B cell response was dominated by the *Irf1*^{-/-} B cells which represented ~90% of the total GC B cell compartment (Fig. 7L). The memory B cell compartment was modestly enriched in *Irf1*^{-/-} B cells (Fig. 7M). Despite the apparent expansion of the GC, the splenic ASC compartment did not appear to be greatly expanded in these aged chimeras (Fig. 7J). Finally, and consistent with our *in vitro* studies (Fig. 1-2), a significantly higher proportion of the ASCs in the aged chimeras were derived from the WT B cells compared to *Irf1*^{-/-} B cells (Fig. 7N). These studies therefore suggest that *Irf1*^{-/-} B cells are intrinsically biased toward entering a GC response even in the absence of exogenous antigen administration.

The bias toward spontaneous GC formation by the *Irf1*^{-/-} B cells in the 50:50 chimeras strongly suggested that these B cells likely expressed BCRs that could react with endogenous or environmental antigens. To test whether *Irf1*^{-/-} B cells were intrinsically prone to generate autoreactive Abs, we examined serum antibodies in aged B-WT and B-*Irf1*^{-/-} mice using a standard autoAb Hep2 anti-nuclear Ab (ANA) assay. Indicative of the presence of anti-nuclear and anti-cytoplasmic autoAbs in the serum from aged B-*Irf1*^{-/-} mice, we observed easily detectable cytoplasmic IgG (Fig. 7O-P). These data therefore demonstrate that B cell intrinsic

expression of *Irf1* is required to prevent the spontaneous development of autoAb production. Taken altogether, the data show that *Irf1* expression by B cells plays a critical role in driving B cell fate decisions and ensures that polyreactive and TLR responsive B cells with the potential to contribute to the autoimmune repertoire are selected into the MZ B cell compartment, which can provide rapid but short-lived responses to systemic pathogens.

DISCUSSION

In the presence of IFN γ T cells require IRF1 to commit to Th1 cell fate through the direct regulation of lineage specifying genes and repressing alternative fates (Kano et al. 2008). Furthermore, IRF1 supports Th1 differentiation through the production of polarizing cytokine in TLR-activated antigen presenting cells (APCs) (Taki et al. 1997). While IRF1 has been characterized in T and myeloid derived lineages, the role of IRF1 in B cell differentiation is not well known. Although it has been shown that IRF1 regulates the expansion of an ASC precursor, germinal center (GC) B cells, the B cell intrinsic role for IRF1 in ASC differentiation has not been fully addressed. We previously reported that cognate encounters between IFN γ producing Th1 effectors and B cells (Be1 cells) resulted in robust production of antibody (Harris et al 2005a). Additionally, *Ifngr1* was required for the upregulation of ASC lineage specifying genes such as *Prdm1* in Be1 cells, suggesting that IFN γ -inducible transcription factors may be required for ASC fate commitment (Stone et al 2019). We predicted IFN γ -inducible IRF1 may be required for ASC differentiation in Be1 cells. Consistent with this prediction, our data shows that IRF1 is indeed required for ASC differentiation in the presence of IFN γ -producing Th1 cells suggesting a role for IRF1 in the development of T-dependent B cell responses in viral infection.

Although we fully expected to find that IRF1 was required for the generation of long-lived antibody following influenza we realized that IRF1 was dispensable for the development of a durable humoral immunity. Instead, we found that IRF1 is required for an early flu-specific IgM response. We recognize not all T-dependent responses were unchanged in the absence of IRF1. Similar to previous reports, we found an expansion of GC B cells, suggesting that IRF1, in some capacity, restricts this B cell subset (Mboko et al 2016). Given the reduction of flu-specific IgM, we speculate that there is diminished viral clearance in the absence of IRF1, resulting in more abundant antigen, thus enhancing the GC B cell response. Alternatively,

IRF1 has been proposed to terminate cell cycle in proliferative B cell precursors in the bone marrow (Yamada et al 1991), thus B cell-intrinsic IRF1 may regulate proliferation in other B cell subsets. In fact, we have observed in flu-infected chimeric models where environmental stimuli are normalized between WT and *Irf1*^{-/-} cells that there is a profound expansion of flu NP specific GC B cells (data not shown). This suggests there is indeed a B cell intrinsic role for IRF1 in the regulation of proliferation, cell cycle arrest, or other mechanisms for seeding the GC.

We previously showed that *Ifngr1*-derived signals were responsible for driving inflammatory programs necessary to initiate ASC differentiation in the presence of Th1 effectors (Stone et al 2019). While we may have expected that IRF1 could be required for cognate, IFN γ -induced ASC differentiation, our data also showed that IRF1 is essential for mounting T-independent antibody unaccompanied by IFN γ including those in response to bacterial antigens. Thus, IRF1 is a global regulator of T-independent humoral immunity. Furthermore, in the absence of IRF1 we found a profound loss of a predominant T-independent ASC precursor, the MZ B cell. Although we found this result wholly unexpected, some key transcription factors important for MZ B cell development are enhanced in the presence of IFN γ . We previously showed B cells in the presence of IFN γ had enriched chromatin accessible regions containing interferon-sensitive response element (ISRE) and composite ETS-IRF (EICE) motifs (Stone et al 2019). Furthermore, it has been reported that ETS and IRF are critical transcription factors in specifying mature B cell fates. It has been shown *Ets1* is required for the development of MZ B cells (Eyquem et al 2004). Conversely, *Irf4* and *Irf8* have been shown to restrict the MZ B cell pool (Simonetti et al 2013; Feng et al 2011). The role of IRF1 cooperating with these transcription factors is completely unknown in the B cell lineage, though well characterized in other cell lineages (Langlais et al 2016). Further study will be needed to understand this complex transcription factor network, though we predict that IRF1 could redirect these transcription factors to specify MZ B cell fate decisions.

Both marginal zone and follicular B cells arise from the bone marrow, and they are continually replenished throughout adult life (Pillai et al 2009). Our data showed B cell intrinsic IRF1 had little effect on B cell development in the bone marrow. This result appears inconsistent with a previous study reporting introduction of a B cell specific IRF1 transgene resulted in

profound B cell depletion in the bone marrow, suggesting that IRF1 does indeed influence B cell development (Yamada et al 1990). This study also proposed a mechanism by which IRF1 regulated IL7R, thus ceasing B cell maturation. However, it has also been reported that IRF4 attenuates IL7 signaling (Johnson et al 2008), therefore suggesting redundancies amongst IRF family members in the regulation of B cell development. Taken together, our result is consistent with established molecular mechanisms for B cell lymphopoiesis. Our data also showed little role for B cell intrinsic IRF1 in regulating splenic, immature, transitional B cells. Given that IRF1 is thought to be an IFN-inducible transcription factor, this result was initially unexpected in that it has been reported that type I IFN can promote the survival of transitional cells (Liu et al 2019; Hamilton et al 2017). However, we also found that IFN α does not induce IRF1 expression in transitional B cells, which suggests that IFN α promotes survival of transitional B cells in an IRF1 independent mechanism. Thus, IRF1 is mostly dispensable for early B cell development.

Our data showed that the IFN-inducible transcription factor IRF1 was dispensable for proper positioning and retention of B cells within the marginal zone. Very little is known about the precise regulation of $\alpha_4\beta_2$ (LFA-1) and $\alpha_4\beta_1$ (VLA-4), though a high avidity conformational change of LFA-1 through antigen receptor signaling has been reported (Dustin et al 1989). Additionally, ligation of LFA-1 has been shown to promote IFN γ production in CD4 $^+$ T cells, though the influence of IFN γ on LFA-1 is relatively unknown (Sherma et al 2018; Verma et al 2016). The respective ligands ICAM-1 and VCAM-1, however, have been shown to be markedly increased in the presence of IFN γ (Chung et al 2002; Parr et al 2008). Therefore, we may have expected a contribution of environmental cues for the retention of B cells within the marginal zone. Indeed, we found a more appreciable IRF1 deficient MZ B cell population in mixed bone marrow chimeras when compared to global IRF1 deficient mice, suggesting a role for B cell extrinsic IRF1 regulating B cell positioning. While it was reported that the stroma of IRF1 deficient mice were developmentally intact (Matsuyama et al.1993), we predict there are some functional losses in this compartment which could influence lymphoid organization. Regardless, our data show B cell intrinsic IRF1 is dispensable for the expression of critical integrins for marginal zone retention which correlates with proper positioning of IRF1 deficient B cells within marginal zone.

Our data showed that IRF1 was expressed by transitional and mature MZ B cells, which suggested that MZ B cells and their precursors experienced signals to induce IRF1 expression. While our data showed that IFN γ could induce IRF1 expression in transitional B cells in vitro, unexpectedly, *Ifngr2* was dispensable for the generation of MZ B cells in vivo. We found this result puzzling in that it is well appreciated that IRF1 is an IFN γ -inducible transcription factor and yet it appears IFN γ is not required for the generation of MZ B cells. To our knowledge there are no studies that report IFN γ is required for the development of MZ B cells, although, it is well appreciated that IFN α/β is important for the survival transitional B cells especially in autoimmune settings (Hamilton et al 2017; Liu et al 2019). While we report no significant role for IFN α in the development of MZ B cells, we also found that IFN α induced little IRF1 expression in transitional B cells in vitro. This suggests that the reported influence of IFN α/β in transitional B cells has no profound effect in the development of MZ B cells. Furthermore, the IFN α -derived pro-survival signals experienced by the transitional cells is likely IRF1-independent.

Given that neither IFN α or IFN γ were solely required for the development of MZ B cells we considered whether IRF1 could be induced through alternative pathways. It has been previously reported that IRF1 can be induced after peptide-specific TCR activation in developing thymocytes and that in the absence of IRF1 positive selection of CD8 $^+$ T cells is severely impaired (Penninger et al 1997). Additionally, it has been reported that TLR9 induced IRF1 expression triggered IFN β production in myeloid derived lineages (Schmitz et al 2007). Therefore, it was conceivable that IRF1 could be induced through BCR or TLR derived signals in transitional B cells. Indeed, we found that IRF1 could be expressed through BCR and TLR signaling, and interestingly, we observed a synergistic effect of BCR and TLR. Given the modest expression of IRF1 in transitional B cells and the augmented expression of IRF1 in MZ B cells, we speculate that transitional B cells experience brief signals derived from endogenous self- or microbiome-derived antigens whereas the sessile MZ B cells may experience more sustained BCR and TLR signaling.

Furthermore, we found that B cell-intrinsic Myd88 was required for sufficient MZ B cell development in our competitive bone marrow chimeric model. Initially, we found this result inconsistent with previous reports proposing that B cell specific Myd88 is dispensable for the generation of autoreactive mature B cells (Silver et al 2006). However, while this study addresses Myd88 in B cell development this study cannot preclude the role of Myd88 in survival or competitive fitness of mature B cell compartments. Given Myd88 is required for MZ B cells in our competitive repopulation model, it is tempting to speculate that signals emanating from TLR are critical for homeostatic proliferation in response to endogenous antigens.

Our data showed in the absence of IRF1, transitional B cells were intolerant or inefficient to BCR/TLR- mediated enhancement of Notch2 pathway, respectively. There is a well appreciated relationship between BCR and Notch2 pathway in developing B cells. Previous studies have demonstrated in the presence of Notch2 ligands, BCR signaling is required to generate efficient frequencies of CD21+IgMhi cells in vitro (Wen et al 2005). Following these studies, it has been shown that BCR-induced kinase, TAOK3, is required for enzymatic activation of Notch2 pathway, and thus, the development of MZ B cells (Hammad et al 2017). Therefore, our data is very consistent with the previous reports of BCR-derived signals supporting Notch2 pathway, thus promoting the development of MZ B cells. Furthermore, TLR-mediated enhancement of Notch1 and Notch2 expression in macrophages has been reported (Palaga et al 2007). Therefore, it is conceivable that TLR stimulated transitional B cells become permissive to Notch ligands, though further study will be necessary to dissect the mechanism for TLR-mediated enhancement of Notch pathway in developing B cells.

Our data showed that IRF1 is required for the robust enrichment of VH transgene-bearing B cells within the MZ B cell compartment. We found this data consistent with studies of lineage-specifying genes bearing restricted Ig rearrangements resulting in fewer MZ B cells (Zhang et al 2012). While our data is suggestive of altered selection mechanisms in the absence of IRF1, aging studies would be required to determine whether IRF1 participates in long-term survival of MZ B cells or mediates initial selection. Given BCR/TLR inducible -IRF1 is required for efficient activation of pro-survival pathways such as Notch (Tan-Pertel et al 2000), it is tempting to speculate that VH-transgene restricted B cells would bear a more severe altered

phenotype over time suggesting IRF1 participates in survival rather than the establishment of nascent B cell repertoire or selection.

Our data showed BCR signaling was predicted to be significantly activated by IPA in the set HOMER-predicted IRF1 target differentially expressed genes comparing MZ B to FoB cells (Haines et al 2019). Furthermore, our data shows IRF1 has a predicted consensus binding motif immediately upstream of the TSS of the Ptpn22 locus. It has been shown that BCR signaling results in a cascade of activating as well as inhibitory molecules which fine tune B cell development, activation, and differentiation (Negro et al 2012; Liu et al 2020). Therefore, our data is very consistent with the established mechanisms of BCR activation. Additionally, we showed the development of autoantibody in aged chimeric mice that selectively lacked IRF1 in all B cells, which correlates to altered Ptpn22 expression in the absence of IRF1 in developing B cells. This data is somewhat inconsistent in that B6 Ptpn22 deficient mice do not develop autoantibody nor any other autoimmune manifestations (Hasegawa et al 2004) in a B cell intrinsic manner. However, like other murine models of autoimmunity, alterations of multiple genes result in overt spontaneous disease (Rawlings et al 2015). Therefore, our data cannot preclude that IRF1 could regulate multiple genes in addition to Ptpn22 resulting in the development of autoantibody. In summary, developing B cells must integrate signals from the microenvironment in the form of cytokine, antigen, TLR ligands, and other specialized cell subsets to develop into MZ B cells. We propose BCR/TLR-inducible IRF1 finely tunes BCR signaling in transitional B cells to promote the generation of the homeostatic MZ B cell compartment, thus preventing the development of autoimmune manifestations.

MATERIALS AND METHODS

Mice and generation of bone marrow chimeras.

All experimental animals were bred and maintained in the UAB animal facilities. All procedures involving animals were approved by the UAB Institutional Animal Care and Use Committee and were conducted in accordance with the principles outlined by the National Research Council. Mouse strains used in these experiments include the following: C57BL/6J (B6), B6.129S2-Ighm^{tm1Cgn}/J (uMT), B6.129S7-Ifngr1^{tm1Agt}/J (*Ifngr1*^{-/-}), B6(Cg)-*Ifnar1*^{tm1Agt}/J (*Ifnar1*^{-/-}), B6.129S2-*Irf1*^{tm1Mak}/J (*Irf1*^{-/-}), B6.SJL.*Ptprc*^a*Pepe*^b/BoyJ (CD45.1⁺B6), and *Vb81X*

transgenic mice. *Vb81X* mice were intercrossed with CD45.1⁺ B6 mice to generate CD45.1⁺.*Vb81X* mice or with *Irf1*^{-/-} mice to generate CD45.2⁺*Irf1*^{-/-}.*Vb81X* animals. The *Vb81X* transgenic strain (Chen et al., 1996) is maintained at UAB and all other strains were obtained from Jackson Laboratory and then bred in the UAB animal facilities. Bone marrow (BM) chimeric mice were generated by irradiating B cell deficient uMT recipient animals with 950 Rads from a high-energy X-ray source, delivered in a split dose at least 4 hrs apart, and then reconstituting the recipients with 10⁷ BM cells by retro-orbital injection. BM cell mixtures were as follows: 80% uMT BM + 20% *Irf1*^{-/-} BM (B-*Irf1*^{-/-} chimeras) or with 80% uMT BM + 20% B6 BM (B-WT chimeras). Competitive 50:50 BM chimeras were generated by reconstituting irradiated uMT recipients with a mixture of: (i) 50% CD45.1⁺B6 BM and 50% B6 BM (control WT:WT competitive chimeras); (ii) 50% CD45.1⁺B6 BM and 50% *Irf1*^{-/-} BM (WT:*Irf1*^{-/-} chimeras); (iii) 50% CD45.1⁺B6 BM and 50% *Ifnar1*^{-/-} BM (WT:*Ifnar1*^{-/-} chimeras); or (iv) 50% CD45.1⁺B6 BM and 50% *Ifngr1*^{-/-} BM (WT:*Ifngr1*^{-/-} chimeras). BM chimeras were used in experiments 6-12 weeks post-reconstitution. Both male and female mice were used in this study. Within each experiment, animals were matched for age (between 6-12 weeks at time zero) and gender. No differences were observed between cohorts of male versus female mice.

Immunizations and Infections

B6, *Irf1*^{-/-} and BM chimeras were immunized (i.v.) with TNP-Ficoll (50 ug per animal in 100 ul of PBS) or with 1x10⁸ heat-killed, pepsin-treated *S. pneumoniae*, strain R36A (Briles et al. 1981). IgM Ab responses to the hapten (nitrophenyl, (NP)) or to the bacterial cell wall component phosphorylcholine (PC) were measured 7 days post immunization. BM chimeric mice were infected (i.n.) with a sublethal dose (1.5 x 10⁴ VFU) of the H1N1 influenza virus, A/PR/8/34 (PR8).

Aging and detection of autoantibodies

Competitive 50:50 BM chimeras and B-WT and B-*Irf1*^{-/-} chimeras were aged 6 months following reconstitution. Spleens from six month-old competitive BM chimeras were analyzed by flow cytometry (see below) for activated B cell populations. Peripheral blood (500-1000 ul) from the renal artery was collected from B-WT and B-*Irf1*^{-/-} chimeras. Serum was isolated using a microtainer serum separator tube (BD365967, 4MDMEDICAL), diluted at 1:200 in PBS and then used to stain (25 ul of diluted serum) Kallestad HEp-2 slides (26100, Biorad).

Positive controls include diluted (1:200) serum from aged systemic lupus erythematosus (SLE), *Yaa. Fcgr2b^{-/-}* (Takai et al. 1996) mice and young naïve C57BL/6J (B6) mice. Bound antibody was detected using FITC-conjugated Goat anti-mouse IgG (F-2761, ThermoFisher Scientific) at 1:200. Slides were mounted using ProLong Diamond anti-fade plus DAPI mountant (P36962; ThermoFisher Scientific). Slides were imaged and analyzed as described in *Immunofluorescence* methods below.

Th1 and B cell co-cultures

Th1 cells were generated *in vitro* as previously described (Harris et al., 2005a). Briefly, splenic CD4⁺ CD45.1⁺ OT-II TCR Tg T cells were purified by positive selection (130-117-043, Miltenyi Biotec) and cultured in complete medium in the presence of platebound anti-CD3 (2 µg/mL, Invitrogen) and anti-CD28 (5 µg/mL, Invitrogen) plus IL-12 (2 ng/mL, R&D Systems) and anti-IL-4 (11B11, 20 µg/mL, R&D Systems). T cells were transferred into new plates after 48-72 hr and cultured for an additional 48 hours in media supplemented with IL-2 (20 Units/mL, R&D Systems) for expansion. Polarized Th1 cells were treated with mitomycin C (50-05-7, Sigma Alderich) washed and then co-cultured for 4 days at a 1:1 ratio with positively selected (130-121-301, Miltenyi Biotec) CD19⁺ splenic B cells in complete B cell media (RPMI 1640, 10% heat inactivated FBS, 0.05 mM 2-ME, 1% nonessential amino acids, 1% penicillin/streptomycin, 10mM HEPES, and 1 mM sodium pyruvate) that was supplemented with OT-II peptide (5 µM), anti-IgM F(ab')₂ (10 µg/mL, Southern Biotech), and IL-2 (20 Unit/mL, R&D Systems).

Transitional and B cell cultures

For B cell cultures positively selected CD19⁺ splenic B cells were cultured in complete B cell media and stimulated with anti-IgM F(ab')₂ (10 µg/mL, Southern Biotech), IFNγ (10 ng/mL, R&D Systems), IL-21 (100 ng/mL, R&D Systems), IL-2 (20 Unit/mL, R&D Systems) plus: (i) R848 (1 µg/mL, tlr1-r848, InvivoGen) or (ii) LPS (10 µg/mL, L2630-10MG; Sigma-Aldrich) for 3 days. For transitional B cell cultures, transitional B cells were enriched by FITC positive selection using an anti-CD93-FITC antibody (AA4.1, BioLegend) with the anti-FITC magnetic microbeads (130-048-701, Miltenyi Biotec) according to manufacturer's instructions. The transitional B cells (2x10⁵ cells in 200 µl) were cultured in B cell media with BAFF alone (10 ng/mL, 8876-BF-010; R&D Systems) or with BAFF plus: (i) LPS (10 µg/mL, L2630-

10MG; Sigma-Aldrich); (ii) anti-IgM F(ab')₂ (1 ug/mL, Southern Biotechnology); or (iii) anti-IgM F(ab')₂ + LPS for 24 hrs.

Ab secretory rate assay

After 3-4 days of activation, B cells were harvested, washed and re-cultured in fresh media for 5-6 hr at 1×10^4 - 1×10^6 live cells/mL. Conditioned media was collected 5-6 hrs later and secreted Ab was quantified by serially diluting conditioned media in ELISA plates coated with anti-Kappa capture antibody (1:2000, Southern Biotech). Bound Ab was detected by using HRP-conjugated total Ig(H+L) (1:2000, Southern Biotech). Absorbance values at 405 nm (OD) were read. Total Ig was quantified by using a IgK standard (1 ug/mL, Sigma) where a dilution from the linear range of the serially diluted sample was used to determine Ab concentration. Secretory rates are reported as IgK (ng)/hour/# cells.

Transitional and OP9 stromal cell co-cultures

OP9-DLL1 or control OP9-GFP cells, obtained from Dr. Robert Welner (UAB), were grown to 80% confluence in T25 flasks in OP9 stromal cell media (500 mL α -MEM, 4% FBS, 10,000 U/mL penicillin, and 10,000 U/mL of streptomycin) as described (Holmes et al., 2009). For co-cultures, 80% confluent OP9-DLL1 or control OP9-GFP cells were seeded in a 24 well plate at a 1:3 dilution overnight. OP9 media was removed from the plate-bound stromal cells and splenic transitional B cells, isolated as described above, were added (5×10^5 cells in 500 ul complete B cell media) to the stromal cell containing wells. To measure Notch2-induced gene expression, transitional B cells were co-cultured with OP9 cells for 5 hrs. To measure MZ B cell development *in vitro*, transitional B cells were co-cultured 1-3 days (refer to figure legends for respective culture time) with BAFF (10 ng/mL; 8876-BF-010; R&D Systems) or with BAFF plus: (i) LPS (10 ug/mL, L2630-10MG; Sigma-Aldrich); (ii) anti-IgM F(ab')₂ (1 ug/mL, Southern Biotechnology); or (iii) anti-IgM F(ab')₂ + LPS.

Influenza (PR8), Phosphorycholine PC, and haptan NP Ab titers.

Serum samples from vaccinated or infected mice were serially diluted in ELISA plates coated with phosphorycholine (PC) antigen (5 mg/mL, Briles et al., 1981) or haptan NP₂BSA (10 ug/mL) or PR8 viral proteins (1:1000 dilution, Lee et al., 2005). Bound Ab was detected using

HRP-conjugated goat anti-mouse heavy chain IgM- or IgG-specific Abs (Southern Biotechnology) and ABTS substrate followed by oxalic acid stop. Absorbance values at 405nm (OD) were read and endpoint titers were defined as the reciprocal of the highest dilution above background where background is determined by using the average OD from naïve samples.

Cell isolation, flow cytometry analysis and cell sorting.

Single cell suspensions from spleen, LN or BM were prepared by gently disrupting tissue on fine wire mesh. Red blood cells were lysed with red blood cell lysing buffer hybrid-max (R7757, Sigma Aldrich). Cell suspensions were filtered through 70um nylon mesh then incubated in FcR blocking antibody 2.4G2 (10 ug/mL). Cells were stained with fluorochrome-conjugated Ab (see Table S4 for Ab staining panels) and LIVE/DEAD fixable dyes (L34957; ThermoFisher Scientific). For the detection of influenza nucleoprotein (NP)-specific B cells, cell suspensions were stained with NP B cell tetramer (Allie et al. 2019) for 45 min at 4°C. For intracellular IRF1 staining, stained cells were incubated with LIVE/DEAD fixable stain, then fixed and permeabilized with the eBioscience Foxp3 transcription factor (TF) staining buffer set (00-5523-00, ThermoFisher) before intracellular staining for 1 hr at room temperature (RT). Stained cells were analyzed using a FACSCanto II (BD Bioscience), Attune NxT (Invitrogen, ThermoFisher) or sort-purified with a FACSAria (BD Biosciences) located in the UAB Comprehensive Flow Cytometry Core.

ImageStream

Cultured transitional B cells were filtered with 70um nylon mesh, incubated in FcR blocking antibody 2.4G2 (10 ug/mL) and stained with LIVE/DEAD fixable dyes (1:500, L34957; ThermoFisher Scientific). Stained cells were resuspended at 1×10^6 cells/50 ul in PBS and were analyzed using ImageStream (Luminex Corp). Data were imported into Image Data Exploration and Analysis Software (IDEAS v6.2) and fluorescence intensities and similarity index were determined using Analysis Wizard software. Collected data were imported as .csv and statistical significance was determined using Prism Graphpad. Representative images of single cells were generated in the IDEAS v6.2 software in the Image Gallery. Images were exported as JPEGs at 600 dpi and cropped in Canvas v12.

Immunofluorescence.

Spleens from naïve mice were embedded in Optimal Cutting Temperature (OCT) medium, flash frozen on dry ice and stored at -80°C. Serial 7 um sections from frozen spleen were deposited onto Superfrost plus microscope slides (22-037-246; Thermo Fisher Scientific), fixed in acetone and stored overnight at 4°C. Tissue sections were treated with blocking buffer (10% FBS and 10 ug/mL FcR blocking antibody 2.4G2) and then stained with fluorochrome-conjugated antibodies diluted in blocking buffer. Primary and secondary antibodies used in this study are described in Supplemental Table 3. Tissue sections were washed in PBS after primary and secondary antibody stains. Stained sections were dried and slides were mounted with ProLong Diamond anti-fade mountant (P36961; ThermoFisher Scientific). Sections were imaged with Nikon Eclipse Ti at RT with NIS-Elements AR 4.20.02 software using stitching for the acquisition of large images. Images were taken with a 20X plan-apochromat 20X/0.8 objective (420650-9901; Zeiss) and an Andor Technology camera. Images were generated by defining a ‘region of interest’ (ROI) from the acquired large image. ROIs were added to a montage and exported from AR4.20.02 software as a 600 dpi JPEG. JPEGs were imported into Canvas v.12 to generate figures. For histocytometry analysis, objects with a ‘positive’ mean fluorescence intensity for one channel were defined by using the masking histogram feature in NIS-Elements AR 4.20.02 software. Fluorescence intensities for all channels, position, and area of ‘positive’ objects were exported into a .csv format. Exported data was imported into R studio (RStudio) to analyze cell localization (position) and phenotype (fluorescence intensities) using ggplot packages.

Quantitative RT-PCR.

RNeasy (Qiagen) was used to isolate total RNA from OP9 co-cultured transitional B cells (2 or more independent experiments with 3 experimental replicates/group per experiment). RNA quantity and quality were assessed using the Nanodrop 6000 and the Agilent 2100 Bioanalyzer. cDNA was generated from total RNA using SuperScript II double stranded cDNA synthesis kit (Invitrogen) with random hexamers according to manufacturer’s protocols. Real-time PCR was performed using TaqMan Gene Expression Master Mix, with the following parameters on a Roche LightCycler 480: 50°C for 2 min, 95°C for 10 min, followed by 45 two-step cycles at 95°C for 15 seconds and at 60°C for 1 minute. Applied Biosystems pre-designed TaqMan Gene Expression Assays were used for real-time PCR

(*Gapdh* Mm99999915_g1, *Hes1* Mm01342805_m1, *Hes5* Mm00439311_g1, *Hey1* Mm00468865_m1, *Dtx1* Mm00492297_m1). *Gapdh* expression in a control WT transitional B cell sample was used to normalize gene expression across all samples. The fold change in expression of each gene was compared to a control WT sample, which was set at 1.0, and was expressed as $2^{-\text{ddCT}}$. Samples with CT values above 32 were considered negative.

Bioinformatic identification of predicted upstream regulatory TFs.

Published raw sequencing reads (GSE132227, [Haines et al., 2019](#)) of MZ B cells and FoB cells were mapped to the mm10 genome using Tophat2 ([Kim et al., 2013](#)). A gene was considered detected if all samples from a sample group had at least 0.1 mRNA/cell (the minimum External RNA Controls Consortium transcript/cell concentration to detect at least 90% of that particular transcript across all samples) or one RPM. DESeq2 ([Love et al., 2014](#)) was used to identify differentially expressed genes (DEGs) based on a fold change of > 2 and a FDR q value < 0.05 . All DEGs are listed in Table S1. DEGs were imported into Ingenuity Pathway Analysis (IPA, QIAGEN Digital Insights) and upstream regulator analysis ([Krämer et al., 2014](#)) was used to identify upstream transcriptional regulators that are predicted to contribute to defining the MZ B cell program. Activation Z-scores were used to characterize regulators as activated or inhibited based on the observed pattern of up-/downregulation of the target molecules compared with expected directions of changes documented in Ingenuity's curated database. The Z-score captures the degree to which the directions of changes of the individual DEGs in the regulator's target set is consistent with its activated or inhibited state based on the IPA curated, expected influences of the regulator on each target. To determine statistical significance of the predicted IPA upstream regulators we used the log transformed Benjamini-Hochberg (B-H) corrected overlap p value as previously described ([Krämer et al., 2014](#)). Genes with an B-H corrected overlap p value < 0.05 by IPA were predicted to be upstream regulators. A Supplemental Table 2 is provided for all IPA-predicted upstream regulators.

Quantification and Statistical Analysis

Statistical details of all experiments including tests used, n , and number of experimental repeats are provided in figure legends. FlowJo (v10.5.3) used for flow cytometric analyses. Prism graphpad (v7.0) used for statistical analyses and graphing except where indicated. R studio (v3.6.1) was used for histometry and IPA analysis where indicated.

ACKNOWLEDGEMENTS

We thank Thomas Scott Simpler, Uma Mudunuru, Rebecca Burnham, Vidya Sagar Hanmanthu, and Holly Bachus for technical support and Dr. Robert Welner (UAB) for providing cell lines and mouse strains used in the experiments. Funding for experiments were provided by 5R01AI110508, R01AI153365 and the Lupus Research Alliance (to F.E.L). AI14782-42 (to JFK). NIH P30 AR048311 and P30 AI027767 provided support for the UAB consolidated flow cytometry core, and G20RR022807-01 provided support for the UAB Animal Resources Program X-irradiator.

REFERENCES

- Allie SR, Bradley JE, Mudunuru U, et al. The establishment of resident memory B cells in the lung requires local antigen encounter. *Nat Immunol.* 2019;20(1):97-108. doi:10.1038/s41590-018-0260-6
- Amano M, Baumgarth N, Dick MD, et al. CD1 expression defines subsets of follicular and marginal zone B cells in the spleen: beta 2-microglobulin-dependent and independent forms. *J Immunol.* 1998;161(4):1710-1717.
- Bajénoff M, Egen JG, Koo LY, et al. Stromal cell networks regulate lymphocyte entry, migration, and territoriality in lymph nodes. *Immunity.* 2006;25(6):989-1001. doi:10.1016/j.immuni.2006.10.011
- Bao Y, Liu X, Han C, et al. Identification of IFN- γ -producing innate B cells. *Cell Res.* 2014;24(2):161-176. doi:10.1038/cr.2013.155
- Baumgarth N, Tung JW, Herzenberg LA. Inherent specificities in natural antibodies: a key to immune defense against pathogen invasion. *Springer Semin Immunopathol.* 2005;26(4):347-362. doi:10.1007/s00281-004-0182-2
- Bos NA, Kimura H, Meeuwsen CG, et al. Serum immunoglobulin levels and naturally occurring antibodies against carbohydrate antigens in germ-free BALB/c mice fed chemically defined ultrafiltered diet. *Eur J Immunol.* 1989;19(12):2335-2339. doi:10.1002/eji.1830191223
- Briles DE, Nahm M, Schroer K, et al. Antiphosphocholine antibodies found in normal mouse serum are protective against intravenous infection with type 3 streptococcus pneumoniae. *J Exp Med.* 1981;153(3):694-705. doi:10.1084/jem.153.3.694
- Chen X, Martin F, Forbush KA, Perlmutter RM, Kearney JF. Evidence for selection of a population of multi-reactive B cells into the splenic marginal zone. *Int Immunol.* 1997;9(1):27-41. doi:10.1093/intimm/9.1.27
- Chen J, Limon JJ, Blanc C, Peng SL, Fruman DA. Foxo1 regulates marginal zone B-cell development. *Eur J Immunol.* 2010;40(7):1890-1896. doi:10.1002/eji.200939817
- Chen L, Flies DB. Molecular mechanisms of T cell co-stimulation and co-inhibition [published correction appears in *Nat Rev Immunol.* 2013 Jul;13(7):542]. *Nat Rev Immunol.* 2013;13(4):227-242. doi:10.1038/nri3405
- Cyster JG, Goodnow CC. Protein tyrosine phosphatase 1C negatively regulates antigen receptor signaling in B lymphocytes and determines thresholds for negative selection. *Immunity.* 1995;2(1):13-24. doi:10.1016/1074-7613(95)90075-6

- Cyster JG, Healy JI, Kishihara K, Mak TW, Thomas ML, Goodnow CC. Regulation of B-lymphocyte negative and positive selection by tyrosine phosphatase CD45. *Nature*. 1996;381(6580):325-328. doi:10.1038/381325a0
- Cyster JG. Signaling thresholds and interclonal competition in preimmune B-cell selection. *Immunol Rev*. 1997;156:87-101. doi:10.1111/j.1600-065x.1997.tb00961.x
- Cyster JG. B cell follicles and antigen encounters of the third kind. *Nat Immunol*. 2010;11(11):989-996. doi:10.1038/ni.1946
- De Silva NS, Klein U. Dynamics of B cells in germinal centres. *Nat Rev Immunol*. 2015;15(3):137-148. doi:10.1038/nri3804
- Elser B, Lohoff M, Kock S, et al. IFN-gamma represses IL-4 expression via IRF-1 and IRF-2. *Immunity*. 2002;17(6):703-712. doi:10.1016/s1074-7613(02)00471-5
- Fasnacht N, Huang HY, Koch U, et al. Specific fibroblastic niches in secondary lymphoid organs orchestrate distinct Notch-regulated immune responses. *J Exp Med*. 2014;211(11):2265-2279. doi:10.1084/jem.20132528
- Flaño E, Kim IJ, Woodland DL, Blackman MA. Gamma-herpesvirus latency is preferentially maintained in splenic germinal center and memory B cells. *J Exp Med*. 2002;196(10):1363-1372. doi:10.1084/jem.20020890
- Fujiyama S, Nakahashi-Oda C, Abe F, Wang Y, Sato K, Shibuya A. Identification and isolation of splenic tissue-resident macrophage sub-populations by flow cytometry. *Int Immunol*. 2019;31(1):51-56. doi:10.1093/intimm/dxy064
- Gamrekelashvili J, Kapanadze T, Sablotny S, et al. Notch and TLR signaling coordinate monocyte cell fate and inflammation. *Elife*. 2020;9:e57007. Published 2020 Jul 29. doi:10.7554/eLife.57007
- Gavin AL, Hoebe K, Duong B, et al. Adjuvant-enhanced antibody responses in the absence of toll-like receptor signaling. *Science*. 2006;314(5807):1936-1938. doi:10.1126/science.1135299
- Ghosn EE, Sadate-Ngatchou P, Yang Y, Herzenberg LA, Herzenberg LA. Distinct progenitors for B-1 and B-2 cells are present in adult mouse spleen. *Proc Natl Acad Sci U S A*. 2011;108(7):2879-2884. doi:10.1073/pnas.1019764108
- Grech AP, Amesbury M, Chan T, Gardam S, Basten A, Brink R. TRAF2 differentially regulates the canonical and noncanonical pathways of NF-kappaB activation in mature B cells. *Immunity*. 2004;21(5):629-642. doi:10.1016/j.immuni.2004.09.011
- Haines RR, Scharer CD, Lobby JL, Boss JM. LSD1 Cooperates with Noncanonical NF- κ B Signaling to Regulate Marginal Zone B Cell Development. *J Immunol*. 2019;203(7):1867-1881. doi:10.4049/jimmunol.1900654

- Hammad H, Vanderkerken M, Pouliot P, et al. Transitional B cells commit to marginal zone B cell fate by Taok3-mediated surface expression of ADAM10. *Nat Immunol.* 2017;18(3):313-320. doi:10.1038/ni.3657
- Hannum LG, Haberman AM, Anderson SM, Shlomchik MJ. Germinal center initiation, variable gene region hypermutation, and mutant B cell selection without detectable immune complexes on follicular dendritic cells. *J Exp Med.* 2000;192(7):931-942. doi:10.1084/jem.192.7.931
- Hardy RR, Hayakawa K, Parks DR, Herzenberg LA. Demonstration of B-cell maturation in X-linked immunodeficient mice by simultaneous three-colour immunofluorescence. *Nature.* 1983;306(5940):270-272. doi:10.1038/306270a0
- Hardy RR, Carmack CE, Shinton SA, Kemp JD, Hayakawa K. Resolution and characterization of pro-B and pre-pro-B cell stages in normal mouse bone marrow. *J Exp Med.* 1991;173(5):1213-1225. doi:10.1084/jem.173.5.1213
- Hardy RR, Hayakawa K. B cell development pathways. *Annu Rev Immunol.* 2001;19:595-621. doi:10.1146/annurev.immunol.19.1.595
- Harris DP, Goodrich S, Gerth AJ, Peng SL, Lund FE. Regulation of IFN-gamma production by B effector 1 cells: essential roles for T-bet and the IFN-gamma receptor. *J Immunol.* 2005;174(11):6781-6790. doi:10.4049/jimmunol.174.11.6781
- Hatton OL, Harris-Arnold A, Schaffert S, Krams SM, Martinez OM. The interplay between Epstein-Barr virus and B lymphocytes: implications for infection, immunity, and disease. *Immunol Res.* 2014;58(2-3):268-276. doi:10.1007/s12026-014-8496-1
- Haury M, Sundblad A, Grandien A, Barreau C, Coutinho A, Nobrega A. The repertoire of serum IgM in normal mice is largely independent of external antigenic contact. *Eur J Immunol.* 1997;27(6):1557-1563. doi:10.1002/eji.1830270635
- Hayakawa K, Hardy RR, Parks DR, Herzenberg LA. The "Ly-1 B" cell subpopulation in normal immunodeficient, and autoimmune mice. *J Exp Med.* 1983;157(1):202-218. doi:10.1084/jem.157.1.202
- Hayakawa K, Hardy RR, Herzenberg LA, Herzenberg LA. Progenitors for Ly-1 B cells are distinct from progenitors for other B cells. *J Exp Med.* 1985;161(6):1554-1568. doi:10.1084/jem.161.6.1554
- Hikida M, Johmura S, Hashimoto A, Takezaki M, Kurosaki T. Coupling between B cell receptor and phospholipase C-gamma2 is essential for mature B cell development. *J Exp Med.* 2003;198(4):581-589. doi:10.1084/jem.20030280
- Holmes R, Zúñiga-Pflücker JC. The OP9-DL1 system: generation of T-lymphocytes from embryonic or hematopoietic stem cells in vitro. *Cold Spring Harb Protoc.* 2009;2009(2):pdb.prot5156. doi:10.1101/pdb.prot5156

- Hooijkaas H, Benner R, Pleasants JR, Wostmann BS. Isotypes and specificities of immunoglobulins produced by germ-free mice fed chemically defined ultrafiltered "antigen-free" diet. *Eur J Immunol*. 1984;14(12):1127-1130. doi:10.1002/eji.1830141212
- Hua Z, Hou B. TLR signaling in B-cell development and activation. *Cell Mol Immunol*. 2013;10(2):103-106. doi:10.1038/cmi.2012.61
- Jandl C, King C. Cytokines in the Germinal Center Niche [published correction appears in *Antibodies (Basel)*. 2016 Apr 27;5(2):]. *Antibodies (Basel)*. 2016;5(1):5. Published 2016 Feb 5. doi:10.3390/antib5010005
- Jondle CN, Johnson KE, Uitenbroek AA, et al. B Cell-Intrinsic Expression of Interferon Regulatory Factor 1 Supports Chronic Murine Gammaherpesvirus 68 Infection. *J Virol*. 2020;94(13):e00399-20. Published 2020 Jun 16. doi:10.1128/JVI.00399-20
- Kano S, Sato K, Morishita Y, et al. The contribution of transcription factor IRF1 to the interferon-gamma-interleukin 12 signaling axis and TH1 versus TH17 differentiation of CD4+ T cells. *Nat Immunol*. 2008;9(1):34-41. doi:10.1038/ni1538
- Kantor AB, Stall AM, Adams S, Herzenberg LA, Herzenberg LA. Adoptive transfer of murine B-cell lineages. *Ann N Y Acad Sci*. 1992;651:168-169. doi:10.1111/j.1749-6632.1992.tb24610.x
- Kim D, Pertea G, Trapnell C, Pimentel H, Kelley R, Salzberg SL. TopHat2: accurate alignment of transcriptomes in the presence of insertions, deletions and gene fusions. *Genome Biol*. 2013;14(4):R36. Published 2013 Apr 25. doi:10.1186/gb-2013-14-4-r36
- Krämer A, Green J, Pollard J Jr, Tugendreich S. Causal analysis approaches in Ingenuity Pathway Analysis. *Bioinformatics*. 2014;30(4):523-530. doi:10.1093/bioinformatics/btt703
- Langlais D, Barreiro LB, Gros P. The macrophage IRF8/IRF1 regulome is required for protection against infections and is associated with chronic inflammation. *J Exp Med*. 2016;213(4):585-603. doi:10.1084/jem.20151764
- Lee BO, Rangel-Moreno J, Moyron-Quiroz JE, et al. CD4 T cell-independent antibody response promotes resolution of primary influenza infection and helps to prevent reinfection. *J Immunol*. 2005;175(9):5827-5838. doi:10.4049/jimmunol.175.9.5827
- Love MI, Huber W, Anders S. Moderated estimation of fold change and dispersion for RNA-seq data with DESeq2. *Genome Biol*. 2014;15(12):550. doi:10.1186/s13059-014-0550-8
- Lu TT, Cyster JG. Integrin-mediated long-term B cell retention in the splenic marginal zone. *Science*. 2002;297(5580):409-412. doi:10.1126/science.1071632
- Luu K, Greenhill CJ, Majoros A, Decker T, Jenkins BJ, Mansell A. STAT1 plays a role in TLR signal transduction and inflammatory responses. *Immunol Cell Biol*. 2014;92(9):761-769. doi:10.1038/icb.2014.51

- MacLennan IC, Gulbranson-Judge A, Toellner KM, et al. The changing preference of T and B cells for partners as T-dependent antibody responses develop. *Immunol Rev.* 1997;156:53-66. doi:10.1111/j.1600-065x.1997.tb00958.x
- Martin F, Chen X, Kearney JF. Development of VH81X transgene-bearing B cells in fetus and adult: sites for expansion and deletion in conventional and CD5/B1 cells. *Int Immunol.* 1997;9(4):493-505. doi:10.1093/intimm/9.4.493
- Martin F, Kearney JF. B-cell subsets and the mature preimmune repertoire. Marginal zone and B1 B cells as part of a "natural immune memory". *Immunol Rev.* 2000;175:70-79.
- Martin F, Oliver AM, Kearney JF. Marginal zone and B1 B cells unite in the early response against T-independent blood-borne particulate antigens. *Immunity.* 2001;14(5):617-629. doi:10.1016/s1074-7613(01)00129-7
- Martin F, Kearney JF. Marginal-zone B cells. *Nat Rev Immunol.* 2002;2(5):323-335. doi:10.1038/nri799
- Mboko WP, Rekow MM, Ledwith MP, et al. Interferon Regulatory Factor 1 and Type I Interferon Cooperate To Control Acute Gammaherpesvirus Infection. *J Virol.* 2016;91(1):e01444-16. Published 2016 Dec 16. doi:10.1128/JVI.01444-16
- Negishi H, Ohba Y, Yanai H, et al. Negative regulation of Toll-like-receptor signaling by IRF-4. *Proc Natl Acad Sci U S A.* 2005;102(44):15989-15994. doi:10.1073/pnas.0508327102
- Negishi H, Fujita Y, Yanai H, et al. Evidence for licensing of IFN-gamma-induced IFN regulatory factor 1 transcription factor by MyD88 in Toll-like receptor-dependent gene induction program. *Proc Natl Acad Sci U S A.* 2006;103(41):15136-15141. doi:10.1073/pnas.0607181103
- New JS, King RG, Kearney JF. Manipulation of the glycan-specific natural antibody repertoire for immunotherapy. *Immunol Rev.* 2016;270(1):32-50. doi:10.1111/imr.12397
- New JS, Dizon BLP, Fucile CF, Rosenberg AF, Kearney JF, King RG. Neonatal Exposure to Commensal-Bacteria-Derived Antigens Directs Polysaccharide-Specific B-1 B Cell Repertoire Development. *Immunity.* 2020;53(1):172-186.e6. doi:10.1016/j.immuni.2020.06.006
- Nutt SL, Hodgkin PD, Tarlinton DM, Corcoran LM. The generation of antibody-secreting plasma cells. *Nat Rev Immunol.* 2015;15(3):160-171. doi:10.1038/nri3795
- Oliver AM, Martin F, Gartland GL, Carter RH, Kearney JF. Marginal zone B cells exhibit unique activation, proliferative and immunoglobulin secretory responses. *Eur J Immunol.* 1997;27(9):2366-2374. doi:10.1002/eji.1830270935
- Penninger JM, Sirard C, Mittrücker HW, et al. The interferon regulatory transcription factor IRF-1 controls positive and negative selection of CD8+ thymocytes. *Immunity.* 1997;7(2):243-254. doi:10.1016/s1074-7613(00)80527-0

- Pirgova G, Chauveau A, MacLean AJ, Cyster JG, Arnon TI. Marginal zone SIGN-R1⁺ macrophages are essential for the maturation of germinal center B cells in the spleen. *Proc Natl Acad Sci U S A*. 2020;117(22):12295-12305. doi:10.1073/pnas.1921673117
- Pillai S. The chosen few? Positive selection and the generation of naive B lymphocytes. *Immunity*. 1999;10(5):493-502. doi:10.1016/s1074-7613(00)80049-7
- Pillai S, Cariappa A, Moran ST. Marginal zone B cells. *Annu Rev Immunol*. 2005;23:161-196. doi:10.1146/annurev.immunol.23.021704.115728
- Pillai S, Cariappa A. The follicular versus marginal zone B lymphocyte cell fate decision. *Nat Rev Immunol*. 2009;9(11):767-777. doi:10.1038/nri2656
- Rawlings DJ, Schwartz MA, Jackson SW, Meyer-Bahlburg A. Integration of B cell responses through Toll-like receptors and antigen receptors. *Nat Rev Immunol*. 2012;12(4):282-294. Published 2012 Mar 16. doi:10.1038/nri3190
- Saito T, Chiba S, Ichikawa M, et al. Notch2 is preferentially expressed in mature B cells and indispensable for marginal zone B lineage development. *Immunity*. 2003;18(5):675-685. doi:10.1016/s1074-7613(03)00111-0
- Samardzic T, Marinkovic D, Danzer CP, Gerlach J, Nitschke L, Wirth T. Reduction of marginal zone B cells in CD22-deficient mice. *Eur J Immunol*. 2002;32(2):561-567. doi:10.1002/1521-4141(200202)32:2<561::AID-IMMU561>3.0.CO;2-H
- Schmitz F, Heit A, Guggemoos S, et al. Interferon-regulatory-factor 1 controls Toll-like receptor 9-mediated IFN-beta production in myeloid dendritic cells. *Eur J Immunol*. 2007;37(2):315-327. doi:10.1002/eji.200636767
- Stone SL, Peel JN, Scharer CD, et al. T-bet Transcription Factor Promotes Antibody-Secreting Cell Differentiation by Limiting the Inflammatory Effects of IFN- γ on B Cells. *Immunity*. 2019;50(5):1172-1187.e7. doi:10.1016/j.immuni.2019.04.004
- Taki S, Sato T, Ogasawara K, et al. Multistage regulation of Th1-type immune responses by the transcription factor IRF-1. *Immunity*. 1997;6(6):673-679. doi:10.1016/s1074-7613(00)80443-4
- Tamura T, Yanai H, Savitsky D, Taniguchi T. The IRF family transcription factors in immunity and oncogenesis. *Annu Rev Immunol*. 2008;26:535-584. doi:10.1146/annurev.immunol.26.021607.090400
- Tanigaki K, Han H, Yamamoto N, et al. Notch-RBP-J signaling is involved in cell fate determination of marginal zone B cells. *Nat Immunol*. 2002;3(5):443-450. doi:10.1038/ni793
- Van Epps HL. Bringing order to early B cell chaos. *J Exp Med*. 2006;203(6):1389. doi:10.1084/jem.2036fta

- Wang H, Beatty N, Chen S, et al. The CXCR7 chemokine receptor promotes B-cell retention in the splenic marginal zone and serves as a sink for CXCL12. *Blood*. 2012;119(2):465-468. doi:10.1182/blood-2011-03-343608
- Wen R, Chen Y, Xue L, et al. Phospholipase Cgamma2 provides survival signals via Bcl2 and A1 in different subpopulations of B cells. *J Biol Chem*. 2003;278(44):43654-43662. doi:10.1074/jbc.M307318200
- Wen L, Brill-Dashoff J, Shinton SA, Asano M, Hardy RR, Hayakawa K. Evidence of marginal-zone B cell-positive selection in spleen. *Immunity*. 2005;23(3):297-308. doi:10.1016/j.immuni.2005.08.007
- Won WJ, Kearney JF. CD9 is a unique marker for marginal zone B cells, B1 cells, and plasma cells in mice. *J Immunol*. 2002;168(11):5605-5611. doi:10.4049/jimmunol.168.11.5605
- Won WJ, Bachmann MF, Kearney JF. CD36 is differentially expressed on B cell subsets during development and in responses to antigen. *J Immunol*. 2008;180(1):230-237. doi:10.4049/jimmunol.180.1.230
- Xu H, Chaudhri VK, Wu Z, et al. Regulation of bifurcating B cell trajectories by mutual antagonism between transcription factors IRF4 and IRF8. *Nat Immunol*. 2015;16(12):1274-1281. doi:10.1038/ni.3287
- Yamada G, Ogawa M, Akagi K, et al. Specific depletion of the B-cell population induced by aberrant expression of human interferon regulatory factor 1 gene in transgenic mice. *Proc Natl Acad Sci U S A*. 1991;88(2):532-536. doi:10.1073/pnas.88.2.532
- Yang Y, Wang C, Yang Q, et al. Distinct mechanisms define murine B cell lineage immunoglobulin heavy chain (IgH) repertoires. *Elife*. 2015;4:e09083. Published 2015 Sep 30. doi:10.7554/eLife.09083
- You Y, Myers RC, Freeberg L, et al. Marginal zone B cells regulate antigen capture by marginal zone macrophages. *J Immunol*. 2011;186(4):2172-2181. doi:10.4049/jimmunol.1002106
- Zhang Z, Zhou L, Yang X, et al. Notch-RBP-J-independent marginal zone B cell development in IgH transgenic mice with VH derived from a natural polyreactive antibody. *PLoS One*. 2012;7(6):e38894. doi:10.1371/journal.pone.0038894
- Zhou Z, Niu H, Zheng YY, Morel L. Autoreactive marginal zone B cells enter the follicles and interact with CD4+ T cells in lupus-prone mice. *BMC Immunol*. 2011;12:7. Published 2011 Jan 20. doi:10.1186/1471-2172-12-7

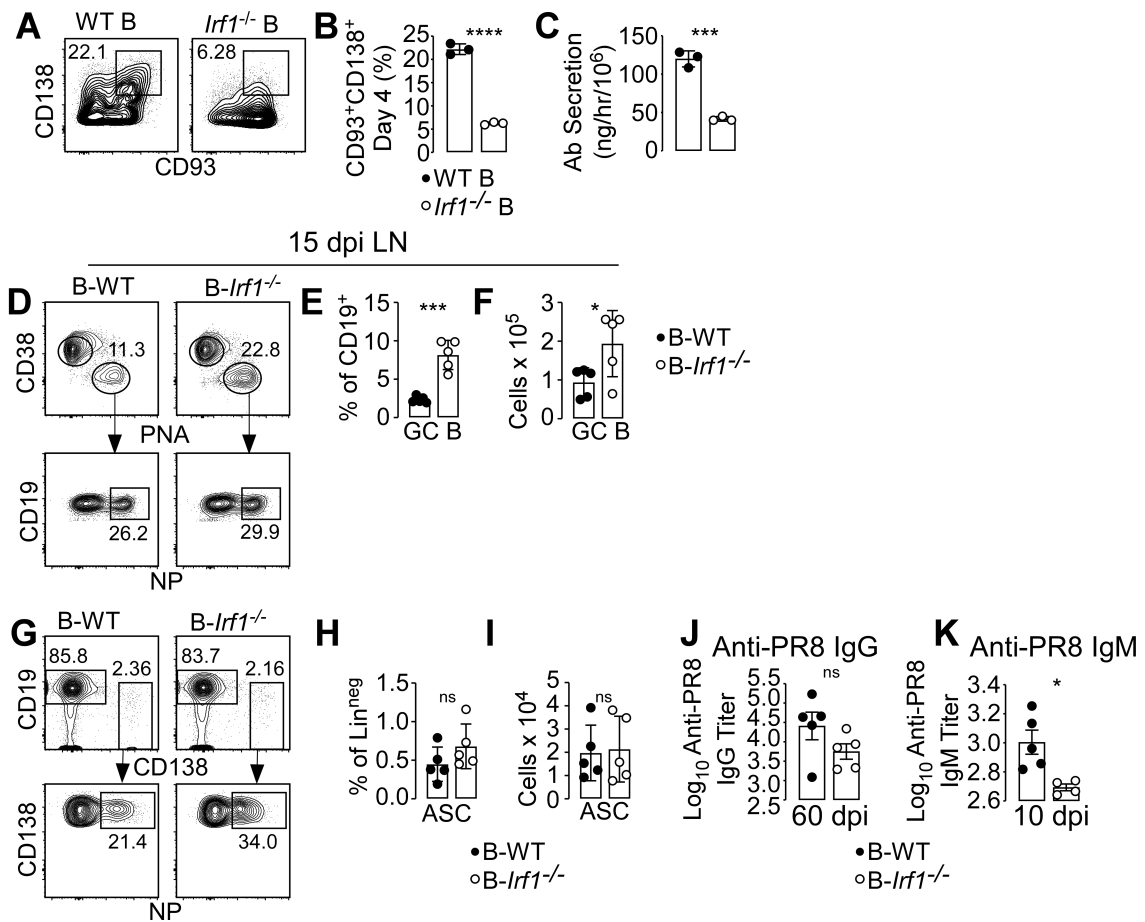


Figure 1. IRF1-expressing B cells are required for IFN γ -dependent IgM antibody responses and early IgM responses to influenza infection.

(A-C) *Irf1* expression by B cells regulates IFN γ -dependent development of IgM-secreting ASCs. B6 or *Irf1*^{-/-} splenic CD19⁺ B cells were co-cultured with Th1 cells in the presence of IL-2 and anti-IgM (Fab'2). The frequency (A-B) of CD138⁺CD93⁺ ASCs in the cultures were determined by flow cytometry on Day 4. (C) Cells from Day 4 cultures were washed and incubated for 5 hrs at 10⁶ cells/ml in fresh media. Ab secretory rates, measured as the amount of total Ig (antibody, Ab) secreted/hr by the cells, were determined by ELISA.

(D-K) *Irf1* expression by B cells regulates early IgM responses to influenza infection. BM chimeric mice that are competent to express *Irf1* in all lineages (B-

WT) or unable to express *Irf1* selectively in B lineage cells (B-*Irf1*^{-/-}, see [Fig. S1A](#) for description) were infected with PR8 influenza virus 8 weeks post-reconstitution. (D-I) Cells from medLN were analyzed by flow cytometry on Day 15. Flu nucleoprotein (NP)-specific PNA^{hi}CD38^{lo} GCB cells (D) and CD138^{hi}CD19^{lo} ASCs (G) were identified and the frequencies (E, H) and numbers (F, I) of NP⁺ GCB and NP⁺ ASCs were determined. (J-K) Serum was collected from infected mice. Day 10 flu-specific IgM (J) and Day 60 flu-specific IgG (K) were measured by ELISA. Data shown as endpoint titers.

Data shown are representative 3(A-C), 2(D-K) independent experiments with 3 experimental replicates per group (A-C) or with 3-5 mice/group (D-K) and are reported as mean ± SEM. *p* values determined using Student's *t* test, **p*≤0.05, ***p*≤0.01, ****p*≤0.001, *****p*≤0.0001 or not significant (ns).

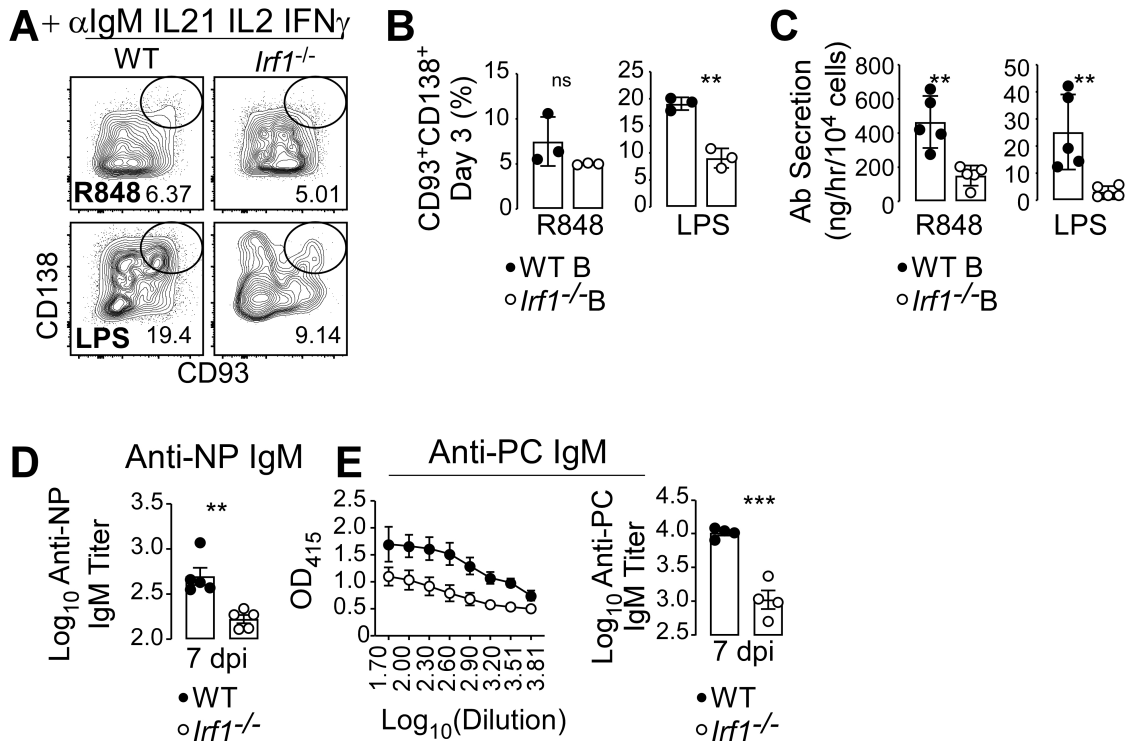


Figure 2. IRF1 regulates IgM Ab responses to TLR ligands and T-independent antigens.

(A-C) *lrf1* expression by B cells regulates TLR-driven IgM⁺ ASC development. WT or *lrf1*^{-/-} splenic CD19⁺ B cells were activated for 3 days with anti-IgM (Fab'2), IL-2, IFN γ , IL-21 plus either R848 or LPS. The frequency (A-B) and number (C) CD138⁺CD93⁺ ASCs in the cultures were determined by flow. (D) Cells from Day 3 cultures were washed and incubated for 6 hrs at 10⁴ cells/ml in fresh media. Ab secretory rates, measured as the amount of total Ig (antibody, Ab) secreted/hr by the cells, were determined by ELISA.

(D-E) T cell independent IgM Ab responses are regulated by IRF1. WT and *lrf1*^{-/-} mice (8 wk old) were immunized i.v. with TNP-Ficoll (D) or heat-killed *Streptococcus pneumonia* (E). Day 7 serum hapten-specific (D) or phosphorylcholine (PC)-specific (E) IgM was measured by ELISA. Data shown as endpoint titers.

Data shown are representative 2(A-B), 2(D-E) independent experiments with 3 experimental replicates per group (A-B) or 3-5 mice/group (D-E). 2C is representative of 2 combined experiments with 2-3 experimental replicates per group per experiment and are reported as mean \pm SEM. *p* values determined using Student's t test, **p*≤0.05, ***p*≤0.01, ****p*≤0.001, *****p*≤0.0001 or not significant (ns).

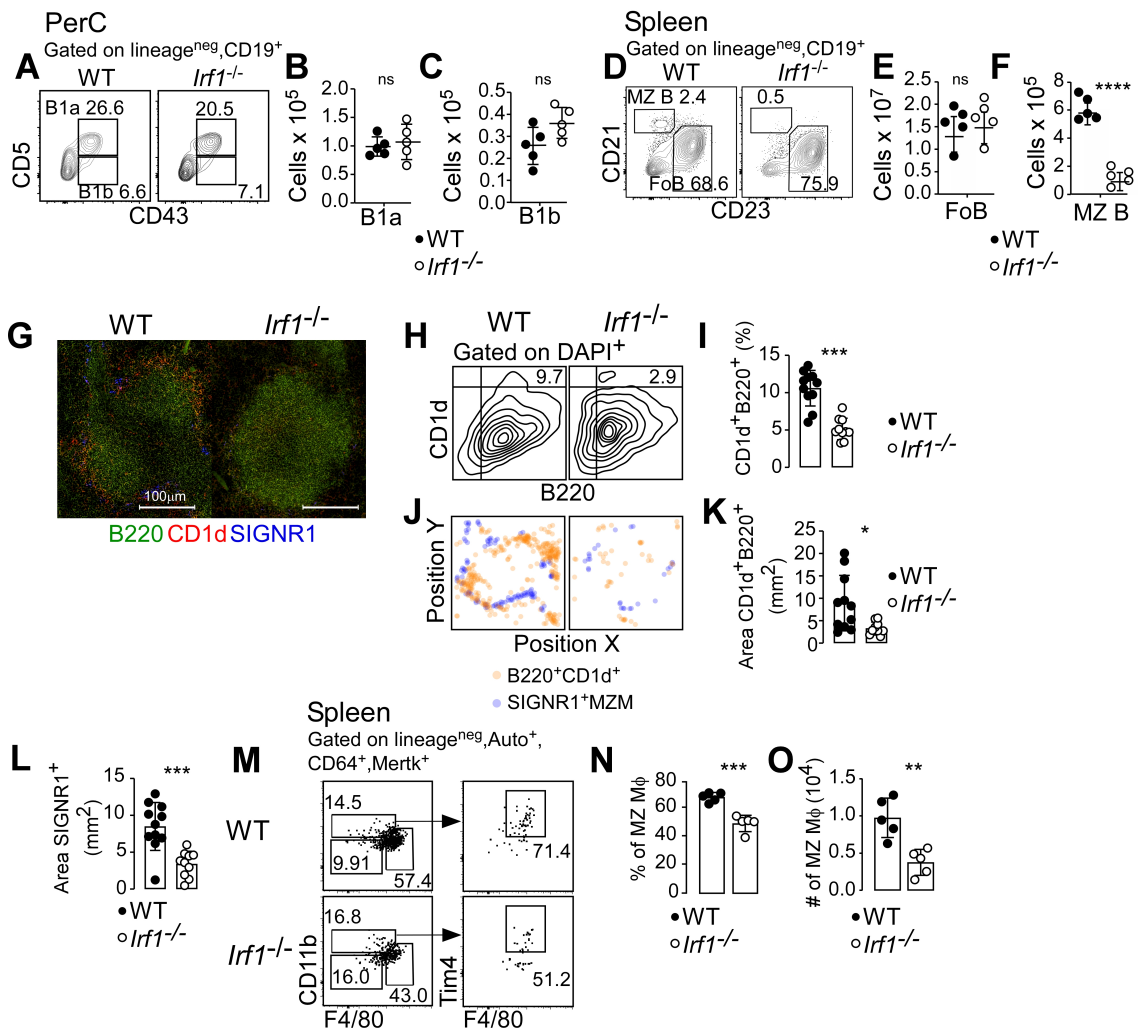


Figure 3. The marginal zone B cell and macrophage compartments rely on IRF1.

(A-F) The splenic MZ B cell compartment is ablated in *Lrf1*^{-/-} mice. Flow cytometric analysis of peritoneal cavity (PerC, A-C) and spleen (D-F) of 8 wk old naïve WT and *Lrf1*^{-/-} mice. Data are shown as the frequency (A) and number of PerC CD19⁺CD43⁺CD5⁺ B1a (B) and CD19⁺CD43⁺CD5^{neg} B1b (C) cells and the frequency (D) and number of splenic CD19⁺CD23⁺CD21^{neg} FoB (E) and CD19⁺CD23^{neg}CD21^{hi} MZ B (F) cells. Enumeration of MZ B cells using additional markers is shown in Fig. S2A-F.

(G-L). The splenic marginal zone is compromised in *Lrf1*^{-/-} mice. Immunohistology analysis of spleen sections from 8 wk naïve WT or *Lrf1*^{-/-} mice stained for B220 (green), CD1d (red), SIGNR1 (blue) and DAPI (shown in Fig. S2G, cyan). Representative sections (G) displaying B cell follicles and the MZ are shown. Histocytometry density plots (H) were generated from the WT and *Lrf1*^{-/-} splenic

follicles shown in panel G. The frequency of B220⁺CD1d⁺ B cells within the DAPI⁺ cells is shown. Frequencies of B220⁺CD1d⁺ B cells (I) in individual splenic follicles (WT n=11, *Irf1*^{-/-} n=9) present in one splenic cross-section. Mapped position plots (J) were generated from the WT and *Irf1*^{-/-} splenic follicles shown in panel G. Localization of B220⁺CD1d⁺ B cells (orange) and SIGNR1⁺ MZM (blue) is shown. Total area occupied by B220⁺CD1d⁺ B cells (K) and SIGNR1⁺ macrophages (L) in individual splenic follicles (WT n=11, *Irf1*^{-/-} n=9) present in one splenic cross-section.

(M-O). MZ macrophages (MZM) compartment is reduced in *Irf1*^{-/-} mice. Flow cytometric analysis to identify MZM cells in spleens of 8 wk naïve WT and *Irf1*^{-/-} mice. Gating strategy (M) to identify CD64⁺Mertk⁺CD11b^{hi}F480^{int}Tim4⁺ MZM (M). The frequencies (N) and numbers (O) of MZM are shown.

Data are representative of 5(A-F), 2(G-O) independent experiments with 3-5 mice/group (A-F),(M-O) or 2 mice/group (G-L) and reported as mean ± SEM. *p* values determined using Student's t test (A-O) **p*≤0.05, ***p*≤0.01, ****p*≤0.001, *****p*≤0.0001 or not significant (ns).

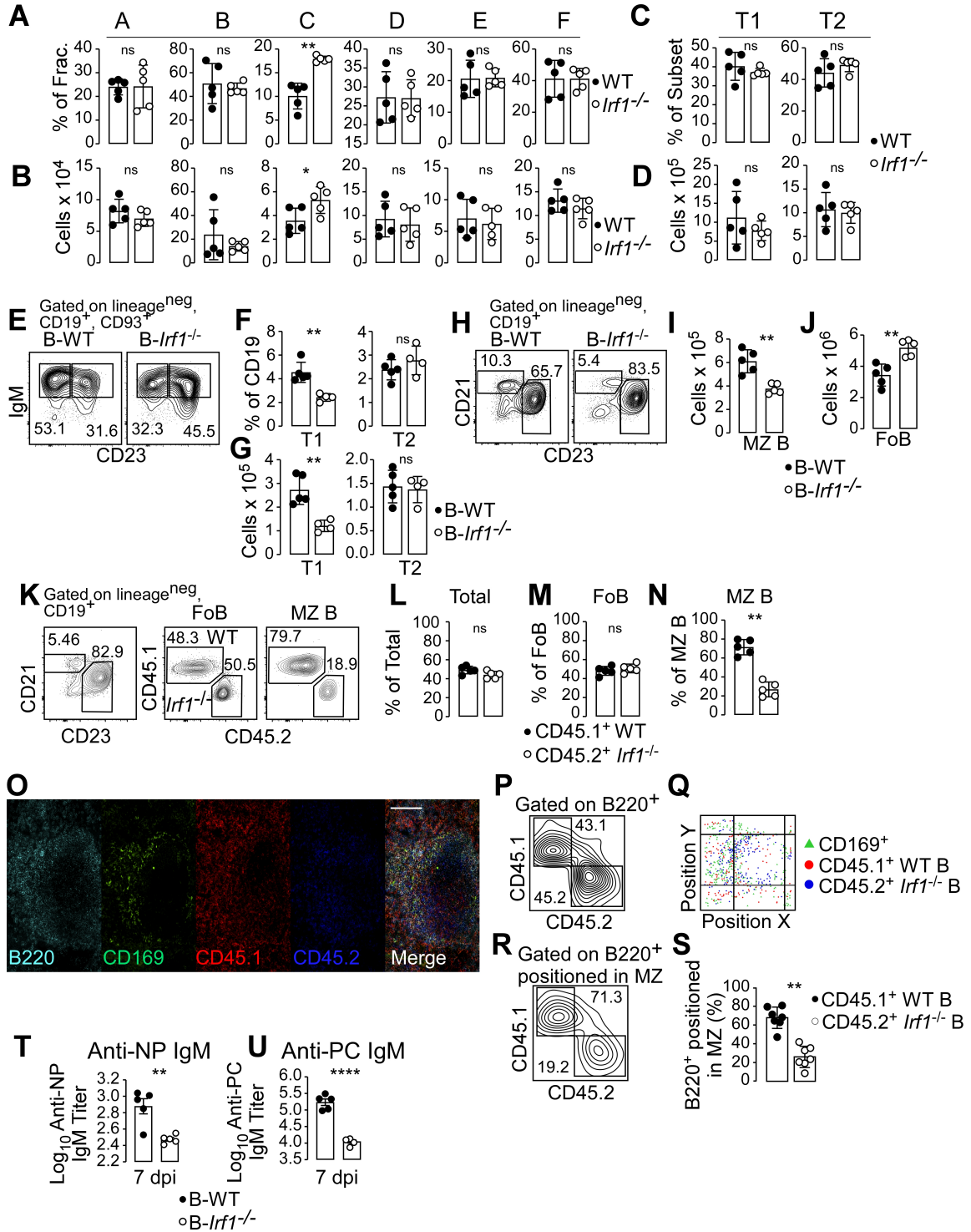


Figure 4. MZ B cells and T cell independent responses require IRF1 expression by B cells.

(A-D) B cell development is not affected in *Irf1*^{-/-} mice. Flow cytometric analysis of BM (A-B) and spleen (C-D) of 8 wk old naïve WT and *Irf1*^{-/-} mice. The frequency (A, C) and number (B, D) of BM B cell subsets (Fraction A-F, gated as in Fig. S3A) and immature splenic B cells (T1 and T2 subsets, gated as in Fig. S3B) are shown.

(E-J) The MZ B cell compartment is dependent on B cell specific expression of *Irf1*. Flow cytometric analysis of spleens from B-WT and B-*Irf1*^{-/-} chimeras (see Fig. S1A for description of chimeras) 8 weeks post-reconstitution. Representative flow plots showing T1 and T2 B cells (E) or FoB and MZ B (H) are shown. Data are displayed as the frequencies (F) and numbers (G) of T1 and T2 transitional B cells and the numbers of FoB (I) and MZ B (J) cells.

(K-S) B cell intrinsic expression of *Irf1* is required for the formation or maintenance of the MZ B cell compartment but not positioning of B cells within the MZ. Flow cytometric (K-N) and immuno-histologic (O-S) analysis of spleens from lethally irradiated recipients reconstituted 8 wks earlier with a mixture of 50% WT (CD45.1⁺) and 50% *Irf1*^{-/-} (CD45.2⁺) BM cells. Representative flow plots (K) identifying CD45.1⁺ WT and CD45.2⁺ *Irf1*^{-/-} FoB and MZ B cells are shown. The frequencies of CD45.1⁺ B6 cells and CD45.2⁺ *Irf1*^{-/-} cells present in total live splenocytes (L), the FoB (M) or MZ B (N) compartments. Immunohistology analysis (O-S) of spleen sections from 50%WT:50%*Irf1*^{-/-} chimeras stained for B220 (cyan), CD169 (green), CD45.1 (red, to identify WT cells) and CD45.2 (blue, to identify *Irf1*^{-/-} cells). Representative section (O) displaying a B cell follicle and the MZ with the boundary between the follicle and MZ delineated by CD169⁺ metallophilic macrophages (MMM). Histocytometry density plots (P, R) and mapped localization plots (Q, S) were generated from the WT and *Irf1*^{-/-} splenic follicle shown in panel O. The frequencies (P) of CD45.1⁺ WT and CD45.2⁺ *Irf1*^{-/-} cells within the B220⁺ compartment is shown. B cells positioned within the MZ were identified by assessing the localization (Q) of the WT and *Irf1*^{-/-} B cells relative to the MMM. The frequencies (R) of MZ-localized WT CD45.1⁺ and *Irf1*^{-/-} CD45.2⁺ B cells were determined in the B cell follicle shown in (O) and in individual splenic follicles (WT n=7, *Irf1*^{-/-} n=7) present in one splenic cross-section.

(T-U) IRF1-expressing B cells are required for T cell-independent IgM Ab responses. B-WT and B-*Irf1*^{-/-} mice were immunized i.v. with TNP-Ficoll (T) or heat-killed *Streptococcus pneumonia* (U) 8 wks post-reconstitution. Day 7 serum hapten (NP)-specific (T) or phosphorylcholine (PC)-specific (U) IgM was measured by ELISA. Data shown as endpoint titers.

Data shown are representative of 3(A-D),2(E-J),4(K-N),2(O-S) with 3-5 (A-N),(T,U) or 2(O-S) mice/group. Data reported as mean ± SEM. *p* values determined using Student's t test, **p*≤0.05, ***p*≤0.01, ****p*≤0.001, *****p*≤0.0001 or not significant (ns).

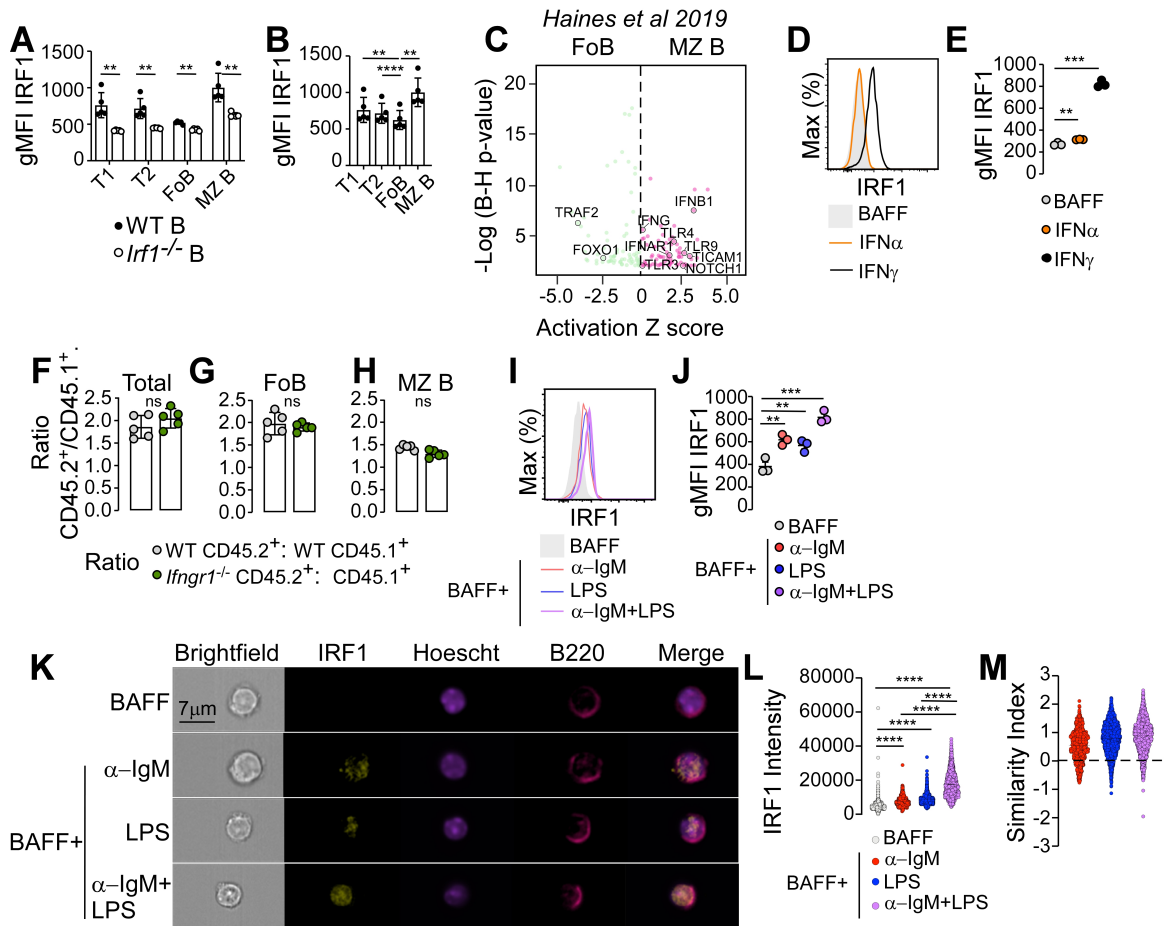


Figure 5. TLR and BCR signals cooperate to induce IRF1 expression in transitional B cells.

(A-B) IRF1 is expressed in transitional and MZ B cells. Flow cytometric analysis of spleens from 8 wk old naïve WT and *Irf1*^{-/-} mice. Data in (A) compare IRF1 levels, shown as geometric mean fluorescence intensities (gMFI), in T1, T2, FoB and MZ B cells from WT and *Irf1*^{-/-} animals. Panel B compares gMFI between WT T1, T2, FoB, and MZ B cells.

(C) IPA-predicted upstream regulators of the published ([Haines et al., 2019](#)) differentially expressed genes (DEGs) between *Cd19*^{cre/+} MZ B cells (pink, up in MZ B cells) and *Cd19*^{cre/+} FoB cells (green, up in FoB cells). DEGs (n=1453, [Table S1](#)) defined as fold-change > 1(log2) or <-1 (log2) and FDR q≤0.05. IPA-predicted upstream regulators provided in [Table S2](#).

(D-E) IFNs induces IRF1 expression in transitional B cells. IRF1 expression by WT CD93⁺ transitional B cells stimulated for 24 hrs with BAFF (grey filled histogram, grey symbols) alone or BAFF in combination with IFN α (orange line histogram, orange symbol) or IFN γ (black line histogram, black symbol). Data are shown from a representative experiment as histograms (D) or as the gMFI of IRF1 (E) in the stimulated cells.

(F-H) B cell intrinsic expression of IFN receptors is not required for MZ B cell development. Assessment of total spleen cells (F), FoB cells (G) and MZ B cells (H) in 50:50 radiation BM chimeras reconstituted with 50% CD45.1⁺WT BM plus 50% CD45.2⁺WT BM (grey) or with 50% CD45.1⁺WT BM plus 50% CD45.2⁺*Ifngr1*^{-/-} BM (green). Data shown as the ratio of CD45.1⁺ cells to CD45.2⁺ cells in each WT:WT and WT:*Ifngr1*^{-/-} chimeric animal. Analysis of WT:WT and WT:*Ifnar*^{-/-} chimeras is shown in [Fig. S4B-S4D](#).

(I-J) IRF1 expression by WT CD93⁺ transitional B cells stimulated for 24 hrs with BAFF (grey filled histogram, grey symbols) alone or BAFF in combination with anti-IgM (red line and symbol), LPS (blue line and symbol) or anti-IgM+LPS (purple line and symbol). Data are shown from a representative experiment as histograms (I) or as the gMFI of IRF1 (J) in the stimulated cells.

(K-M) IRF1 translocates to the nucleus in BCR or TLR stimulated transitional B cells. Analysis of WT CD93⁺ transitional B cells stimulated for 24 hrs with BAFF alone (grey) or BAFF in combination with anti-IgM (red), LPS (blue) or anti-IgM+LPS (purple), and then stained with Hoescht, anti-IRF1 and anti-B220. Cells were visualized by ImageStream. Representative images of cells from each stimulation condition show co-localization of IRF1 (yellow) with Hoescht (purple) in the nucleus of B220⁺ (pink) transitional B cells. IRF1 expression levels (L) in each cell (BAFF n= 2698, BAFF+anti-IgM n= 860, BAFF+LPS n=2142, or BAFF+anti-IgM+LPS n=1782 cells) from the different stimulation conditions were measured as fluorescence intensity using IDEAS ImageStream analysis software. IRF1 nuclear localization in each cell (BAFF n= 2698, BAFF+anti-IgM n= 860, BAFF+LPS n=2142, or BAFF+anti-IgM+LPS n=1782 cells) from the different stimulation conditions was assessed using IDEAS ImageStream analysis software to determine the similarity index (M), which is defined as pixel intensity overlap between the nucleus (Hoescht, purple) and the IRF1 probe (yellow). Similarity index not shown for BAFF alone stimulation as IRF1 levels were too low to make a determination.

Data shown are representative of 2(A-B),2(D-E),3(F-H),2(I-J) independent experiments with experimental replicates/condition or 2(K-M) independent experiments with individual cells/condition. Data reported as mean \pm SEM. *p* values determined using unpaired Student's t test (A), paired Student's t test (F-H) or one-way ANOVA (B, E, J, L) **p*≤0.05, ***p*≤0.01, ****p*≤0.001, *****p*≤0.0001 or not significant (ns).

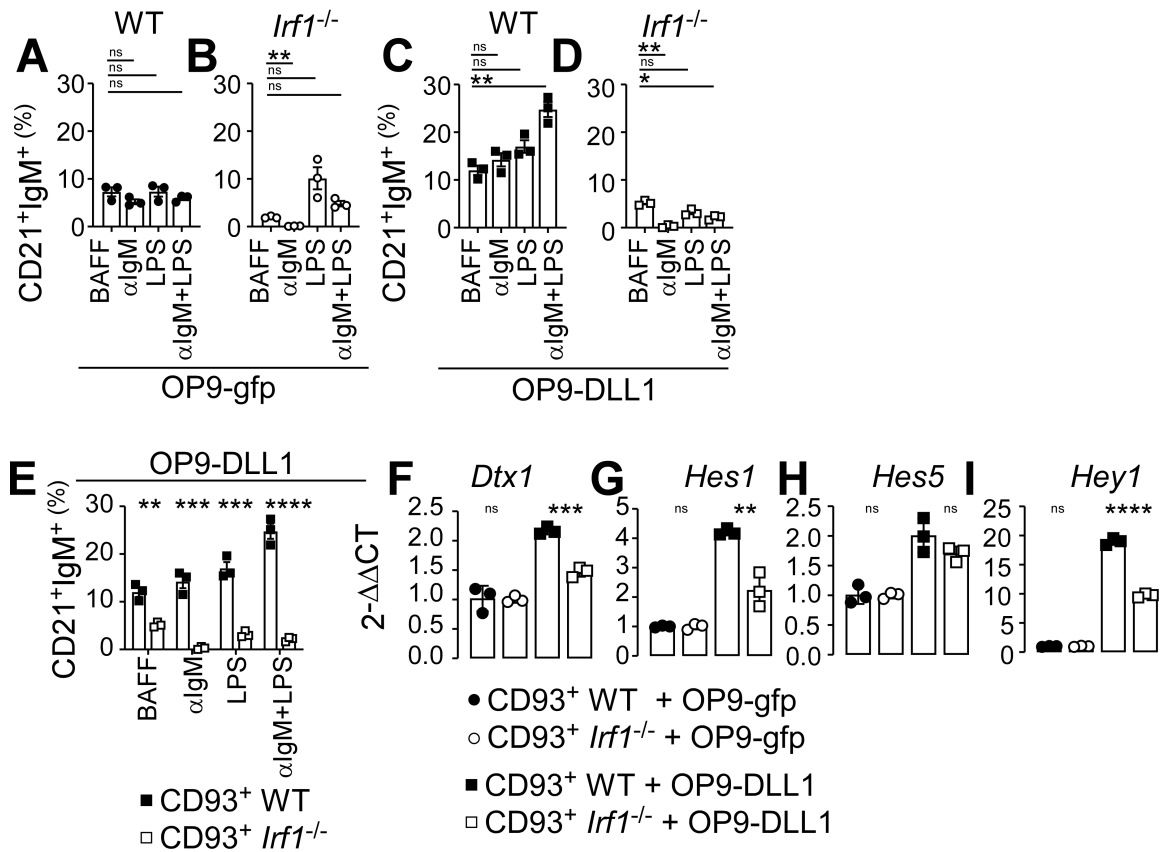


Figure 6. IRF1 Regulates Notch signaling in Transitional B Cells.

(A-E) BCR and TLR signals cooperate to promote the development of MZ B cells from IRF1-expressing MZ B cell precursors. Development of CD23^{neg}CD21^{hi}IgM⁺ MZ B-like cells from purified WT (black) or *Irf1*^{-/-} (white) CD93⁺ transitional B cells that were co-cultured with OP9-gfp (circles, (A-B)) or OP9-DLL1 (squares, (C-E)) stromal cells for 3 days in the presence of BAFF alone or BAFF in combination with anti-IgM, LPS or anti-IgM+LPS. Data are shown as the frequency of CD23^{neg}CD21⁺IgM⁺ cells in the cultures.

(F-I) Upregulation of Notch-dependent target genes requires IRF1 expression by transitional B cells. qPCR analysis of CD93⁺ WT (black) or CD93⁺ *Irf1*^{-/-} (white) co-cultured for 5 hrs with either OP9-gfp (circle) or OP9-DLL1 (square) stromal cells. Data are shown as the fold change in expression of *Dtx1* (F), *Hes1* (G), *Hes5* (H) and *Hey1* (I) calculated as the 2^{-ΔΔCT} normalized to a co-culture control sample containing WT CD93⁺ transitional B cells and *Irf1* OP9-gfp cells. Samples with CT values above 32 were considered negative.

Data shown are representative of 2(A-I) independent experiments with 3 experimental replicates/group and reported as mean ± SEM. *p* values determined using one-way ANOVA (A-D) or Student's *t* test (E-I) **p*≤0.05, ***p*≤0.01, ****p*≤0.001, *****p*≤0.0001 or not significant (ns).

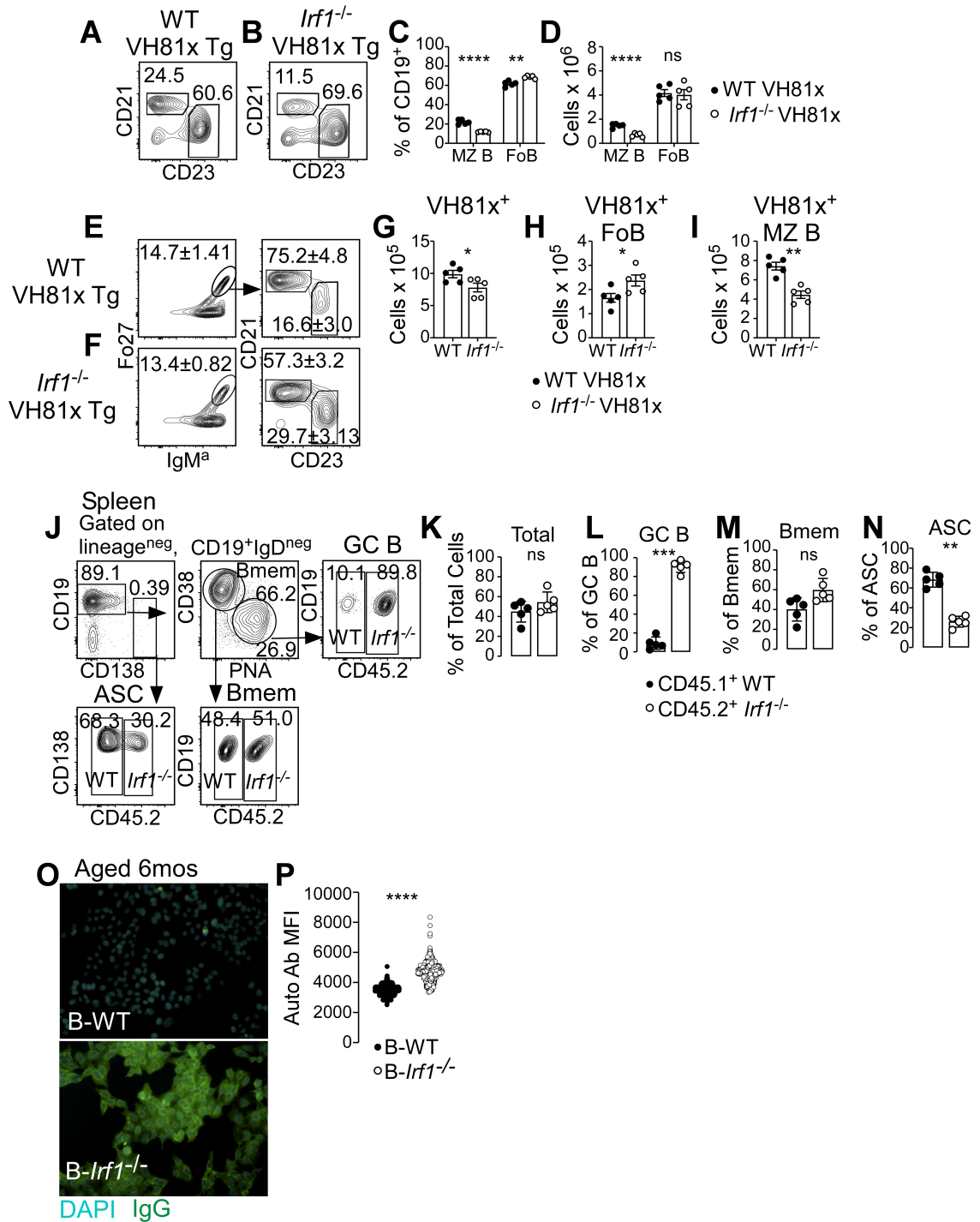


Figure 7. IRF1 regulates selection of B cells into the polyreactive and autoreactive repertoire.

(A-I) IRF1 supports selection of polyreactive BCRs into the MZ B cell compartment. Flow cytometric analysis of splenic CD19⁺ CD21^{lo}CD23⁺ FoB and CD21^{hi}CD23^{neg} MZ B cells from 8 wk old naive WT VH81x (WT VH81x Tg, black symbols) and *Irf1*^{-/-} VH81x (*Irf1*^{-/-} VH81x Tg, white symbols) transgenic mice. Representative flow plots are shown in (A-B). Data are reported as the frequency (C) and number (D) of total MZ B cells and FoB cells in each animal. Identification of splenic B cells expressing the VH81x transgene in WT VH81x (E) and *Irf1*^{-/-} VH81x (F) mice by flow cytometry using the RS3.1 Ab to identify the IgMa⁺ VH81X transgene and Fo27 Ab to identify the predominant VK1C light chain that pairs with VH81x transgene. Data are shown as the absolute number of VH81X⁺ (G), VH81X⁺ FoB cells (H), and VH81X⁺MZ B cells (I) in each mouse.

(J-N) *Irf1*^{-/-} B cells form spontaneous GC B cells in aged mice. Flow cytometric analysis of B cells in the spleens of aged (6 months) irradiated μ MT recipients reconstituted with 50% CD45.1⁺WT BM plus 50% CD45.2⁺*Irf1*^{-/-} BM. CD45.1⁺WT and CD45.2⁺*Irf1*^{-/-} ASCs, memory B cells (Bmem) and GC B cells were identified (J) and enumerated as the frequencies of CD45.1⁺WT (black) or CD45.2⁺*Irf1*^{-/-} (white) lymphocytes (K), GC B cells (L), Bmem (M) or ASCs (N) in each recipient.

(O-P) B cell intrinsic expression of *Irf1* prevents autoAb development. Detection of IgG autoAbs in serum of aged (6 month) B-WT or B-*Irf1*^{-/-} BM chimeras (see Fig. S1A for description). HEp-2 cells were stained with serum from aged B-WT (top) or B-*Irf1*^{-/-} (bottom) chimeric mice and developed with a pan anti-IgG (green) to identify autoAbs and DAPI (cyan) to identify the nucleus. Representative images of autoAb staining are shown in (O) and Fig. S7. Data are reported as mean fluorescent intensities (MFI) of serum IgG autoantibody binding (P) to individual cells (B-WT n = 1119, B-*Irf1*^{-/-} n= 962).

Data shown are representative of 2(A-I),2(J-N), 2(O-P) independent experiments with 3-5 mice/group and reported as mean \pm SEM. *p* values determined using Student's t test (C, D, G-I, P) or Paired Student's t test (K-N). **p*≤0.05, ***p*≤0.01, ****p*≤0.001, *****p*≤0.0001 or not significant (ns).

NP-specific PNA^{hi}CD38^{lo} GCB cells and CD138^{hi}CD19^{lo}ASCs are shown. Data shown are representative of 3 independent experiments.

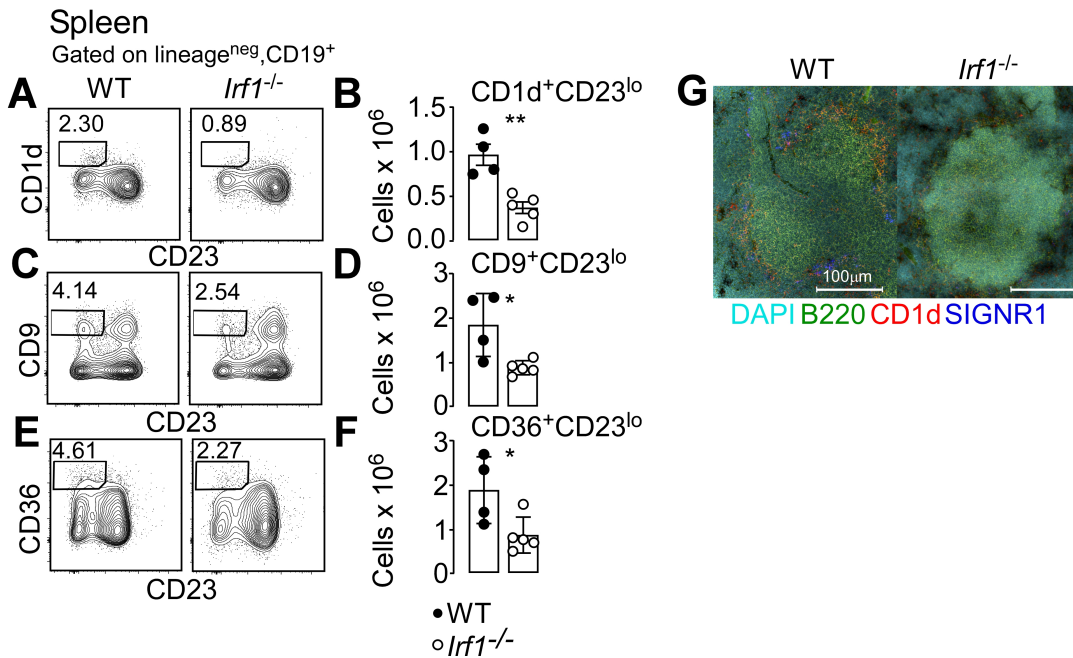


Figure S2. Characterization of splenic MZ B cells in naive WT and *Irf1*^{-/-} mice (related to Figure 3).

(A-F) Flow cytometric analysis of spleens from 8 wk old naive WT and *Irf1*^{-/-} mice. Data are shown as the frequency (A,C,E) and number of CD1d⁺CD23^{lo} MZ B cells (B), CD9⁺CD23^{lo} MZ B cells (D), or CD36⁺CD23^{lo} MZ B cells (F).

(G) Immunohistology analysis of spleen sections from 8 wk naive WT or *Irf1*^{-/-} mice stained for B220 (green), CD1d (red), SIGNR1 (blue) and DAPI (cyan). Representative sections (G) displaying B cell follicles and the MZ are shown.

Data shown are representative of 3(A-F),2(G) independent experiments with 4-5(A-F),2(G) mice/group and reported as mean ± SEM. *p* values are determined using Student's t test **p*≤0.05, ***p*≤0.01, ****p*≤0.001, *****p*≤0.0001.

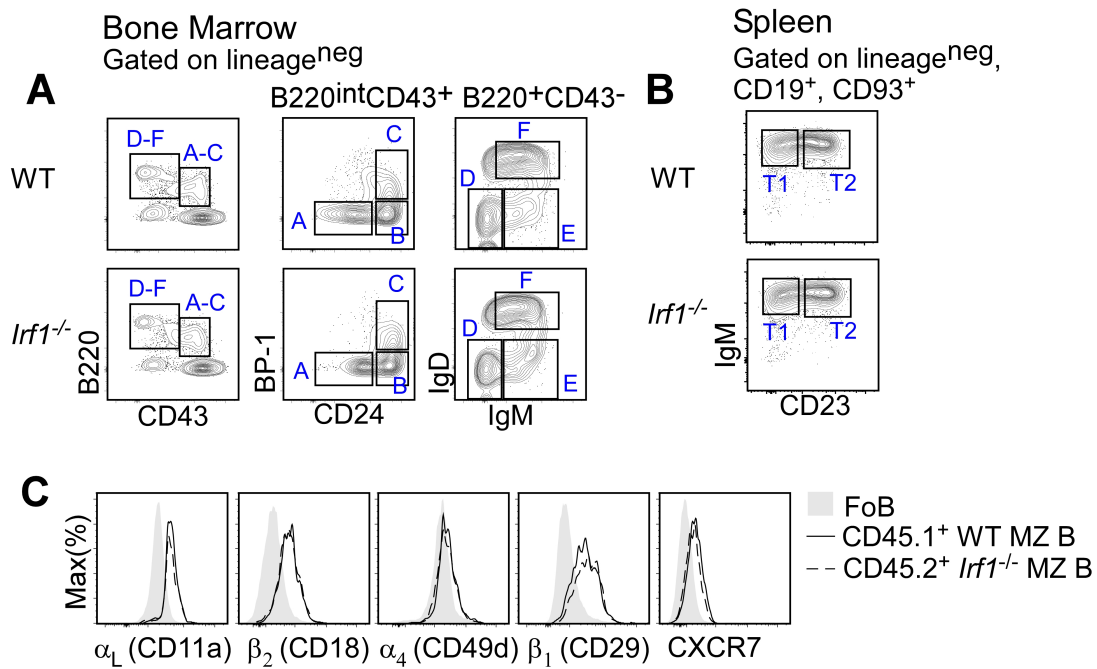


Figure S3. *Irf1* is mostly dispensable for BM and splenic B cell development and intact integrin and chemokine receptor expression in the absence of *Irf1* (related to Figure 4).

(A-B) *Irf1* is mostly dispensable for BM and splenic B cell development. Flow cytometry gating strategy to identify B cell subsets in the BM (A) and spleen (B) of 8 wk naïve WT and *Irf1*^{-/-} mice. Representative flow plots showing BM pre-pro B (Fraction A (Fr. A)), BM pro-B (Fr. B-C), BM pre-B (Fr. D), BM immature B (Fr. E) BM mature B (Fr. F) (A) and splenic T1 plus T2 transitional B cells (B).

(C) *Irf1* expression by B cell is not required for the expression of integrins and chemokine receptors that mediate retention of B cells in the MZ. Flow cytometric analysis of spleens from lethally irradiated recipients reconstituted 8 wks earlier with a mixture of 50% CD45.1⁺WT and 50%*Irf1*^{-/-} BM cells. Representative histograms (n=3 independent experiments) showing the expression of CD11a, CD18, CD49d, CD29, and CXCR7 by CD19⁺CD21^{neg}CD23⁺ FoB (grey filled), CD45.1⁺ CD19⁺CD21^{hi}CD23^{lo} WT MZ B cells (solid black line) or CD45.2⁺ CD19⁺CD21^{hi}CD23^{lo} *Irf1*^{-/-} MZ B cells (dashed black line).

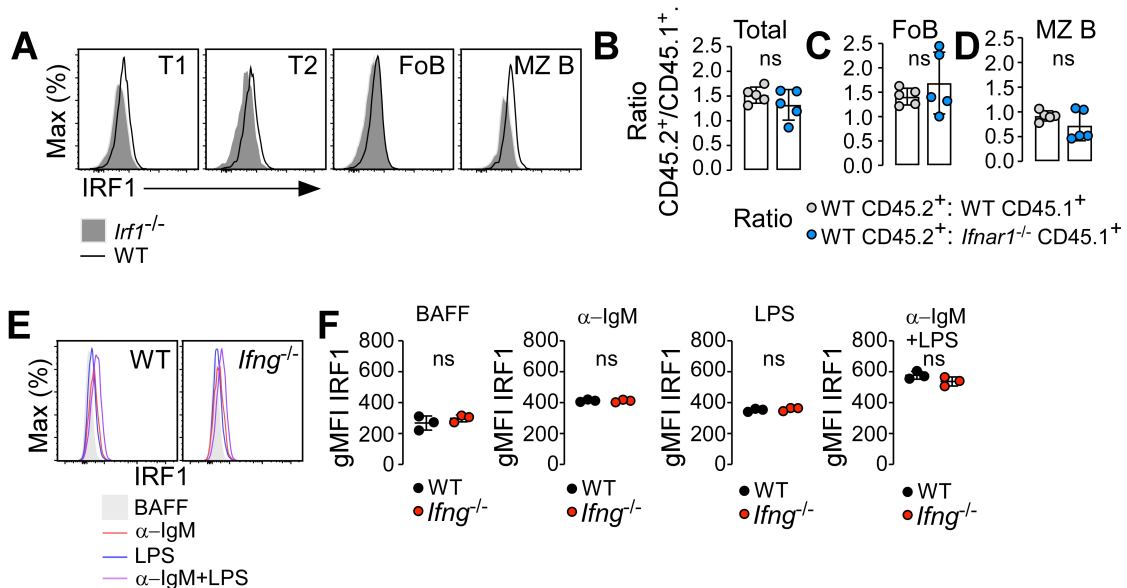


Figure S4. IRF1 expression in transitional and MZ B cells does not require IFN signals (related to Figure 5).

(A) IRF1 expression by transitional and MZ B cells. Flow cytometric analysis of spleens of 8 wk old naïve WT (black line) and *Irfl*^{-/-} (grey filled) mice showing IRF1 expression in CD19⁺CD93⁺ T1, CD19⁺CD93⁺ T2, CD19⁺CD21^{neg}CD23⁺ FoB and CD19⁺CD21^{hi}CD23^{lo} MZ B cells.

(B-D) *Ifnar1* expression is not required for MZ B cell development. Flow cytometry analysis of competitive mixed BM chimeras that were generated by reconstituting lethally irradiated μ MT recipients with a mixture of (i) 50% CD45.1⁺WT BM plus 50% CD45.2⁺WT BM (grey symbols) or (ii) 50% CD45.1⁺WT BM plus 50% CD45.2⁺*Ifnar1*^{-/-} (blue symbols). Total spleen cells (B), CD19⁺CD21^{neg}CD23⁺ FoB cells (C) and CD19⁺CD21^{hi}CD23^{lo} MZ B cells (D) were identified and the proportion of CD45.1⁺WT and CD45.2⁺*Ifnar1*^{-/-} cells in each subset was determined. Data shown as ratios of CD45.1⁺WT to CD45.2⁺WT cells within each subset and are compared to the ratios of CD45.1⁺WT to CD45.2⁺*Ifnar1*^{-/-} cells in each subset.

(E-F) BCR and TLR stimulated IRF1 expression in transitional B cells does not require IFN γ production by the B cells. IRF1 expression measured by flow cytometry in magnetically purified WT CD93⁺ or *Ifng*^{-/-} CD93⁺ transitional B cells stimulated 24 hrs with BAFF alone (grey filled) or BAFF in combination with anti-IgM F(ab)[']2 (red), LPS (blue) or anti-IgM+LPS (purple). Quantitation of IRF1 expression (F) by 24 hr stimulated transitional B cells represented as the geometric mean fluorescence intensities (gMFI) of IRF1 from stimulated WT CD93⁺ (black) or *Ifng*^{-/-}CD93⁺ (red) transitional B cells.

Data shown are representative of 2 (A, E-F) or 3 (B) independent experiments with 3-5 mice/group (A-B) or 3 experimental replicates/group/condition (E) and reported

as mean \pm SEM. p values are determined using Student's t test * $p \leq 0.05$, ** $p \leq 0.01$, *** $p \leq 0.001$, **** $p \leq 0.0001$ or not significant (ns).

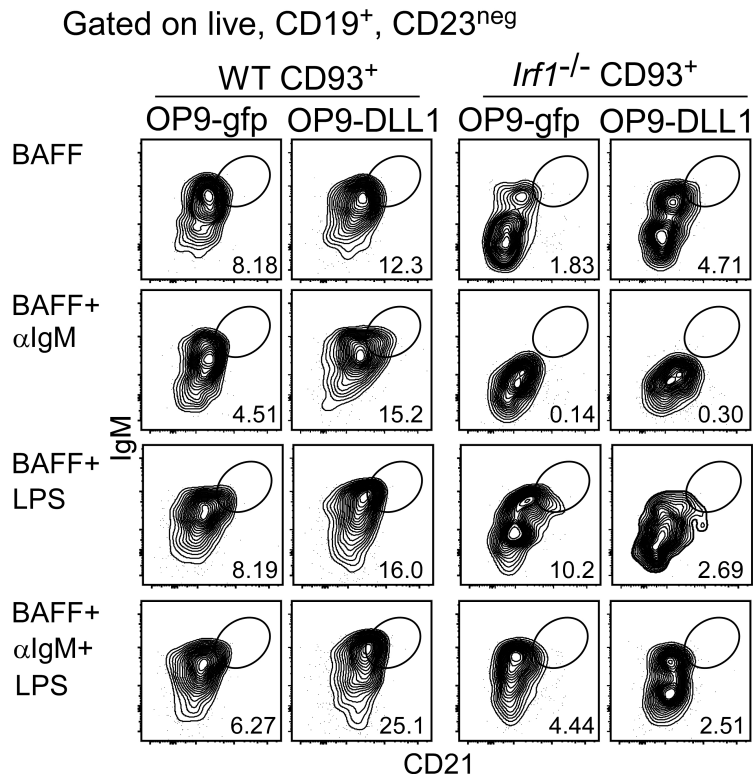


Figure S5. Activated *Irf1*^{-/-} transitional B cells do not adopt a mature MZ B cell phenotype *in vitro* (related to Figure 6).

Purified WT and *Irf1*^{-/-} CD93⁺ transitional B cells were co-cultured with OP9-gfp or OP9-DLL1 stromal cells for 3 days in the presence of BAFF alone or BAFF in combination with anti-IgM F(ab)'₂, LPS or anti-IgM F(ab)'₂ +LPS. Representative flow cytometric analysis of WT and *Irf1*^{-/-} CD93⁺ transitional B cells on day 3. B cells exhibiting a mature MZ B cell phenotype (CD23^{neg}CD21⁺IgM^{hi}) after 3 days of co-culture were identified and the frequency of these cells was determined.

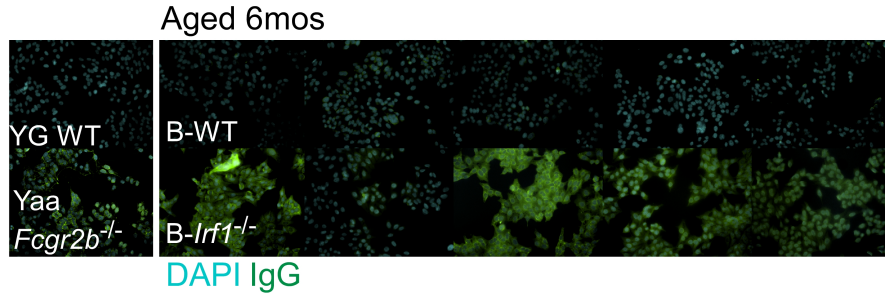


Figure S6. IRF1 regulates selection of B cells into the polyreactive and autoreactive repertoire. (related to Figure 7).

B cell intrinsic expression of *Irf1* prevents autoAb development. Detection of IgG autoAbs in serum of aged (6 month) B-WT or B-*Irf1*^{-/-} BM chimeras (see Fig. S1A for description). HEp-2 cells were stained with serum from aged (5) B-WT (top) or (5) B-*Irf1*^{-/-} (bottom) chimeric mice and developed with a pan anti-IgG (green) to identify autoAbs and DAPI (cyan) to identify the nucleus. 8 wk old or Young (YG, top left) WT and aged (12 month, bottom left) Yaa *Fcgr2b*^{-/-} mice included at controls.

SINGLE-DOSE INTRANASAL ADMINISTRATION OF ADCOVID ELICITS
SYSTEMIC AND MUCOSAL IMMUNITY AGAINST SARS-COV-2 IN MICE

by

RODNEY G. KING, AARON SILVA-SANCHEZ, JESSICA N. PEEL, DAVIDE BOTTA,
SELENE MEZA-PEREZ, S. RAMEEZA ALLIE, MICHAEL D. SCHULTZ,
MINGYONG LIU, JOHN E. BRADLEY, SHIHONG QIU, GUANG YANG, FEN
ZHOU, ESTHER ZUMAQUERO, THOMAS S. SIMPLER, BETTY MOUSSEAU, JOHN
T. KILLIAN JR., BRITTANY DEAN, QIAO SHANG, JENNIFER L. TIPPER,
CHRISTOPHER RISLEY, KEVIN S. HARROD, RAY FENG, YOUNG LEE,
BETHLEHEM SHIBERU, VYJAYANTHI KRISHNAN, ISABELLE PEGUILLET,
JIANFENG ZHANG, J. TODD GREEN, TROY D. RANDALL, JOHN J. SUSCHAK,
BERTRAND GEORGES, FRANCES E. LUND, SCOT ROBERTS

Vaccines

King RG, Silva-Sanchez A, Peel JN, Botta D, Dickson AM, Pinto AK, Meza-Perez S,
Allie SR, Schultz MD, Liu M, Bradley JE, Qiu S, Yang G, Zhou F, Zumaquero E,
Simpler TS, Mousseau B, Killian JT Jr., Dean B, Shang Q, Tipper JL, Risley CA, Harrod
KS, Feng T, Lee Y, Shiberu B, Krishnan V, Peguillet I, Zhang J, Green TJ, Randall TD,
Suschak JJ, Georges B, Brien JD, Lund FE, Roberts MS. Single-Dose Intranasal
Administration of AdCOVID Elicits Systemic and Mucosal Immunity against SARS-
CoV-2 and Fully Protects Mice from Lethal Challenge. *Vaccines*. 2021; 9(8):881.

<https://doi.org/10.3390/vaccines9080881>

Copyright

2021

by

Frances E. Lund

Used by permission

Format adapted for dissertation

SUMMARY

Background: The coronavirus disease 2019 (COVID-19) pandemic has highlighted the urgent need for effective prophylactic vaccination to reduce burden and spread of severe acute respiratory syndrome coronavirus 2 (SARS-CoV-2) in humans. Intranasal vaccination is an attractive strategy to prevent COVID-19 as the nasal mucosa represents the first-line barrier to SARS-CoV-2 entry before viral spread to the upper and lower respiratory tracts. Although SARS-CoV-2 vaccine development has been rapidly progressing, the current intramuscular vaccines are designed to elicit systemic immunity but not necessarily high-level mucosal immunity.

Methods: Here, we tested the immunogenicity of a single intranasal dose of our candidate adenovirus type 5-vectored vaccine encoding the receptor binding domain of the SARS-CoV-2 spike protein (AdCOVID) in both inbred and outbred strains of mice.

Findings: A single intranasal vaccination with AdCOVID elicited a strong and focused immune response against RBD through the induction of mucosal IgA, serum neutralizing antibodies, and CD4+ and CD8+ T cells with a Th1-like cytokine expression profile. A single intranasal AdCOVID administration also resulted in sustained immunity that is detectable for over six months.

Conclusions: This study demonstrates that intranasal AdCOVID vaccination induces both cellular and humoral immunity in mice. These data suggest that AdCOVID promotes concomitant systemic and mucosal immunity and represents a promising COVID-19 vaccine candidate.

Funding: This study was supported by Altimmune, Inc. with additional support from the Barbara Ingalls Shook Foundation and the National Institutes of Health.

KEYWORDS

INTRODUCTION

First reported in late 2019 in China, severe acute respiratory syndrome coronavirus 2 (SARS-CoV-2) evolved into a global pandemic within a few months.¹ As of this report, the World Health Organization estimates over 131 million cases of coronavirus disease 2019 (COVID-19) worldwide, with 2.8 million associated deaths.^{2,3} Morbidity from SARS-CoV-2 infection can be severe, especially in high-risk groups (e.g., the elderly, individuals with chronic comorbidities such as hypertension, obesity, and diabetes).⁴ Early evidence from convalescent COVID-19 patients and survivors of similar ~~to~~ coronaviruses such as SARS-CoV-1 and Middle East respiratory syndrome (MERS), suggests that COVID-19 survivors may suffer long-term sequelae (e.g., inflammation resulting in damage to the lungs and heart).^{5,6} The global impact on human health and well-being underscores the immediate need for safe and effective vaccines against SARS-CoV-2 to end this pandemic and prevent its return.

Despite the well-recognized role of mucosal immunity in prevention of disease^{7,8}, all of the COVID-19 vaccines that have achieved emergency use authorization or have been advanced to Phase 3 clinical trials are administered via intramuscular injection.⁹⁻¹² Intramuscular injection elicits systemic immunity but generally does not result in potent mucosal immune responses. Suboptimal mucosal immunity may limit the utility of intramuscularly administered COVID-19 vaccines since transmission of SARS-CoV-2 is primarily via respiratory droplets released by infected individuals in enclosed spaces¹³, with the nose and other portions of the respiratory mucosa being the primary routes of entry.¹⁴ The nasal compartment shows particular susceptibility to SARS-CoV-2 infection due to abundant co-expression of the viral entry receptor (angiotensin-converting enzyme-2, ACE-2) and a required activating protease (TMPRSS2) in nasal goblet and ciliated cells.¹⁵ These cells are thought to be the primary route of infection and it is hypothesized that the nasal cavity serves as the initial reservoir for subsequent seeding of the virus to the lungs.¹⁶ The well-documented association of anosmia with COVID-19 further supports the nasal cavity as a principle reservoir of infection¹⁷, and the presence of high viral load in the nasal cavity may facilitate transmission of the virus.

A vaccination route targeting the mucosa presents an attractive alternative to intramuscular delivery. Intranasal delivery may be more appealing to patients as intranasal administration is non-invasive and obviates the need for needles.¹⁸ In addition, data suggest that intranasal delivery may increase vaccine uptake¹⁹, and in contrast to intramuscular injection, mucosal vaccination via the intranasal route has the potential to confer sterilizing immunity in the respiratory tract thereby reducing virus-induced disease and transmission of COVID-19.²⁰ Entry of SARS-CoV-2 into host cells depends on engagement of the receptor-binding domain (RBD) of the spike protein to ACE-2, leading to fusion of the virus with the cell membrane.²¹ In human convalescent serum, the majority of neutralizing antibodies are directed against the RBD.^{22,23} While most clinically advanced SARS-CoV-2 vaccine candidates deliver the trimeric spike ectodomain as the target antigen⁹, subdomains of the spike protein such as RBD represent alternative vaccine antigens for stimulation of a more focused immune response targeting well-conserved domains. Such an approach may also limit the induction of non-protective antibodies, mitigating the risk of enhanced respiratory diseases (ERD).²⁴

Here, we report results of preclinical immunogenicity testing of AdCOVID, an intranasal replication-deficient adenovirus serotype 5 (Ad5)-vectored vaccine candidate against COVID-19 that encodes the RBD from SARS-CoV-2 spike protein. We demonstrate immunogenicity of AdCOVID following a single administration of the vaccine in two strains of mice, which resulted in induction of spike-specific IgG and IgA antibody in sera and bronchoalveolar lavage (BAL) fluids that endured for at least six months. We show functionality of these vaccine-elicited antibodies in live virus neutralization assays. In addition to the induction of robust neutralizing antibody responses and mucosal IgA against SARS-CoV-2, the RBD vaccine candidate stimulated systemic and mucosal cell-mediated immune responses characterized by the induction of type 1 cytokine-producing CD4+ and CD8+ T cells, including lung-resident memory T cells. These data support the clinical development of AdCOVID in response to a serious global health threat.

RESULTS

Intranasal vaccination with AdCOVID elicits systemic and mucosal antibody responses

Researchers at Altimmune, Inc. generated a candidate COVID-19 vaccine using a replication-deficient E1- and E3-deleted Ad5 vector platform.²⁵ The Ad5 vector was engineered to encode the human codon-optimized gene for the RBD (residues 302 to 543) from the spike antigen of the Wuhan-1 strain of SARS-CoV-2 (accession number QHD43416). The immunogenicity of the RBD vector (hereafter referred to as AdCOVID) was evaluated in both inbred C57BL/6J and outbred CD-1 mice. Mice received a single intranasal administration of the control vehicle or AdCOVID at $3.35\text{E}+08$ infectious units (ifu) (high dose), $6\text{E}+07$ ifu (mid dose) or $6\text{E}+06$ ifu (low dose). Following vaccine administration on day 0, sera and BAL samples were collected between days 7-21 (CD-1) or days 7-28 (C57BL/6J). IgG antibodies specific for SARS-CoV-2 spike were measured in sera samples using a spike cytometric bead array (CBA). Systemic spike-specific IgG antibody responses in sera were detected in both CD-1 (Figure 1A) and C57BL/6J (Figure 1B) mice following a single intranasal administration of AdCOVID. This effect appeared to be dose-dependent as the antibody response in the low dose group was not significantly increased above that seen in the vehicle control group. Notably, anti-spike IgG was detectable in sera of vaccinated mice for at least 180 days after a single intranasal dose of $3.78\text{E}+08$ ifu (Figure 1C). These data are in agreement with the sustained presence of IgG-secreting, RBD-specific plasma cell populations in the mediastinal lymph node (medLN) and bone marrow of AdCOVID vaccinated mice (Supplementary Figure 1).

The ability of AdCOVID-elicited antibodies to neutralize SARS-CoV-2 were then tested in a focus reduction neutralization test (FRNT) using the wild-type SARS-CoV-2 isolate USA-WA1/2020. The analysis included AdCOVID samples from C57BL/6J mice 4-weeks after vaccination with either the mid ($6\text{E}+07$ ifu) or high dose ($3.35\text{E}+08$ ifu), and AdCOVID samples from CD-1 mice 3-weeks after vaccination with the high dose ($3.35\text{E}+08$ ifu). AdCOVID vaccination yielded neutralizing systemic antibodies in both strains of mice (Figure 2A). At the highest intranasal AdCOVID dose, neutralizing antibody responses above background were detected in 10 of 10 C57BL/6J mice and 8 out of 10 CD-1 mice with a median titer of 563 and 431, respectively. The level of the neutralizing antibody response was well-correlated with the magnitude of the spike-specific serum IgG response measured in individual animals (Figure 2B and 2C), indicating that robust antibody responses to RBD were associated with generation of potentially protective neutralizing antibodies.

IgA-mediated immunity is crucial for controlling SARS-CoV-2 infection.²⁶ We therefore quantified the presence of anti-spike IgA in the BAL of CD-1 and C57BL/6J mice following a single intranasal dose of 6.25E+08 ifu AdCOVID. As shown in Figure 3, AdCOVID induced a lung mucosal spike-specific IgA response in both strains of mice. As was previously measured in the sera, a single intranasal administration (3.78E+08 ifu) of AdCOVID yielded long-lasting mucosal immunity with anti-spike specific IgA remaining at high levels 180 days post-vaccination (Figure 3B). These mice also had RBD-specific IgA-secreting plasma cells in both the BAL and medLN (Supplementary Figure 2). When combined with the presence of anti-spike IgG in the sera at day 180, these data suggest that AdCOVID elicits robust and long-lived humoral responses in both the mucosa and the periphery.

Intranasal AdCOVID administration recruits innate and adaptive immune cells to the respiratory tract

Given the potent neutralizing antibody titers measured in AdCOVID vaccinated mice, we next evaluated the ability of AdCOVID to elicit cellular immunity. Flow cytometric analysis of immune cells (Supplementary Table 1) was performed on lung, BAL, medLN, and spleen samples following intranasal administration of AdCOVID (3.35E+08 ifu) in C57BL/6J mice. Consistent with the hypothesis that mucosal administration of the vaccine would induce innate and adaptive pulmonary immune responses, rapid recruitment of immune cells into the lung was observed following AdCOVID administration. Indicative of early innate immune activation, significant increases in the number of dendritic cells, macrophages, polymorphonuclear (PMN) cells, and natural killer (NK) cells were observed compared to control mice (Figure 4A). These responses peaked at day 7 post-vaccination. Rapid recruitment of adaptive immune cells to the lung, including T follicular helper-like cells (T_{fh}-like) and multiple B lineage subsets, was also observed peaking between days 7-28 (Figure 4B). Similar trends were observed in the BAL (Supplementary Figure 3) and medLN (Supplementary Figure 4) but were less obvious in the spleen (Supplementary Figure 5).

AdCOVID elicits mucosal and systemic RBD-specific CD4+ and CD8+ T cell responses

Animal models have shown that CD4+ and CD8+ T cells residing in the respiratory tract are important for local protection immediately after viral infection.²⁷⁻²⁹ Moreover, emerging data suggest a critical role for T cell responses in COVID-19 immunity independent of antibody responses³⁰⁻³², particularly when directed against the SARS-CoV-2 RBD.³³ To assess vaccine-induced SARS-CoV-2-specific T cell responses, AdCOVID was administered intranasally to

outbred CD-1 mice at a single dose of $3.78\text{E}+08$ ifu. Control animals received vehicle alone administered intranasally. RBD-specific T cell cytokine responses in lung and spleen samples were assessed by ELISpot following ex vivo re-stimulation with a pool of 54 peptides (15a.a. long, 11a.a. overlap) covering the SARS-CoV-2 RBD residues 319-541. A high frequency of RBD-specific IFN- γ + T cells were detected in the lung at 10- (Fig. 5A) and 14 (Fig. 5B) -days post-vaccination, reaching a mean response of 915 and 706 spot forming cells (SFC) per million input cells respectively. IFN- γ producing, RBD-specific T cells were also detected by ELISpot in the spleen (Fig. 5A-B), albeit at lower frequency compared to the lung. These results prove that mucosally-delivered vaccines can elicit functional effector T cells that are distributed in secondary lymphoid tissues.

To further characterize the RBD-specific CD4+ and CD8+ T cell responses to mucosal vaccination, intracellular cytokine staining was performed on lung and spleen cells from vaccinated CD-1 mice ($3.78\text{E}+08$ ifu). Consistent with ELISpot data, we observed a significant induction of IFN- γ - or TNF- α -producing T cells in the lung and spleen of vaccinated animals. These included both CD11a+CD8+ (Figure 6A) and CD11a+CD4+ (Figure 6B) T cells, although the response was strongly biased toward the induction of CD8+ T cells, especially in lung samples. Expression of integrin CD11a, which is only upregulated in recently activated T cells and is required for optimal vascular adhesion in the tissue and retention within the respiratory tract³⁴, supports the hypothesis that these cells were recently recruited to the lung. To assess whether these cells are resident memory T cells (T_{rm}), the expression of the T_{rm} markers CD103 and CD69 on pulmonary CD4+ and CD8+ cells was measured.²⁹ Consistent with the intranasal administration route, induction of lung RBD-specific CD8+ and CD4+ T_{rm} expressing either IFN- γ , TNF- α or both cytokines was observed (Figure 7).

Intranasal AdCOVID vaccination yields a type 1 cytokine-biased immune response

Concerns exist that a vaccine-elicited Th2 biased immune response may result in ERD following SARS-CoV-2 infection. Our data showed that intranasal administration of AdCOVID induced both monofunctional and polyfunctional T cells capable of producing type 1-associated cytokines, such as IFN- γ and TNF- α . In addition, the vaccine elicited high frequencies of antigen-specific CD8+ T cells that generally correlate with an interferon-regulated T cell response necessary for control of viral infection. To further assess the

cytokine-producing potential of T cells from AdCOVID vaccinated CD-1 mice (3.78E+08 ifu), splenic T cells were stimulated with RBD peptides for 48 hours and then the presence of secreted cytokines was measured in harvested supernatant by multiplex cytokine bead array (Figure 8). As expected, induction of IFN- γ and TNF- α by T cells was observed. Moreover, T cells from the vaccinated animals produced moderate levels of IL-10 compared to T cells from the vehicle control treated mice. Importantly, the levels of the Th2 and Th17-derived cytokines, including Interleukin (IL)-4, IL-5, IL-13 and IL-17a, were statistically equivalent in the supernatants of peptide-stimulated cells isolated from the spleens of vaccinated and control animals. These data therefore indicated that intranasal administration of AdCOVID did not potentiate a deleterious Th2 response but rather induced the expected antiviral T cell responses.

DISCUSSION

To date, the COVID-19 vaccine candidates that have achieved emergency use approval or that have advanced to Phase 3 clinical trials are delivered by intramuscular injection. In preclinical and clinical studies, these candidates have demonstrated stimulation of serum neutralizing antibodies and peripheral T cell responses. However, a fundamental limitation of these approaches is that they are not designed to target the distinct immune microenvironment of the respiratory tract mucosa, and there is no widespread expectation that the current intramuscular vaccine candidates will provide sterilizing immunity in the nasal cavity. In a SARS-CoV-2 challenge model in rhesus macaques, a single intramuscular administration of an adenovectored vaccine candidate was shown to significantly reduce viral load in the bronchoalveolar lavage fluid and lower respiratory tract tissue but the level of viral replication in the nasal cavity was unaffected.³⁵ Conversely, nasal administration of replication-deficient human Ad5-vectored vaccines, like AdCOVID, mimic natural infection of respiratory viruses and stimulate strong protective immunity, both systemically and mucosally.³⁶⁻³⁸ Intranasal vaccination stimulates mucosal IgA antibodies, providing a first line of defense at the point of respiratory pathogen inoculation³⁹, which correlates well with protection from respiratory infections such as influenza.⁴⁰⁻⁴² Moreover, numerous studies have demonstrated the ability of intranasally administered vaccines to block transmission of influenza between infected and naïve cage-mates.^{43,44} Consistent with these reports, several studies assessing other COVID-19

vaccine candidates have shown that the intranasal route, as opposed to the intramuscular route, stimulated local mucosal immune responses in addition to systemic neutralizing antibody and T cell responses, resulting in significantly reduced oropharyngeal virus shedding compared to intramuscularly vaccinated animals.^{20,45,46}

In agreement with these reports, we showed here that AdCOVID, an intranasal adenovirus-vectored vaccine encoding the RBD of the SARS-CoV-2 spike protein, is highly immunogenic in both inbred and outbred mice and elicits robust systemic and local antibody and T cell responses. Following a single intranasal vaccination, AdCOVID elicited a strong and focused immune response against SARS-CoV-2 spike antigen through the induction of functional serum antibodies that neutralized wild-type SARS-CoV-2 virus. Importantly, AdCOVID vaccination resulted in antigen-specific IgA, IgG, and polyfunctional CD8⁺ and CD4⁺ T cell responses in the respiratory tract. Cell-mediated responses induced by AdCOVID were biased toward antiviral type 1 cytokine responses as demonstrated by the high rates of antigen-specific CD8⁺ T cells and an effector cytokine profile including IFN- γ and TNF- α .

Key to these findings, intranasal AdCOVID vaccination appears to yield a significant memory response, both locally and systemically. AdCOVID promoted persistent spike-specific sera IgG responses with no evidence of significant decline 6 months after a single vaccination. Likewise, IgA levels in the respiratory tract remained elevated throughout the course of the study. When combined with the establishment of a resident memory CD8⁺ T cell population in the lungs, our data suggest that AdCOVID has the potential to confer long lasting immunity, particularly within the bronchoalveolar space and lungs, which represent major sites of infection and clinical disease.

Moreover, adenoviral vector-based vaccines are an attractive platform for combating the SARS-CoV-2 pandemic as they have an established safety profile in the clinic.^{47,48} Additionally, intranasal administration has been demonstrated to bypass preexisting immunity to the vector.³⁶

By what mechanism was AdCOVID able to elicit such robust memory responses? One possibility is that the immune response induced by AdCOVID vaccination was targeted to the RBD domain, which contains the major critical neutralizing epitopes in the spike protein. This is consistent with results obtained during the development of vaccines for SARS-CoV-1.⁴⁹ We

postulate that an Ad5-vector expressing RBD vaccine may offer three advantages over other forms of the spike antigen that have been used in COVID-19 vaccine candidates currently in clinical development. First, it is reported that RBD-based vaccines can promote equivalent or higher titer antibody responses than the full-length or S1/S2 ectodomain of spike from SARS-CoV-2 and that the antibodies induced by the RBD vaccine were of higher affinity.^{49,50} Second, recent data suggest that neutralizing antibody responses directed against the RBD are less impacted by escape mutations present in the currently circulating SARS-CoV-2 variants compared to neutralizing antibodies that target other regions of the spike protein.⁵¹ Third, focusing the immune response on the RBD domain could decrease the production of potentially pathogenic non-neutralizing antibodies, which can contribute to ERD.⁵² These factors suggest that RBD-only vaccines, like AdCOVID, have the potential to provide significant protection from SARS-CoV-2 infection while avoiding the negative side-effects that may be associated with vaccines targeting respiratory pathogens.

In summary, there is a clear need for a vaccine to prevent SARS-CoV-2 infection, preferably one that elicits mucosal immunity so as to reduce viral shedding in the upper respiratory tract, thereby reducing transmission. In these experiments, AdCOVID induced systemic and mucosal immune responses within days following a single-dose vaccination. In the context of a pandemic, intranasally administered AdCOVID has two compelling advantages. First, non-invasive intranasal administration makes it particularly well-suited for wide-spread vaccinations of large cohorts. Intranasal administration may also provide incentive for the subset of the population displaying hesitance towards vaccination due to trypanophobia.¹⁸ Second, intranasal AdCOVID may control SARS-CoV-2 infection within both the upper and lower respiratory tract. This has the advantages of potentially preventing infection at the site of virus entry, reducing the risk of significant respiratory disease, and decreasing the likelihood of subsequent virus transmission by vaccinated individuals. Collectively, these findings support further development of AdCOVID for the prevention of SARS-CoV-2 infections and its transmission. These aspects will be investigated as the intranasal AdCOVID vaccine progresses through ongoing clinical trials.

MATERIALS AND METHODS

Ethics statement and Mice

Mice used in these studies were obtained from the Jackson Laboratory (C56BL/6J) or Charles River Laboratories (CD-1). Animal procedures performed at University of Alabama at Birmingham (UAB) or Noble Life Sciences (Noble) were conducted in accordance with Public Health Service Policy on the Humane Care and Use of Laboratory Animals and Guide for the Care and Use of Laboratory Animals. Studies performed at UAB were performed under IACUC Approval Number 21203. Studies performed at Noble were performed under the IACUC Approval Number NLS-591.

Vaccine candidate

The vaccine candidate evaluated in this study was based on a replication-deficient, E1- and E3-deleted adenovirus type 5 vector platform²⁵ and expresses a human codon-optimized gene for the RBD domain (residues 302 to 543) of SARS-CoV-2 spike protein (accession number QHD43416.1). The Ad5-vectored RBD transgene includes a human tissue plasminogen activator leader sequence and is expressed under the control of the cytomegalovirus immediate early promoter/enhancer. An initial seed stock was obtained from transfection of recombinant vector plasmid into E1-complementing PER.C6 cells using a scalable transfection system (MaxCyte STX-100; MaxCyte). Cell transfection was performed by static electroporation using the CL1.1 Processing Assembly procedure.⁵³ Following vector expansion, replication-deficient vector was obtained from infected cell lysates and was purified over a CsCl gradient, dialyzed against a formulation buffer containing 10 mM Tris (pH 7.4), 75 mM NaCl, 1 mM MgCl₂, 10 mM histidine, 5% (wt/vol) sucrose, 0.02% polysorbate-80 (wt/vol), 0.1 mM EDTA, and 0.5% (vol/vol) ethanol and then frozen and stored at -65°C.

Adenovirus vaccine titer measurement

293 HEK cells were seeded in a 96-well plate one day before Ad vector infection. After inoculation of the appropriate dilutions of adenovirus control and test sample(s) onto duplicate wells, the infected cells were incubated for 3 days. At the end of the infection period, media were removed, and cells were fixed with cold methanol. Following drying and rinsing with phosphate-buffered saline, mouse anti-adenovirus-5 hexon antibody was added to each

well of cells and incubated at 37°C for at least 60 minutes. After removal of the mouse anti-adenovirus-5 hexon antibody and additional phosphate-buffered saline washes, HRP-conjugated rat anti-mouse antibody was added to each well and incubated at least 60 minutes at 37°C. After removal of the detection antibody and additional phosphate-buffered saline washes, cells were stained with DAB (3, 3-diaminobenzidine) working solution for at least 10 minutes. After removal of DAB working solution and additional washing steps with phosphate-buffered saline, the stained foci were enumerated using a microscope with a 20X objective.

Vaccination

Inbred female C57BL/6J (The Jackson Laboratory) and outbred CD-1 (Charles River Laboratories) mice of at least 6 weeks of age were randomly allocated into vaccination groups. Replication-deficient Ad5 vector encoding the RBD (AdCOVID) from the SARS-CoV-2 spike protein was administered intranasally at the described doses in a volume of 50 µL. The control group received 50 µL of vehicle alone by intranasal administration.

Serum Collection

Blood samples were collected from the submandibular vein of vaccinated mice into BD Microtainer blood collection tubes (BD Biosciences). The samples were centrifuged at 13000 rpm at RT for 8-10 minutes and the serum was collected, aliquoted and frozen at -80°C until analyzed.

Tissue processing and single cell isolation

Spleen, medLN, and lung tissues were isolated from vaccinated mice at the indicated timepoints. Lung tissue was minced and then digested in RPMI-1640 medium containing collagenase (1.25 mg/mL; Millipore-Sigma) and DNase I (150 units/mL; Millipore-Sigma) for 30 minutes at 37°C. To generate single cell suspensions, digested lung, spleen, and draining lymph nodes were passed through a fine wire mesh. The single cell suspensions were treated with red blood cell lysis buffer and filtered (100 µm) to remove debris.

BAL collection

BAL samples were collected using ethyl vinyl acetate (EVA) microbore tubing (Cole-Parmer) with inner and outer diameters of 0.02 in and 0.06 inches, respectively. One end of the tube

was fitted to a 23G syringe needle attached to a 3-way stopcock. The other end of the tube was inserted postmortem into an incised trachea. BAL fluid was collected as a single 1 mL lavage fraction using ice-cold phenol-free Hank's Buffered Salt Solution (HBSS, without Ca^{2+} and Mg^{2+}) containing 2mM EDTA. BAL cells were separated from the supernatant by centrifugation at 1800 rpm for 5 minutes at 4°C.

Recombinant SARS-CoV-2 protein production

To produce recombinant SARS-CoV-2 spike ectodomain protein, two human codon-optimized constructs were generated with linear sequence order encoding: a human IgG leader sequence, the SARS-CoV-2 spike ectodomain (amino acids 14-1211), a GGSG linker, T4 fibrin foldon sequence, a GS linker, and finally an AviTag (construct 1) or 6X-HisTag (construct 2). Each construct was engineered with two sets of mutations to stabilize the protein in a pre-fusion conformation. These included substitution of RRAR>SGAG (residues 682 to 685)⁵⁴ at the S1/S2 cleavage site and the introduction of two proline residues; K983P, V984P.^{54,55} Avi/His-tagged trimers were produced by co-transfecting plasmid constructs 1 and 2 (1:2 ratio) into FreeStyle 293-F cells. Cells were grown for three days and the supernatant (media) was recovered by centrifugation. Recombinant spike trimers were purified from media by Fast protein liquid chromatography (FPLC) using a HisTrap HP Column (GE Biosciences) and elution with 250mM of imidazole. After exchanging into either 10mM Tris-HCl, pH 8.0 or 50mM Bicine, pH 8.3, purified spike ectodomain trimers were biotinylated by addition of biotin-protein ligase (Avidity). Biotinylated spike ectodomain trimers were buffer exchanged into PBS, sterile filtered, aliquoted, then stored at -80°C until used.

SARS-CoV-2 spike cytometric bead array

To generate the spike cytometric bead array (CBA), recombinant SARS-CoV-2 ectodomain trimers were passively absorbed onto streptavidin functionalized fluorescent microparticles (3.6 μm ; Spherotech). 500 μg of biotinylated SARS2-CoV-2 was incubated with $2\text{E}+07$ streptavidin functionalized fluorescent microparticles in 400 μL of 1% BSA in PBS. Following coupling, the SARS-CoV-2 spike conjugated beads were washed twice in 1 mL of 1% BSA, PBS, 0.05% NaN₃, resuspended at $1\text{E}+08$ beads/mL and stored at 4°C. The loading of recombinant SARS2-CoV-2 spike onto the beads was evaluated by staining $1\text{E}+05$ beads with

dilutions ranging from 1 $\mu\text{g}/\text{mL}$ to 2 ng/mL of the recombinant anti-SARS spike antibody CR3022 and visualized with an anti-human IgG secondary antibody.

CBA IgG and IgA standards

IgG and IgA standards were generated by covalent coupling of isotype-specific polyclonal antibodies to fluorescent particles. Briefly, 0.2 mg of goat polyclonal anti-mouse IgG (SouthernBiotech), anti-IgM (SouthernBiotech), and anti-IgA (SouthernBiotech) antibodies in PBS were mixed with $5\text{E}+07$ fluorescent microparticles each with a unique fluorescent intensity in the far-red channels (3.6 μm ; Spherotech) resuspended in 0.1 M MES buffer pH 5.0. An equal volume of EDC (1-Ethyl-3-(3-dimethylaminopropyl)-carbodiimide), 10 mg/mL , in 0.1 M MES (2-(N-morpholino) ethanesulfonic acid) buffer pH 5.0 was added and the mixture was incubated overnight at RT. The beads were washed twice by pelleting by centrifugation and resuspension in PBS. Following washing, beads were resuspended in 1% BSA in PBS with 0.005% NaN_3 as a preservative.

CBA measurement of spike-specific IgG and IgA responses

The quantification of SARS-CoV-2 spike IgG and IgA was performed in serum or BAL samples obtained from immunized animals using the spike CBA described above. BAL samples (diluted 1/4-8) or serum samples (diluted to 1/1000-5000) in 50 μL of PBS were arrayed in 96-well u-bottom polystyrene plates along with 50 μL of standards consisting of either mouse IgG, IgM, or IgA ranging from 1 $\mu\text{g}/\text{mL}$ to 2 ng/mL at 0.75 x dilutions (SouthernBiotech). 5 μL of a suspension containing $5\text{E}+05$ of each SARS-CoV-2 spike, anti-IgM, anti-IgA, and anti-IgG beads was added to the diluted samples. The suspensions were mixed by pipetting and incubated for 15 minutes at RT. The beads were washed by the addition of 200 μL of PBS and centrifuged at 3000 x g for 5 minutes at RT. The CBA particles were resuspended in a secondary staining solution consisting of polyclonal anti-IgG 488 (SouthernBiotech), and either a goat polyclonal anti-IgM (SouthernBiotech) or anti-IgA (SouthernBiotech) conjugated to PE diluted 1/400 in 1% BSA in PBS. The suspension was incubated for 15 minutes in the dark at RT. The beads were washed by the addition of 200 μL of PBS and pelleted by centrifugation at 3000 x g for 5 minutes at RT. The particles were resuspended in 75 μL of PBS and directly analyzed on a BD Cytotflex flow cytometer in plate mode at sample rate of 100 uL/minute . Sample collection was stopped following the

acquisition of 75 μL . Following acquisition, the resulting FCS files were analyzed in FlowJo (Tree Star). Briefly, the beads were identified by gating on singlet 3.6 μm particles in log scale in the forward scatter and side scatter parameters. APC-Cy7 channel fluorescence gates were used to segregate the particles by bead identity. Geometric mean fluorescent intensity was calculated in the PE and 488 channels. Best fit power curves were generated from the Ig capture beads using the known concentration of standards on a plate-by-plate basis. This formula was applied to the MFI of the SARS-CoV-2 spike particles for all samples of the corresponding assay converting MFI to ng/mL or $\mu\text{g/mL}$ concentrations. These calculated values were corrected for the dilution factor.

Neutralizing antibody titers

A focus reduction neutralization test (FRNT) was used to quantify the titer of neutralizing antibodies against SARS-CoV-2 isolate USA-WA1/2020. Vero E6 cells were grown to confluence on 96-well plates. On the day of the infection phase of the assay, serial dilutions (1:20-1:2560) of antisera were made and combined and incubated with an equal volume of viral stock, at a specified dilution for 30 minutes at RT, such that the final dilutions of antisera ranged from 1:40 to 1:5120. The viral stock was diluted from a concentrated working stock to produce an estimated 30 viral focal units per well. After incubation, the sera:virus mixtures were added to the wells (100 μL), and infection allowed to proceed for 1 hour on the Vero E6 cells at 35°C. At the completion of the 1-hour incubation, a viscous overlay of Eagle's MEM with 4% FBS and antibiotics and 1.2% Avicell were added to sera:virus mixture on the cell monolayers such that the final volume was 200 μL per well. The infection was allowed to proceed for 24 hours. The next day, each plate was fixed by submerging the entire plate and contents in 10% formalin/PBS for 24 hours. Detection of virus foci reduction was performed on the fixed 96-well plates. Briefly, plates were rinsed in H_2O , and methanol:hydrogen peroxide added to the wells for 30 minutes with rocking to quench endogenous peroxidase activity. After quenching, plates were rinsed in H_2O to remove methanol and 5% Blotto was added to the wells as a blocking solution for 1 hour. For primary antibody detection, a SARS-CoV-2 spike/RBD antibody (Sino Biological) was added to 5% Blotto and incubated on the monolayers overnight. Plates were washed five times with PBS, and further incubated with a goat anti-rabbit IgG conjugated to horseradish peroxidase (Boster Bio) in 5% Blotto for 1 hour. Plates were rinsed once with 0.05% Tween in 1X PBS followed by 5 washes in 1X PBS.

Impact DAB detection kit (Vector Labs) was used to detect peroxidase activity. Brown foci were counted manually from the scanned image of each well, recorded, and the reduction of foci as compared to equivalent naïve mouse sera controls was determined. FRNT₅₀ titers were calculated using a 4PL curve fit to determine the serum dilution corresponding to a 50% reduction in the foci present in control wells.

Flow cytometry analysis of innate and adaptive immune cells

Cell numbers per tissue were determined by mixing 20 uL of each single cell suspension into a 96-well plate with 50 uL of 8.4E+04 Fluoresbrite Carboxylate YG 10 µm microspheres/mL (Polysciences Inc.) and 180 uL staining media (dPBS + 2% FBS) containing 2 mM EDTA (SME) and 7-AAD (1:720 dilution). To perform flow cytometric analysis, 200 µL of each sample were placed into 3 separate V-bottom 96-well plates for antibody staining for flow cytometric analysis. Samples were incubated for 10 minutes at 4°C in the dark with Fc-Block (clone 24G2, 10 µg/mL), washed with 200 µL staining media (SME) and then stained with myeloid, B cell, or BAL antibody panels. The myeloid panel consisted of B220/CD45R-FITC (clone RA3-6B2; 1:200 dilution), Ly6G-PE (clone 1A8; 1:200 dilution), CD64-PerCP-Cy5.5 (clone X54-5/7.1; 1:150 dilution), CD11b-APC (clone M1/70; 1:200 dilution), CD11c-PE-Cy7 (clone N418; 1:300 dilution), Ly6C-APC-Cy7 (clone AL-21; 1:200 dilution), MHCII-PB (clone M5/114.15.4; 1:600 dilution) and Aqua LIVE/DEAD (1:1000 dilution). Cells stained with the myeloid panel were incubated with the antibody mix (50 uL total volume) for 20 minutes at 4°C in the dark. The B cell panel consisted of CD95/FAS-FITC (clone Jo2; 1:200 dilution), F4/80-PerCP-Cy5.5 (clone BM8; 1:200 dilution), CD3-PerCP-Cy5.5 (clone 17A2; 1:200 dilution), CD38-PE-Cy7 (clone 90; 1:400 dilution), CD19-APC-Fire750 (clone 6D5; 1:200 dilution), CD138-BV421 (clone 281-2; 1:200 dilution) and IgD-BV510 (clone 11-26c.2a; 1:500 dilution). Cells stained with the B cell panel were incubated with antibody mix (50 uL total volume) for 45 minutes at 4°C in the dark. The BAL panel consisted of Ly6G-PE (clone 1A8; 1:200 dilution), CD64-PerCP-Cy5.5 (clone X54-5/7.1; 1:150 dilution), CD8a-APC (clone 53-6.7; 1:200 dilution), CD11c-PE-Cy7 (clone N418; 1:200 dilution), CD19-APC/Fire750 (clone 6D5; 1:200 dilution; CD4-eFLUOR450 (clone GK1.5; 1:200 dilution) and Aqua LIVE/DEAD (1:1000 dilution). Cells stained with the BAL panel were incubated with the antibody mix (50 uL total volume) for 20 minutes at 4°C in the dark. Following incubation with the different flow cytometry panels, the cells were washed, resuspended in 100 µL of

eBioscience fixation buffer and incubated for 20 minutes at 4 °C. After incubation, the cells were spun down and resuspended in 200 uL SME. Stained and fixed cells from all antibody panels and cell counting panels were analyzed on a BD FACSCanto II. Cellular markers are summarized in Supplementary Table 1. The gating strategies for T cells (Supplementary Figure 6), B cells (Supplementary Figure 7), myeloid cells (Supplementary Figure 8), and Trm cells (Supplementary Figure 9) are presented.

Intracellular cytokine staining

The analysis of CD4⁺ and CD8⁺ T cell responses in lung tissues and spleens by flow cytometry was performed as follows. Spleen and lung single cell suspensions were stimulated with the RBD peptide pool for 5 hours in the presence of 12.5 µg/mL Brefeldin A (BD Biosciences). Cells were then incubated on ice with a combination of fluorescent dye-labelled antibodies including anti-CD4-V500 (clone GK1.5; 1:200 dilution), anti-CD8α-APC-Fire750 (clone 53-6.7; 1:200 dilution), anti-CD11a/CD18-Pacific Blue (H155-78; 1:200 dilution), anti-CD103-PE (M290; 1:200 dilution), anti-CD69-FITC (H1-2F3; 1:200 dilution), anti-Ly6G-PerCP-Cy5.5 (clone 1A8; 1:200 dilution), anti-CD64-PerCP-Cy5.5 (clone X54-5/7.1; 1:200 dilution), anti-B220/CD45R-PerCP (clone RA3-6B2; 1:200 dilution), and Red LIVE/DEAD (1:1000 dilution). Following surface staining, cells were permeabilized using BD Biosciences Cytofix/Cytoperm kit and stained with anti-IFN-γ-PE-Cy7 (XMG1.2; 1:200 dilution) and anti-TNF-α-APC (MP6-XT22; 1:200 dilution). Following incubation with the antibodies, cells were washed and resuspended before analysis on a BD FACSCanto II within 12 hours.

IFN-γ ELISpot

Spleen and lung cell suspensions (150,000 cells/well) were placed in individual wells of ELISpot plates (Millipore-Sigma) that were pre-coated with anti-IFN-γ (AN18, 5 µg/mL). Cells were stimulated with the RBD peptide pool described above at 2 µg/peptide/mL. Following 24-hour stimulation, plates were stained with biotinylated anti-IFN-γ (R4-6A2), followed by washing steps, and incubation with streptavidin-AP. Secreted IFN-γ was detected following incubation with NBT/NCPI substrate for 7-10 minutes. The number of IFN-γ spot-forming cells were manually counted from digital images of each well.

Synthetic RBD peptides

For analysis of T cell responses, a pool of 53 peptides derived from a peptide scan through the RBD of spike protein of SARS-CoV-2 (319-541) was designed and synthesized by JPT (JPT Peptide Technologies). Peptides were designed with a length of 15 a.a. and an overlap of 11 a.a. Before use, each vial containing 15 nmol (appr. 25 µg) of each peptide per vial was reconstituted in 50 µL of DMSO before dilution into complete culture media.

B cell ELISpot

Single cell suspensions from bone marrow, BAL and medLN cells were prepared from vaccinated mice. Cells were serially diluted in duplicate in complete media and incubated for 5 hours at 37°C on multiscreen cellulose filter ELISPOT plates (Millipore-Sigma) that were previously coated with purified recombinant RBD protein (Sino Biological). RBD-specific antibodies secreted by plasma cells present in these tissues were detected using AP-conjugated goat anti-mouse IgG (Jackson ImmunoResearch) or AP-conjugated goat anti-mouse IgA (Jackson ImmunoResearch). ELISpots were imaged and counted using S6 Ultra-V Analyzer (Cellular Technology Limited).

Measurement of inflammatory cytokines in culture supernatants

Protein levels of IFN- γ , IL-2, IL-4, IL-5, IL-10, IL-13, IL-17A and TNF- α were quantified in culture supernatants using the mouse-specific Milliplex® multi-analyte panel kit MT17MAG-47K (Millipore-Sigma) and the MagPix® instrument platform with related xPONENT® software (Luminex Corporation). The readouts were analyzed with the standard version of EMD Millipore's Milliplex® Analyst software (Millipore-Sigma and Vigene Tech).

Quantification and statistical analysis

Statistical significance was assigned when P values were < 0.05 using Prism Version 9.0.1 (GraphPad). All tests and values are indicated in the relevant Figure legends.

REFERENCES

- Zhu, N., Zhang, D., Wang, W., Li, X., Yang, B., Song, J., Zhao, X., Huang, B., Shi, W., Lu, R., *et al.* (2020). A Novel Coronavirus from Patients with Pneumonia in China, 2019. *N Engl J Med* *382*, 727-733.
- World Health Organization. (2020). Coronavirus disease 2019 (COVID-19) [2020] <https://covid19.who.int/>
- Centers for Disease Control and Prevention. (2020). Coronavirus disease 2019 (COVID-19): Scientific Brief: SARS-CoV-2 and Potential Airborne Transmission. [2020] <https://www.cdc.gov/coronavirus/2019-ncov/more/scientific-brief-sars-cov-2.html>
- Centers for Disease Control and Prevention. (2020). Coronavirus disease 2019 (COVID-19): People who are at increased risk for severe illness. [2020] <https://www.cdc.gov/coronavirus/2019-ncov/need-extra-precautions/people-at-increased-risk.html>
- Huang, C., Huang, L., Wang, Y., Li, X., Ren, L., Gu, X., Kang, L., Guo, L., Liu, M., Zhou, X., *et al.* (2021). 6-month consequences of COVID-19 in patients discharged from hospital: a cohort study. *Lancet* *397*, 220-232.
- Shafi, A.M.A., Shaikh, S.A., Shirke, M.M., Iddawela, S., and Harky, A. (2020). Cardiac manifestations in COVID-19 patients-A systematic review. *J Card Surg* *35*, 1988-2008.
- van Ginkel, F.W., Nguyen, H.H., and McGhee, J.R. (2000). Vaccines for mucosal immunity to combat emerging infectious diseases. *Emerg Infect Dis* *6*, 123-132.
- Holmgren, J., and Czerkinsky, C. (2005). Mucosal immunity and vaccines. *Nat Med* *11*, S45-53.
- Funk, C.D., Laferriere, C., and Ardakani, A. (2020). A Snapshot of the Global Race for Vaccines Targeting SARS-CoV-2 and the COVID-19 Pandemic. *Front Pharmacol* *11*, 937.
- Polack, F.P., Thomas, S.J., Kitchin, N., Absalon, J., Gurtman, A., Lockhart, S., Perez, J.L., Perez Marc, G., Moreira, E.D., Zerbini, C., *et al.* (2020). Safety and Efficacy of the BNT162b2 mRNA Covid-19 Vaccine. *N Engl J Med* *383*, 2603-2615.

- Baden, L.R., El Sahly, H.M., Essink, B., Kotloff, K., Frey, S., Novak, R., Diemert, D., Spector, S.A., Roupael, N., Creech, C.B., *et al.* (2021). Efficacy and Safety of the mRNA-1273 SARS-CoV-2 Vaccine. *N Engl J Med* *384*, 403-416.
- Sadoff, J., Le Gars, M., Shukarev, G., Heerwegh, D., Truyers, C., de Groot, A.M., Stoop, J., Tete, S., Van Damme, W., Leroux-Roels, I., *et al.* (2021). Interim Results of a Phase 1-2a Trial of Ad26.COV2.S Covid-19 Vaccine. *N Engl J Med*.
- Shen, Y., Li, C., Dong, H., Wang, Z., Martinez, L., Sun, Z., Handel, A., Chen, Z., Chen, E., Ebell, M.H., *et al.* (2020). Community Outbreak Investigation of SARS-CoV-2 Transmission Among Bus Riders in Eastern China. *JAMA Intern Med* *180*, 1665-1671.
- Li, H., Wang, Y., Ji, M., Pei, F., Zhao, Q., Zhou, Y., Hong, Y., Han, S., Wang, J., Wang, Q., *et al.* (2020). Transmission Routes Analysis of SARS-CoV-2: A Systematic Review and Case Report. *Front Cell Dev Biol* *8*, 618.
- Sungnak, W., Huang, N., Becavin, C., Berg, M., Queen, R., Litvinukova, M., Talavera-Lopez, C., Maatz, H., Reichart, D., Sampaziotis, F., *et al.* (2020). SARS-CoV-2 entry factors are highly expressed in nasal epithelial cells together with innate immune genes. *Nat Med* *26*, 681-687.
- Hou, Y.J., Okuda, K., Edwards, C.E., Martinez, D.R., Asakura, T., Dinnon, K.H., 3rd, Kato, T., Lee, R.E., Yount, B.L., Mascenik, T.M., *et al.* (2020). SARS-CoV-2 Reverse Genetics Reveals a Variable Infection Gradient in the Respiratory Tract. *Cell* *182*, 429-446 e414.
- Brann, D.H., Tsukahara, T., Weinreb, C., Lipovsek, M., Van den Berge, K., Gong, B., Chance, R., Macaulay, I.C., Chou, H.J., Fletcher, R.B., *et al.* (2020). Non-neuronal expression of SARS-CoV-2 entry genes in the olfactory system suggests mechanisms underlying COVID-19-associated anosmia. *Sci Adv* *6*.
- Taddio, A., Ipp, M., Thivakaran, S., Jamal, A., Parikh, C., Smart, S., Sovran, J., Stephens, D., and Katz, J. (2012). Survey of the prevalence of immunization non-compliance due to needle fears in children and adults. *Vaccine* *30*, 4807-4812.
- Yusuf, H., and Kett, V. (2017). Current prospects and future challenges for nasal vaccine delivery. *Hum Vaccin Immunother* *13*, 34-45.
- Hassan, A.O., Kafai, N.M., Dmitriev, I.P., Fox, J.M., Smith, B.K., Harvey, I.B., Chen, R.E., Winkler, E.S., Wessel, A.W., Case, J.B., *et al.* (2020). A Single-Dose Intranasal ChAd Vaccine Protects Upper and Lower Respiratory Tracts against SARS-CoV-2. *Cell* *183*, 169-184 e113.
- Letko, M., Marzi, A., and Munster, V. (2020). Functional assessment of cell entry and receptor usage for SARS-CoV-2 and other lineage B betacoronaviruses. *Nat Microbiol* *5*, 562-569.
- Seydoux, E., Homad, L.J., MacCamy, A.J., Parks, K.R., Hurlburt, N.K., Jennewein, M.F., Akins, N.R., Stuart, A.B., Wan, Y.H., Feng, J., *et al.* (2020). Characterization of neutralizing antibodies from a SARS-CoV-2 infected individual. [bioRxiv](https://doi.org/10.1101/2020.08.19.20164111).

Premkumar, L., Segovia-Chumbez, B., Jadi, R., Martinez, D.R., Raut, R., Markmann, A., Cornaby, C., Bartelt, L., Weiss, S., Park, Y., *et al.* (2020). The receptor binding domain of the viral spike protein is an immunodominant and highly specific target of antibodies in SARS-CoV-2 patients. *Sci Immunol* 5.

Lee, W.S., Wheatley, A.K., Kent, S.J., and DeKosky, B.J. (2020). Antibody-dependent enhancement and SARS-CoV-2 vaccines and therapies. *Nat Microbiol* 5, 1185-1191.

Tang, D.C., Zhang, J., Toro, H., Shi, Z., and Van Kampen, K.R. (2009). Adenovirus as a carrier for the development of influenza virus-free avian influenza vaccines. *Expert Rev Vaccines* 8, 469-481.

Planas, D., Bruel, T., Grzelak, L., Guivel-Benhassine, F., Staropoli, I., Porrot, F., Planchais, C., Buchrieser, J., Rajah, M.M., Bishop, E., *et al.* (2021). Sensitivity of infectious SARS-CoV-2 B.1.1.7 and B.1.351 variants to neutralizing antibodies. *Nat Med*.

Pizzolla, A., Nguyen, T.H.O., Smith, J.M., Brooks, A.G., Kedzieska, K., Heath, W.R., Reading, P.C., and Wakim, L.M. (2017). Resident memory CD8(+) T cells in the upper respiratory tract prevent pulmonary influenza virus infection. *Sci Immunol* 2.

Laidlaw, B.J., Zhang, N., Marshall, H.D., Staron, M.M., Guan, T., Hu, Y., Cauley, L.S., Craft, J., and Kaech, S.M. (2014). CD4+ T cell help guides formation of CD103+ lung-resident memory CD8+ T cells during influenza viral infection. *Immunity* 41, 633-645.

Takamura, S. (2017). Persistence in Temporary Lung Niches: A Survival Strategy of Lung-Resident Memory CD8(+) T Cells. *Viral Immunol* 30, 438-450.

Sekine, T., Perez-Potti, A., Rivera-Ballesteros, O., Stralin, K., Gorin, J.B., Olsson, A., Llewellyn-Lacey, S., Kamal, H., Bogdanovic, G., Muschiol, S., *et al.* (2020). Robust T Cell Immunity in Convalescent Individuals with Asymptomatic or Mild COVID-19. *Cell* 183, 158-168 e114.

McMahan, K., Yu, J., Mercado, N.B., Loos, C., Tostanoski, L.H., Chandrashekar, A., Liu, J., Peter, L., Atyeo, C., Zhu, A., *et al.* (2021). Correlates of protection against SARS-CoV-2 in rhesus macaques. *Nature* 590, 630-634.

Sun, J., Zhuang, Z., Zheng, J., Li, K., Wong, R.L., Liu, D., Huang, J., He, J., Zhu, A., Zhao, J., *et al.* (2020). Generation of a Broadly Useful Model for COVID-19 Pathogenesis, Vaccination, and Treatment. *Cell* 182, 734-743 e735.

Zhuang, Z., Lai, X., Sun, J., Chen, Z., Zhang, Z., Dai, J., Liu, D., Li, Y., Li, F., Wang, Y., *et al.* (2021). Mapping and role of T cell response in SARS-CoV-2-infected mice. *J Exp Med* 218.

Thatte, J., Dabak, V., Williams, M.B., Braciale, T.J., and Ley, K. (2003). LFA-1 is required for retention of effector CD8 T cells in mouse lungs. *Blood* 101, 4916-4922.

van Doremalen, N., Lambe, T., Spencer, A., Belij-Rammerstorfer, S., Purushotham, J.N., Port, J.R., Avanzato, V.A., Bushmaker, T., Flaxman, A., Ulaszewska, M., *et al.* (2020). ChAdOx1

nCoV-19 vaccine prevents SARS-CoV-2 pneumonia in rhesus macaques. *Nature* 586, 578-582.

Croyle, M.A., Patel, A., Tran, K.N., Gray, M., Zhang, Y., Strong, J.E., Feldmann, H., and Kobinger, G.P. (2008). Nasal delivery of an adenovirus-based vaccine bypasses pre-existing immunity to the vaccine carrier and improves the immune response in mice. *PloS one* 3, e3548.

Zhang J, T.E., Feng T, Shi Z, Van Kampen KR, Tang DC. (2011). Adenovirus-vectored drug-vaccine duo as a rapid-response tool for conferring seamless protection against influenza. *PloS one* 6, e22605.

Krishnan, V., Andersen, B.H., Shoemaker, C., Sivko, G.S., Tordoff, K.P., Stark, G.V., Zhang, J., Feng, T., Duchars, M., and Roberts, M.S. (2015). Efficacy and immunogenicity of single-dose AdVAV intranasal anthrax vaccine compared to anthrax vaccine absorbed in an aerosolized spore rabbit challenge model. *Clin Vaccine Immunol* 22, 430-439.

Boyaka, P.N. (2017). Inducing Mucosal IgA: A Challenge for Vaccine Adjuvants and Delivery Systems. *J Immunol* 199, 9-16.

Gould, V.M.W., Francis, J.N., Anderson, K.J., Georges, B., Cope, A.V., and Tregoning, J.S. (2017). Nasal IgA Provides Protection against Human Influenza Challenge in Volunteers with Low Serum Influenza Antibody Titre. *Front Microbiol* 8, 900.

Belshe, R.B., Gruber, W.C., Mendelman, P.M., Mehta, H.B., Mahmood, K., Reisinger, K., Treanor, J., Zangwill, K., Hayden, F.G., Bernstein, D.I., *et al.* (2000). Correlates of immune protection induced by live, attenuated, cold-adapted, trivalent, intranasal influenza virus vaccine. *J Infect Dis* 181, 1133-1137.

Tasker, S., Wight O'Rourke, A., Suyundikov, A., Jackson Booth, P.-G., Bart, S., Krishnan, V., Zhang, J., Anderson, K.J., Georges, B., and Roberts, M.S. (2021). Safety and Immunogenicity of a Novel Intranasal Influenza Vaccine (NasoVAX): A Phase 2 Randomized, Controlled Trial. *Vaccines* 9, 224.

Lowen, A.C., Steel, J., Mubareka, S., Carnero, E., Garcia-Sastre, A., and Palese, P. (2009). Blocking interhost transmission of influenza virus by vaccination in the guinea pig model. *J Virol* 83, 2803-2818.

Price, G.E., Lo, C.Y., Mispion, J.A., and Epstein, S.L. (2014). Mucosal immunization with a candidate universal influenza vaccine reduces virus transmission in a mouse model. *J Virol* 88, 6019-6030.

Wu, S., Zhong, G., Zhang, J., Shuai, L., Zhang, Z., Wen, Z., Wang, B., Zhao, Z., Song, X., Chen, Y., *et al.* (2020). A single dose of an adenovirus-vectored vaccine provides protection against SARS-CoV-2 challenge. *Nat Commun* 11, 4081.

van Doremalen, N., Purushotham, J., Schulz, J., Holbrook, M., Bushmaker, T., Carmody, A., Port, J., Yinda, K.C., Okumura, A., Saturday, G., *et al.* (2021). Intranasal ChAdOx1 nCoV-

19/AZD1222 vaccination reduces shedding of SARS-CoV-2 D614G in rhesus macaques. bioRxiv.

Zhang, C., and Zhou, D. (2016). Adenoviral vector-based strategies against infectious disease and cancer. *Hum Vaccin Immunother* 12, 2064-2074.

Wold, W.S., and Toth, K. (2013). Adenovirus vectors for gene therapy, vaccination and cancer gene therapy. *Curr Gene Ther* 13, 421-433.

Ravichandran, S., Coyle, E.M., Klenow, L., Tang, J., Grubbs, G., Liu, S., Wang, T., Golding, H., and Khurana, S. (2020). Antibody signature induced by SARS-CoV-2 spike protein immunogens in rabbits. *Sci Transl Med* 12.

Walsh, E.E., Frenck, R., Falsey, A.R., Kitchin, N., Absalon, J., Gurtman, A., Lockhart, S., Neuzil, K., Mulligan, M.J., Bailey, R., *et al.* (2020). RNA-Based COVID-19 Vaccine BNT162b2 Selected for a Pivotal Efficacy Study. medRxiv.

Amanat, F., Thapa, M., Lei, T., Ahmed, S.M.S., Adelsberg, D.C., Carreno, J.M., Strohmeier, S., Schmitz, A.J., Zafar, S., Zhou, J.Q., *et al.* (2021). The plasmablast response to SARS-CoV-2 mRNA vaccination is dominated by non-neutralizing antibodies that target both the NTD and the RBD. medRxiv.

Zost, S.J., Gilchuk, P., Case, J.B., Binshtein, E., Chen, R.E., Nkolola, J.P., Schafer, A., Reidy, J.X., Trivette, A., Nargi, R.S., *et al.* (2020). Potently neutralizing and protective human antibodies against SARS-CoV-2. *Nature* 584, 443-449.

Li, L.H., Shivakumar, R., Feller, S., Allen, C., Weiss, J.M., Dzekunov, S., Singh, V., Holaday, J., Fratantoni, J., and Liu, L.N. (2002). Highly efficient, large volume flow electroporation. *Technol Cancer Res Treat* 1, 341-350.

Walls, A.C., Park, Y.J., Tortorici, M.A., Wall, A., McGuire, A.T., and Veesler, D. (2020). Structure, Function, and Antigenicity of the SARS-CoV-2 Spike Glycoprotein. *Cell* 183, 1735.

Wrapp, D., Wang, N., Corbett, K.S., Goldsmith, J.A., Hsieh, C.L., Abiona, O., Graham, B.S., and McLellan, J.S. (2020). Cryo-EM structure of the 2019-nCoV spike in the prefusion conformation. *Science* 367, 1260-1263.

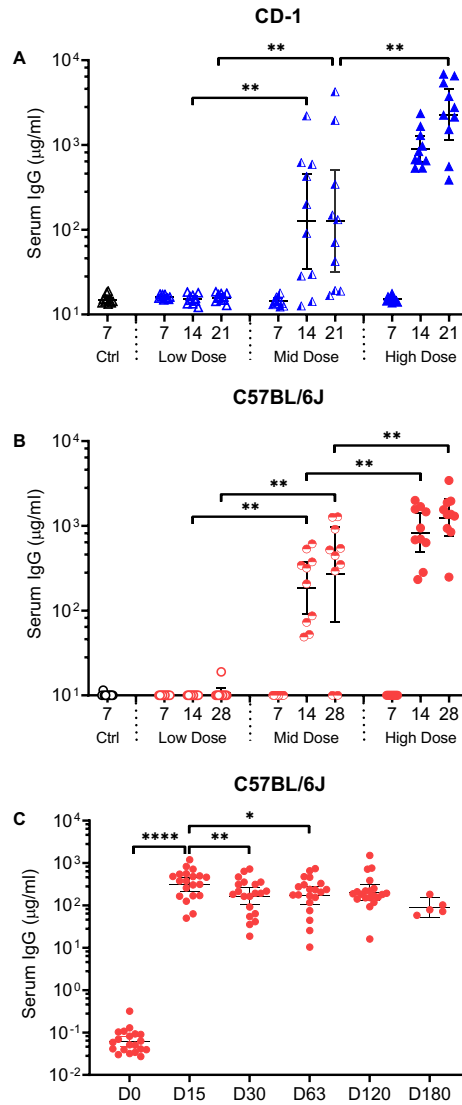


Figure 1. Spike-specific IgG responses in sera following a single intranasal administration of AdCOVID

(A) CD-1 and (B) C57BL/6J mice received a single intranasal administration of vehicle (Ctrl) or AdCOVID at a low, mid, or high dose as described. Sera were collected from euthanized animals between days (A) 7-21 or (B) 7-28 post-vaccination (n=10 animals/group/timepoint) and analyzed individually for quantification of spike-specific IgG. (C) A single cohort of C57BL/6J mice (n=20) received a single intranasal administration of AdCOVID at a dose of 3.78×10^8 ifu. Sera were collected longitudinally between days 0-180 post-vaccination and analyzed individually for quantification of spike-specific IgG. All results are expressed in $\mu\text{g/mL}$. Data are the geometric mean response \pm 95% confidence interval. Statistical analysis was performed with a Mann-Whitney test: *, $P < 0.05$; **, $P < 0.01$; ****, $P < 0.0001$.

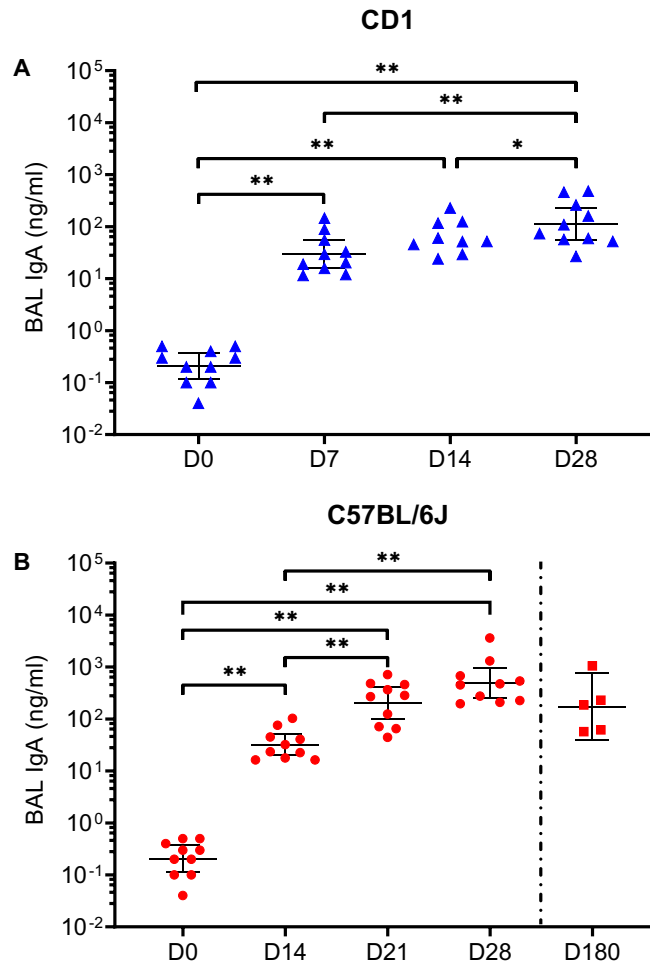


Figure 3. Spike-specific IgA responses in BAL following single intranasal administration of AdCOVID

(A) CD-1 mice (n=10 animals/timepoint) received a single intranasal administration of $6.25E+08$ ifu AdCOVID. BAL samples were collected at the indicated timepoints and analyzed individually for the quantification of spike-specific IgA. (B) C57BL/6J mice received a single intranasal administration of $6.25E+08$ ifu AdCOVID. BAL samples were collected on days 0, 14, 21, and 28 (n=10 animals/timepoint). In a separate study, C57BL/6J mice (n=5) received a single intranasal administration of $3.78E+08$ ifu AdCOVID on day 0 and were euthanized on day 180 for BAL collection. BAL samples were analyzed individually for the quantification of spike-specific IgA. All results are expressed in ng/mL. Data are the geometric mean response \pm 95% confidence interval. Statistical analysis was performed with a Mann-Whitney test: *, $P < 0.05$; **, $P < 0.01$.

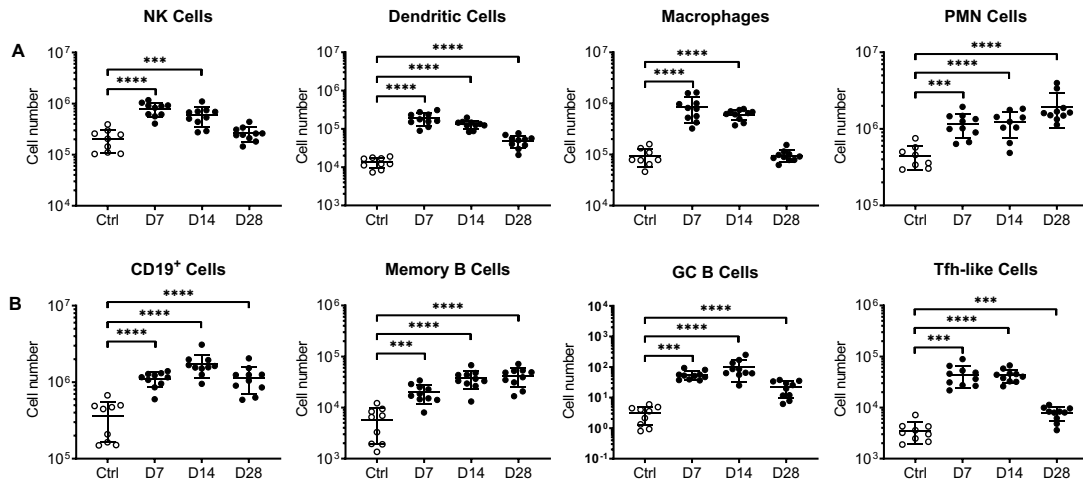


Figure 4. Flow cytometry analysis of immune cells in lungs from C57BL/6J mice following a single intranasal dose of AdCOVID

C57BL/6J mice were given a single intranasal administration of vehicle (Ctrl) or 3.35×10^8 ifu AdCOVID. Lung cells were isolated from the vaccinated mice at the timepoints indicated (10 mice/timepoint) and analyzed individually by flow cytometry using markers of (A) innate immune cells or (B) B and Tfh-like cells as described in Material and Methods. Results are expressed as cell number. Different Y-axis scales are used across the graphics. Data are the mean response \pm SD. Statistical analysis was performed with a Mann-Whitney test: ***, $P < 0.001$; ****, $P < 0.0001$.

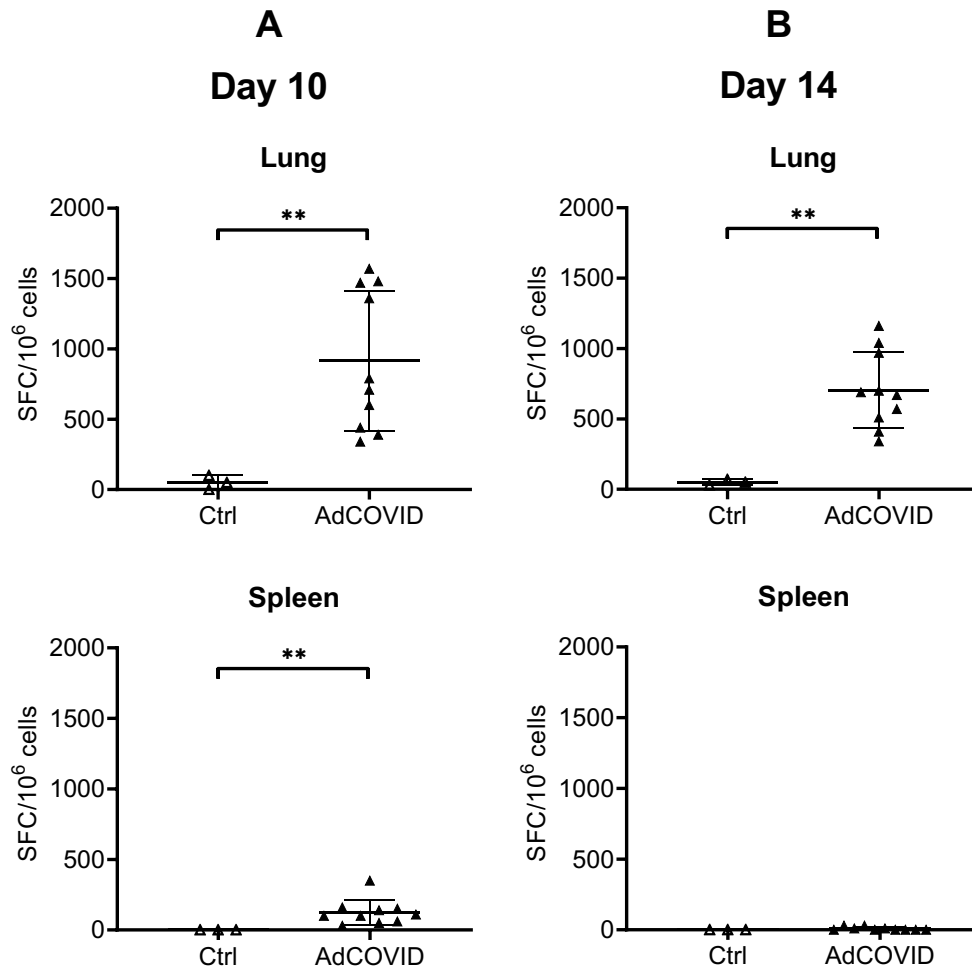


Figure 5. Intranasal AdCOVID vaccination elicits mucosal and systemic IFN- γ ⁺ T cells

CD-1 mice were given a single intranasal administration of vehicle (Ctrl) or 3.78E+08 ifu AdCOVID. Lung and spleen cells were isolated on days (A) 10 and (B) 14 following vaccination, re-stimulated with an RBD peptide pool, and analyzed by IFN- γ ELISpot. Results are expressed as Spot Forming Cells (SFC) per million input cells. Data are the mean response +/- SD. Statistical analysis was performed with a Mann-Whitney test: **, P <0.01.

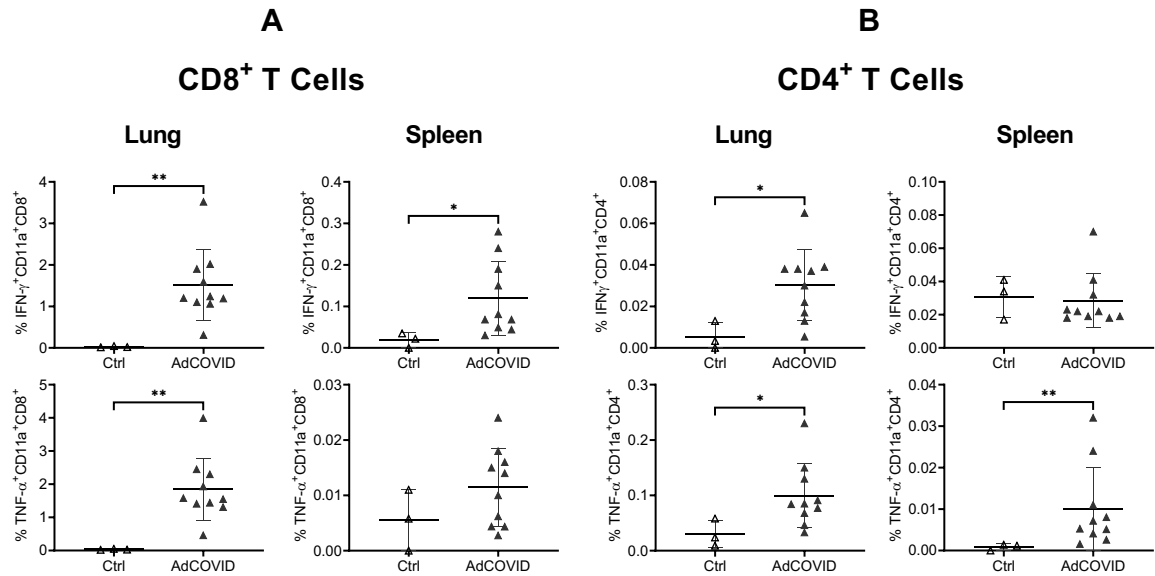


Figure 6. Intracellular cytokine production by pulmonary and splenic T cells 14 days after intranasal AdCOVID vaccination. CD-1 mice were given a single intranasal administration of vehicle (Ctrl) or 3.78E+08 ifu AdCOVID. Lung cells (n= 10 mice/vaccine, 3 mice/control) were isolated on day 14, re-stimulated with the RBD peptide pool for 5 hours, and analyzed by flow cytometry. Results are expressed as the percentage of IFN- γ or TNF- α expressing (A) CD11a⁺CD8⁺ or (B) CD11a⁺CD4⁺ T cells for individual mice. Different Y-axis scales are used across the graphics. Data are the mean response +/- SD. Statistical analysis was performed with a Mann-Whitney test: *, P < 0.05; **, P < 0.01.

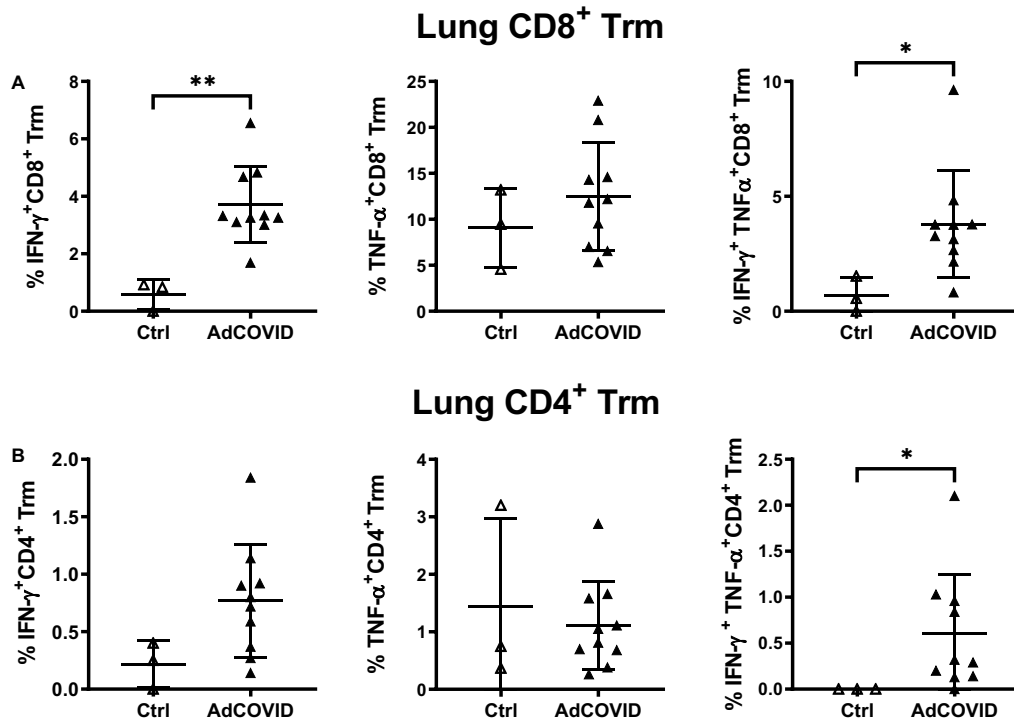


Figure 7. Intranasal AdCOVID vaccination elicits polyfunctional memory T cell populations in the lung 14 days after vaccination

CD-1 mice were given a single intranasal administration of vehicle (Ctrl) or 3.78E+08 ifu AdCOVID. Lung cells (n= 10 mice/vaccine, 3 mice/control) were isolated at day 14, re-stimulated with the RBD peptide pool for 5 hours, and analyzed by flow cytometry to identify CD69⁺CD103⁺ resident memory T cells (Trm). Results are expressed as the percentage of IFN- γ ⁺, TNF- α ⁺ or double positive IFN- γ ⁺/TNF- α ⁺ expressing (A) CD8⁺ or (B) CD4⁺ Trm cells for individual mice. Different Y-axis scales are used across the graphics. Data are the mean response +/- SD for the groups. Statistical analysis was performed with a Mann-Whitney test: *, P < 0.05; **, P < 0.01.

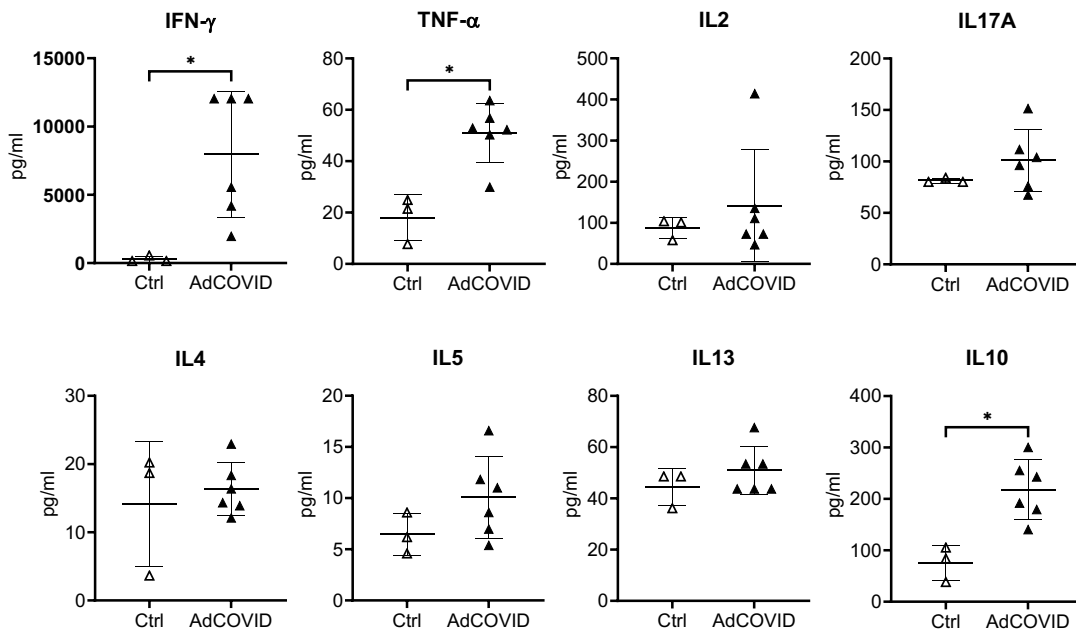
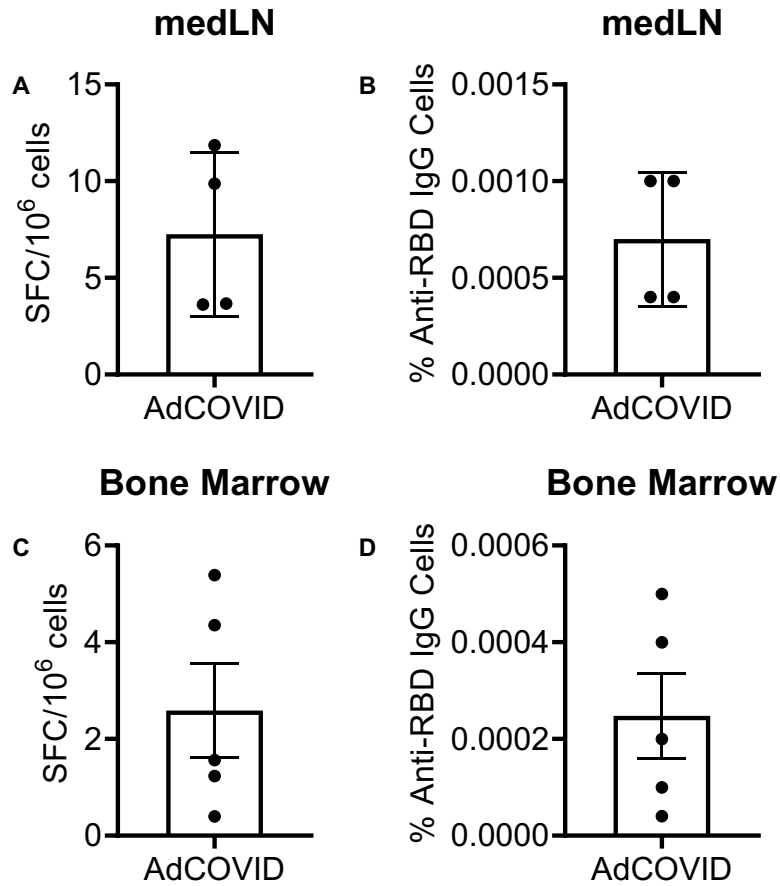


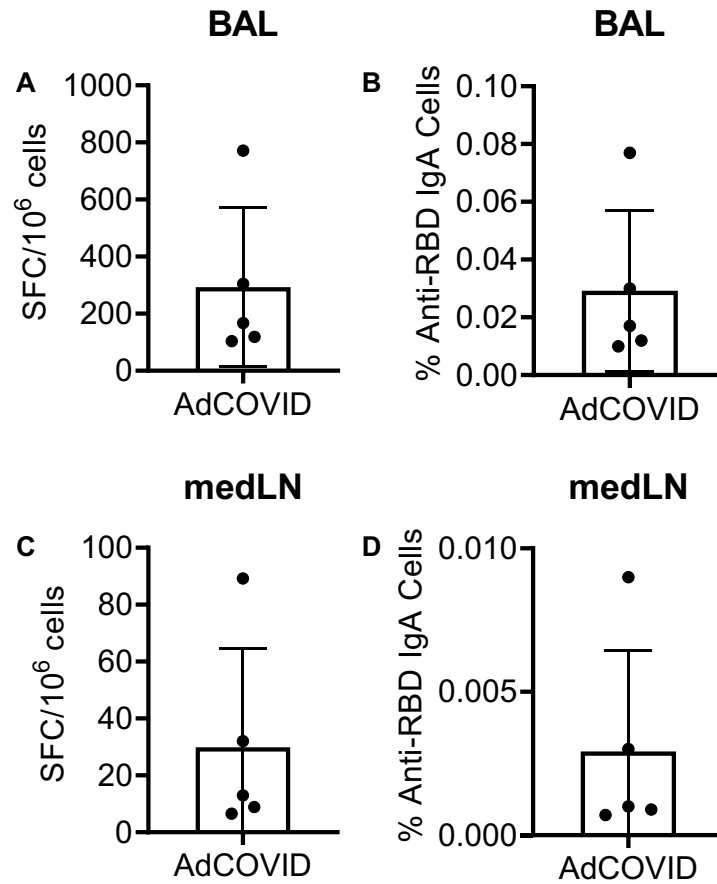
Figure 8. Intranasal AdCOVID vaccination does not elicit a Th2 or Th17-biased immune response

CD-1 mice were given a single intranasal administration of vehicle (Ctrl) or 3.78E+08 ifu AdCOVID. Splenocytes (n= 10 mice/vaccine, 3 mice/control) were isolated at day 10 and re-stimulated with the RBD peptide pool for 48 hours. Secreted cytokines were detected in the supernatant using a cytokine multiplex assay. Results are expressed in pg/mL. Different Y-axis scales are used across the graphics. Data are mean response +/- SD. Statistical analysis was performed with a Mann-Whitney test: *, P < 0.05.



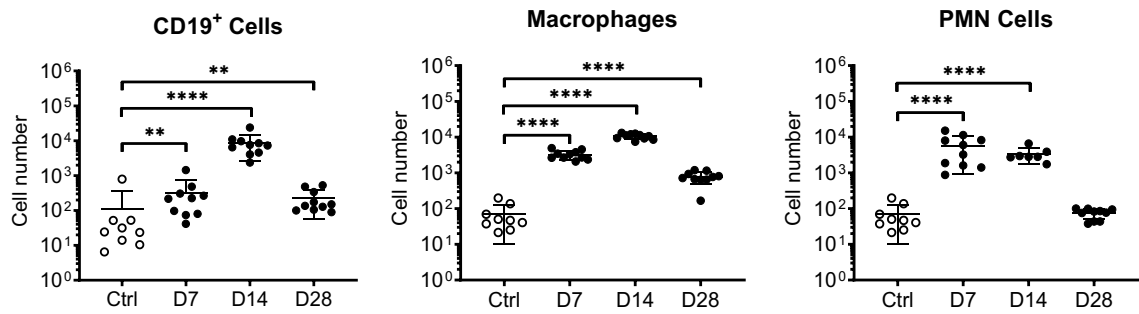
Supplementary Figure 1. A single intranasal dose of AdCOVID generates long-lived anti-RBD IgG-secreting B cell populations in the periphery

C57BL/6J mice (n=10) received a single intranasal administration of AdCOVID at a dose of 3.78E+08 ifu on day 0. Mice were euthanized on day 193 and (A, B) medLN or (C, D) bone marrow were harvested for B cell ELISpot. Results are expressed as (A, C) Spot Forming Cells (SFC) per million input cells or (B, D) frequency of RBD-specific IgG-secreting cells isolated. Data are the mean response +/- SD.



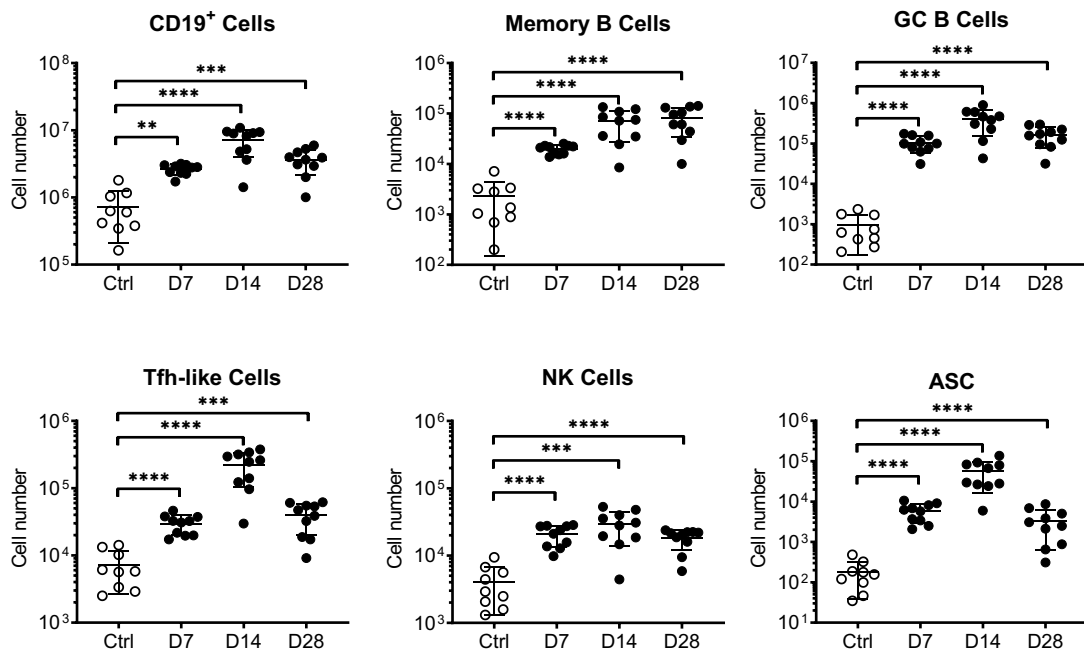
Supplementary Figure 2. A single intranasal dose of AdCOVID generates long-lived anti-RBD IgA-secreting B cell populations

C57BL/6J mice (n=5) received a single intranasal administration of AdCOVID at a dose of 3.78E+08 ifu on day 0 and were euthanized on day 180. Cells were isolated from the (A, B) BAL and (C, D) medLN for analysis by B cell ELISpot. Results are expressed as (A, C) Spot Forming Cells (SFC) per million input cells or (B, D) frequency of RBD-specific IgA-secreting cells isolated. Data are the mean response +/- SD.



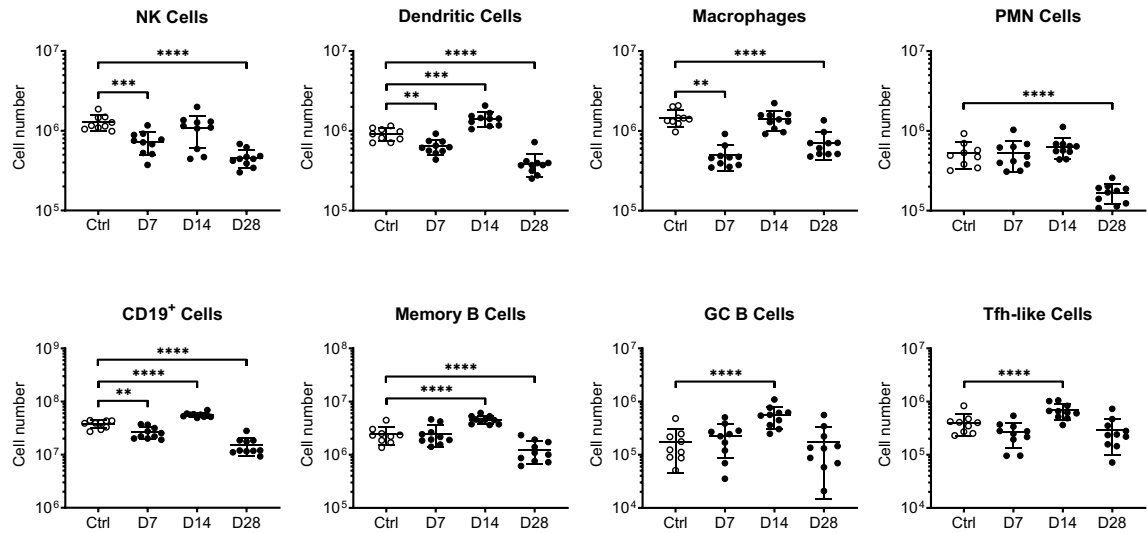
Supplementary Figure 3. Flow cytometry analysis of immune cells in BAL from C57BL/6J mice following intranasal vaccination with single dose of AdCOVID

C57BL/6J mice were given a single intranasal administration of vehicle (ctrl) or 3.35E+08 ifu AdCOVID (high dose). BAL cells were collected from vaccinated animals at the indicated timepoints (10 mice/timepoint) and analyzed individually by flow cytometry. Results are expressed as cell number. Data are means +/- SD. Statistical analysis was performed with Mann-Whitney test: **, P<0.01; ****, P<0.0001.



Supplementary Figure 4. Flow cytometry analysis of immune cells in medLN from C57BL/6J mice following intranasal vaccination with single dose of AdCOVID

C57BL/6J mice were given a single intranasal administration of vehicle (ctrl) or 3.35E+08 ifu AdCOVID (high dose). medLN cells were isolated from vaccinated animals at the indicated timepoints (10 mice/timepoint) and analyzed individually by flow cytometry. Results are expressed as cell number. Data are means +/- SD. Statistical analysis was performed with Mann-Whitney test: **, P<0.01;***, P<0.001; ****, P<0.0001.

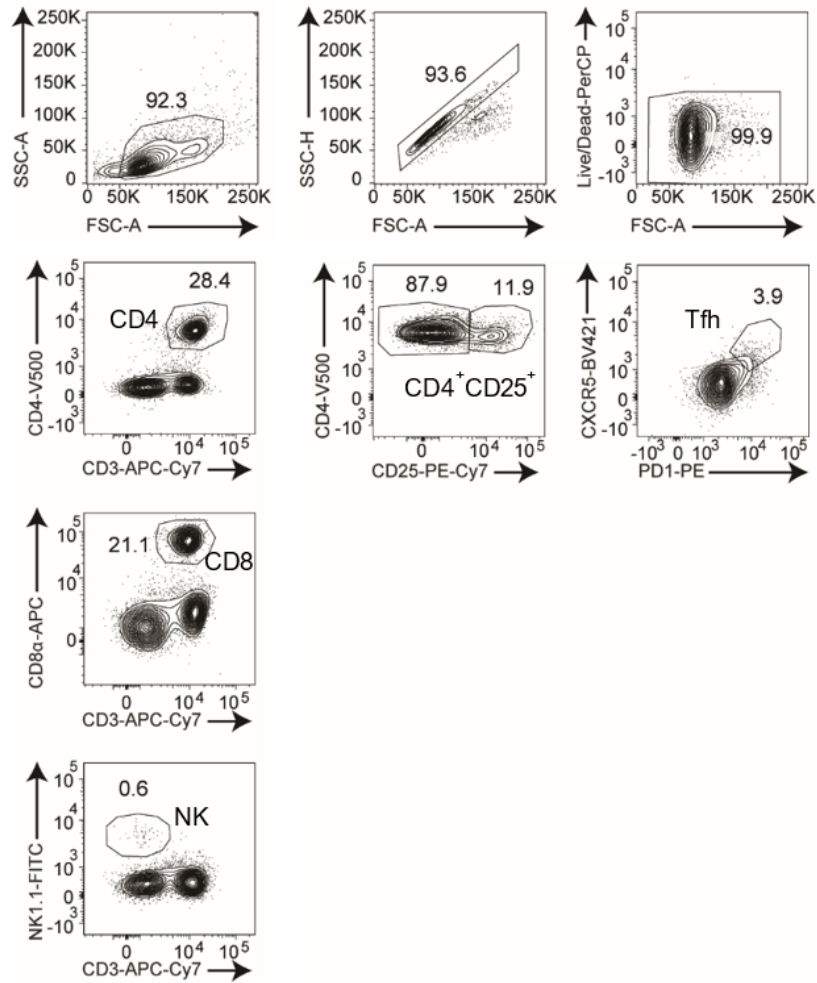


Supplementary Figure 5. Flow cytometry analysis of immune cells in spleens from C57BL/6J mice following intranasal vaccination with single dose of AdCOVID

C57BL/6J mice were given a single intranasal administration of vehicle (ctrl) or 3.35×10^8 ifu AdCOVID (high dose). Splenocytes were collected from vaccinated animals at the indicated timepoints (10 mice/timepoint) and analyzed individually by flow cytometry. Results are expressed as cell number. Data are means \pm SD. Statistical analysis was performed with Mann-Whitney test: **, $P < 0.01$; ***, $P < 0.001$; ****, $P < 0.0001$.

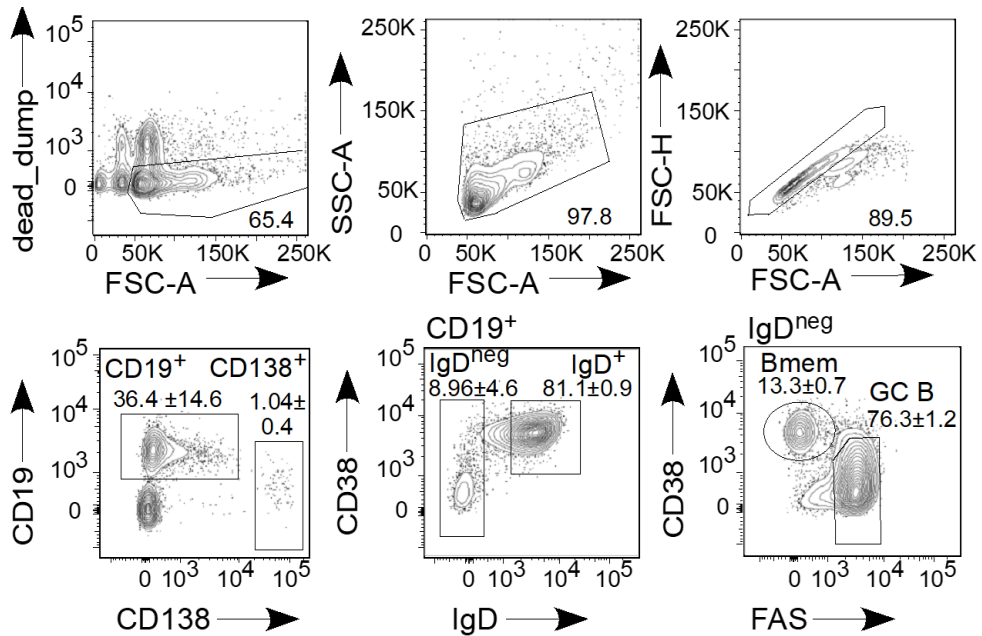
Cell Type	Cellular Markers
CD4 T Cell	CD3 ⁺ CD4 ⁺
CD8 T Cell	CD3 ⁺ CD8 ⁺
T Follicular Helper-like (Tfh)	CD4 ⁺ CXCR5 ⁺ PD-1 ^{hi}
CD19 B Cell	CD19 ⁺ CD138 ^{neg}
Memory B Cell	IgD ^{neg} CD38 ⁺ Fas ^{neg}
Germinal Center B Cell (GC)	IgD ^{neg} CD38 ^{lo} Fas ⁺
Antibody Secreting Cells (ASC)	CD19 ^{lo} CD138 ^{hi}
Natural Killer (NK)	CD3 ^{ne} gNK1.1 ⁺
Polymorphonuclear (PMN)	Ly6G ^{hi} autofluorescent ^{neg} CD3 ^{neg} NK1.1 ⁺
Macrophage	CD11b ⁺ CD64 ^{hi}
Dendritic Cell	MHCII ⁺ CD11c ⁺

Supplementary Table 1. Flow Cytometry Cellular Markers



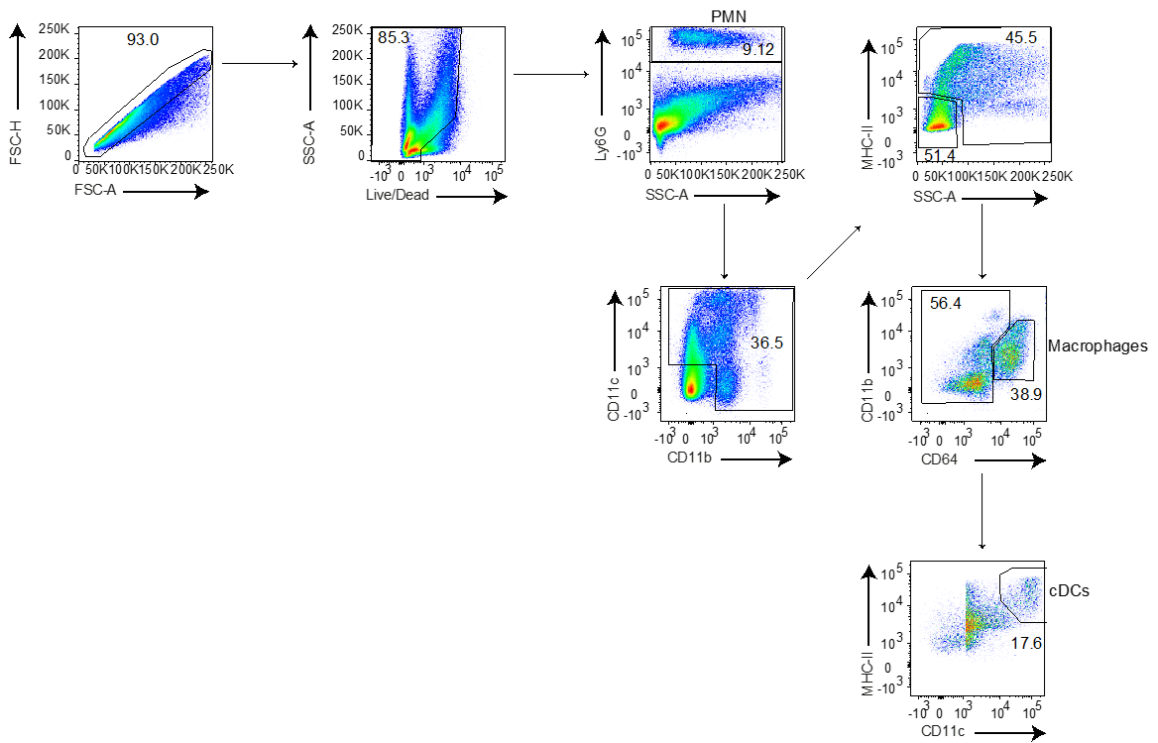
Supplementary Figure 6. Representative flow cytometry plots for gating of T cells isolated from mice

Gating strategy to identify CD3+CD4+ (CD4+ T cells), CD3+CD8+ (CD8+ T cells), CD3negNK1.1+(NK cells), CD25+CD4+ T cells and CXCR5+PD-1hi T follicular helper-like cells (Tfh)



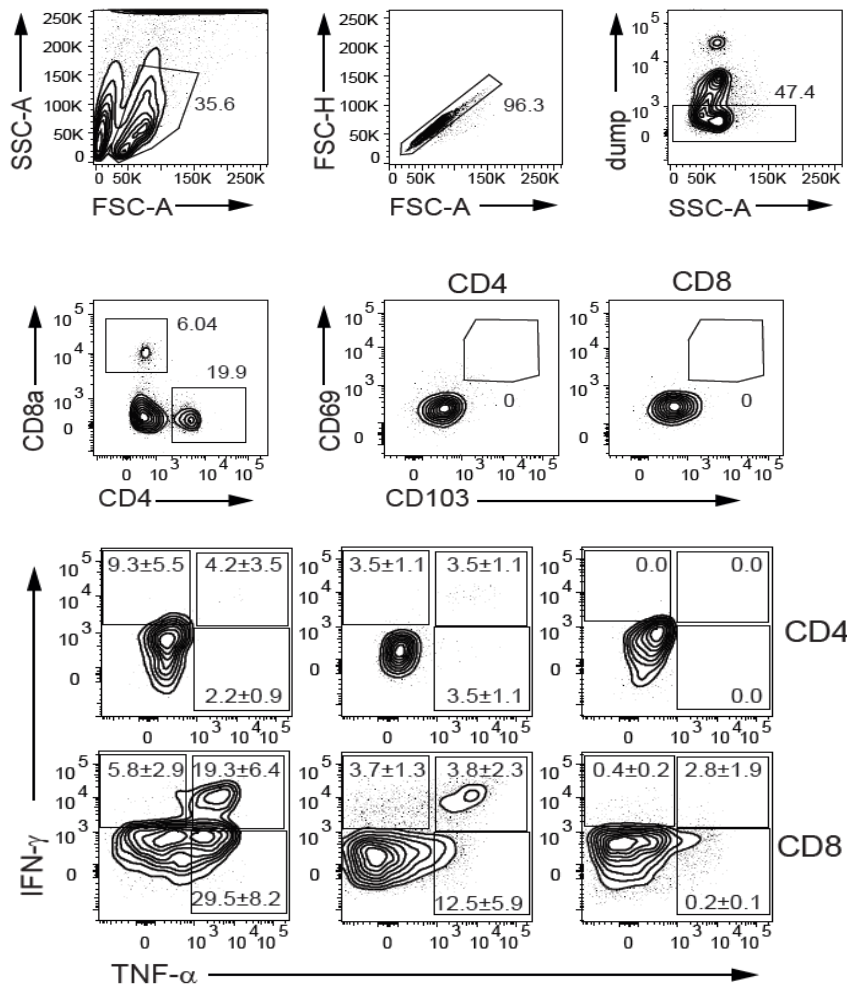
Supplementary Figure 7. Representative flow cytometry plots for gating B cells isolated from mice

Gating strategy to identify total CD19⁺ B cells, CD19^{lo}CD138^{hi} antibody secreting cells (ASCs), IgD⁺ naïve B cells, IgD^{neg} antigen-experienced B cells, IgD^{neg}CD38⁺Fas^{neg} memory B cells (Bmem) and IgD^{neg}CD38^{lo}Fas⁺ germinal center (GC) B cells



Supplementary Figure 8. Representative flow cytometry plots for gating of myeloid cells isolated from mice.

Gating strategy to identify Ly6G^{hi} neutrophils (PMN), CD11b⁺CD64^{hi} macrophages, and MHCII⁺CD11c⁺ dendritic cells (cDCs).



for gating for

Gating strategy to identify CD69⁺CD103⁺ resident memory (RM) CD4⁺ or CD8⁺ cells.

DISCUSSION

Our data demonstrate, for the first time, how IFN- γ and IFN- γ -inducible transcription factors (TFs), T-bet and IRF1, promote ASC differentiation from IFN- γ -activated B cell precursors *in vitro* and upon viral infection *in vivo*. We previously reported that cognate encounters between B cells and either Th1 or Th2 effectors resulted in preferential antibody generation in the presence of IFN- γ -producing Th1 cells rather than Th2 cells *in vitro*^{238,245}. We soon realized that IFN- γ -activated B cells upregulated T-bet, a well appreciated TF in coordinating Th1 cell fate decisions^{216,238,245,258,265}. We predicted only one other TF, IRF1, as a driver of IFN- γ -induced ASC differentiation by the intersect of four bioinformatic analysis. Consistent with our prediction, we found that while T-bet is indispensable for the development of long-lived ASCs upon viral infection, IRF1 is required for the generation of early antigen-specific IgM in response to viral infection and bacterial immunization. Lastly, we found a local IFN- γ -producing T cell response that corresponds to the production of durable RBD-specific antibody upon intranasal Ad5COVID vaccination. Therefore, we have established an unprecedented role for IFN- γ and IFN- γ -inducible TFs in B cell biology-driving the differentiation of ASCs from activated B cell precursors.

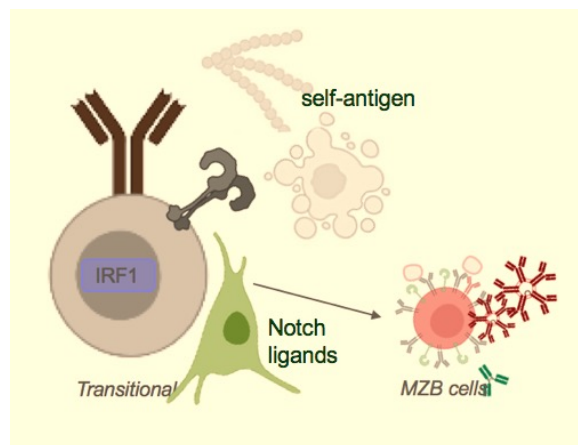


Figure 8 Model of BCR/TLR-inducible IRF1 in transitional cells.

BCR/TLR-inducible IRF1 in transitional cells promotes the efficient transduction of the key developmental pathway of the MZ B cells, Notch. In response to endogenous ligands IRF1-expressing B cells are selected into the MZ B cell pool.

T-bet and IFN- γ repress alternative B cell fates

In CD4⁺ T cells, *Il6*, *Batf*, and *Rorc*, have been shown to be important for the differentiation of Th17 cells²⁷⁶⁻²⁷⁹. In the presence of IL-6 and TGF- β , which are Th17-polarizing conditions, *Batf*^{-/-} CD4⁺ T cells are unable to express the “master” transcription factor of the Th17 program, ROR γ T (encoded by the gene *Rorc*)²⁷⁶. *Rorc*^{-/-} CD4⁺ T cells, however, are only partially impaired in their ability to produce the Th17 signature cytokine, IL-17²⁸⁰. In response to IL-6 and TGF- β , CD4⁺ T cells express another transcription factor, ROR α (encoded by the gene *Rora*), and together, ROR γ T and ROR α cooperate to promote Th17 differentiation and production of IL-17²⁸⁰. Since it is known that T-bet can oppose Th17 differentiation through obstructing the activation of *Rorc*, it is conceivable that T-bet may repress alternative B cell fates in a similar fashion²⁸¹. Indeed, our data showed that *Il6*, *Batf*, and *Rorc*, were more highly expressed in both *Ifngr1*^{-/-} and *Tbx21*^{-/-} Be1 cells when compared to B6 Be1 cells. This result suggests that IFN- γ R signaling may oppose expression of alternate fate-specifying TFs in Be1 cells through the activation of T-bet.

Very little is known about *Rorc* and *Rora* in B cells. While it has been shown that B cells can produce IL-17, it appears they do so independently of *Rorc*²⁸². We have yet to show that in the absence of T-bet, activated B cells produce other signature cytokines, although the differential transcript expression of key “master regulators” suggests that they may have acquired alternative B effector fates. In support of this, we do show that B cell intrinsic loss of *Tbx21* biased NP⁺ Bmem causes them to express an alternative, TGF- β -induced, secondary Ig subclass, IgG2b²⁵¹. Additionally, it is proposed that class switched B cells may represent transcriptionally and functionally distinct Bmem populations²⁸³. Separable programs for IgG2a and IgA Bmem have been described and largely determined by the expression of *Tbx21* and *Rora*, respectively²⁸³. Indeed, Bmem populations characterized by the expression of IgG2a or IgA are distinctive in cell surface phenotype and migratory potential²⁸³. Therefore, it is tempting to speculate that like the Th1/Th2 paradigm for T cells there exists a similar dichotomy for B cells.

In agreement with this speculation, we have some preliminary data that suggests in the absence of *Tbx21*, B cells may produce alternative class switched antibody in addition to IgG2b. We have observed *Tbx21* deficient B cells preferentially secrete IgA in response to influenza infection (Figure 1A-C). It is well understood that *Igba* CSR is initiated by TGF- β

and TGF- β R-induced transcription factors (TFs), including SMAD and Runx3²³⁷. Therefore, we propose that like Th1 cell differentiation where T-bet may redirect Runx3 to silence *I μ* , T-bet may redirect Runx3 in B cells to silence to *Igba* or other lineage defining genes^{238,239}. In support of this, we identify a T-bet dependent differentially accessible region (DAR) within the *Rorc* locus in B6 Be1 cells. Within that T-bet-dependent DAR, we find a predicted a T-bet-Runx composite consensus binding motif along with concomitant decreased transcript expression of *Rorc* over time. This suggests that repression of *Rorc* occurs through cooperation of T-bet and Runx in B cells. Altogether, our data is suggestive of alternative B cell fates which are repressed by IFN- γ -induced T-bet.

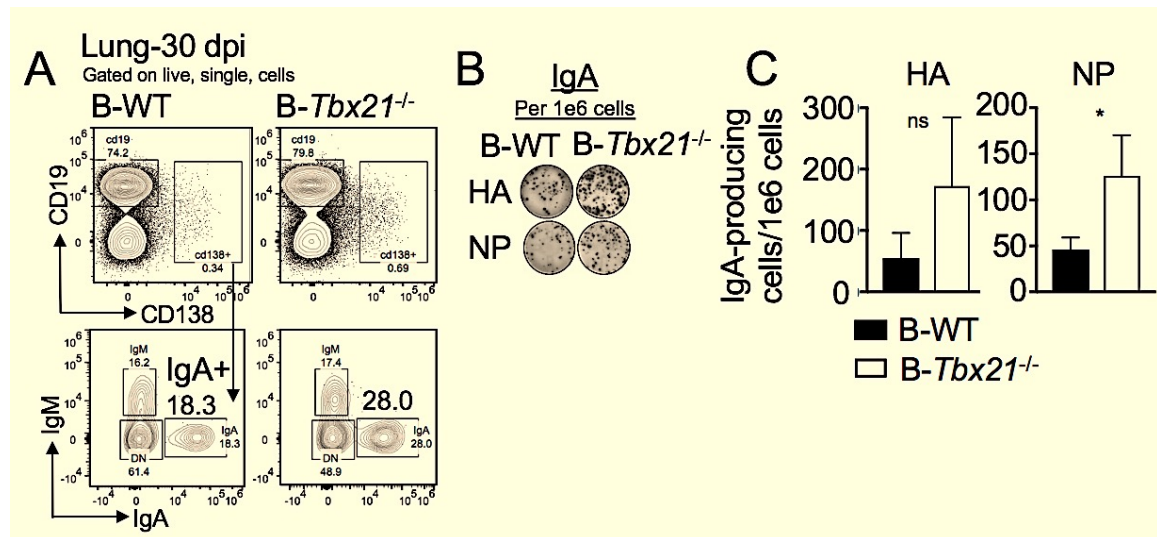


Figure 9 T-bet opposes IgA-producing cells in response to influenza infection in the lung.

(A-C) Irradiated μ MT recipients are reconstituted with a mix of either 20% B6 + 80% μ MT (B-WT) or 20% *Tbx21*^{-/-} + 80% μ MT BM (B-*Tbx21*^{-/-}). B chimeric mice were infected with influenza (PR8) 8 weeks post reconstitution and analyzed 30 days later.

(A) Representative flow plot of lung CD138⁺ cells in B chimeric mice 30 dpi

(B-C) ELISPOT of influenza NP or HA –specific IgA cells from the lungs 30 dpi of influenza infected B chimeric mice (B) and quantification (C)

T-bet paradox: Stable B effector state

Our data showed that T-bet restrained the expression of *Stat*, *Irf*, and *Nfkb* family members. Indeed, the expression of many *Stat*, *Irf*, and *Nfkb* family members declined in Be1 cells when compared to Be2 cells, whereas *Tbx21*^{-/-} Be1 cells maintained the expression of *Stat*, *Irf*, and *Nfkb* family members relative to B6 Be1 cells. Furthermore, continued NF-κB activation through the addition of an NF-κB activator in the B6 Be1 cultures blocked the generation of ASCs. Therefore, T-bet promotes ASC differentiation by limiting the activity of NF-κB in B cells. Initially, this was somewhat unexpected in that *Nfkb* family members are known to support the activation of B cells and their subsequent differentiation into ASCs²⁸⁴. Although, the transcription factor, Blimp1, may promote ASC differentiation by repressing genes that support B cell proliferation like the *Nfkb* family member, *Rel*^{285,286}. This could suggest, like Blimp1, T-bet may drive the generation of ASCs through negatively regulating pro-proliferation genes in IFN-γ-activated B cells.

Consistent with our observations *in vitro*, we found the highly proliferative, T-dependent, GC B cells express T-bet 12 days following influenza infection. It has also been shown that Tfh cells may transiently express T-bet and produce IFN-γ relatively early following immunization^{287,289}. Therefore, it is likely that GC B cells are responding to IFN-γ-producing Tfh cells at this time. Since we showed that T-bet promotes the differentiation of ASCs by limiting genes that may support B cell proliferation, we predict that T-bet may actively suppress the formation of the highly proliferative GC B cells. In support of this prediction, we found that *Tbx21*^{-/-}GC B cells expand over time when in competition with B6 GC B cells (Figure 2A-C). Therefore, this observation is very consistent with our findings that T-bet prevents the continued expression of pro-proliferative genes like *Nfkb* family members *in vitro*. However, we also observed high T-bet expression in GC B cells. How can this be? We speculate that this is a question of occupancy. *In vitro*, B6 B cells are activated by IFN-γ-producing Th1 cells and BCR stimulation. Consequently, T-bet is expressed early in B6 Be1 cells, coincident with the expression of *Stat*, *Irf*, and *Nfkb* family members. We propose at this time, T-bet is rendered functionally inactive as a result of active STAT, IRF, and NF-κB family members at some, but not all loci. Once B6 Be1 cells are no longer exposed to T cell help and/or have effectively consumed IFN-γ/BCR stimulation, T-bet is then able

to enact its repressive function. Therefore, IFN- γ -induced ASC differentiation is a consequence of the relative abundance of T-bet, STAT, IRF, and NF- κ B family members. In support of this, it has been shown that a high expression of T-bet repressed *Pdcd1*, the gene that encodes for PD-1, thus sustaining antigen specific CD8⁺ T cells during chronic viral infection²⁹⁰. Thus, T-bet may function in an expression-dependent fashion during IFN- γ -induced ASC differentiation. Therefore, while we show that sustained NF- κ B activity can block the formation of ASCs, much remains to be understood about how the interplay between T-bet and NF- κ B family members determines B cell fate decisions.

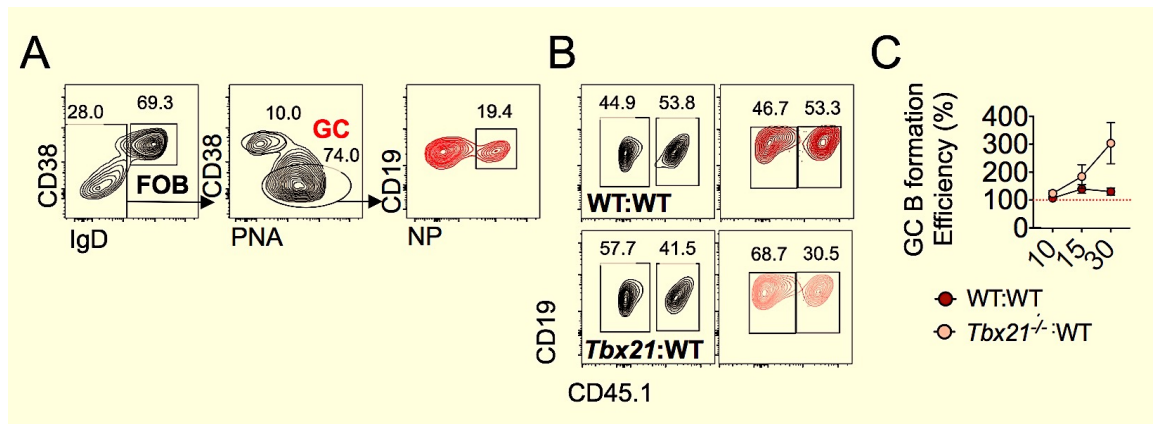


Figure 10 T-bet represses GC B cell formation after influenza infection.

(A-C) Irradiated μ MT recipients are reconstituted with a mix of either 50% CD45.1 B6 + 50% CD45.2 B6 (WT:WT) or 50% CD45.1 B6 + 50% CD45.2 *Tbx21*^{-/-} BM (*Tbx21*^{-/-}:WT). Competitive chimeric mice were infected with influenza (PR8) 8 weeks post reconstitution and draining lymphnode (LN) analyzed at 10,15 and 30 days later.

(A) Representative gating strategy for influenza nucleoprotein (NP) GC B cells

(B-C) Representative flow plots assessing the contribution of CD45.1 or CD45.2 cells to NP+GC B cells 30 days after influenza infection in competitive chimeric mice groups (B) and quantification of (B) by normalized GC B formation efficiency = (CD45.2 GC B / CD45.1 GC B) / (CD45.2 FoB / CD45.1 FoB) (C)

IRF1 as a regulator of the protective, innate-like B cell populations

Our data showed that *Irf1* was required for mounting optimal early antigen specific IgM in response to influenza infection and prototypical T-independent (T-I) immunizations. While these data support our conclusion that *Irf1* is required for the generation of MZ B cells in that these cells contribute to innate-like, protective antibody responses, we cannot yet

preclude the possibility that the B-1 B cells are functionally defective in the absence of *Irf1*. Indeed, our data showed that B-1a and B-1b cells are intact by cell surface phenotype, but whether these cells require *Irf1* to generate antibody remains an open question. Given that phosphorylcholine (PC)-specific IgM arises from the fetally derived T15 clone, we predict that B-1 B cells are functionally censored since our data showed that *Irf1* was required to efficiently generate PC-specific IgM upon PC-containing *Streptococcus pneumoniae* immunization⁷¹. Furthermore, we have observed that there is a significant reduction in total IgG3 in the preimmune sera of *Irf1* deficient mice (data not shown). As B-1 B cells are the primary producers of natural antibody, those data would also suggest that B-1 B cells are functionally defective. Therefore, our data suggests that *Irf1* expression is important for all innate-like B cells and how *Irf1* may influence neonatal B cell lymphopoiesis will require further study.

The influence of TLR signaling in the development of mature B cells

Our data showed that co-signaling of BCR and TLR promotes high IRF1 expression, where *Irf1* is required for the development of MZ B cells. It is currently unclear whether the sensing of microbial or self components through TLRs influences the clonal selection or expansion of immature B cells into the primary B cell repertoire. It appears that *Myd88* and *Trif*, the direct downstream adaptors of TLRs, are mostly dispensable for mature B cell development⁹⁸. Given that innate-like B cells express broadly reactive BCRs similar to TLRs in regards to specificity, it is conceivable that compensatory BCR signaling in the absence of *Myd88* and *Trif* could result in a mostly complete mature B cell pool, provided that FoB cells do not require TLR signaling. Indeed, in addition to specificity, TLR and BCR signaling share central components of the NF- κ B pathway²⁹¹⁻²⁹³. Furthermore, we have observed high IRF1 expression in transitional B cells in the presence of high dose TLR and/or BCR stimulation. Therefore, some of our data seem very consistent with the notion that *Myd88* and *Trif* are not required for the development of mature B cells.

However, humans deficient in *MYD88* exhibit increased autoreactivity within the naïve B cell compartment, implying that TLR signaling pathways are required for the elimination of autoreactive BCRs during B cell development²⁹⁴. Similarly, multiple components of TLR signaling are essential for shaping the BCR repertoire of B-1 B cells²⁹⁵. Therefore, while mature B cells are sufficiently generated in the absence of TLR signaling, the composition of the primary B cell repertoire is significantly altered. One possibility is that

TLR signaling lends itself to mechanisms of clonal selection. Indeed, our data shows that *Irf1*^{-/-} B cells bearing the self-reactive V_H81X transgene are not appropriately selected into the MZ B cell pool, where the putative autoantigen may also engage TLRs^{51,52}. Alternatively, as TLR ligands are known mitogens, engagement of TLRs could promote clonal expansion²¹⁰. Since *Myd88*^{-/-} mice can sufficiently develop all mature B cells and MZ B cells may undergo homeostatic proliferation, we predicted that *Myd88*^{-/-} MZ B cells are at a competitive disadvantage^{98,296}. Indeed, our data shows there are fewer *Myd88*^{-/-} MZ B cells when in competition with B6 MZ B cells. How might BCR and TLR co-signaling grant a competitive advantage to developing, peripheral B cells? It is well appreciated that TLR engagement can promote responsiveness to the pro-survival factor, BAFF, in transitional B cells^{68,218-221,297-299}. Additionally, TLR signaling could initiate an IFN β –feedforward loop to support the survival of developing, peripheral B cells²⁴⁹. Therefore, it is tempting to speculate on a model of MZ B cell interclonal competition, where TLR and BCR co-signaling in transitional B cells bestows a competitive advantage in clonal selection and/or expansion.

IRF1 and the development of autoimmunity

Our data showed that IRF1 regulates expression of *Ptprn22*, a proposed negative regulator of BCR signaling. This dampening of BCR signaling not only promotes the development of the MZ B cell compartment but also prevents the clonal selection of autoreactive B cells into the FoB cell repertoire. The inclusion of those autoreactive specificities may then facilitate the development of self-reactive GCs and autoantibodies. It is well appreciated that distinct populations of B cells require different BCR signaling thresholds for their development. While relatively “weak” BCR signaling in transitional B cells will favor the selection into the MZ B cell compartment, a “strong” signal will promote the development of FoB cells^{40,43,300}. Therefore, our data is very consistent with the proposed “Goldilocks” model for the positive selection of MZ B cells^{34,40}. However, the loss of MZ B cells in the absence of *Irf1*, initially, seems at odds with the development of autoimmunity. Indeed, the activation and/or expansion of the MZ B cell pool is often observed in models of Rheumatoid Arthritis (RA), Systemic lupus erythematosus (SLE), and type 1 diabetes³⁰¹⁻³⁰³. Although, these studies identify the expanded MZ B cell population as a correlate at the onset of autoimmune disease, where antigen presentation is the proposed primary function of these cells³⁰¹⁻³⁰³.

Therefore, it is difficult to determine the exact role of MZ B cells in those settings. In contrast, MZ B cells express BCRs that often recognize self-antigen exposed on potentially pro-inflammatory apoptotic cells^{54,304-306}. Consequently, MZ B cells can participate in the clearance of self-antigen generated by senescent cells, which could otherwise promote the development of autoimmunity^{54,304-306}. Thus, our data support a model where *Irf1*-dependent MZ B cells perform essential “housekeeping” functions to prevent the pathogenesis of autoimmune disease.

Our data also showed that IRF1 may promote the development of the homeostatic MZ B cell compartment through the upregulation of the gene *Ptpn22*, where the loss-of-function variant is often associated with the increased susceptibility to many autoimmune diseases²⁰²⁻²⁰⁸. Similar to the role of PTPN22 inhibiting TCR signaling, we found that B cells display enhanced calcium influx and reduced tolerance in response to BCR stimulation²⁰⁹. These results initially appeared inconsistent with a previous study reporting that *Ptpn22* is completely dispensable for BCR signaling²⁰⁹. However, this study evaluated bulk mature B cells, therefore B cell-type specific BCR signaling could not be adequately assessed. Therefore, our data is consistent with the notion that MZ B cell precursors may require developmentally distinct mechanisms for their maturation^{46,93-95}. However, our data also showed that *Irf1*^{-/-} B cells preferentially developed into GC B cells in response to endogenous antigens in aged competitive chimeric mice, suggesting that IRF1 may regulate the generation of FoB cells in addition to MZ B cells. Given that IRF1 inhibits BCR signaling thresholds in transitional B cells, it is tempting to speculate that the composition of the primary mature B cell repertoire is altered, where the redistribution of self-reactive specificities may promote the production of high affinity, pathogenic autoantibody. Therefore, B cell intrinsic-IRF1 may play a multifactorial role in the prevention of autoimmune disease.

Additionally, IRF1 was originally described as directly promoting the transcription of human *IFNA1* and *IFNB1*, well appreciated type I IFNs implicated in autoimmune disease^{307,308}. While we have yet to evaluate the contribution of B cell-intrinsic IRF1 to the production of IFN α/β , we speculate that populations of innate immune cells may be an adequate source^{309,310}. Although, B cell-intrinsic IFN β has been shown to regulate the survival of autoreactive B cells^{249,311}. Thus, it is possible that *Irf1*^{-/-} B cells are more vulnerable to apoptosis^{249,311}. Alternatively, the survival of autoreactive B cells may depend on the balance of BCR, TLR, and IFN, where compensatory BCR/TLR signaling may be sufficient⁶⁸.

Collectively, these data indicate that IRF1, induced in response to BCR and TLR signals, regulates the amplitude of BCR signaling in developing, peripheral B cells which promotes the generation of an innocuous primary B cell repertoire.

COVID-19 vaccination strategies

The currently approved vaccination strategies for COVID-19 are delivered by intramuscular injection and elicit robust systemic humoral responses. While these vaccination strategies significantly reduced viral load in the bronchoalveolar lavage fluid (BAL) and lower respiratory tract tissue, the levels of viral replication in the nasal cavity are unaffected, suggesting the potential for transmission³¹². Therefore, the Ad5COVID intranasal vaccine offers an attractive strategy to induce local, protective enduring immune responses.

Our data showed that Ad5COVID intranasally vaccinated mice were protected against viral challenge. However, while the phase I/II clinical trial demonstrated safety the Ad5COVID vaccine proved ineffective in eliciting protective immune responses when compared to placebo control groups. These studies exemplify the considerable differences between man and mouse. While intranasal vaccination strategies offer an attractive immunization route to induce local, mucosal immunity we know relatively little about the immune responses established in situ in humans. Indeed, due to the limitations of human studies we currently understand the Waldeyer's ring as a functional equivalent to the nasal associated lymphoid tissue (NALT) in the mouse³²⁸. Therefore, the very tissues or the organization of local lymphoid tissues that give rise to nasal immune responses could be vastly different between the mouse and man³²⁸. In addition to distinct local lymphoid associated tissues, there are other confounding factors of experimental mouse model systems including housing cleanliness, limited exposure to other viral and microbial agents, and reduced susceptibility to COVID-19³²⁹. These differences are well appreciated and are perhaps the underlying cause to the robust responses observed in the Ad5COVID murine preclinical trial.

Even though Ad5COVID intranasal vaccination strategy proved ineffective, we currently know very little about the mechanistic basis for the generation of protective antibody upon other COVID-19 vaccination platforms or natural COVID-19 infection. Furthermore, the lifespan of efficacious antibody responses induced upon vaccination or infection are continuing to be evaluated. It has been shown anti-SARS-CoV-2 antibody seropositivity has persisted for 6 months after vaccination and up to 10 months post infection³¹³⁻³¹⁶. Although,

it has also been reported anti-SARS-CoV-2 antibodies rapidly decay in those that experienced mild SARS-CoV-2 infection³¹⁷. Therefore, it is paramount to understand how to elicit long-lived, protective antibody responses. Our data, while limited to mouse models, showed that upon Ad5COVID intranasal vaccination we induced a local, IFN- γ -producing T cell response along with enduring anti-RBD IgG and IgA antibody. Our previous studies identify that the IFN- γ -inducible TF, T-bet, is indispensable for the generation of long-lived antibody in response to influenza infection. Therefore, it is conceivable that T-bet may also be required to form durable anti-RBD antibody upon Ad5COVID intranasal vaccination. In support of this idea, it has been shown that T-bet⁺ activated B cell populations strongly corresponded to the induction of neutralizing SARS-CoV-2-specific antibodies as well as autoreactive antibodies in response to SARS-CoV-2 infection³¹⁸. Although, these features are enriched in those that were critically ill, suggesting both pathogenic and protective roles for the correlating T-bet⁺ B cell subset³¹⁸. Therefore, it will be interesting to profile activated B cell subsets for T-bet expression in response to COVID-19 vaccination strategies. Furthermore, to evaluate the requirement for T-bet or other IFN- γ -inducible TFs in the generation of durable SARS-CoV-2-specific antibody. Therefore, assessing the roles of T-bet expressing B cells in infection and immunization could offer beneficial insight in the design of future vaccination protocols.

Future directions and concluding remarks

Collectively, these data underscore the importance of IFN- γ and IFN- γ -inducible TFs in B cell biology. We show for the first time, how two IFN- γ -inducible TFs shape B cell fate decisions upon activation and in development. Originally described as the “B cell growth factor,” IL-4 is often recognized as the cytokine to support B cell proliferation, CSR, and ASC differentiation^{235-242,319}. However, we have established a new paradigm by which IFN- γ -inducible TFs provide lasting humoral immunity upon viral infection and protective, broadly reactive early antibody responses to bacterial and viral pathogens.

We previously observed that Th1-activated B cells preferentially produced antibody and we soon realized IFN- γ -inducible T-bet was required for ASC differentiation *in vitro*. We show unlike any other appreciated ASC specifying TFs, T-bet was dispensable for upregulation of *Prdm1*. Instead T-bet limited an IFN- γ -induced inflammatory program which was incompatible for ASC formation. While T-bet was not a global regulator of ASC

differentiation, we show that T-bet was indispensable for the development of long-lived ASC responses upon influenza infection. While these data provide a mechanism for IFN- γ -induced ASC differentiation, many questions remain. Our data indicate that perhaps like the established Th1/Th2 paradigm there may be a similar dichotomy for B cells. Is there a separable lineage-defining program for IgA or IgG2b-expressing B cells? Additionally, how might the interplay between T-bet and NF- κ B family members influence B cell fate decisions?

Our data also predicted the TF, IRF1, as a regulator for IFN- γ -induced ASC differentiation. Consistent with our prediction, IRF1 is required for the generation of early antigen-specific IgM in response to viral infection and bacterial immunization. Unexpectedly, we found that IRF1 is indispensable for the generation of innate-like MZ B cells. While IFNs can induce IRF1 expression in MZ B precursors, IFN signaling is not required for MZ B cell development. Instead we find that BCR/TLR signals, which can influence MZ B cell development, induced high expression of IRF1 in transitional B cells^{40,46,47,294,295}. IRF1 then regulates the expression of *Ptpn22*, a negative regulator of antigen receptor signaling^{208,209}. Collectively, we find an unanticipated role for BCR/TLR-induced IRF1 for the selection of MZ B cells. A long-standing question is how TLR signals may influence the primary B cell repertoire. Our data indicates that TLR signals may bestow a competitive advantage to developing, peripheral B cells. Additionally, our data suggests that dual BCR/TLR-induced IRF1 ensures the generation of an innocuous B cell repertoire. Exactly how might the redistribution of self-reactive specificities promote the development of autoimmune disease?

Lastly, we provide data that supports the use of an intranasal Ad5COVID vaccination strategy. We show that local polyfunctional T cell responses and durable RBD-specific IgG and IgA are elicited upon intranasal Ad5COVID immunization. We currently appreciate that approved vaccination strategies can induce long-lived SARS-CoV-2-specific antibody and yet we do not understand the mechanistic basis for the generation of this response, nor have we fully established how only some vaccination strategies grants longevity to ASCs. Our previous studies provide some indication that T-bet is required for the generation of long-lived antibody in response to viral infection. Furthermore, T-bet⁺ B cells have shown to be a correlate of neutralizing SARS-CoV-2-specific antibody. Thus, defining the basic underlying mechanism for the generation of durable antibody could be invaluable for informing future vaccination strategies.

GENERAL LIST OF REFERENCES

1. Manz RA, Hauser AE, Hiepe F, Radbruch A. Maintenance of serum antibody levels. *Annu Rev Immunol.* 2005;23:367-86. doi: 10.1146/annurev.immunol.23.021704.115723. PMID: 15771575.
2. Kearney JF. Innate-like B cells. *Springer Semin Immunopathol.* 2005;26(4):377-383. doi:10.1007/s00281-004-0184-0
3. Allman D, Pillai S. Peripheral B cell subsets., *Curr Opin Immunol*, 20 (2008) pp. 149-157
4. Jacob J, Kassir R, Kelsoe G. In situ studies of the primary immune response to (4-hydroxy-3-nitrophenyl)acetyl. I. The architecture and dynamics of responding cell populations. *J Exp Med.* 1991;173(5):1165-1175. doi:10.1084/jem.173.5.1165
5. Garside P, Ingulli E, Merica RR, Johnson JG, Noelle RJ, Jenkins MK. Visualization of specific B and T lymphocyte interactions in the lymph node. *Science.* 1998;281(5373):96-99. doi:10.1126/science.281.5373.96
6. Kometani K, Kurosaki T. Differentiation and maintenance of long-lived plasma cells. *Curr Opin Immunol.* (2015) 33:64–9. doi: 10.1016/j.coi.2015.01.017
7. Smith KG, Light A, Nossal GJ, Tarlinton DM. The extent of affinity maturation differs between the memory and antibody-forming cell compartments in the primary immune response. *EMBO J.* (1997) 16:2996–3006. doi: 10.1093/emboj/16.11.2996
8. Amanna IJ, Carlson NE, Slifka MK. Duration of humoral immunity to common viral and vaccine antigens. *N Engl J Med.* 2007;357(19):1903-1915. doi:10.1056/NEJMoa066092
9. Janeway CA Jr, Travers P, Walport M, et al. Immunobiology: The Immune System in Health and Disease. 5th edition. New York: Garland Science; 2001. Part V, The Immune System in Health and Disease. Available from: <https://www.ncbi.nlm.nih.gov/books/NBK10775/>
10. Nutt SL, Hodgkin PD, Tarlinton DM, Corcoran LM. The generation of antibody-secreting plasma cells. *Nat Rev Immunol.* 2015;15(3):160-171. doi:10.1038/nri3795
11. Phan TG, Paus D, Chan TD, et al. High affinity germinal center B cells are actively selected into the plasma cell compartment. *J Exp Med.* 2006;203(11):2419-2424. doi:10.1084/jem.20061254
12. Tew JG, Mandel TE, Phipps RP, Szakal AK. Tissue localization and retention of antigen in relation to the immune response. *Am J Anat.* 1984;170(3):407-420. doi:10.1002/aja.1001700314
13. Schwickert TA, Victora GD, Fooksman DR, et al. A dynamic T cell-limited checkpoint regulates affinity-dependent B cell entry into the germinal center. *J Exp Med.* 2011;208(6):1243-1252. doi:10.1084/jem.20102477
14. Koike T, Harada K, Horiuchi S, Kitamura D. The quantity of CD40 signaling determines the differentiation of B cells into functionally distinct memory cell subsets. *Elife.* 2019;8:e44245. Published 2019 Jun 21. doi:10.7554/eLife.44245
15. Rubtsova K, Rubtsov AV, van Dyk LF, Kappler JW, Marrack P. T-box transcription factor T-bet, a key player in a unique type of B-cell activation essential for effective

- viral clearance. *Proc Natl Acad Sci U S A*. 2013;110(34):E3216-E3224. doi:10.1073/pnas.1312348110
16. Barnett BE, Staupe RP, Odorizzi PM, et al. Cutting Edge: B Cell-Intrinsic T-bet Expression Is Required To Control Chronic Viral Infection. *J Immunol*. 2016;197(4):1017-1022. doi:10.4049/jimmunol.1500368
 17. Jenks SA, Cashman KS, Zumaquero E, et al. Distinct Effector B Cells Induced by Unregulated Toll-like Receptor 7 Contribute to Pathogenic Responses in Systemic Lupus Erythematosus [published correction appears in *Immunity*. 2020 Jan 14;52(1):203]. *Immunity*. 2018;49(4):725-739.e6. doi:10.1016/j.immuni.2018.08.015
 18. Rubtsova K, Marrack P, Rubtsov AV. TLR7, IFN γ , and T-bet: their roles in the development of ABCs in female-biased autoimmunity. *Cell Immunol*. 2015;294(2):80-83. doi:10.1016/j.cellimm.2014.12.002
 19. Nakayama T, Yoshimura M, Higashioka K, et al. Type 1 helper T cells generate CXCL9/10-producing T-bet⁺ effector B cells potentially involved in the pathogenesis of rheumatoid arthritis. *Cell Immunol*. 2021;360:104263. doi:10.1016/j.cellimm.2020.104263
 20. Serre K, Cunningham AF, Coughlan RE, et al. CD8 T cells induce T-bet-dependent migration toward CXCR3 ligands by differentiated B cells produced during responses to alum-protein vaccines. *Blood*. 2012;120(23):4552-4559. doi:10.1182/blood-2012-03-417733
 21. Gerth AJ, Lin L, Peng SL. T-bet regulates T-independent IgG2a class switching. *Int Immunol*. 2003;15(8):937-944. doi:10.1093/intimm/dxg093
 22. Stone SL, Peel JN, Scharer CD, et al. T-bet Transcription Factor Promotes Antibody-Secreting Cell Differentiation by Limiting the Inflammatory Effects of IFN- γ on B Cells. *Immunity*. 2019;50(5):1172-1187.e7. doi:10.1016/j.immuni.2019.04.004
 23. Flaño E, Kim IJ, Woodland DL, Blackman MA. Gamma-herpesvirus latency is preferentially maintained in splenic germinal center and memory B cells. *J Exp Med*. 2002;196(10):1363-1372. doi:10.1084/jem.20020890
 24. Jondle CN, Johnson KE, Uitenbroek AA, et al. B Cell-Intrinsic Expression of Interferon Regulatory Factor 1 Supports Chronic Murine Gammaherpesvirus 68 Infection. *J Virol*. 2020;94(13):e00399-20. Published 2020 Jun 16. doi:10.1128/JVI.00399-20
 25. Matsuyama T, Kimura T, Kitagawa M, et al. Targeted disruption of IRF-1 or IRF-2 results in abnormal type I IFN gene induction and aberrant lymphocyte development. *Cell*. 1993;75(1):83-97
 26. Slocombe T, Brown S, Miles K, Gray M, Barr TA, Gray D. Plasma cell homeostasis: the effects of chronic antigen stimulation and inflammation. *J Immunol*. 2013;191(6):3128-3138. doi:10.4049/jimmunol.1301163
 27. Slifka MK, Matloubian M, Ahmed R. Bone marrow is a major site of long-term antibody production after acute viral infection. *J Virol*. 1995;69(3):1895-1902. doi:10.1128/JVI.69.3.1895-1902.1995
 28. Hardy RR, Li YS, Allman D, Asano M, Gui M, Hayakawa K. B-cell commitment, development and selection. *Immunol Rev*. 2000;175:23-32.
 29. Hardy RR, Carmack CE, Shinton SA, Kemp JD, Hayakawa K. Resolution and characterization of pro-B and pre-pro-B cell stages in normal mouse bone marrow. *J Exp Med*. 1991;173(5):1213-1225. doi:10.1084/jem.173.5.1213
 30. Allman D, Li J, Hardy RR. Commitment to the B lymphoid lineage occurs before DH-JH recombination. *J Exp Med*. 1999;189(4):735-740. doi:10.1084/jem.189.4.735

31. Hartley SB, Crosbie J, Brink R, Kantor AB, Basten A, Goodnow CC. Elimination from peripheral lymphoid tissues of self-reactive B lymphocytes recognizing membrane-bound antigens. *Nature*. 1991;353(6346):765-769. doi:10.1038/353765a0
32. Nemazee DA, Bürki K. Clonal deletion of B lymphocytes in a transgenic mouse bearing anti-MHC class I antibody genes. *Nature*. 1989;337(6207):562-566. doi:10.1038/337562a0
33. Pelanda R, Schwers S, Sonoda E, Torres RM, Nemazee D, Rajewsky K. Receptor editing in a transgenic mouse model: site, efficiency, and role in B cell tolerance and antibody diversification. *Immunity*. 1997;7(6):765-775. doi:10.1016/s1074-7613(00)80395-7
34. Nemazee D. Mechanisms of central tolerance for B cells. *Nat Rev Immunol*. 2017;17(5):281-294. doi:10.1038/nri.2017.19
35. Allman DM, Ferguson SE, Cancro MP. Peripheral B cell maturation. I. Immature peripheral B cells in adults are heat-stable antigenhi and exhibit unique signaling characteristics. *J Immunol*. 1992;149(8):2533-2540.
36. Allman D, Lindsley RC, DeMuth W, Rudd K, Shinton SA, Hardy RR. Resolution of three nonproliferative immature splenic B cell subsets reveals multiple selection points during peripheral B cell maturation. *J Immunol*. 2001;167(12):6834-6840. doi:10.4049/jimmunol.167.12.6834
37. Wen L, Brill-Dashoff J, Shinton SA, Asano M, Hardy RR, Hayakawa K. Evidence of marginal-zone B cell-positive selection in spleen. *Immunity*. 2005;23(3):297-308. doi:10.1016/j.immuni.2005.08.007
38. Srivastava B, Quinn WJ 3rd, Hazard K, Erikson J, Allman D. Characterization of marginal zone B cell precursors. *J Exp Med*. 2005;202(9):1225-1234. doi:10.1084/jem.20051038
39. Allman D, Srivastava B, Lindsley RC. Alternative routes to maturity: branch points and pathways for generating follicular and marginal zone B cells. *Immunol Rev*. 2004;197:147-160. doi:10.1111/j.0105-2896.2004.0108.x
40. Cyster JG. Signaling thresholds and interclonal competition in preimmune B-cell selection. *Immunol Rev*. 1997;156:87-101. doi:10.1111/j.1600-065x.1997.tb00961.x
41. Lam KP, Kühn R, Rajewsky K. In vivo ablation of surface immunoglobulin on mature B cells by inducible gene targeting results in rapid cell death. *Cell*. 1997;90(6):1073-1083. doi:10.1016/s0092-8674(00)80373-6
42. Ekland EH, Forster R, Lipp M, Cyster JG. Requirements for follicular exclusion and competitive elimination of autoantigen-binding B cells. *J Immunol*. 2004;172(8):4700-4708. doi:10.4049/jimmunol.172.8.4700
43. Cyster JG, Goodnow CC. Protein tyrosine phosphatase 1C negatively regulates antigen receptor signaling in B lymphocytes and determines thresholds for negative selection. *Immunity*. 1995;2(1):13-24. doi:10.1016/1074-7613(95)90075-6
44. Casola S, Otipoby KL, Alimzhanov M, et al. B cell receptor signal strength determines B cell fate. *Nat Immunol*. 2004;5(3):317-327. doi:10.1038/ni1036
45. Pillai S, Cariappa A, Moran ST. Marginal zone B lymphocyte cells. *Annu Rev Immunol*. 2005;23:161-196. doi:10.1146/annurev.immunol.23.021704.115728
46. Martin F, Kearney JF. B-cell subsets and the mature preimmune repertoire. Marginal zone and B1 B cells as part of a "natural immune memory". *Immunol Rev*. 2000;175:70-79.

47. Martin F, Kearney JF. Positive selection from newly formed to marginal zone B cells depends on the rate of clonal production, CD19, and btk. *Immunity*. 2000;12(1):39-49. doi:10.1016/s1074-7613(00)80157-0
48. Rolink AG, Brocker T, Bluethmann H, Kosco-Vilbois MH, Andersson J, Melchers F. Mutations affecting either generation or survival of cells influence the pool size of mature B cells. *Immunity*. 1999;10(5):619-628. doi:10.1016/s1074-7613(00)80061-8
49. Turner M, Gulbranson-Judge A, Quinn ME, Walters AE, MacLennan IC, Tybulewicz VL. Syk tyrosine kinase is required for the positive selection of immature B cells into the recirculating B cell pool. *J Exp Med*. 1997;186(12):2013-2021. doi:10.1084/jem.186.12.2013
50. Torres RM, Flaswinkel H, Reth M, Rajewsky K. Aberrant B cell development and immune response in mice with a compromised BCR complex. *Science*. 1996;272(5269):1804-1808. doi:10.1126/science.272.5269.1804
51. Chen X, Martin F, Forbush KA, Perlmutter RM, Kearney JF. Evidence for selection of a population of multi-reactive B cells into the splenic marginal zone. *Int Immunol*. 1997;9(1):27-41. doi:10.1093/intimm/9.1.27
52. Martin F, Chen X, Kearney JF. Development of VH81X transgene-bearing B cells in fetus and adult: sites for expansion and deletion in conventional and CD5/B1 cells. *Int Immunol*. 1997;9(4):493-505. doi:10.1093/intimm/9.4.493
53. Silverman GJ. Protective natural autoantibodies to apoptotic cells: evidence of convergent selection of recurrent innate-like clones. *Ann N Y Acad Sci*. 2015;1362(1):164-175. doi:10.1111/nyas.12788
54. New JS, King RG, Kearney JF. Glycan Reactive Natural Antibodies and Viral Immunity. *Viral Immunol*. 2020;33(4):266-276. doi:10.1089/vim.2019.0136
55. Sigal NH, Pickard AR, Metcalf ES, Gearhart PJ, Klinman NR. Expression of phosphorylcholine-specific B cells during murine development. *J Exp Med*. 1977;146(4):933-948.
56. Fiskesund R, Steen J, Amara K, et al. Naturally occurring human phosphorylcholine antibodies are predominantly products of affinity-matured B cells in the adult. *J Immunol*. 2014;192(10):4551-4559. doi:10.4049/jimmunol.1303035
57. Storb U, Pinkert C, Arp B, et al. Transgenic mice with mu and kappa genes encoding antiphosphorylcholine antibodies. *J Exp Med*. 1986;164(2):627-641. doi:10.1084/jem.164.2.627
58. Nemazee D. Mechanisms of central tolerance for B cells. *Nat Rev Immunol*. 2017;17(5):281-294. doi:10.1038/nri.2017.19
59. Goodnow CC, Crosbie J, Adelstein S, et al. Altered immunoglobulin expression and functional silencing of self-reactive B lymphocytes in transgenic mice. *Nature*. 1988;334(6184):676-682. doi:10.1038/334676a0
60. Cyster JG, Hartley SB, Goodnow CC. Competition for follicular niches excludes self-reactive cells from the recirculating B-cell repertoire. *Nature*. 1994;371(6496):389-395. doi:10.1038/371389a0
61. Berland R, Wortis HH. Origins and functions of B-1 cells with notes on the role of CD5. *Annu Rev Immunol*. 2002;20:253-300.
62. Pillai S, Cariappa A. The follicular versus marginal zone B lymphocyte cell fate decision. *Nat Rev Immunol*. 2009;9(11):767-777. doi:10.1038/nri2656
63. Hardy RR, Hayakawa K, Parks DR, Herzenberg LA. Demonstration of B-cell maturation in X-linked immunodeficient mice by simultaneous three-colour immunofluorescence. *Nature*. 1983;306(5940):270-272. doi:10.1038/306270a0

64. Justement LB, Campbell KS, Chien NC, Cambier JC. Regulation of B cell antigen receptor signal transduction and phosphorylation by CD45. *Science*. 1991;252(5014):1839-1842.
65. Cyster JG, Healy JI, Kishihara K, Mak TW, Thomas ML, Goodnow CC. Regulation of B-lymphocyte negative and positive selection by tyrosine phosphatase CD45. *Nature*. 1996;381(6580):325-328. doi:10.1038/381325a0
66. Goodnow CC, Brink R, Adams E. Breakdown of self-tolerance in anergic B lymphocytes. *Nature*. 1991;352(6335):532-536. doi:10.1038/352532a0
67. Lesley R, Xu Y, Kalled SL, et al. Reduced competitiveness of autoantigen-engaged B cells due to increased dependence on BAFF. *Immunity*. 2004;20(4):441-453. doi:10.1016/s1074-7613(04)00079-2
68. Rawlings DJ, Metzler G, Wray-Dutra M, Jackson SW. Altered B cell signalling in autoimmunity. *Nat Rev Immunol*. 2017;17(7):421-436. doi:10.1038/nri.2017.24
69. Pillai S. The chosen few? Positive selection and the generation of naive B lymphocytes. *Immunity*. 1999;10(5):493-502. doi:10.1016/s1074-7613(00)80049-7
70. Hayakawa K, Hardy RR, Parks DR, Herzenberg LA. The "Ly-1 B" cell subpopulation in normal immunodeficient, and autoimmune mice. *J Exp Med*. 1983;157(1):202-218. doi:10.1084/jem.157.1.202
71. Benedict CL, Kearney JF. Increased junctional diversity in fetal B cells results in a loss of protective anti-phosphorylcholine antibodies in adult mice. *Immunity*. 1999;10(5):607-617. doi:10.1016/s1074-7613(00)80060-6
72. Marshall AJ, Doyen N, Bentolila LA, Paige CJ, Wu GE. Terminal deoxynucleotidyl transferase expression during neonatal life alters D(H) reading frame usage and Ig-receptor-dependent selection of V regions. *J Immunol*. 1998;161(12):6657-6663.
73. New JS, King RG, Kearney JF. Glycan Reactive Natural Antibodies and Viral Immunity. *Viral Immunol*. 2020;33(4):266-276. doi:10.1089/vim.2019.0136
74. Yang Y, Wang C, Yang Q, et al. Distinct mechanisms define murine B cell lineage immunoglobulin heavy chain (IgH) repertoires. *Elife*. 2015;4:e09083. Published 2015 Sep 30. doi:10.7554/eLife.09083
75. Bos NA, Kimura H, Meeuwse CG, et al. Serum immunoglobulin levels and naturally occurring antibodies against carbohydrate antigens in germ-free BALB/c mice fed chemically defined ultrafiltered diet. *Eur J Immunol*. 1989;19(12):2335-2339. doi:10.1002/eji.1830191223
76. Haury M, Sundblad A, Grandien A, Barreau C, Coutinho A, Nobrega A. The repertoire of serum IgM in normal mice is largely independent of external antigenic contact. *Eur J Immunol*. 1997;27(6):1557-1563. doi:10.1002/eji.1830270635
77. Hooijkaas H, Benner R, Pleasants JR, Wostmann BS. Isotypes and specificities of immunoglobulins produced by germ-free mice fed chemically defined ultrafiltered "antigen-free" diet. *Eur J Immunol*. 1984;14(12):1127-1130. doi:10.1002/eji.1830141212
78. Won WJ, Kearney JF. CD9 is a unique marker for marginal zone B cells, B1 cells, and plasma cells in mice. *J Immunol*. 2002;168(11):5605-5611. doi:10.4049/jimmunol.168.11.5605
79. Won WJ, Bachmann MF, Kearney JF. CD36 is differentially expressed on B cell subsets during development and in responses to antigen. *J Immunol*. 2008;180(1):230-237. doi:10.4049/jimmunol.180.1.230
80. Pan C, Baumgarth N, Parnes JR. CD72-deficient mice reveal nonredundant roles of CD72 in B cell development and activation. *Immunity*. 1999;11(4):495-506. doi:10.1016/s1074-7613(00)80124-7

81. Haas KM, Johnson KL, Phipps JP, Do C. CD22 Promotes B-1b Cell Responses to T Cell-Independent Type 2 Antigens. *J Immunol.* 2018;200(5):1671-1681. doi:10.4049/jimmunol.1701578
82. Waffarn EE, Hastey CJ, Dixit N, et al. Infection-induced type I interferons activate CD11b on B-1 cells for subsequent lymph node accumulation. *Nat Commun.* 2015;6:8991. Published 2015 Nov 27. doi:10.1038/ncomms9991
83. Allard D, Charlebois R, Gilbert L, Stagg J, Chrobak P. CD73-A2a adenosine receptor axis promotes innate B cell antibody responses to pneumococcal polysaccharide vaccination. *PLoS One.* 2018;13(1):e0191973. Published 2018 Jan 29. doi:10.1371/journal.pone.0191973
84. Gu H, Tarlinton D, Müller W, Rajewsky K, Förster I. Most peripheral B cells in mice are ligand selected. *J Exp Med.* 1991;173(6):1357-1371. doi:10.1084/jem.173.6.1357
85. Mebius RE, Kraal G. Structure and function of the spleen. *Nat Rev Immunol.* 2005;5(8):606-616. doi:10.1038/nri1669
86. Amano M, Baumgarth N, Dick MD, et al. CD1 expression defines subsets of follicular and marginal zone B cells in the spleen: beta 2-microglobulin-dependent and independent forms. *J Immunol.* 1998;161(4):1710-1717.
87. Cerutti A, Cols M, Puga I. Marginal zone B cells: virtues of innate-like antibody-producing lymphocytes. *Nat Rev Immunol.* 2013;13(2):118-132. doi:10.1038/nri3383
88. Attanavanich K, Kearney JF. Marginal zone, but not follicular B cells, are potent activators of naive CD4 T cells. *J Immunol.* 2004;172(2):803-811. doi:10.4049/jimmunol.172.2.803
89. Tull TJ, Pitcher MJ, Guesdon W, et al. Human marginal zone B cell development from early T2 progenitors. *J Exp Med.*
90. Takeuchi T, Nakagawa T, Maeda Y, et al. Functional defect of B lymphocytes in a patient with selective IgM deficiency associated with systemic lupus erythematosus. *Autoimmunity.* 2001;34(2):115-122. doi:10.3109/08916930109001959
91. Saito T, Chiba S, Ichikawa M, et al. Notch2 is preferentially expressed in mature B cells and indispensable for marginal zone B lineage development. *Immunity.* 2003;18(5):675-685. doi:10.1016/s1074-7613(03)00111-0
92. Kuroda K, Han H, Tani S, et al. Regulation of marginal zone B cell development by MINT, a suppressor of Notch/RBP-J signaling pathway. *Immunity.* 2003;18(2):301-312. doi:10.1016/s1074-7613(03)00029-3
93. Tanigaki K, Han H, Yamamoto N, et al. Notch-RBP-J signaling is involved in cell fate determination of marginal zone B cells. *Nat Immunol.* 2002;3(5):443-450. doi:10.1038/ni793
94. Cariappa A, Tang M, Parng C, et al. The follicular versus marginal zone B lymphocyte cell fate decision is regulated by Aiolos, Btk, and CD21. *Immunity.* 2001;14(5):603-615. doi:10.1016/s1074-7613(01)00135-2
95. Hammad H, Vanderkerken M, Pouliot P, et al. Transitional B cells commit to marginal zone B cell fate by Taok3-mediated surface expression of ADAM10. *Nat Immunol.* 2017;18(3):313-320. doi:10.1038/ni.3657
96. Iwahashi S, Maekawa Y, Nishida J, et al. Notch2 regulates the development of marginal zone B cells through Fos. *Biochem Biophys Res Commun.* 2012;418(4):701-707. doi:10.1016/j.bbrc.2012.01.082

97. Yamashita K, Sakamoto A, Ohkubo Y, et al. c-fos overexpression in splenic B cells augments development of marginal zone B cells. *Mol Immunol.* 2005;42(5):617-625. doi:10.1016/j.molimm.2004.09.011
98. Gavin AL, Hoebe K, Duong B, et al. Adjuvant-enhanced antibody responses in the absence of toll-like receptor signaling. *Science.* 2006;314(5807):1936-1938. doi:10.1126/science.1135299
99. Silver K, Ferry H, Crockford T, Cornall RJ. TLR4, TLR9 and MyD88 are not required for the positive selection of autoreactive B cells into the primary repertoire. *Eur J Immunol.* 2006;36(6):1404-1412. doi:10.1002/eji.200636019
100. You Y, Myers RC, Freeberg L, et al. Marginal zone B cells regulate antigen capture by marginal zone macrophages. *J Immunol.* 2011;186(4):2172-2181. doi:10.4049/jimmunol.1002106
101. Lanoue A, Clatworthy MR, Smith P, et al. SIGN-R1 contributes to protection against lethal pneumococcal infection in mice. *J Exp Med.* 2004;200(11):1383-1393. doi:10.1084/jem.20040795
102. Kang YS, Do Y, Lee HK, et al. A dominant complement fixation pathway for pneumococcal polysaccharides initiated by SIGN-R1 interacting with C1q. *Cell.* 2006;125(1):47-58. doi:10.1016/j.cell.2006.01.046
103. You Y, Zhao H, Wang Y, Carter RH. Cutting edge: Primary and secondary effects of CD19 deficiency on cells of the marginal zone. *J Immunol.* 2009;182(12):7343-7347. doi:10.4049/jimmunol.0804295
104. Lu TT, Cyster JG. Integrin-mediated long-term B cell retention in the splenic marginal zone. *Science.* 2002;297(5580):409-412. doi:10.1126/science.1071632
105. Cinamon G, Matloubian M, Lesneski MJ, et al. Sphingosine 1-phosphate receptor 1 promotes B cell localization in the splenic marginal zone. *Nat Immunol.* 2004;5(7):713-720. doi:10.1038/ni1083
106. Tedford K, Steiner M, Koshutin S, et al. The opposing forces of shear flow and sphingosine-1-phosphate control marginal zone B cell shuttling. *Nat Commun.* 2017;8(1):2261. Published 2017 Dec 22. doi:10.1038/s41467-017-02482-4
107. Sixt M, Kanazawa N, Selg M, et al. The conduit system transports soluble antigens from the afferent lymph to resident dendritic cells in the T cell area of the lymph node. *Immunity.* 2005;22(1):19-29. doi:10.1016/j.immuni.2004.11.013
108. Gretz JE, Norbury CC, Anderson AO, Proudfoot AE, Shaw S. Lymph-borne chemokines and other low molecular weight molecules reach high endothelial venules via specialized conduits while a functional barrier limits access to the lymphocyte microenvironments in lymph node cortex. *J Exp Med.* 2000;192(10):1425-1440. doi:10.1084/jem.192.10.1425
109. Carrasco YR, Batista FD. B cells acquire particulate antigen in a macrophage-rich area at the boundary between the follicle and the subcapsular sinus of the lymph node. *Immunity.* 2007;27(1):160-171. doi:10.1016/j.immuni.2007.06.007
110. Berney C, Herren S, Power CA, Gordon S, Martinez-Pomares L, Kosco-Vilbois MH. A member of the dendritic cell family that enters B cell follicles and stimulates primary antibody responses identified by a mannose receptor fusion protein. *J Exp Med.* 1999;190(6):851-860. doi:10.1084/jem.190.6.851
111. Colino J, Shen Y, Snapper CM. Dendritic cells pulsed with intact *Streptococcus pneumoniae* elicit both protein- and polysaccharide-specific immunoglobulin isotype responses in vivo through distinct mechanisms. *J Exp Med.* 2002;195(1):1-13. doi:10.1084/jem.20011432

112. Ferguson AR, Youd ME, Corley RB. Marginal zone B cells transport and deposit IgM-containing immune complexes onto follicular dendritic cells. *Int Immunol.* 2004;16(10):1411-1422. doi:10.1093/intimm/dxh142
113. Roco JA, Mesin L, Binder SC, et al. Class-Switch Recombination Occurs Infrequently in Germinal Centers. *Immunity.* 2019;51(2):337-350.e7. doi:10.1016/j.immuni.2019.07.001
114. Matsuoka M, Yoshida K, Maeda T, Usuda S, Sakano H. Switch circular DNA formed in cytokine-treated mouse splenocytes: evidence for intramolecular DNA deletion in immunoglobulin class switching. *Cell.* 1990;62(1):135-142. doi:10.1016/0092-8674(90)90247-c
115. Park SR, Seo GY, Choi AJ, Stavnezer J, Kim PH. Analysis of transforming growth factor-beta1-induced Ig germ-line gamma2b transcription and its implication for IgA isotype switching. *Eur J Immunol.* 2005;35(3):946-956. doi:10.1002/eji.200425848
116. Wagner SD, Neuberger MS. Somatic hypermutation of immunoglobulin genes. *Annu Rev Immunol.* 1996;14:441-457. doi:10.1146/annurev.immunol.14.1.441
117. Muramatsu M, Kinoshita K, Fagarasan S, Yamada S, Shinkai Y, Honjo T. Class switch recombination and hypermutation require activation-induced cytidine deaminase (AID), a potential RNA editing enzyme. *Cell.* 2000;102(5):553-563. doi:10.1016/s0092-8674(00)00078-7
118. Kometani K, Nakagawa R, Shinnakasu R, et al. Repression of the transcription factor Bach2 contributes to predisposition of IgG1 memory B cells toward plasma cell differentiation. *Immunity.* 2013;39(1):136-147. doi:10.1016/j.immuni.2013.06.011
119. Paus D, Phan TG, Chan TD, Gardam S, Basten A, Brink R. Antigen recognition strength regulates the choice between extrafollicular plasma cell and germinal center B cell differentiation. *J Exp Med.* 2006;203(4):1081-1091. doi:10.1084/jem.20060087
120. Jacob J, Przylepa J, Miller C, Kelsoe G. In situ studies of the primary immune response to (4-hydroxy-3-nitrophenyl)acetyl. III. The kinetics of V region mutation and selection in germinal center B cells. *J Exp Med.* 1993;178(4):1293-1307. doi:10.1084/jem.178.4.1293
121. Takahashi Y, Dutta PR, Cerasoli DM, Kelsoe G. In situ studies of the primary immune response to (4-hydroxy-3-nitrophenyl)acetyl. V. Affinity maturation develops in two stages of clonal selection. *J Exp Med.* 1998;187(6):885-895. doi:10.1084/jem.187.6.885
122. Smith KG, Light A, Nossal GJ, Tarlinton DM. The extent of affinity maturation differs between the memory and antibody-forming cell compartments in the primary immune response. *EMBO J.* 1997;16(11):2996-3006. doi:10.1093/emboj/16.11.2996
123. Blink EJ, Light A, Kallies A, Nutt SL, Hodgkin PD, Tarlinton DM. Early appearance of germinal center-derived memory B cells and plasma cells in blood after primary immunization. *J Exp Med.* 2005;201(4):545-554. doi:10.1084/jem.20042060
124. Obukhanych TV, Nussenzweig MC. T-independent type II immune responses generate memory B cells. *J Exp Med.* 2006;203(2):305-310. doi:10.1084/jem.20052036
125. Weisel FJ, Zuccarino-Catania GV, Chikina M, Shlomchik MJ. A Temporal Switch in the Germinal Center Determines Differential Output of Memory B and Plasma Cells. *Immunity.* 2016;44(1):116-130. doi:10.1016/j.immuni.2015.12.004

126. Bortnick A, Chernova I, Quinn WJ 3rd, Mugnier M, Cancro MP, Allman D. Long-lived bone marrow plasma cells are induced early in response to T cell-independent or T cell-dependent antigens. *J Immunol.* 2012;188(11):5389-5396. doi:10.4049/jimmunol.1102808
127. Bortnick A, Allman D. What is and what should always have been: long-lived plasma cells induced by T cell-independent antigens. *J Immunol.* 2013;190(12):5913-5918. doi:10.4049/jimmunol.1300161
128. Oldfield S, Jenkins S, Yeoman H, Gray D, MacLennan IC. Class and subclass anti-pneumococcal antibody responses in splenectomized patients. *Clin Exp Immunol.* 1985;61(3):664-673.
129. Oldfield S, Jenkins S, Yeoman H, Gray D, MacLennan IC. Class and subclass anti-pneumococcal antibody responses in splenectomized patients. *Clin Exp Immunol.* 1985;61(3):664-673.
130. Slifka MK, Antia R, Whitmire JK, Ahmed R. Humoral immunity due to long-lived plasma cells. *Immunity.* 1998;8(3):363-372. doi:10.1016/s1074-7613(00)80541-5
131. Yeung YA, Foletti D, Deng X, et al. Germline-encoded neutralization of a Staphylococcus aureus virulence factor by the human antibody repertoire. *Nat Commun.* 2016;7:13376. Published 2016 Nov 18. doi:10.1038/ncomms13376
132. Ju B, Zhang Q, Ge J, et al. Human neutralizing antibodies elicited by SARS-CoV-2 infection. *Nature.* 2020;584(7819):115-119. doi:10.1038/s41586-020-2380-z
133. Lee BO, Rangel-Moreno J, Moyron-Quiroz JE, et al. CD4 T cell-independent antibody response promotes resolution of primary influenza infection and helps to prevent reinfection. *J Immunol.* 2005;175(9):5827-5838. doi:10.4049/jimmunol.175.9.5827
134. Baumgarth N, Herman OC, Jager GC, Brown L, Herzenberg LA, Herzenberg LA. Innate and acquired humoral immunities to influenza virus are mediated by distinct arms of the immune system. *Proc Natl Acad Sci U S A.* 1999;96(5):2250-2255. doi:10.1073/pnas.96.5.2250
135. Baumgarth N, Herman OC, Jager GC, Brown LE, Herzenberg LA, Chen J. B-1 and B-2 cell-derived immunoglobulin M antibodies are nonredundant components of the protective response to influenza virus infection. *J Exp Med.* 2000;192(2):271-280. doi:10.1084/jem.192.2.271
136. Choi YS, Baumgarth N. Dual role for B-1a cells in immunity to influenza virus infection. *J Exp Med.* 2008;205(13):3053-3064. doi:10.1084/jem.20080979
137. Nussenzweig V, Benacerraf B. Antihapten antibody specificity and L chain type. *J Exp Med.* 1967;126(4):727-743. doi:10.1084/jem.126.4.727
138. Victora GD, Nussenzweig MC. Germinal centers. *Annu Rev Immunol.* 2012;30:429-457. doi:10.1146/annurev-immunol-020711-075032
139. Paweletz N. Walther Flemming: pioneer of mitosis research. *Nat Rev Mol Cell Biol.* 2001;2(1):72-75. doi:10.1038/35048077
140. Nieuwenhuis P, Opstelten D. Functional anatomy of germinal centers. *Am J Anat.* 1984;170(3):421-435. doi:10.1002/aja.1001700315
141. Hannum LG, Haberman AM, Anderson SM, Shlomchik MJ. Germinal center initiation, variable gene region hypermutation, and mutant B cell selection without detectable immune complexes on follicular dendritic cells. *J Exp Med.* 2000;192(7):931-942. doi:10.1084/jem.192.7.931

142. Wu X, Jiang N, Fang YF, et al. Impaired affinity maturation in Cr2^{-/-} mice is rescued by adjuvants without improvement in germinal center development. *J Immunol.* 2000;165(6):3119-3127. doi:10.4049/jimmunol.165.6.3119
143. Chen Z, Koralov SB, Gendelman M, Carroll MC, Kelsoe G. Humoral immune responses in Cr2^{-/-} mice: enhanced affinity maturation but impaired antibody persistence. *J Immunol.* 2000;164(9):4522-4532. doi:10.4049/jimmunol.164.9.4522
144. Victora GD, Schwickert TA, Fooksman DR, et al. Germinal center dynamics revealed by multiphoton microscopy with a photoactivatable fluorescent reporter. *Cell.* 2010;143(4):592-605. doi:10.1016/j.cell.2010.10.032
145. Gitlin AD, Shulman Z, Nussenzweig MC. Clonal selection in the germinal centre by regulated proliferation and hypermutation. *Nature.* 2014;509(7502):637-640. doi:10.1038/nature13300
146. Tas JM, Mesin L, Pasqual G, et al. Visualizing antibody affinity maturation in germinal centers. *Science.* 2016;351(6277):1048-1054. doi:10.1126/science.aad3439
147. Schwickert TA, Lindquist RL, Shakhar G, et al. In vivo imaging of germinal centres reveals a dynamic open structure. *Nature.* 2007;446(7131):83-87. doi:10.1038/nature05573
148. Batista FD, Iber D, Neuberger MS. B cells acquire antigen from target cells after synapse formation. *Nature.* 2001;411(6836):489-494. doi:10.1038/35078099
149. Ersching J, Efeyan A, Mesin L, et al. Germinal Center Selection and Affinity Maturation Require Dynamic Regulation of mTORC1 Kinase. *Immunity.* 2017;46(6):1045-1058.e6. doi:10.1016/j.immuni.2017.06.005
150. Liu YJ, Joshua DE, Williams GT, Smith CA, Gordon J, MacLennan IC. Mechanism of antigen-driven selection in germinal centres. *Nature.* 1989;342(6252):929-931. doi:10.1038/342929a0
151. Han S, Hathcock K, Zheng B, Kepler TB, Hodes R, Kelsoe G. Cellular interaction in germinal centers. Roles of CD40 ligand and B7-2 in established germinal centers. *J Immunol.* 1995;155(2):556-567.
152. Zotos D, Coquet JM, Zhang Y, et al. IL-21 regulates germinal center B cell differentiation and proliferation through a B cell-intrinsic mechanism. *J Exp Med.* 2010;207(2):365-378. doi:10.1084/jem.20091777
153. Linterman MA, Beaton L, Yu D, et al. IL-21 acts directly on B cells to regulate Bcl-6 expression and germinal center responses. *J Exp Med.* 2010;207(2):353-363. doi:10.1084/jem.20091738
154. Rolf J, Bell SE, Kovesdi D, et al. Phosphoinositide 3-kinase activity in T cells regulates the magnitude of the germinal center reaction. *J Immunol.* 2010;185(7):4042-4052. doi:10.4049/jimmunol.1001730
155. Bachmann MF, Odermatt B, Hengartner H, Zinkernagel RM. Induction of long-lived germinal centers associated with persisting antigen after viral infection. *J Exp Med.* 1996;183(5):2259-2269. doi:10.1084/jem.183.5.2259
156. Smith KG, Light A, Nossal GJ, Tarlinton DM. The extent of affinity maturation differs between the memory and antibody-forming cell compartments in the primary immune response. *EMBO J.* 1997;16(11):2996-3006. doi:10.1093/emboj/16.11.2996
157. Zhang Y, Meyer-Hermann M, George LA, et al. Germinal center B cells govern their own fate via antibody feedback. *J Exp Med.* 2013;210(3):457-464. doi:10.1084/jem.20120150

158. Meffre E, Catalan N, Seltz F, Fischer A, Nussenzweig MC, Durandy A. Somatic hypermutation shapes the antibody repertoire of memory B cells in humans. *J Exp Med*. 2001;194(3):375-378. doi:10.1084/jem.194.3.375
159. Taylor JJ, Pape KA, Jenkins MK. A germinal center-independent pathway generates unswitched memory B cells early in the primary response. *J Exp Med*. 2012;209(3):597-606. doi:10.1084/jem.20111696
160. Dogan I, Bertocci B, Vilmont V, et al. Multiple layers of B cell memory with different effector functions. *Nat Immunol*. 2009;10(12):1292-1299. doi:10.1038/ni.1814
161. Weisel F, Shlomchik M. Memory B Cells of Mice and Humans. *Annu Rev Immunol*. 2017;35:255-284. doi:10.1146/annurev-immunol-041015-055531
162. Toyama H, Okada S, Hatano M, et al. Memory B cells without somatic hypermutation are generated from Bcl6-deficient B cells. *Immunity*. 2002;17(3):329-339. doi:10.1016/s1074-7613(02)00387-4
163. Suan D, Kräutler NJ, Maag JLV, et al. CCR6 Defines Memory B Cell Precursors in Mouse and Human Germinal Centers, Revealing Light-Zone Location and Predominant Low Antigen Affinity. *Immunity*. 2017;47(6):1142-1153.e4. doi:10.1016/j.immuni.2017.11.022
164. Elgueta R, Marks E, Nowak E, et al. CCR6-dependent positioning of memory B cells is essential for their ability to mount a recall response to antigen. *J Immunol*. 2015;194(2):505-513. doi:10.4049/jimmunol.1401553
165. Smith KG, Weiss U, Rajewsky K, Nossal GJ, Tarlinton DM. Bcl-2 increases memory B cell recruitment but does not perturb selection in germinal centers. *Immunity*. 1994;1(9):803-813. doi:10.1016/s1074-7613(94)80022-7
166. Ozaki K, Spolski R, Feng CG, et al. A critical role for IL-21 in regulating immunoglobulin production. *Science*. 2002;298(5598):1630-1634. doi:10.1126/science.1077002
167. Allen RC, Armitage RJ, Conley ME, et al. CD40 ligand gene defects responsible for X-linked hyper-IgM syndrome. *Science*. 1993;259(5097):990-993. doi:10.1126/science.7679801
168. Lee BO, Rangel-Moreno J, Moyron-Quiroz JE, et al. CD4 T cell-independent antibody response promotes resolution of primary influenza infection and helps to prevent reinfection. *J Immunol*. 2005;175(9):5827-5838. doi:10.4049/jimmunol.175.9.5827
169. Ahonen C, Manning E, Erickson LD, et al. The CD40-TRAF6 axis controls affinity maturation and the generation of long-lived plasma cells. *Nat Immunol*. 2002;3(5):451-456. doi:10.1038/ni792
170. Jourdan M, Cren M, Robert N, et al. IL-6 supports the generation of human long-lived plasma cells in combination with either APRIL or stromal cell-soluble factors. *Leukemia*. 2014;28(8):1647-1656. doi:10.1038/leu.2014.61
171. Kawano MM, Mihara K, Huang N, Tsujimoto T, Kuramoto A. Differentiation of early plasma cells on bone marrow stromal cells requires interleukin-6 for escaping from apoptosis. *Blood*. 1995;85(2):487-494.
172. Tellier J. BAFF bestows longevity on splenic plasma cells. *Blood*. 2018;131(14):1500-1501. doi:10.1182/blood-2018-02-832089
173. Ise W, Kohyama M, Schraml BU, et al. The transcription factor BATF controls the global regulators of class-switch recombination in both B cells and T cells. *Nat Immunol*. 2011;12(6):536-543. doi:10.1038/ni.2037

174. Sciammas R, Shaffer AL, Schatz JH, Zhao H, Staudt LM, Singh H. Graded expression of interferon regulatory factor-4 coordinates isotype switching with plasma cell differentiation. *Immunity*. 2006;25(2):225-236. doi:10.1016/j.immuni.2006.07.009
175. Ochiai K, Maienschein-Cline M, Simonetti G, et al. Transcriptional regulation of germinal center B and plasma cell fates by dynamical control of IRF4. *Immunity*. 2013;38(5):918-929. doi:10.1016/j.immuni.2013.04.009
176. Willis SN, Good-Jacobson KL, Curtis J, et al. Transcription factor IRF4 regulates germinal center cell formation through a B cell-intrinsic mechanism. *J Immunol*. 2014;192(7):3200-3206. doi:10.4049/jimmunol.1303216
177. Lin KI, Angelin-Duclos C, Kuo TC, Calame K. Blimp-1-dependent repression of Pax-5 is required for differentiation of B cells to immunoglobulin M-secreting plasma cells. *Mol Cell Biol*. 2002;22(13):4771-4780. doi:10.1128/MCB.22.13.4771-4780.2002
178. Shaffer AL, Lin KI, Kuo TC, et al. Blimp-1 orchestrates plasma cell differentiation by extinguishing the mature B cell gene expression program. *Immunity*. 2002;17(1):51-62. doi:10.1016/s1074-7613(02)00335-7
179. Kallies A, Hasbold J, Tarlinton DM, et al. Plasma cell ontogeny defined by quantitative changes in blimp-1 expression. *J Exp Med*. 2004;200(8):967-977. doi:10.1084/jem.20040973
180. Savage HP, Yenson VM, Sawhney SS, Mousseau BJ, Lund FE, Baumgarth N. Blimp-1-dependent and -independent natural antibody production by B-1 and B-1-derived plasma cells. *J Exp Med*. 2017;214(9):2777-2794. doi:10.1084/jem.20161122
181. Todd DJ, McHeyzer-Williams LJ, Kowal C, et al. XBP1 governs late events in plasma cell differentiation and is not required for antigen-specific memory B cell development. *J Exp Med*. 2009;206(10):2151-2159. doi:10.1084/jem.20090738
182. Shinnakasu R, Inoue T, Kometani K, et al. Regulated selection of germinal-center cells into the memory B cell compartment. *Nat Immunol*. 2016;17(7):861-869. doi:10.1038/ni.3460
183. Laidlaw BJ, Duan L, Xu Y, Vazquez SE, Cyster JG. The transcription factor Hhex cooperates with the corepressor Tle3 to promote memory B cell development. *Nat Immunol*. 2020;21(9):1082-1093. doi:10.1038/s41590-020-0713-6
184. Woyach JA, Johnson AJ, Byrd JC. The B-cell receptor signaling pathway as a therapeutic target in CLL. *Blood*. 2012;120(6):1175-1184. doi:10.1182/blood-2012-02-362624
185. Rolli V, Gallwitz M, Wossning T, et al. Amplification of B cell antigen receptor signaling by a Syk/ITAM positive feedback loop. *Mol Cell*. 2002;10(5):1057-1069. doi:10.1016/s1097-2765(02)00739-6
186. Yamamoto T, Yamanashi Y, Toyoshima K. Association of Src-family kinase Lyn with B-cell antigen receptor. *Immunol Rev*. 1993;132:187-206. doi:10.1111/j.1600-065x.1993.tb00843.x
187. Smith KG, Tarlinton DM, Doody GM, Hibbs ML, Fearon DT. Inhibition of the B cell by CD22: a requirement for Lyn. *J Exp Med*. 1998;187(5):807-811. doi:10.1084/jem.187.5.807
188. Adachi T, Flaswinkel H, Yakura H, Reth M, Tsubata T. The B cell surface protein CD72 recruits the tyrosine phosphatase SHP-1 upon tyrosine phosphorylation. *J Immunol*. 1998;160(10):4662-4665.

189. Bikah G, Carey J, Ciallella JR, Tarakhovsky A, Bondada S. CD5-mediated negative regulation of antigen receptor-induced growth signals in B-1 B cells. *Science*. 1996;274(5294):1906-1909. doi:10.1126/science.274.5294.1906
190. Ono M, Bolland S, Tempst P, Ravetch JV. Role of the inositol phosphatase SHIP in negative regulation of the immune system by the receptor Fc(gamma)RIIB. *Nature*. 1996;383(6597):263-266. doi:10.1038/383263a0
191. Scharenberg AM, El-Hillal O, Fruman DA, et al. Phosphatidylinositol-3,4,5-trisphosphate (PtdIns-3,4,5-P3)/Tec kinase-dependent calcium signaling pathway: a target for SHIP-mediated inhibitory signals. *EMBO J*. 1998;17(7):1961-1972. doi:10.1093/emboj/17.7.1961
192. Alsadeq A, Hobeika E, Medgyesi D, Kläsener K, Reth M. The role of the Syk/Shp-1 kinase-phosphatase equilibrium in B cell development and signaling. *J Immunol*. 2014;193(1):268-276. doi:10.4049/jimmunol.1203040
193. Penninger JM, Sirard C, Mittrücker HW, et al. The interferon regulatory transcription factor IRF-1 controls positive and negative selection of CD8+ thymocytes. *Immunity*. 1997;7(2):243-254. doi:10.1016/s1074-7613(00)80527-0
194. Dolmetsch RE, Lewis RS, Goodnow CC, Healy JI. Differential activation of transcription factors induced by Ca²⁺ response amplitude and duration [published correction appears in *Nature* 1997 Jul 17;388(6639):308]. *Nature*. 1997;386(6627):855-858. doi:10.1038/386855a0
195. DeFranco AL, Chan VW, Lowell CA. Positive and negative roles of the tyrosine kinase Lyn in B cell function. *Semin Immunol*. 1998;10(4):299-307. doi:10.1006/smim.1998.0122
196. Gross AJ, Proekt I, DeFranco AL. Elevated BCR signaling and decreased survival of Lyn-deficient transitional and follicular B cells. *Eur J Immunol*. 2011;41(12):3645-3655. doi:10.1002/eji.201141708
197. Lamagna C, Hu Y, DeFranco AL, Lowell CA. B cell-specific loss of Lyn kinase leads to autoimmunity. *J Immunol*. 2014;192(3):919-928. doi:10.4049/jimmunol.1301979
198. Kil LP, de Bruijn MJ, van Nimwegen M, et al. Btk levels set the threshold for B-cell activation and negative selection of autoreactive B cells in mice. *Blood*. 2012;119(16):3744-3756. doi:10.1182/blood-2011-12-397919
199. Crofford LJ, Nyhoff LE, Sheehan JH, Kendall PL. The role of Bruton's tyrosine kinase in autoimmunity and implications for therapy. *Expert Rev Clin Immunol*. 2016;12(7):763-773. doi:10.1586/1744666X.2016.1152888
200. Conley ME. B cells in patients with X-linked agammaglobulinemia. *J Immunol*. 1985;134(5):3070-3074.
201. Ng YS, Wardemann H, Chelnis J, Cunningham-Rundles C, Meffre E. Bruton's tyrosine kinase is essential for human B cell tolerance. *J Exp Med*. 2004;200(7):927-934. doi:10.1084/jem.20040920
202. Burn GL, Svensson L, Sanchez-Blanco C, Saini M, Cope AP. Why is PTPN22 a good candidate susceptibility gene for autoimmune disease?. *FEBS Lett*. 2011;585(23):3689-3698. doi:10.1016/j.febslet.2011.04.032
203. Begovich AB, Carlton VE, Honigberg LA, et al. A missense single-nucleotide polymorphism in a gene encoding a protein tyrosine phosphatase (PTPN22) is associated with rheumatoid arthritis. *Am J Hum Genet*. 2004;75(2):330-337. doi:10.1086/422827

204. Bottini N, Musumeci L, Alonso A, et al. A functional variant of lymphoid tyrosine phosphatase is associated with type I diabetes. *Nat Genet.* 2004;36(4):337-338. doi:10.1038/ng1323
205. Kyogoku C, Langefeld CD, Ortmann WA, et al. Genetic association of the R620W polymorphism of protein tyrosine phosphatase PTPN22 with human SLE. *Am J Hum Genet.* 2004;75(3):504-507. doi:10.1086/423790
206. Habib T, Funk A, Rieck M, et al. Altered B cell homeostasis is associated with type I diabetes and carriers of the PTPN22 allelic variant. *J Immunol.* 2012;188(1):487-496. doi:10.4049/jimmunol.1102176
207. Menard L, Saadoun D, Isnardi I, et al. The PTPN22 allele encoding an R620W variant interferes with the removal of developing autoreactive B cells in humans. *J Clin Invest.* 2011;121(9):3635-3644. doi:10.1172/JCI45790
208. Metzler G, Dai X, Thouvenel CD, et al. The Autoimmune Risk Variant PTPN22 C1858T Alters B Cell Tolerance at Discrete Checkpoints and Differentially Shapes the Naive Repertoire. *J Immunol.* 2017;199(7):2249-2260. doi:10.4049/jimmunol.1700601
209. Hasegawa K, Martin F, Huang G, Tumas D, Diehl L, Chan AC. PEST domain-enriched tyrosine phosphatase (PEP) regulation of effector/memory T cells. *Science.* 2004;303(5658):685-689. doi:10.1126/science.1092138
210. Hua Z, Hou B. TLR signaling in B-cell development and activation. *Cell Mol Immunol.* 2013;10(2):103-106. doi:10.1038/cmi.2012.61
211. Frauwirth KA, Thompson CB. Activation and inhibition of lymphocytes by costimulation. *J Clin Invest.* 2002;109(3):295-299. doi:10.1172/JCI14941
212. Clark EA, Ledbetter JA. Activation of human B cells mediated through two distinct cell surface differentiation antigens, Bp35 and Bp50. *Proc Natl Acad Sci U S A.* 1986;83(12):4494-4498. doi:10.1073/pnas.83.12.4494
213. Liu YJ, Joshua DE, Williams GT, Smith CA, Gordon J, MacLennan IC. Mechanism of antigen-driven selection in germinal centres. *Nature.* 1989;342(6252):929-931. doi:10.1038/342929a0
214. McAdam AJ, Farkash EA, Gewurz BE, Sharpe AH. B7 costimulation is critical for antibody class switching and CD8(+) cytotoxic T-lymphocyte generation in the host response to vesicular stomatitis virus. *J Virol.* 2000;74(1):203-208. doi:10.1128/jvi.74.1.203-208.2000
215. Mak TW, Shahinian A, Yoshinaga SK, et al. Costimulation through the inducible costimulator ligand is essential for both T helper and B cell functions in T cell-dependent B cell responses. *Nat Immunol.* 2003;4(8):765-772. doi:10.1038/ni947
216. McAdam AJ, Greenwald RJ, Levin MA, et al. ICOS is critical for CD40-mediated antibody class switching. *Nature.* 2001;409(6816):102-105. doi:10.1038/35051107
217. Hua Z, Hou B. TLR signaling in B-cell development and activation. *Cell Mol Immunol.* 2013;10(2):103-106. doi:10.1038/cmi.2012.61
218. Abu-Rish EY, Amrani Y, Browning MJ. Toll-like receptor 9 activation induces expression of membrane-bound B-cell activating factor (BAFF) on human B cells and leads to increased proliferation in response to both soluble and membrane-bound BAFF. *Rheumatology* (Oxford). 2013;52(7):1190-1201. doi:10.1093/rheumatology/ket006

219. Batten M, Groom J, Cachero TG, et al. BAFF mediates survival of peripheral immature B lymphocytes. *J Exp Med.* 2000;192(10):1453-1466. doi:10.1084/jem.192.10.1453
220. Do RK, Hatada E, Lee H, Tourigny MR, Hilbert D, Chen-Kiang S. Attenuation of apoptosis underlies B lymphocyte stimulator enhancement of humoral immune response. *J Exp Med.* 2000;192(7):953-964. doi:10.1084/jem.192.7.953
221. Lesley R, Xu Y, Kalled SL, et al. Reduced competitiveness of autoantigen-engaged B cells due to increased dependence on BAFF. *Immunity.* 2004;20(4):441-453. doi:10.1016/s1074-7613(04)00079-2
222. Kuraoka M, Snowden PB, Nojima T, et al. BCR and Endosomal TLR Signals Synergize to Increase AID Expression and Establish Central B Cell Tolerance. *Cell Rep.* 2017;18(7):1627-1635. doi:10.1016/j.celrep.2017.01.050
223. Heer AK, Shamshiev A, Donda A, et al. TLR signaling fine-tunes anti-influenza B cell responses without regulating effector T cell responses. *J Immunol.* 2007;178(4):2182-2191. doi:10.4049/jimmunol.178.4.2182
224. Khan AQ, Chen Q, Wu ZQ, Paton JC, Snapper CM. Both innate immunity and type 1 humoral immunity to *Streptococcus pneumoniae* are mediated by MyD88 but differ in their relative levels of dependence on toll-like receptor 2. *Infect Immun.* 2005;73(1):298-307. doi:10.1128/IAI.73.1.298-307.2005
225. Kawai T, Akira S. The role of pattern-recognition receptors in innate immunity: update on Toll-like receptors. *Nat Immunol.* 2010;11(5):373-384. doi:10.1038/ni.1863
226. Kawasaki T, Kawai T. Toll-like receptor signaling pathways. *Front Immunol.* 2014;5:461. Published 2014 Sep 25. doi:10.3389/fimmu.2014.00461
227. Honda K, Yanai H, Negishi H, et al. IRF-7 is the master regulator of type-I interferon-dependent immune responses. *Nature.* 2005;434(7034):772-777. doi:10.1038/nature03464
228. Schmitz F, Heit A, Guggemoos S, et al. Interferon-regulatory-factor 1 controls Toll-like receptor 9-mediated IFN-beta production in myeloid dendritic cells. *Eur J Immunol.* 2007;37(2):315-327. doi:10.1002/eji.200636767
229. Negishi H, Fujita Y, Yanai H, et al. Evidence for licensing of IFN-gamma-induced IFN regulatory factor 1 transcription factor by MyD88 in Toll-like receptor-dependent gene induction program. *Proc Natl Acad Sci U S A.* 2006;103(41):15136-15141. doi:10.1073/pnas.0607181103
230. Altan-Bonnet G, Mukherjee R. Cytokine-mediated communication: a quantitative appraisal of immune complexity. *Nat Rev Immunol.* 2019;19(4):205-217. doi:10.1038/s41577-019-0131-x
231. Corcoran AE, Riddell A, Krooshoop D, Venkitaraman AR. Impaired immunoglobulin gene rearrangement in mice lacking the IL-7 receptor. *Nature.* 1998;391(6670):904-907. doi:10.1038/36122
232. Durum SK, Candèias S, Nakajima H, et al. Interleukin 7 receptor control of T cell receptor gamma gene rearrangement: role of receptor-associated chains and locus accessibility. *J Exp Med.* 1998;188(12):2233-2241. doi:10.1084/jem.188.12.2233
233. Nakae S, Asano M, Horai R, Sakaguchi N, Iwakura Y. IL-1 enhances T cell-dependent antibody production through induction of CD40 ligand and OX40 on T cells. *J Immunol.* 2001;167(1):90-97. doi:10.4049/jimmunol.167.1.90

234. Hawrylowicz CM, Duncan LM, Fuhlbrigge RC, Unanue ER. Regulation of antigen presentation. II. Anti-Ig and IL-2 induce IL-1 production by murine splenic B cells. *J Immunol.* 1989;142(10):3361-3368.
235. Gui L, Zeng Q, Xu Z, et al. IL-2, IL-4, IFN- γ or TNF- α enhances BAFF-stimulated cell viability and survival by activating Erk1/2 and S6K1 pathways in neoplastic B-lymphoid cells. *Cytokine.* 2016;84:37-46. doi:10.1016/j.cyto.2016.05.017
236. Naradikian MS, Myles A, Beiting DP, et al. Cutting Edge: IL-4, IL-21, and IFN- γ Interact To Govern T-bet and CD11c Expression in TLR-Activated B Cells. *J Immunol.* 2016;197(4):1023-1028. doi:10.4049/jimmunol.1600522
237. Weinstein JS, Herman EI, Lainez B, et al. TFH cells progressively differentiate to regulate the germinal center response. *Nat Immunol.* 2016;17(10):1197-1205. doi:10.1038/ni.3554
238. Harris DP, Goodrich S, Mohrs K, Mohrs M, Lund FE. Cutting edge: the development of IL-4-producing B cells (B effector 2 cells) is controlled by IL-4, IL-4 receptor α , and Th2 cells. *J Immunol.* 2005;175(11):7103-7107. doi:10.4049/jimmunol.175.11.7103
239. Dell'Aringa M, Reinhardt RL, Friedman RS, Jacobelli J. Live Imaging of IL-4-Expressing T Follicular Helper Cells in Explanted Lymph Nodes. *Methods Mol Biol.* 2018;1799:225-235. doi:10.1007/978-1-4939-7896-0_17
240. Snapper CM, Finkelman FD, Stefany D, Conrad DH, Paul WE. IL-4 induces co-expression of intrinsic membrane IgG1 and IgE by murine B cells stimulated with lipopolysaccharide. *J Immunol.* 1988;141(2):489-498.
241. Kitayama D, Sakamoto A, Arima M, Hatano M, Miyazaki M, Tokuhisa T. A role for Bcl6 in sequential class switch recombination to IgE in B cells stimulated with IL-4 and IL-21. *Mol Immunol.* 2008;45(5):1337-1345. doi:10.1016/j.molimm.2007.09.007
242. Avery DT, Bryant VL, Ma CS, de Waal Malefyt R, Tangye SG. IL-21-induced isotype switching to IgG and IgA by human naive B cells is differentially regulated by IL-4. *J Immunol.* 2008;181(3):1767-1779. doi:10.4049/jimmunol.181.3.1767
243. Heine G, Drozdenko G, Grün JR, Chang HD, Radbruch A, Worm M. Autocrine IL-10 promotes human B-cell differentiation into IgM- or IgG-secreting plasmablasts. *Eur J Immunol.* 2014;44(6):1615-1621. doi:10.1002/eji.201343822
244. Lund FE, Garvy BA, Randall TD, Harris DP. Regulatory roles for cytokine-producing B cells in infection and autoimmune disease. *Curr Dir Autoimmun.* 2005;8:25-54. doi:10.1159/000082086
245. Harris DP, Goodrich S, Gerth AJ, Peng SL, Lund FE. Regulation of IFN-gamma production by B effector 1 cells: essential roles for T-bet and the IFN-gamma receptor. *J Immunol.* 2005;174(11):6781-6790. doi:10.4049/jimmunol.174.11.6781
246. Ruane D, Chorny A, Lee H, et al. Microbiota regulate the ability of lung dendritic cells to induce IgA class-switch recombination and generate protective gastrointestinal immune responses. *J Exp Med.* 2016;213(1):53-73. doi:10.1084/jem.20150567
247. Ito T, Carson WF 4th, Cavassani KA, Connett JM, Kunkel SL. CCR6 as a mediator of immunity in the lung and gut. *Exp Cell Res.* 2011;317(5):613-619. doi:10.1016/j.yexcr.2010.12.018

248. Lin YL, Ip PP, Liao F. CCR6 Deficiency Impairs IgA Production and Dysregulates Antimicrobial Peptide Production, Altering the Intestinal Flora. *Front Immunol.* 2017;8:805. Published 2017 Jul 11. doi:10.3389/fimmu.2017.00805
249. Hamilton JA, Wu Q, Yang P, et al. Cutting Edge: Endogenous IFN- β Regulates Survival and Development of Transitional B Cells. *J Immunol.* 2017;199(8):2618-2623. doi:10.4049/jimmunol.1700888
250. Cazac BB, Roes J. TGF-beta receptor controls B cell responsiveness and induction of IgA in vivo. *Immunity.* 2000;13(4):443-451. doi:10.1016/s1074-7613(00)00044-3
251. McIntyre TM, Klinman DR, Rothman P, et al. Transforming growth factor beta 1 selectivity stimulates immunoglobulin G2b secretion by lipopolysaccharide-activated murine B cells. *J Exp Med.* 1993;177(4):1031-1037. doi:10.1084/jem.177.4.1031
252. Liu Q, Zhou YH, Yang ZQ. The cytokine storm of severe influenza and development of immunomodulatory therapy. *Cell Mol Immunol.* 2016;13(1):3-10. doi:10.1038/cmi.2015.74
253. Graham MB, Dalton DK, Giltinan D, Braciale VL, Stewart TA, Braciale TJ. Response to influenza infection in mice with a targeted disruption in the interferon gamma gene. *J Exp Med.* 1993;178(5):1725-1732. doi:10.1084/jem.178.5.1725
254. Turner SJ, Olivas E, Gutierrez A, Diaz G, Doherty PC. Disregulated influenza A virus-specific CD8+ T cell homeostasis in the absence of IFN-gamma signaling. *J Immunol.* 2007;178(12):7616-7622. doi:10.4049/jimmunol.178.12.7616
255. Platanias LC. Mechanisms of type-I- and type-II-interferon-mediated signalling. *Nat Rev Immunol.* 2005;5(5):375-386. doi:10.1038/nri1604
256. Darnell JE Jr, Kerr IM, Stark GR. Jak-STAT pathways and transcriptional activation in response to IFNs and other extracellular signaling proteins. *Science.* 1994;264(5164):1415-1421. doi:10.1126/science.8197455
257. Ihle JN. The Janus protein tyrosine kinase family and its role in cytokine signaling. *Adv Immunol.* 1995;60:1-35. doi:10.1016/s0065-2776(08)60582-9
258. Zhu J, Yamane H, Paul WE. Differentiation of effector CD4 T cell populations (*). *Annu Rev Immunol.* 2010;28:445-489. doi:10.1146/annurev-immunol-030409-101212
259. Bradley LM, Dalton DK, Croft M. A direct role for IFN-gamma in regulation of Th1 cell development. *J Immunol.* 1996;157(4):1350-1358.
260. Djuretic IM, Levanon D, Negreanu V, Groner Y, Rao A, Ansel KM. Transcription factors T-bet and Runx3 cooperate to activate Ifng and silence Il4 in T helper type 1 cells. *Nat Immunol.* 2007;8(2):145-153. doi:10.1038/ni1424
261. Szabo SJ, Kim ST, Costa GL, Zhang X, Fathman CG, Glimcher LH. A novel transcription factor, T-bet, directs Th1 lineage commitment. *Cell.* 2000;100(6):655-669. doi:10.1016/s0092-8674(00)80702-3
262. Miller SA, Mohn SE, Weinmann AS. Jmjd3 and UTX play a demethylase-independent role in chromatin remodeling to regulate T-box family member-dependent gene expression. *Mol Cell.* 2010;40(4):594-605. doi:10.1016/j.molcel.2010.10.028
263. Bradley LM, Dalton DK, Croft M. A direct role for IFN-gamma in regulation of Th1 cell development. *J Immunol.* 1996;157(4):1350-1358.

264. Oestreich KJ, Mohn SE, Weinmann AS. Molecular mechanisms that control the expression and activity of Bcl-6 in TH1 cells to regulate flexibility with a TFH-like gene profile. *Nat Immunol.* 2012;13(4):405-411. Published 2012 Mar 11. doi:10.1038/ni.2242
265. Iwata S, Mikami Y, Sun HW, et al. The Transcription Factor T-bet Limits Amplification of Type I IFN Transcriptome and Circuitry in T Helper 1 Cells. *Immunity.* 2017;46(6):983-991.e4. doi:10.1016/j.immuni.2017.05.005
266. Yates JL, Racine R, McBride KM, Winslow GM. T cell-dependent IgM memory B cells generated during bacterial infection are required for IgG responses to antigen challenge. *J Immunol.* 2013;191(3):1240-1249. doi:10.4049/jimmunol.1300062
267. Racine R, Chatterjee M, Winslow GM. CD11c expression identifies a population of extrafollicular antigen-specific splenic plasmablasts responsible for CD4 T-independent antibody responses during intracellular bacterial infection. *J Immunol.* 2008;181(2):1375-1385. doi:10.4049/jimmunol.181.2.1375
268. Papillion AM, Kenderes KJ, Yates JL, Winslow GM. Early derivation of IgM memory cells and bone marrow plasmablasts. *PLoS One.* 2017;12(6):e0178853. Published 2017 Jun 2. doi:10.1371/journal.pone.0178853
269. Peng SL, Szabo SJ, Glimcher LH. T-bet regulates IgG class switching and pathogenic autoantibody production. *Proc Natl Acad Sci U S A.* 2002;99(8):5545-5550. doi:10.1073/pnas.082114899
270. Lohoff M, Ferrick D, Mittrucker HW, et al. Interferon regulatory factor-1 is required for a T helper 1 immune response in vivo. *Immunity.* 1997;6(6):681-689. doi:10.1016/s1074-7613(00)80444-6
271. Unutmaz D, Vilcek J. IRF1: a deus ex machina in TH1 differentiation. *Nat Immunol.* 2008;9(1):9-10. doi:10.1038/ni0108-9
272. Taki S, Sato T, Ogasawara K, et al. Multistage regulation of Th1-type immune responses by the transcription factor IRF-1. *Immunity.* 1997;6(6):673-679. doi:10.1016/s1074-7613(00)80443-4
273. Kano S, Sato K, Morishita Y, et al. The contribution of transcription factor IRF1 to the interferon-gamma-interleukin 12 signaling axis and TH1 versus TH-17 differentiation of CD4+ T cells. *Nat Immunol.* 2008;9(1):34-41. doi:10.1038/ni1538
274. Elser B, Lohoff M, Kock S, et al. IFN-gamma represses IL-4 expression via IRF-1 and IRF-2. *Immunity.* 2002;17(6):703-712. doi:10.1016/s1074-7613(02)00471-5
275. Yamada G, Ogawa M, Akagi K, et al. Specific depletion of the B-cell population induced by aberrant expression of human interferon regulatory factor 1 gene in transgenic mice. *Proc Natl Acad Sci U S A.* 1991;88(2):532-536. doi:10.1073/pnas.88.2.532
276. Silverstein AM. A History of Immunology. Second ed. San Diego: *Acad. Pr.*; 1989.
277. Schraml BU, Hildner K, Ise W, et al. The AP-1 transcription factor Batf controls T(H)17 differentiation. *Nature.* 2009;460(7253):405-409. doi:10.1038/nature08114
278. Ise W, Kohyama M, Schraml BU, et al. The transcription factor BATF controls the global regulators of class-switch recombination in both B cells and T cells. *Nat Immunol.* 2011;12(6):536-543. doi:10.1038/ni.2037

279. Ivanov II, McKenzie BS, Zhou L, et al. The orphan nuclear receptor ROR γ directs the differentiation program of proinflammatory IL-17+ T helper cells. *Cell*. 2006;126(6):1121-1133. doi:10.1016/j.cell.2006.07.035
280. Betz BC, Jordan-Williams KL, Wang C, et al. Batf coordinates multiple aspects of B and T cell function required for normal antibody responses. *J Exp Med*. 2010;207(5):933-942. doi:10.1084/jem.20091548
281. Yang XO, Pappu BP, Nurieva R, et al. T helper 17 lineage differentiation is programmed by orphan nuclear receptors ROR α and ROR γ . *Immunity*. 2008;28(1):29-39. doi:10.1016/j.immuni.2007.11.016
282. Lazarevic V, Chen X, Shim JH, et al. T-bet represses T(H)17 differentiation by preventing Runx1-mediated activation of the gene encoding ROR γ t. *Nat Immunol*. 2011;12(1):96-104. doi:10.1038/ni.1969
283. Bermejo DA, Jackson SW, Gorosito-Serran M, et al. Trypanosoma cruzi trans-sialidase initiates a program independent of the transcription factors ROR γ t and Ahr that leads to IL-17 production by activated B cells. *Nat Immunol*. 2013;14(5):514-522. doi:10.1038/ni.2569
284. Wang NS, McHeyzer-Williams LJ, Okitsu SL, Burris TP, Reiner SL, McHeyzer-Williams MG. Divergent transcriptional programming of class-specific B cell memory by T-bet and ROR α . *Nat Immunol*. 2012;13(6):604-611. Published 2012 May 6. doi:10.1038/ni.2294
285. Heise N, De Silva NS, Silva K, et al. Germinal center B cell maintenance and differentiation are controlled by distinct NF- κ B transcription factor subunits. *J Exp Med*. 2014;211(10):2103-2118. doi:10.1084/jem.20132613
286. Shaffer AL, Lin KI, Kuo TC, et al. Blimp-1 orchestrates plasma cell differentiation by extinguishing the mature B cell gene expression program. *Immunity*. 2002;17(1):51-62. doi:10.1016/s1074-7613(02)00335-7
287. Roy K, Mitchell S, Liu Y, et al. A Regulatory Circuit Controlling the Dynamics of NF κ B cRel Transitions B Cells from Proliferation to Plasma Cell Differentiation. *Immunity*. 2019;50(3):616-628.e6. doi:10.1016/j.immuni.2019.02.004
288. Fang D, Cui K, Mao K, et al. Transient T-bet expression functionally specifies a distinct T follicular helper subset. *J Exp Med*. 2018;215(11):2705-2714. doi:10.1084/jem.20180927
289. Pepper M, Pagán AJ, Igyártó BZ, Taylor JJ, Jenkins MK. Opposing signals from the Bcl6 transcription factor and the interleukin-2 receptor generate T helper 1 central and effector memory cells. *Immunity*. 2011;35(4):583-595. doi:10.1016/j.immuni.2011.09.009
290. Chodisetti SB, Fike AJ, Domeier PP, et al. Type II but Not Type I IFN Signaling Is Indispensable for TLR7-Promoted Development of Autoreactive B Cells and Systemic Autoimmunity. *J Immunol*. 2020;204(4):796-809. doi:10.4049/jimmunol.1901175
291. Kao C, Oestreich KJ, Paley MA, et al. Transcription factor T-bet represses expression of the inhibitory receptor PD-1 and sustains virus-specific CD8+ T cell responses during chronic infection. *Nat Immunol*. 2011;12(7):663-671. Published 2011 May 29. doi:10.1038/ni.2046
292. Hua Z, Hou B. TLR signaling in B-cell development and activation. *Cell Mol Immunol*. 2013;10(2):103-106. doi:10.1038/cmi.2012.61

293. Kuraoka M, Snowden PB, Nojima T, et al. BCR and Endosomal TLR Signals Synergize to Increase AID Expression and Establish Central B Cell Tolerance. *Cell Rep.* 2017;18(7):1627-1635. doi:10.1016/j.celrep.2017.01.050
294. Pone EJ, Zhang J, Mai T, et al. BCR-signalling synergizes with TLR-signalling for induction of AID and immunoglobulin class-switching through the non-canonical NF- κ B pathway. *Nat Commun.* 2012;3:767. Published 2012 Apr 3. doi:10.1038/ncomms1769
295. Isnardi I, Ng YS, Srdanovic I, et al. IRAK-4- and MyD88-dependent pathways are essential for the removal of developing autoreactive B cells in humans. *Immunity.* 2008;29(5):746-757. doi:10.1016/j.immuni.2008.09.015
296. Kreuk LS, Koch MA, Slayden LC, et al. B cell receptor and Toll-like receptor signaling coordinate to control distinct B-1 responses to both self and the microbiota. *Elife.* 2019;8:e47015. Published 2019 Aug 21. doi:10.7554/eLife.47015
297. Rothausler K, Baumgarth N. Evaluation of intranuclear BrdU detection procedures for use in multicolor flow cytometry. *Cytometry A.* 2006;69(4):249-259. doi:10.1002/cyto.a.20252
298. Abu-Rish EY, Amrani Y, Browning MJ. Toll-like receptor 9 activation induces expression of membrane-bound B-cell activating factor (BAFF) on human B cells and leads to increased proliferation in response to both soluble and membrane-bound BAFF. *Rheumatology (Oxford).* 2013;52(7):1190-1201. doi:10.1093/rheumatology/ket006
299. Mackay F, Woodcock SA, Lawton P, et al. Mice transgenic for BAFF develop lymphocytic disorders along with autoimmune manifestations. *J Exp Med.* 1999;190(11):1697-1710. doi:10.1084/jem.190.11.1697
300. Mackay F, Browning JL. BAFF: a fundamental survival factor for B cells. *Nat Rev Immunol.* 2002;2(7):465-475. doi:10.1038/nri844
301. Kil LP, de Bruijn MJ, van Nimwegen M, et al. Btk levels set the threshold for B-cell activation and negative selection of autoreactive B cells in mice. *Blood.* 2012;119(16):3744-3756. doi:10.1182/blood-2011-12-397919
302. Grimaldi CM, Michael DJ, Diamond B. Cutting edge: expansion and activation of a population of autoreactive marginal zone B cells in a model of estrogen-induced lupus. *J Immunol.* 2001;167(4):1886-1890. doi:10.4049/jimmunol.167.4.1886
303. Rolf J, Motta V, Duarte N, et al. The enlarged population of marginal zone/CD1d(high) B lymphocytes in nonobese diabetic mice maps to diabetes susceptibility region Idd11. *J Immunol.* 2005;174(8):4821-4827. doi:10.4049/jimmunol.174.8.4821
304. Carnrot C, Prokopec KE, Råsbo K, Karlsson MC, Kleinau S. Marginal zone B cells are naturally reactive to collagen type II and are involved in the initiation of the immune response in collagen-induced arthritis. *Cell Mol Immunol.* 2011;8(4):296-304. doi:10.1038/cmi.2011.2
305. Bendelac A, Bonneville M, Kearney JF. Autoreactivity by design: innate B and T lymphocytes. *Nat Rev Immunol.* 2001;1(3):177-186. doi:10.1038/35105052
306. Shaw PX, Hörkkö S, Chang MK, et al. Natural antibodies with the T15 idiotype may act in atherosclerosis, apoptotic clearance, and protective immunity. *J Clin Invest.* 2000;105(12):1731-1740. doi:10.1172/JCI8472
307. Vas J, Grönwall C, Marshak-Rothstein A, Silverman GJ. Natural antibody to apoptotic cell membranes inhibits the proinflammatory properties of lupus

- autoantibody immune complexes. *Arthritis Rheum.* 2012;64(10):3388-3398. doi:10.1002/art.34537
308. Miyamoto M, Fujita T, Kimura Y, et al. Regulated expression of a gene encoding a nuclear factor, IRF-1, that specifically binds to IFN-beta gene regulatory elements. *Cell.* 1988;54(6):903-913. doi:10.1016/s0092-8674(88)91307-4
 309. Hooks JJ, Moutsopoulos HM, Geis SA, Stahl NI, Decker JL, Notkins AL. Immune interferon in the circulation of patients with autoimmune disease. *N Engl J Med.* 1979;301(1):5-8. doi:10.1056/NEJM197907053010102
 310. Cervantes-Barragan L, Lewis KI, Firner S, et al. Plasmacytoid dendritic cells control T-cell response to chronic viral infection. *Proc Natl Acad Sci U S A.* 2012;109(8):3012-3017. doi:10.1073/pnas.1117359109
 311. Swiecki M, Gilfillan S, Vermi W, Wang Y, Colonna M. Plasmacytoid dendritic cell ablation impacts early interferon responses and antiviral NK and CD8(+) T cell accrual. *Immunity.* 2010;33(6):955-966. doi:10.1016/j.immuni.2010.11.020
 312. Liu M, Guo Q, Wu C, et al. Type I interferons promote the survival and proinflammatory properties of transitional B cells in systemic lupus erythematosus patients. *Cell Mol Immunol.* 2019;16(4):367-379. doi:10.1038/s41423-018-0010-6
 313. Van Doremalen N, Lambe T, Spencer A, et al. ChAdOx1 nCoV-19 vaccine prevents SARS-CoV-2 pneumonia in rhesus macaques [published correction appears in *Nature.* 2021 Feb;590(7844):E24]. *Nature.* 2020;586(7830):578-582. doi:10.1038/s41586-020-2608-y
 314. Muecksch F, Wise H, Batchelor B, et al. Longitudinal analysis of clinical serology assay performance and neutralising antibody levels in COVID19 convalescents. Preprint. *medRxiv.* 2020;2020.08.05.20169128. Published 2020 Aug 6. doi:10.1101/2020.08.05.20169128
 315. Isho B, Abe KT, Zuo M, et al. Persistence of serum and saliva antibody responses to SARS-CoV-2 spike antigens in COVID-19 patients. *Sci Immunol.* 2020;5(52):eabe5511. doi:10.1126/sciimmunol.abe5511
 316. Alfego D, Sullivan A, Poirier B, Williams J, Adcock D, Letovsky S. A population-based analysis of the longevity of SARS-CoV-2 antibody seropositivity in the United States. *EClinicalMedicine* 2021; doi:10.1016/j.eclinm.2021.100902
 317. Doria-Rose N, Suthar MS, Makowski M, et al. Antibody Persistence through 6 Months after the Second Dose of mRNA-1273 Vaccine for Covid-19. *N Engl J Med.* 2021;384(23):2259-2261. doi:10.1056/NEJMc2103916
 318. Bölke E, Matuschek C, Fischer JC. Loss of Anti-SARS-CoV-2 Antibodies in Mild Covid-19. *N Engl J Med.* 2020;383(17):1694-1695. doi:10.1056/NEJMc2027051
 319. Woodruff MC, Ramonell RP, Nguyen DC, et al. Extrafollicular B cell responses correlate with neutralizing antibodies and morbidity in COVID-19. *Nat Immunol.* 2020;21(12):1506-1516. doi:10.1038/s41590-020-00814-z
 320. Broxmeyer HE, Lu L, Cooper S, et al. Synergistic effects of purified recombinant human and murine B cell growth factor-1/IL-4 on colony formation in vitro by hematopoietic progenitor cells. Multiple actions. *J Immunol.* 1988;141(11):3852-3862.
 321. New JS, Dizon BLP, Fucile CF, Rosenberg AF, Kearney JF, King RG. Neonatal Exposure to Commensal-Bacteria-Derived Antigens Directs Polysaccharide-Specific B-1 B Cell Repertoire Development. *Immunity.* 2020;53(1):172-186.e6. doi:10.1016/j.immuni.2020.06.006

322. Su TT, Rawlings DJ. Transitional B lymphocyte subsets operate as distinct checkpoints in murine splenic B cell development. *J Immunol.* 2002;168(5):2101-2110. doi:10.4049/jimmunol.168.5.2101
323. Meyer-Bahlburg A, Andrews SF, Yu KO, Porcelli SA, Rawlings DJ. Characterization of a late transitional B cell population highly sensitive to BAFF-mediated homeostatic proliferation. *J Exp Med.* 2008;205(1):155-168. doi:10.1084/jem.20071088
324. Lechner M, Engleitner T, Babushku T, et al. Notch2-mediated plasticity between marginal zone and follicular B cells. *Nat Commun.* 2021;12(1):1111. Published 2021 Feb 17. doi:10.1038/s41467-021-21359-1
325. Baumgarth N. The double life of a B-1 cell: self-reactivity selects for protective effector functions. *Nat Rev Immunol.* 2011;11(1):34-46. doi:10.1038/nri2901
326. Jenks SA, Cashman KS, Zumaquero E, et al. Distinct Effector B Cells Induced by Unregulated Toll-like Receptor 7 Contribute to Pathogenic Responses in Systemic Lupus Erythematosus [published correction appears in *Immunity.* 2020 Jan 14;52(1):203]. *Immunity.* 2018;49(4):725-739.e6. doi:10.1016/j.immuni.2018.08.015
327. Knox JJ, Myles A, Cancro MP. T-bet+ memory B cells: Generation, function, and fate. *Immunol Rev.* 2019;288(1):149-160. doi:10.1111/imr.12736
328. Debertin AS, Tschernig T, Tönjes H, Kleemann WJ, Tröger HD, Pabst R. Nasal-associated lymphoid tissue (NALT): frequency and localization in young children. *Clin Exp Immunol.* 2003;134(3):503-507. doi:10.1111/j.1365-2249.2003.02311.x
329. Muñoz-Fontela C, Dowling WE, Funnell SGP, et al. Animal models for COVID-19. *Nature.* 2020;586(7830):509-515. doi:10.1038/s41586-020-2787-6

APPENDIX A
IACUC PROTOCOLS



MEMORANDUM

DATE: 24-Mar-2017
TO: Lund, Frances E.
FROM: 
Robert A. Kesterson, Ph.D., Chair
Institutional Animal Care and Use Committee (IACUC)
SUBJECT: NOTICE OF APPROVAL

The following application was approved by the University of Alabama at Birmingham Institutional Animal Care and Use Committee (IACUC) on 24-Mar-2017.

Protocol PI: Lund, Frances E.
Title: Plasma Cells in Health and Disease (Ignacio Sanz- Emory University); Project 2: Promoting the Development of Epigenetically and Functionally Distinct Plasma Cell Populations by Modulating the Cytokine Microenvironment
Sponsor: Emory University
Animal Project Number (APN): IACUC-20353

This institution has an Animal Welfare Assurance on file with the Office of Laboratory Animal Welfare (OLAW), is registered as a Research Facility with the USDA, and is accredited by the Association for Assessment and Accreditation of Laboratory Animal Care International (AAALAC).

This protocol is due for full review by 23-Mar-2020.

Institutional Animal Care and Use Committee (IACUC)		Mailing Address:
CH19 Suite 403		CH19 Suite 403
933 19th Street South		1530 3rd Ave S
(205) 934-7692		Birmingham, AL 35294-0019
Fax (205) 934-1188		